Rock Avalanches on Glaciers:

Processes and Implications

A thesis submitted in partial fulfilment of the requirements

for the Degree of

Doctor of Philosophy in Geology

in the University of Canterbury

by

Natalya Victorovna

Reznichenko

University of Canterbury

2012

Frontispiece

View of the Hooker Glacier from the carapace of Mt. Beatrice rock avalanche.

Abstract

This thesis examines the role of rock avalanches in tectonically active terrains including the effects of the deposits on glacier behaviour and their contribution to moraine formation. The chronologies of mountain glacier fluctuations, based on moraine ages, are widely used to infer regional climate change and are often correlated globally. In actively uplifting mountain ranges rock avalanches that travel onto the ablation zone of a glacier can reduce ice-surface melting by insulating the ice. This can cause buried ice to thicken due to slower ablation and can significantly alter the overall glacier mass balance. This glacier response to supraglacial rock avalanche deposits can confound apparent climatic signals extracted from moraine chronologies. This thesis investigates the processes through which rock avalanche deposits may affect glaciers and develops a new technique to identify the presence of rock avalanche debris in glacial moraines.

From laboratory experiments on the effects of debris on ice ablation it is demonstrated that the rate of underlying ice ablation is controlled by diurnal cyclicity and is amplified at high altitude and in lower latitudes. The relatively low permeability of rock avalanche sediment in comparison with non-rock avalanche supraglacial debris cover contributes to the suppression of ablation, at least partly because it greatly reduces the advection of heat from rain water to the underlying ice.

The laboratory findings are supplemented by field investigations of two recent rock avalanche deposits on glaciers in the Southern Alps of New Zealand. This work demonstrates that the rock avalanche deposits are very thick (10 m at Aoraki/Mt. Cook and 7m at Mt. Beatrice) and almost stopped the ablation of the overlying ice. This resulted in the formation of an ice-platform more than 30 m high. This led to a reduction of the existing negative mass balance of the affected Tasman and Hooker Glaciers. There was little noticeable alteration of the overall glacial regime due to the small scale of the debris covered area (4 and 1% of the ablation zones for the Tasman and Hooker Glaciers, respectively) but there is a significant contribution to supraglacial debris, which is passively transported toward the terminus. A conceptual model of the response of mountain valley glaciers to emplacement of extensive rock avalanche debris on the ablation zone has been proposed for the effect of this type of debris on terminal moraine formation based on enhanced ‘dumping’ of supraglacial sediments.

A new technique has been developed to distinguish rock-avalanche-derived sediment from sediment of glacial origin, based on the sedimentary characteristics of the finest fraction. Examination of rock avalanche sediment under the Scanning Electron Microscope showed that finer particles tend to form strong clumps, which comprise many smaller (down to nanometre-scale) clasts, named here 'agglomerates'. These agglomerates are present in the fine fraction of all examined rock avalanche deposits and absent in known non-rock-avalanche-derived glacial sediments. The agglomerates are characteristics of sediment produced under the high-stress conditions of rock avalanche emplacement and contrast with lower-stress process sub- and en-glacial environments. It is demonstrated that these agglomerates are present in some moraines in the Southern Alps of New Zealand that have been attributed to climate fluctuation. Consequently, this technique has the potential to resolve long-standing arguments about the role of rock avalanches in moraine formation, and to enhance the use of moraines in palaeoclimatological studies.

Acknowledgements

I am sincerely grateful to my supervisory team, without whom my research would not have been possible. Thank you to Professor Tim Davies for providing a level of support and encouragement beyond expectations and for allowing me to develop my ideas using experiments that evolved as a result of our many discussions. I also thank Professor Jamie Shulmeister for supporting me during my thesis years and for the best supervision that a student could ever have, and for giving me the opportunity to have a really great and productive time at the Queensland University. A special note of appreciation to Dr. Mauri McSaveney for acting as guide during my research and for very invaluable and informative discussions and advise associated with so many of the questions and ideas that developed as my work progressed.

I am grateful to colleagues who kindly advised me during my research and with whom I had many interesting discussions: to Trevor Chinn, Stuart Dunning, Martin Kirkbride, Martin Brook, Alexander Strom, Glenn Thackray, Stuart Larsen and Philip Deline, a huge thank you. I also acknowledge the support of the University of Canterbury for the provision of a Doctoral Scholarship, this in combination with grants from the Department of Geological Sciences' Mason Trust Fund made this research possible and allowed me to continue my fieldwork and to present some of my results at national and international conferences. Thank you to the wonderful academic staff in the Department of Geological Sciences who have helped me so much, especially Stefan Winkler, David Nobes, Kate Pedley. Thank you to the technical staff who contributed so much to the construction and testing of my experimental installations, to sediment analysis and for assistance with field work in remote areas right through to those final days prior to thesis submission: Chris Grimshaw, Rob Spiers, Cathy Higgins, Vanessa Tappenden, Sacha Baldwin-Cunningham, Matt Cockcroft, John Southward, Anekant Wandres, Pat Roberts, Janet Warburton, Stephen Brown and others. Special thanks and appreciation to Kerry Swanson for continued support of my research, for indispensable advice concerning my laboratory work, and time consuming proof reading of some of my chapters. Thanks to the postgraduates and fellow PhDs in Department who I have had opportunity to work with, who have contributed so much in terms of field work help, and for good times both work and play. I thank all the field assistants I have had during my research among with a special thanks to Olivia for introducing me to the New Zealand setting and sedimentology, and to Sam who has been the best ever field companion, David for long

scientific discussions, Blair for the shear hard work he put in helping me with my fieldwork and all other students I have been privileged to meet over these three years. I`m grateful to technical and academic staff from other Departments (Biology, Geography and Engineering) who not only provided the opportunity for me to access their equipment, a situation compounded by the earthquakes, but were also willing to discuss and solve and operational problems as they arose.

I thank the Department of Conservation staff in New Zealand for the opportunity to conduct my research in often remote areas and for the understanding and help they provided with respect to access and permits: Ray Bellringer and staff from DOC of Aoraki/Mt. Cook National Part, Canterbury DOC, West Coast DOC; and to all owners of properties who generously allowed me to carry out my field studies and to collect those all important samples.

I am grateful to my partner Dylan, who bravely went with me through my journey and has supported my ambitions over all these years. I owe so much to my family, who have always supported and believed in me and for that reason, I dedicate the thesis to my parents.

Table of Contents

List of Figures

List of Tables

1. Introduction

1.1. PURPOSE AND OBJECTIVES

Although large rock avalanches are infrequent, sediment production in active orogens is dominated by such events, and they strongly influence geomorphic processes. Where rock avalanches fall onto glaciers, they may affect glacier behaviour and cause moraines to form that do not reflect climate forcing. The climatic signals extracted from the moraine chronologies of such glaciers may consequently have significant errors. Although accurate reconstruction of glacier chronologies is crucial for understanding global climate-change dynamics, the evidence of aclimatic glacier responses to catastrophic events and their potential impact on geomorphic processes has received particular attention only recently (Porter, 2000; Hewitt et al., 2008; Tovar et al., 2008) and still is not totally accepted by the glacial-chronology community (Schaefer et al., 2009; Putnam et al., 2010a). The impact of supraglacial rock avalanches on glaciers, starting from the mechanism of the emplacement and immediate effect of the deposit on glaciers through to the final re-deposition of rock avalanche sediment as a moraine by an affected glacier, requires systematic investigation.

This thesis is a study of the impact of rock avalanches upon glaciers and moraine formation. It presents integrated research on mass slope processes, glaciology and glacial geomorphology. This thesis is based firstly on observational and physical experimentation methods to assess the effect of reduced surface ablation on supraglacially emplaced materials. Secondly it investigates the microsedimentology of rock avalanche deposits and glacially produced sediments to determine the contribution of supraglacial rock avalanche deposits to moraine formation. The identification of rock avalanche sediment in moraines is critical to understanding rock avalanche effects on glaciers and in resolving potential uncertainties in any palaeoclimatic interpretation of moraines.

This thesis has the following objectives:

- To determine the effect of rock-avalanche cover on the surface ablation of glaciers.
- To assess the effect of rock avalanches on glaciers through examining modern supraglacial rock avalanches in the Aoraki/Mt. Cook region, Southern Alps, New Zealand.

- To develop a conceptual model of moraine formation from enhanced sediment supply from rock avalanche deposits.
- To determine the differences, if any, between the sedimentology of rock avalanche deposits and glacially-produced sediment.
- If such a difference in the sediment is found, to develop and test a technique for the identification of rock avalanche sediment in modern moraines;
- To investigate the palaeoclimate interpretations of some recent moraine dating work.

1.2. THESIS STRUCTURE

There are eight chapters in this thesis:

Chapter 2 is the literature review. It presents summary information on rock avalanche events, their mechanics of emplacement and the geomorphological and sedimentological characteristics of their deposits. The main aspect of the valley glaciers are discussed in the next section. Finally, there is a discussion on the rock avalanches that have travelled onto glaciers which summarises the rare research concerning their impact on glacier behaviour and the final sediment budget. The main outcome of this review is the identification of the research directions that were investigated in the rest of the thesis.

Chapter 3 covers the physical settings and description of study sites in the Southern Alps of New Zealand, Jostedalsbreen in Norway and coastal glacial sediment in the Kaliningrad region of Western Russia, in the South-Eastern Baltic.

Chapter 4 is the study of the effect of debris cover on ice surface ablation. This is regarded as the main effect of supraglacial rock avalanche deposit. Here I report the results from laboratory studies of the effects of debris thickness, diurnally cyclic radiation and rainfall on melt rates beneath rock-avalanche debris and sand (representing typical highly permeable supraglacial debris).

In **Chapter 5** a field investigation of the effects of rock avalanche deposits on two glaciers in the Aoraki/Mt. Cook National Park area, Southern Alps of New Zealand is reported. This study involves ground penetrating radar investigations of the rock avalanche deposits and adjacent areas of the glaciers. As a result, the glaciological and geomorphological implications, including glacial regime changes, effects on the glacial sediment transportation

and contribution to the moraine formation are discussed. Finally, I developed a conceptual model of rock-avalanche-induced advance and resultant moraine formation of the glacier.

The following two chapters are devoted to development and testing of a microsedimentological technique for differentiating rock avalanche material in glacial sediments. The implications for palaeoclimate studies are also discussed.

Chapter 6 describes the development of a microsedimentological technique to indentify rock avalanche sediment from glacially-derived sediment. The technique is based on characteristics of rock avalanche sediment that relate to the high stress conditions of its formation.

Chapter 7 applies the technique to identification of the rock avalanche material and glacial sediment in moraines sequences in some valleys in the Southern Alps of New Zealand. The results from this exercise are discussed in terms of the implications of the proposed technique, its importance in understanding of the palaeoclimate history in the area and the importance of the supraglacial rock avalanche deposits for geomorphology in such areas.

Chapter 8 summarises the major findings of this thesis and briefly discusses directions for future work.

Seven appendices accompany these chapters. These contain two published papers, two papers in press and additional data for the thesis that are briefly outlined below.

Appendix A: Reznichenko, N.V., Davies, T.R.H. Shulmeister, J., and McSaveney, M.J., 2010. Effects of debris on ice-surface melting rates: an experimental study. *Journal of Glaciology*, v. 56, no.197, p. 385-394. This paper is the outcome of Chapter 4.

Appendix B: Reznichenko, N.V., Davies, T.R.H. and Alexander, D.J., 2011. Effects of rock avalanches on glacier behaviour and moraine formation. *Geomorphology*, v. 132, is.3-4, p. 327-338. This paper is mostly the outcome of Chapter 5.

Appendix C: Reznichenko, N.V., Davies, T.R.H., Shulmeister, J. and Winkler, S. Accepted. Influence of rock avalanches upon the formation of moraines and their subsequent palaeoclimatic interpretation: a critical appraisal. *Zeitschrift für Geomorphologie*. This paper is mostly the outcome of Chapters 5, 6 and 7.

Appendix D: Reznichenko, N.V., Davies, T.R.H., Shulmeister, J. and Larsen S.H. 2012. A new technique for identifying rock-avalanche-sourced sediment in moraines and some

paleoclimatic implications. *Geology*, in press. This paper is mostly the outcome of Chapters 6 and 7.

Appendix E: Detailed descriptions of sample sites.

Appendix F: Laser diffraction method plots as particle size distributions output: examples of Round top rock avalanche and Franz Josef terminal moraine samples.

Appendix G: Method and index of microtextures identified on the quartz grains surfaces. Quantitative summary of grain microtextures for analysed glacial and rock avalanche sediments with examples of analyzed separate grains, SEM micrographs.

2. Literature review: rock avalanches in glacial environments

2.1. INTRODUCTION

The number of identified historical and prehistorical catastrophic rock avalanches in high mountain areas has increased significantly over the last 30 years (e.g., Whitehouse and Griffiths, 1983; Geertsema et al., 2006; Hewitt et al., 2008; Ivy-Ochs et al., 2009, Prager et al., 2009; McColl and Davies, 2011). Many of these large rock avalanches run out onto glaciers (e.g., Post, 1967; McSaveney, 1975, 2002; Gordon et al., 1978; Evans and Clague, 1988; Gardner and Hewitt, 1990; Jibson et al., 2004, 2006; Deline, 2009; Decaulne et al., 2010; Jiskoot, 2011). However, the impact of such events on the glaciers' mass balance, sediment transport and deposition are poorly understood. To date, most research has concentrated on rock avalanches in isolation, or on glacier mass balance and climate change responses. Additionally, the processes of rock avalanche deposition, modification and preservation in glacial and paraglacial environments are not well described.

Therefore, this chapter attempts to combine insights from mass slope failure processes and glaciology to address the deficiencies highlighted above. The first section defines rock avalanches and describes their causes, frequencies and characteristic deposits in glaciated valleys. The second part gives an overview of current knowledge of valley glacier systems and associated processes. Finally, rock avalanches that have travelled onto glaciers are characterised with a description of their emplacement and how they affect glacier behaviour. As a result of this review (and the research described herein), future directions for research will also be suggested.

2.2. ROCK AVALANCHES

Rock avalanches are large-volume mass rock slope failures that are mainly confined to high-relief mountain areas and fall from the upper-most parts of mountain slopes. If glaciers are present in the valleys, rock avalanches are likely to fall onto them. In order to determine their effect on glacier behaviour and glacial deposition, some of the important diagnostic features of this phenomenon are discussed. These include: initiation, motion, emplacement,

geomorphological characteristics and sedimentology, and in the present work these discussions will be supported with field observations.

2.2.1. Main characteristics of rock avalanches

Rock avalanches, or catastrophic rock slope failures, are extremely rapid (in the order of tens of metres per second), large-scale (a million cubic metres or more) rock slope failures leading to travel of the fragmenting rock mass for distances often in the order of kilometres across a landscape (Fort et al., 2009). Such events are most common in tectonically active mountain regions and have high destructive potential (Voight, 1978; Eisbacher and Clague, 1984; Hungr et al., 2001; Hewitt et al., 2008). Rock avalanches can occur in most types of rocks which have structural defects or closed fracture patterns (Hungr et al., 2001; Strom and Korup, 2006), and the frequency of these events is a reflection of how steep mountains slopes adjust to high uplift and erosion rates (Montgomery and Brandon, 2002; Korup et al., 2007, 2010).

In principle, rock avalanches are distinguishable from rockfalls and rockslides. Rockfalls represent the detachment of (individual or a few) rock clasts or blocks from a steep slope, and are controlled by gravity. The detachment is centred along discontinuities or tension failure surfaces but occurs without shear displacement (Fig. 2.1) (Fort et al., 2009), and the individual rocks move largely independently of each other. In contrast, rockslides are the downslope movement of a failed rockslope, which may be as rapid and (if sufficiently large) as destructive as a rock avalanche. The term “rock avalanche” was introduced by Heim (in Hsü, 1978) and is synonymous with other commonly used terms such as long-runout/large landslide, Sturzstrom, or debris-avalanche. These mass movements are conventionally distinguished from other rock mass movements by parameters such as velocity, volume and runout length. Thus, “rock avalanche” describes one of the fastest mass movements resulting from the instantaneous release of large quantities of rock which then develops into a mass flow (Angeli et al., 1996; Blikra and Anda, 1997; Hewitt et al., 2008). If the volume of the mass exceeds a certain value, the runout behaviour is likely to differ from that of smaller events. It is widely accepted that this threshold is achieved when the volume reaches of the order of a million of cubic metres, acknowledging that this will vary with the geological setting of the source rock, triggering mechanism, volume of the detached rock mass and parameters of the descent path (Eisbacher and Clague, 1984; Davies et al., 1999; Hewitt,

2002). Herein, I will try to eliminate the confusion of this particular mass movement (rock avalanche), with others, e.g. rockfalls, landslides, and will refer solely to these types of events by the term of "rock avalanches" in the text.

2.2.1.1. Initiation, motion and emplacement

A rock avalanche starts as a large, relatively intact mass of rock that detaches from the upper part of a mountain slope and descends under the influence of gravity down the mountainside. The process of formation includes the initial failure of the rock mass, the down-slope movement of this mass (often travelling many kilometres from the source) and its progressive fragmentation (Evans, 2006), and eventually its cessation of movement and deposition. Following detachment, the body of rock will progressively and rapidly collapse into large, joint-controlled blocks. Then, increasingly, these blocks will be caused to fragment, that is, to fail on newly-generated cracks. This fragmentation will result in the generation of large quantities of fine particles that form an increasing dust cloud during runout and immediately after the deposition.

After observing the 1881 Elm rock avalanche in the Swiss Alps, Heim postulated that the avalanche did not slide but flowed as a sheet of debris, produced by internal deformation during the emplacement (Hsü, 1978). From numerous observations (Evans, 1989; Hewitt, 2001; Dunning, 2004; Strom and Korup, 2006) it is also evident that rock avalanches exhibit impressive mobility such that they are able to move over or around obstacles, and climb up distal slopes resulting in elevated deposits and super-elevation in valley bends. Evans (1989) suggested a simple formula for estimating the velocity of a rock avalanche (noting, however, such a calculation does not include frictional losses during the movement):

$$V^2=2\ gH \tag{2.1}$$

where g = acceleration due to gravity and H = height of run-up (Fig. 2.1).

The velocities of rock avalanches thus estimated exceed tens of metres per second, with ranges of 30-55 m/s (Hewitt, 1999), and to up 60 m/s when travelling over snow and ice (McSaveney, 2002). Speeds >100 m/s have been estimated for mega-rock avalanches (Strom, 2004). Another important characteristic of rock avalanche motion is the length of the runout (often several kilometres) with consequent deposition of material over a long distance and large area. However, the motion is constrained by the rock avalanche source and runout

pathways in the valley topography through which it travels (Nicoletti and Sorriso-Valvo, 1991; Hewitt, 2002; Strom and Korup, 2006).

Some large rockfalls in order of 10^{-5}-10^{-6} m^3 under special conditions could behave as rock avalanches. Heim (1932) recognized that avalanche mobility is directly related to avalanche volume, and Scheidegger (1973) reinforced this finding with statistical analyses showing that that the minimum volume of rock required to initiate the streaming behaviour of a rock avalanche is 0.5×10^6 m^3. For example, several large rock falls that were emplaced after Alaskan earthquake of 1964, behaved in a way more appropriate for rock avalanches with development of a flow current in the rock mass and similar deposit morphology (Post, 1968). Equivalent examples are found in the Southern Alps, New Zealand, with particular reference to the Mt. Vampire and Mt. Beatrice rock avalanches in the Aoraki/Mt. Cook National Park area that had very high vertical travel distances (Cox et al., 2008).

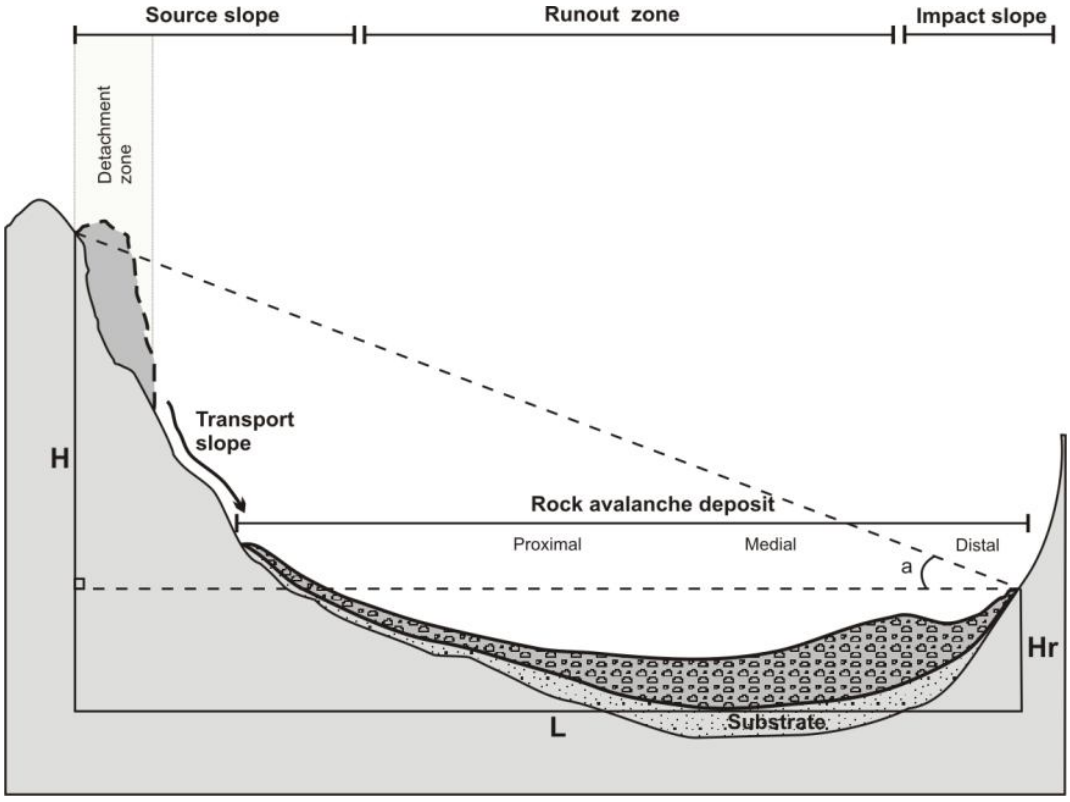

Figure 2.1. Schematic longitudinal section of rock avalanche in a mountain valley. H - vertical distance between highest point of detachment zone and lowest reach of debris; Hr – run up height to raised distal rim; L - maximum horizontal travel; a - travel slope angle from highest point in detachment zone to furthest travel distance, or "Fahrböschung" (adapted from Hewitt, 2002).

Once the deposit reaches the foot of the initial slope, the now-granular and intensely-fragmenting debris mass will continue to flow across the landscape. The fragmentation of the deposit continues due to the very high stresses being experienced by individual clasts, particularly at the base of the mass. There are several theories relating to why different flow regimes develop during the motion of a rock avalanche, these include: granular flow (Komorowski et al., 1991); Bingham or plug flow (Voight et al., 1983); seismic energy fluidisation (Hazlett et al., 1991) and dynamic rock fragmentation (Davies and McSaveney, 2009). The theory of Davies and McSaveney (1999, 2002, and 2009) claims that rock fragmentation during emplacement causes isotropic dispersive stress within the translating rock mass, resulting in the acceleration of the front of the debris sheet and additional fragmentation-induced spreading. This, however, requires a flow depth on the order of metres and does not apply to events with volumes smaller than those appropriate for rock avalanches because the required overburden stress for fragmentation of clasts is not reached.

The characteristic and extraordinary mobility of rock avalanches debris is usually explained by processes occurring in the basal region of the avalanche. Amongst these are concepts of a trapped air cushion inducing low-friction sliding as proposed by Shreve (1968), the presence of a wet basal shear zone (Voight and Sousa, 1994) or basal pressure wave propagation (Kobayashi, 1994). Hewitt et al. (2008) argued that even snow, moisture or wet sediments possibly contribute to the mobility of some rock avalanches, but how this might contribute to associated long travel distances remains unclear.

2.2.1.2. Causes and triggers of rock avalanches in glaciated valleys

The major rock avalanche triggers are defined as direct stimuli following which rock avalanche emplacement occurs (Wieczorek, 1996). Rock avalanche events may have several interconnected causes, but only one trigger. Some events may simply be the culmination of a progressive process, the end point of which is slope failure. The major causes for catastrophic slope failures in glaciated valleys include seismic activity in the valley, oversteepening of the slopes due to deglaciation and erosion processes, rock dilation by rock weathering, heavy rainfall events or permafrost degradation. Human influences are also worthy of mention since human interaction is known to have caused several historical rock avalanches. The classic example is the Elm rock avalanche of 1881 in Switzerland (Heim, 1932) where as a result of quarrying a rock avalanche killed 115 people.

Seismic activity

Seismic activity is the most easily understood and a common trigger for rock avalanches. Intense fracturing progressively reduces rock strength, and as a result of seismic shaking weakening a rock mass, existing fractures widen and ultimately lead to a point where another earthquake initiates large-scale motion (Voight, 1978; Eisbacher and Clague, 1984). In modern glaciated orogens earthquakes have led to catastrophic rock avalanches (e.g. Post, 1967; McSaveney, 1975; Whitehouse and Griffiths, 1983; Keefer, 1984, 1994, 2002; Jibson et al., 2006) with dozens of rock avalanches in order of 10^6 m^3 (the Great Alaskan Earthquake of magnitude 8.4 to 8.6, 27 March 1964; Post, 1967; and the M 7.9 Denali Fault earthquake of 3 November 2002, Alaska; Jibson et al., 2006). Malamud et al. (2004a) suggest that the minimum earthquake magnitude for generation of landslides is M=4.3±0.4, while Keefer (1999) estimated that triggering of landslide volumes in the order of 10^9 m^3 would require an earthquake of M>8, which however depend on the depth of the epicentre. During the period of seismic shaking, shear strength in rock is reduced through widening fractures resulting in an increased chance of failure (Voight, 1978).

Recently, seismic triggering of mass movements has received more attention because of the possibility of using rock avalanches for palaeoseismic reconstruction (e.g. Crozier et al., 1995; Bull, 1996; Jibson, 1996). While the frequency of the events could be determined, the earthquake magnitudes would be harder to reconstruct due to influence of other factors, such as geology and seismic parameters, or the size of a rock avalanche (Keefer, 1984; Gerrard, 1994; Malamud et al., 2004a and 2004b).

Because earthquakes may trigger rock avalanches, some research has focussed on the relationship between earthquake events moraine formation. In New Zealand, Larsen et al. (2005) correlated deposition of terminal moraines with Alpine Fault ruptures that occurred during the last 1000 years. This is based on the assumption that rock avalanches which have spilled onto a glacier will cause the glacier to deposit large moraines composed of materials from the rock avalanche deposit. As a result, they concluded, the dates of such moraines could provide a basis for the development of an earthquake event chronology.

Oversteepening of slopes

During periods of climatic warming, denudation processes are accelerated as a result of glaciers retreating and the consequent exposure of extensive areas of steep ice-free slopes to erosion. According to Augustinus (1995), in mountainous terrain glacial erosion steepens rock slopes, and deepening of troughs may increase the height of rock faces, both of which

increase self-weight stresses. Tensile stress conditions at the toe of the slope are generated and these increase the possibility of rock-slope failure during or after ice retreat. Whitehouse and Griffiths (1983) point out, however, that slope steepening is simply a precondition for failures, and it is the trigger that leads to the rock avalanche.

Another related theory is based on the "debuttressing effect", or paraglacial readjustment, that occurs in rock walls as a response to the alteration of stress within it caused by rapidly retreating glaciers (Evans and Clague, 1994; Ballantyne, 2002; Holm et al., 2004; Deline, 2005). In areas once occupied by ice sheets, loading of the rock induced by the weight of overlying ice leads to increased internal stress levels within the valley walls. Conversely, when the ice retreats, strain energy will be released, causing relaxation. This relaxation may lead to an immediate or delayed rock slope failure during deglaciation. The model proposed by Cruden and Hu (1993) of paraglacial rock-slope failure exhaustion within the period since the last glaciation suggests that there are a potential number of sites that such events can occur only once and that through time, the probability of failure progressively reduces. However, some examples used to support the concept of decreased rock-slope failure rates may be attributed to fact that the deposits are reworked and as a result, their origins misinterpreted. Recent re-examination of the "debuttressing concept' indicates that this is not one of the ways in which deglaciation can significantly affect rock slope stability (Davies and Smart, 2009; McColl et al., 2010), rather it is more likely that slope failure from the glacial deepening would occur while ice was still present, simply because ice is a lightweight but very viscous fluid that cannot resist long-term shear stresses.

It has been noted that majority of documented rock avalanches in the Karakoram Himalaya originated on oversteepened rock walls that have been ice-free for some thousands of years (Hewitt, 2002). In the central Southern Alps, New Zealand, a number of large historic avalanches (1991 Aoraki/Mt. Cook summit failure, 1992 Mt. Fletcher and 1999 Mt. Adams rock avalanches (McSaveney, 2002) originated from oversteepened slopes that are in excess of 49°. For the majority, however, the triggering mechanism has not been identified (Cox and Allen, 2009).

Rock weathering

Climate warming in mountainous areas can lead to rapid permafrost degradation (Geertsema et al., 2006) and increased rock slope failures. Seasonal freezing and thawing of the water in joint networks may facilitate failure and further promote disaggregation of rock masses; and

with time chemical weathering reduces cohesion and frictional resistance along joints, resulting in reduced shear strength along potential failure surfaces (Ballantyne, 2002). The recent hypothesis that permafrost degradation has led to increasing instability of steep rock walls in high-mountain areas is supported by an increasing number of field observations (Haeberli et al., 1997; Noetzli et al., 2003; Fort et al., 2009), but results from other investigations are less compelling in that regard (Allen et al., 2011). It was found that scars associated with rock avalanches of the last century in the Mount Blanc massif were located in the areas of permafrost degradation (Fort et al., 2009), as indicated by measurements and modelling of temperature change in the rockwalls.

Frequent and/or heavy rainfall increases the possibility of rock slope failure by increasing water pressure in joints and thus reducing the frictional strength of the rock (Evans and Clague, 1994; Soldati et al., 2004; Benn and Evans, 2010). In the Southern Alps relatively few large-scale rock-slope failures appear to have been triggered by rainfall, which is in line with observations made elsewhere (Melosh, 1987), but in reality, the triggers for these rock avalanches remain unknown. Such events usually leave a very indistinct source-area scar impacting a large area of the slope to relatively shallow depths (up to 10 – 50 m).

2.2.2. Rock avalanche deposit characteristics

From the geomorphology, sedimentology and material composition of rock avalanches, it is possible to reconstruct these events and distinguish them from the many other deposits found in glaciated valleys which have entirely different origins.

2.2.2.1. Geomorphology

Rock-avalanche deposits may be preserved in the landscape for millennia or longer and usually present features which are out of character with respect to the surrounding morphology, including irregular blocky deposit surfaces and constructional landforms. Several different morphological classifications based on the morphological features of rock-avalanche deposits have been proposed. Nicoletti and Sorriso-Valvo (1991) suggested a classification of the cross-sectional morphology of rock-avalanche deposits based on the topography of the run-out zone, including channelling, unobstructed spreading of the debris mass and the effect of impact against the opposite slope. However, Strom (1999) proposed a

classification which indicated the mode of formation of rock-avalanche deposits based on the foothill junction of the runout path, or the point at which the moving rock avalanche reaches the valley floor.

Several authors, most recently Dunning (2004) have summarised the diagnostic criteria of rock avalanches deposits:

1. Deposits have longer runout than other mass movements (Melosh, 1987).
2. During its emplacement the deposit conforms to the local morphology (Heim, 1932; Nicoletti and Sorriso-Valvo, 1991).
3. The deposits have sharply-defined margins with little spreading of debris beyond these (Cruden and Hungr, 1986).
4. On the deposit surface are formed characteristic ridges and troughs (McSaveney, 1978; Dufresne and Davies, 2009).
5. The deposit runs up opposing valley slopes (up to several hundreds of m) with deposition of material ('brandung'; Heim, 1932; Hewitt, 1999), whereas no other mass failure deposits exhibit such mobility.

Many rock-avalanche deposits typically have a hummocky surface. Among the features of such surfaces, longitudinal ridges are prominent in large avalanches that were emplaced onto deformable substrates and glaciers. Dufresne and Davies (2009) suggest that the form of longitudinal ridges form is determined by the material properties, emplacement dynamics, and environmental factors, such as topography and substrates. Rock-avalanche deposits may also form marginal, levee-like ridges (Blikra and Nemec, 1998) and terminal transverse ridges (Kääb and Weber, 2004). Eisbacher and Clague (1984) attributed these to sliding of the deposit during the final stage of emplacement, where after a sudden halt of the motion, steep margins are formed.

If the rock avalanche occurs within a narrow, confined valley, it is often possible to observe deposits on the opposite valley slope/wall, the result of the avalanche climbing up over obstacles or overrunning into the distal parts of the valley. The resulting deposit features will be determined by the relationship between the rock-avalanche size and valley geometry (Hewitt, 2002). One type of runup is the so-called 'Brandung', where a portion of the avalanche climbs up a hillslope higher than main accumulation deposit then falls back

leaving a small levee (the Brandung) at the highest point reached, providing spectacular evidence of rock-avalanche mobility. Hewitt (2002) provides examples of several such events within a sequence of rock avalanches in Karakoram, where some runups reached heights of 1000 metres above the valley floor.

An important geomorphological signature that provides evidence of a rock avalanche event are large detachment scars at the source; such structures remain evident for thousands of years (e.g., Aa et al., 2007; Strom and Korup, 2006; Turnbull and Davies, 2006; Tovar et al., 2008; McColl and Davies, 2011). Most rock avalanches originate from the upper parts of slopes and often involve the summit ridge which is, as a result, lowered and displaced laterally. A good example of the latter is Shattered Peak, the source of the 1964 Sherman rock avalanche, Alaska (McSaveney, 1978), and the 10×10^6 m^3 bowl-shape depression of the co-seismic Acheron rock avalanche in Canterbury, New Zealand (Turnbull and Davies, 2006) (Fig. 2.2). The characteristics of the scar may also indicate what triggered the rock avalanche. Thus, coseismic rock avalanches usually leave a deep, bowl-shaped scar, whereas a shallow scar covering a large area of a slope will indicate failure due to weathering or stress corrosion factors.

2.2.2.2. Sedimentology

During the downslope movement and runout of a rock avalanche, material derived from masses of hard, largely intact bedrock is fractured, crushed and ground (Hewitt, 2006). This rapid comminution under high stress conditions during rock avalanche emplacement (McSaveney and Davies, 2007) results in specific internal sediment characteristics. Whether the fragmentation occurs during the initial detachment of rock from the source only, or continues until the cessation of rock avalanche motion, is still unclear and hard to determine from contrasting characteristics of deposits presented from case studies (Dunning, 2004). Additionally, there is debate as to whether during the emplacement, formation of new joint sets and fragmentation constantly reoccur. Davies and McSaveney (2009) argued for fragmentation continuing during the entire runout, and that this significantly alters the dynamics of the flow. As a result, the runout of the rock avalanche can be very long where the granular debris mass flows across the landscape and continues to fragment because of the very high stresses being experienced by individual clasts within the mass.

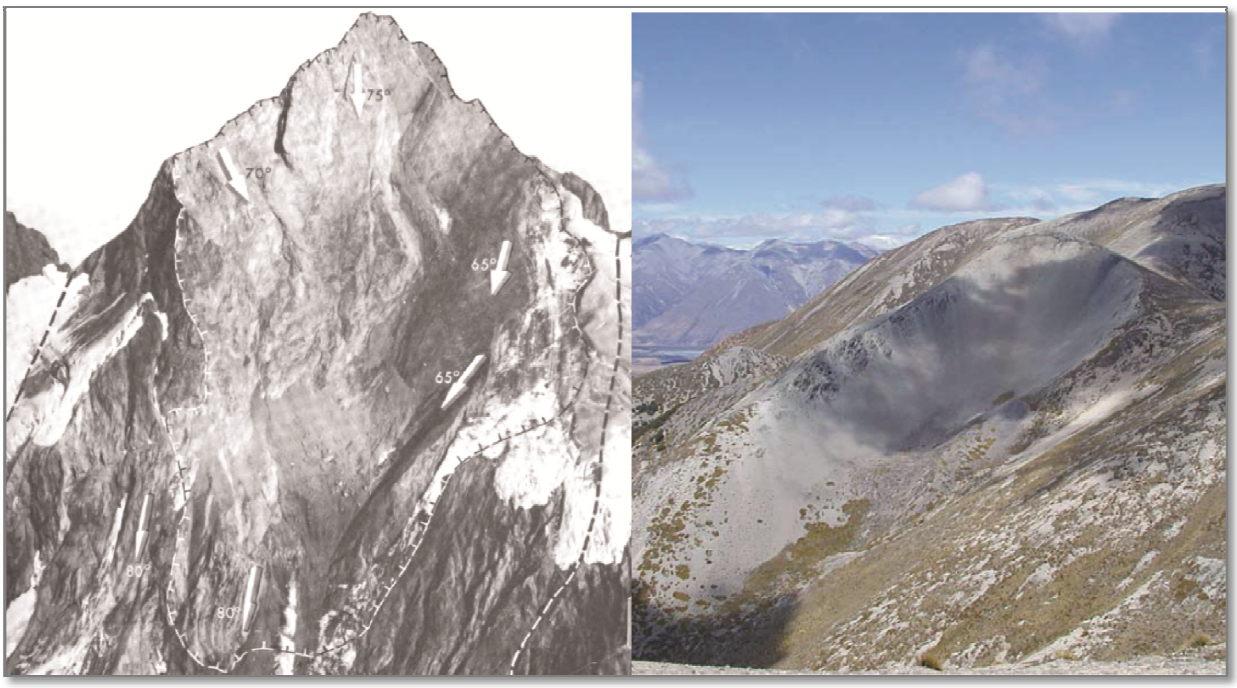

Figure 2.2. Examples of source-area scars of co-seismic rock avalanches. On the left the slide scar of the Shattered Peak (T line) with dashed lines indicating faults, the source of the 1964 Sherman rock avalanches, Alaska (pictures from Plafker, 1968). On the right the cirque-shaped headscarp of the Acheron rock avalanche, Canterbury, New Zealand (from Smith et al., 2006).

Rock-avalanche deposit sediment is usually very angular or angular, unsorted, and contains fractured clasts of all sizes from metre- to sub-micron-size (Fig. 2.3). It is dominated by clast-supported debris with recorded matrix proportions ranging from as little as 5% to 25% or more, ("matrix-poor" and "matrix-rich" debris respectively; Hewitt, 1999). Typically, deposits are composed of very angular, jigsaw-fractured clasts. The facies is characterised by tightly interlocked matrix grains, imbrications and impact fracturing of megaclasts (Hewitt, 1999, 2006; Dunning, 2004) with distinctive deformation structures, such as jigsaw breccia and mosaics of clasts (Laznicka, 1988; Hungr et al., 2001; Kariya et al., 2011). This jigsaw effect is attributed to specific types of motion in the rock avalanche such as semi-coherent mass flow, which Davies and McSaveney (2002) compared to motion with heavy vapour concentrations under positive pressure. Undisturbed, or fresh, rock avalanche deposits usually have a surface or "carapace" layer of relatively less-fragmented angular boulders. This surface layer results from the lower overburden pressure closer to the surface (McSaveney and Davies, 2007) and to partial sorting of the material during movement (McSaveney, *personal comm.*, 2011). This coarser layer overlies densely compacted, highly-fragmented sediment with a full range of sizes from boulders to clays that form the main body of the deposit. The rock avalanche material usually originates from a relatively restricted area of

mountain slope so as a result, the deposit is often composed of a single lithology. If differing lithologies are present in the source area, they are preserved in the deposit as uniform bands in the same relative positions as in the source with a lack of mixing (e.g. Shreve, 1968; Hewitt, 1988, 2009).

Because rock avalanche debris is intensively fragmented during fall and runout, the bulk of the sediment is extremely fine (Heim, 1932; Strom, 2004; Hewitt et al., 2008). For example, McSaveney and Davies (2007) recorded that 99.5% of the deposit fragments from the 1991 Aoraki/Mt. Cook rock avalanche were <10 microns in diameter. The bulk density of this debris is high due to the wide grain-size distribution, such that the voids ratio and permeability are both relatively low. By contrast Hewitt et al. (2008) stated that in rock avalanche deposits the quantity (volume) of sand generally exceeds that of silt, and, in contrast to many tills, clay is a minor component. Thus, Hewitt (1999) found that in matrix samples of rock avalanches in Karakoram Himalaya the 0.2–2 mm range particles dominated, whereas the silt fraction usually ranged between 10 and 35%. This apparent contradiction results from the differences between particle-size distributions measured by number and by volume; in typical fractal rock-avalanche size distributions there are about 10^8 times more 1 μm grains than 1 mm grains, while 1 mm grains occupy 10 times the volume of 1 μm grains (Davies and McSaveney, 2009).

Because of the rapid deceleration and cessation of movement, the main rock-avalanche body is a highly compacted mass characterised by high strength (Hewitt et al., 2008). The large volumes (from 10^7 to 10^{11} m^3) of terrestrial subaerial rock avalanches can be partly preserved in a valley for several thousand years (Keefer, 1984; Hewitt, 1998; Braathen et al., 2004; Strom and Korup, 2006; Wilson, 2009). Often rock avalanche deposits are generally only reworked by river incision, with the main body of the deposit remaining in its original condition (the Lake Coleridge rock avalanche deposits are up to 1000 years old, Lee et al., 2009; and the Mt. Vora rock avalanche deposit in Norway has been preserved for a minimum of 3000 years since emplacement; Aa et al., 2007). The area of a rock avalanche deposit that has crossed a river is progressively removed by river erosion but often, recognisable traces of its initial extent in the form of remnant large angular boulders and vestigial high terraces (Chevalier et al., 2009; Lee et al., 2009).

During emplacement, rock avalanche material is rarely mixed with the underlying substrate (Yarnold and Lombard, 1989; Abbot et al., 2002) and the buried contact with the underlying

soil can usually be traced (e.g. the Acheron rock avalanche deposit, Smith et al., 2006; Fig. 2.3). Dates obtained for boulders and buried trees and soils in comparison with landforms of known age may also be used to support the concept of a rock avalanche origin for a particular landform (Orombelli and Porter, 1988; Deline and Kirkbride, 2009; Ivy-Ochs et al., 2009; Kariya et al., 2011).

Figure 2.3. Examples of rock avalanche deposits: 1. Basal exposure of the 1929 Falling Mountain rock avalanche, the Southern Alps of New Zealand; 2. Acheron rock avalanche deposit (indicated by red arrow) resting on alluvial gravels, outcrop along the Acheron stream, Canterbury, New Zealand; note the overridden soil layer at the deposit base.

2.3. VALLEY GLACIERS AND THEIR SEDIMENT BUDGETS

Glacier-occupied valleys may be found in all climatic zones, where conditions allow sufficient snow accumulation and preservation. The geological setting, slope topography and orientation to the prevailing air masses in a valley, all affect glacier morphology and mass balance. A valley glacier is a complex system with many different factors that affect its sediment production, transport and deposition.

In order to determine the contribution of each process in valley development, Benn and Evans (2010) distinguished low-relief valleys in older mountain belts lower than 1-2 km (Type 1: Canadian Shield, Scandinavia, e.g. Norway) from and high-relief valleys which are confined to young, seismically-active mountains with peaks and highly erodible steep slopes several km high (Type 2: the European Alps, the Southern Alps of NZ, Himalaya, Andes, Alaskan ranges).

Figure 2.4. Low-relief type of valley in older mountain belts with comparatively meagre supraglacial debris and infrequent supraglacial rock avalanche emplacements onto glaciers. The valley Nigardsbreen Glacier is the ice cap outlet from Jostedalsbreen, the highest mountains in southern Norway from 1910 to 350 m in altitude. Photo: Reznichenko N., July, 2010.

Figure 2.5. A high-relief glacierized valley with sharp peaks of the Southern Alps, New Zealand. Aoraki/Mt. Cook peak (3,754 metres) in the background, and glaciers that are extensively covered with debris and often with rock avalanche deposits (the Mueller Glacier at front and the Hooker Glacier at rear). The heavily covered glaciers terminuses in well-developed proglacial lakes surrounded by high terminal and lateral moraines. Photo: Reznichenko N., March, 2009.

In low-relief valleys the supraglacial component usually is insignificant in the glacier sediment budget in contrast with the high-relief Type 2 (Figs. 2.4. and 2.5). The greater volume of supraglacial sediment in Type 2 results from rapid subaerial denudation of steepened slopes by small- and large-scale rock slope failures (Korup and Clague, 2009). These landscapes represent a special case with respect to temperate ice-marginal landsystems, and are characterised by a high proportion of debris and topographic controls on sedimentation from the valley walls (Benn and Evans, 2010).

2.3.1. Glacier mass balance

Valley glaciers gain mass as a result of precipitation (snow, hail, freezing rain) and snow/ice avalanching in the accumulation zone, while mass loss occurs in the ablation zone through melting, sublimation, evaporation, ice calving and avalanching. These two zones meet at the equilibrium line altitude (ELA), at which the mass budget is equal to zero (Fig. 2.6).

The morphology of the glacier is determined by climate and the topography of the valley, while the mass budget of the glacier determines ice mass gains or losses (Østrem and Brugman, 1991). Glacier mass balance is one of the fundamental characteristics used to determine glacier regime and response to climate change (e.g. Paterson, 2004; Marshall, 2009; Benn and Evans, 2010).

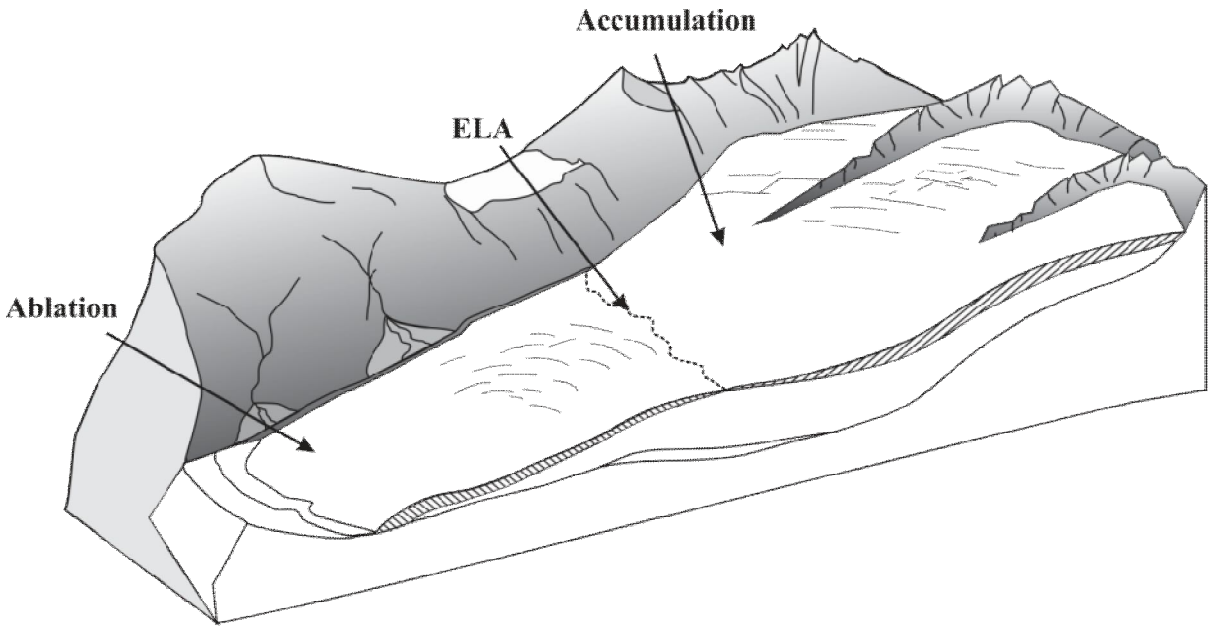

Figure 2.6. Schematic diagram showing the main mass balance parameters of a valley glacier with the accumulation zone in the upper catchment and the ablation zone in lower catchment; at the ELA the amount of accumulation is equal to the amount of ablation.

Changes in atmospheric characteristics are the main causes for glacier fluctuations (Chinn, 1996). The geographical location (latitude, altitude and continentality) and the current climate will determine local meteorological conditions (precipitation and temperature) and, as a result, control the mass balance of a specific glacier. It is evident that with increasing latitude, solar irradiance and thus net radiation and temperature generally decrease; however, latitude is also an important influence with respect to seasonal and diurnal climatic rhythms. Thus, low latitudes are characterised by small seasonal changes of solar radiation, day length and temperature but with relatively large diurnal temperature range (with a mean monthly seasonal range in order of 1-2C^{o}). For middle and higher latitudes, seasonal effects substantially exceed diurnal changes (< 10C^{o}). Continentality (caused by the much lower effective heat capacities of land surfaces compared to oceans and resulting in greater temperature variations) also has a significant effect on a glacier's mass balance; glaciers in areas with a humid climate have a larger mass turnover and extend to lower altitudes where air temperatures are relatively high (e.g. glaciers in the Southern Alps of New Zealand, Alaska and western Norway). Thus they respond faster to climatic fluctuation (Oerlemans and Fortuin, 1992).

Glacier mass-balance responds directly to atmospheric change, resulting in glacier front or terminus position fluctuations determined by the ice flow and the net mass balance. The lag time of the terminus response is defined as the period from the initiation of the mass balance change until the glacier has fully adjusted to a new equilibrium size. For temperate valley glaciers this is in the order of 10^{1}-10^{2} years (Oerlemans and Fortuin, 1992). However, changes of the glacier ice volume could also be reflected by ice surface elevation alterations. For example, a low surface gradient and thick debris-cover close to the terminus of the downwasting Tasman Glacier (the Southern Alps of New Zealand) resulted in negative mass balances with an almost stable terminus position over the 150 years preceding proglacial lake development (Kirkbride, 1989).

The slope and morphology of glaciers control their advance/retreat response to a change in climate ("sensitivity"; Chinn, 1996). For example, flat accumulation and steep ablation zone gradients have resulted in rapid responses by the maritime Nigardsbreen Glacier, Norway, and the Franz Josef and Fox Glaciers, New Zealand (Oerlemans and Fortuin, 1992). Because sensitivity to negative mass balance perturbations about a given terminus position is not necessarily the same as that for positive balance changes, these should be considered

individually for each glacier and based on long-term observation of regional changes in glacier geometries (Chinn, 1999).

The relative sizes of the accumulation and ablation zones (Accumulation Area Ratio, AAR) will also affect the glacier response. The AAR is based on the assumption that under steady state conditions the accumulation area of a glacier represents a fixed proportion of the total glacier area (Benn and Evans, 2010):

$$AAR = \frac{\text{accumulation area}}{\text{total glacier area}} \quad (2.2)$$

Thus, many mid- and high- altitude glaciers have AAR between 0.55-0.65, indicating that the accumulation area is about 60% of the total glacier area (Meier and Post, 1962), where in different conditions AAR could be as low as 0.3-0.4 (debris-covered or cirque glacier) or as high as 0.8-0.9 (for steep slope maritime glaciers, tropical or rapidly calving glaciers; Kulkarni, 1992; Kaser and Osmaston, 2002; Fig. 2.7). When certain threshold values of AAR are crossed due to external changes a glacier can switch from one regime to another because glaciers always tend to move towards a state of equilibrium. For example, in a glacier with a wide, shallow accumulation zone but steep, narrow ablation zone, equilibrium will be reached when the ice accumulation is able to match the rapidly melting and fast flowing ablation zone ice. This observation applies to steep maritime glaciers that terminate at low elevation (e.g. the Franz Josef and Fox Glaciers of South Westland, New Zealand, AAR of the order of 0.8) and tropical glaciers with intensive melting in the ablation zone. Alternatively, when the ablation zone has a slower rate of ablation as a result of extensive debris-cover reducing surface melting, the glacier maintains equilibrium by having a longer ablation area (AAR ~ 0.3-0.4). In order to maintain equilibrium of cirque glaciers their steep and small accumulation zones, and shallow topography of the ablation zone, result in a larger ablation zone (AAR of the order of 0.4 as for the Ivory Glacier, the Southern Alps). As a consequence, these glaciers have a slower response to the climate changes (Chinn, 1999; Trevor Chinn, personal communication, February, 2011). Because glaciers always tend towards an equilibrium state any non-climatic disturbances of their net balance must also be included in estimations as to how any glacier responds to climate change.

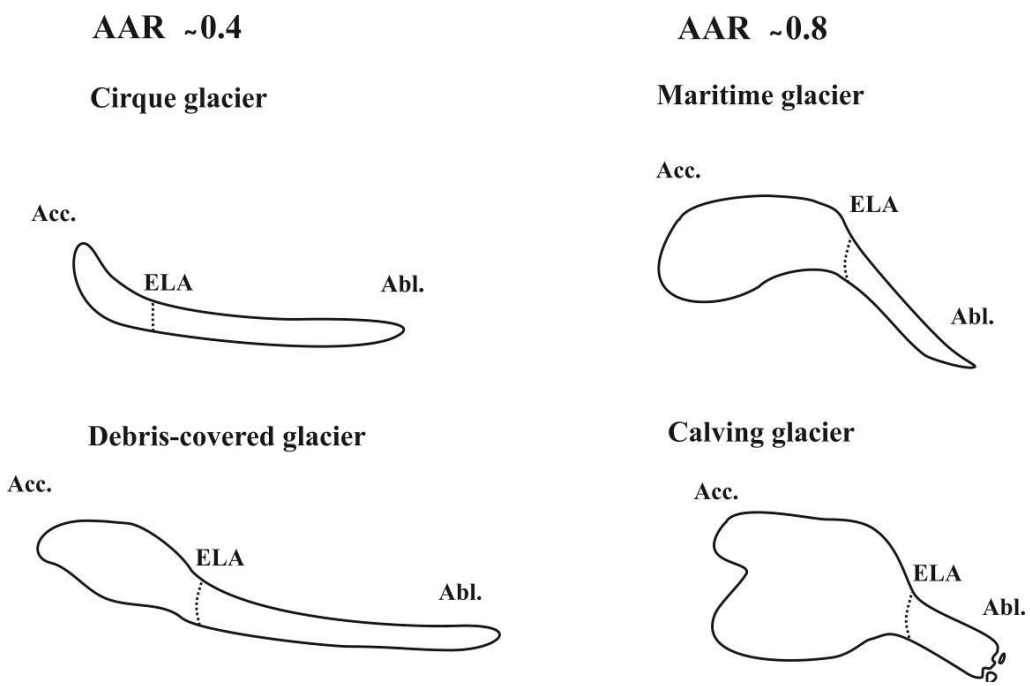

Figure 2.7. Examples for the extreme AAR of the glaciers with different regimes due to topographic (such as cirque or steep maritime glaciers) or ablation peculiarities (debris-covered or calving ablation zone).

2.3.2. Glacier ice flow and movement

Glaciers tend to maintain gravitational equilibrium through ice flow that occurs because ice is a viscous solid, and any increase in stress in a body of ice results in increase in strain rate. Glen (1952) and Nye (1959) established the general flow law for glacier ice:

$$\dot{E} = A\tau^n \tag{2.3}$$

where $\dot{E}$ is the strain rate, τ is a shear stress, A and n are constants. Note that this implies that the strength of ice is zero - it will flow in response to *any* level of applied shear stress.

The basal shear stress of the glacier is calculated from:

$$\tau = \rho g H \tan\alpha \tag{2.4}$$

where ρ is the density of ice (900 kg/m^3), g is the acceleration due to gravity (9.80 m/sec^2), H is the glacier thickness measured vertically and α is the surface slope (note the new formulation of the driving stress that changed *sin* in an older equation to *tan*; in Benn and Evans, 2010, p.114). For valley glaciers, this equation is modified to account for the frictional effects of the valley walls using a shape factor (f):

$$\tau_1 = f\rho g H \tan\alpha, \quad \text{where } f = \frac{A}{Hp} \tag{2.5}$$

where A is the cross-sectional area of the glacier and *p* is the perimeter of the cross section.

The average glacier flow velocity at the surface due to internal ice deformation can be calculated:

$$U_{av} = \frac{2A\tau^{n}H^{n+1}}{(n+2)} \quad (2.6)$$

However, for warm-based glaciers, movement is a result of both internal ice deformation and basal sliding on the substrate. Despite the numerous proposed theories, basal sliding in glaciers is extremely difficult to observe and measure, primarily because the roughness of the bedrock, substrate properties and the basal hydrology are not well constrained. Hence, calculations of glacier flow velocity are estimates at best.

In general, the different flow velocities along and across a glacier result in mostly compressive flow in the ablation zone and extensional flow in the accumulation zone (Andrews, 1975). It should also be noted that topographic constraints inevitably affect the nature of the flow in valley glaciers and, as a result, the terminus position of the glacier. Thus, in a widening valley with extensional flow at the glacier snout, the frontal position will be more stable, whereas in a narrowing valley compressive flow will be more important and the terminus less stable. Topographic controls will influence the position of the terminal moraine.

Through ice flow or kinematic wave propagation, glaciers are constantly responding to fluctuations of accumulation and ablation. Temperate valley-glaciers with steep profiles, high accumulation rates and englacial temperatures close to 0ºC have velocities of up to 300 m/yr (Andrews, 1975). However, some glaciers also display specific short-term responses, such as those exhibited when a glacier alternates between rapid and slow flow over periods of few to several decades of years, or surging cycles (e.g. Post, 1969; Paterson, 2004; Murray et al., 2003; Benn and Evans, 2010). These cycles consist of a period of active surge with up to 10^3 times normal ice velocities; stagnation, a renewed build-up and then another surge. Despite the fact that the surging behaviour of some glaciers may be explained by the stress release that built up beyond the yield stress, the mechanism(s) of glacier surges are poorly understood. This explains why, after catastrophic rock avalanche emplacement onto this type of glacier, it is often unclear whether the rock avalanche deposit has triggered glacial surge or it is a response to some other mechanism/event (e.g. Bualtar Glacier, Karakoram Himalaya; Hewitt, 2009).

2.3.3. Sediment in glacial systems

2.3.3.1. Sources

The main sources of the sediment incorporated into the glacier transportation system are 1) subglacial erosion and entrainment of material by glacier itself and 2) external inputs to the glacier from subaerial denudation processes, which are mostly transported supra- and englacially but also subglacially.

Subglacial processes

Subglacial erosion is dominated by plucking and abrasion, where the type and intensity of erosion is determined by relationship between stresses imposed on the substrate and its strength (Boulton, 1974, 1978; Morris, 1976, 1979; Boulton and Eyles, 1979; Hallet, 1979; Kirkbride, 1995; Benn and Evans, 2010). Three main erosional processes have been described for basal zone of glaciers: bedrock abrasion by debris embedded in the glacier basal ice; bedrock crushing caused by pressure differences due to glacier flow over uneven bedrock surfaces; and entrainment of existing subglacial debris (Boulton, 1974). In the last of these, previously deposited sediment is removed from the base and incorporated into the glacier-sediment transportation system (Kirkbride, 1995). Two main concepts in glacier erosion are proposed. Boulton (1974) considered the contact force as the sum of buoyant weight of the clast in ice and the net weight of the ice above, while Hallet (1981) emphasized the importance of the sediment concentration. Hallet (1981) proposed that abrasion is controlled by the ice flowing towards the bed and its sliding velocity parallel with the bed, and as a result, significant abrasion will occur only at the bases of glaciers which have debris concentrations from 10 to 30%) at the basal layer (Despite continued research on all of these processes (e.g. Boulton, 1974, 1978; Hallet, 1979, 1981; Eyles and Menzies, 1983) their physical reality remains questionable.

Within the glacier environment all sizes of sediment may be produced by physical degradation of rock. Sand and silt fractions result from the combination of basal sliding and two mechanisms of erosion: *abrasion* and *crushing* (Rogers et al., 1963; Smalley and Vita-Finzi, 1968; Boulton, 1978; Smalley and Krinsley, 1978; Wright, 1995). Jansson et al., (2005) point out that comminution at the base of the glacier requires temperate basal conditions with basal ice at the pressure melting point, although sometimes sliding and deformation of basal sediments may occur even when the base is frozen. Silt is mostly produced by abrasion of coarser clasts, while sand is the result of the crushing of grains

generally coarser than 0.5 mm (e.g. Rogers et al., 1963; Haldorsen, 1981; Wright, 1995; Fig. 2.8). Thus, resistant quartz particles comminute softer minerals but are themselves remarkably stable (Sharp and Gomez, 1986). According to Haldorsen (1981) the glacier deposit matrix correlates closely with the granulometric composition of the parent bedrock and, consequently, if the source rock is fine-grained the amount of silt particles produced by crushing would overlap that produced by abrasion and complicate differentiation between these two. The statement that glacier plucking and abrasion are the *only* origin of rock flour, however, can be questioned due to the impossibility of separating purely glacier-basal-erosion products from fines derived from slope mass wasting, or from sediment previously deposited at the glacier base, in the final product output from the glacier (Whalley, 1978; Wright, 1995).

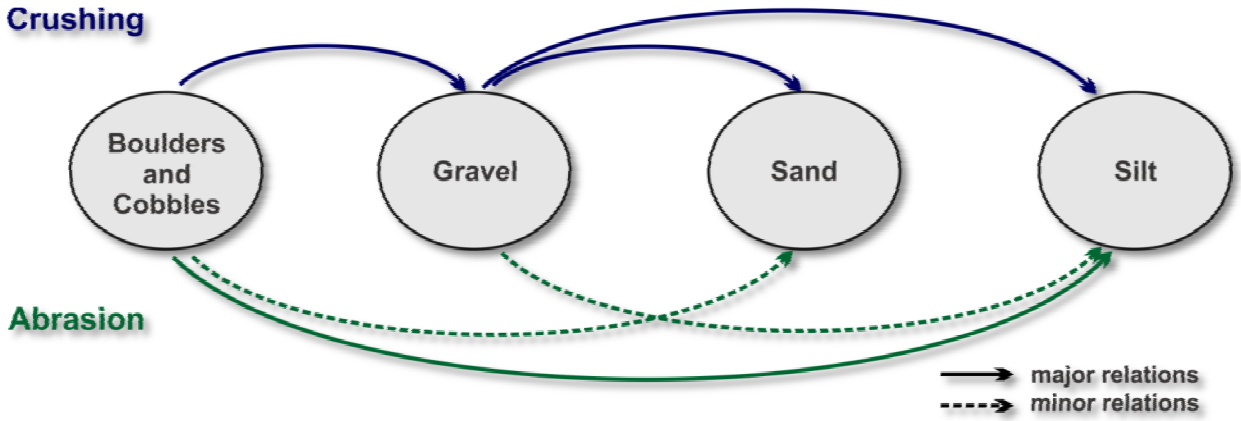

Figure 2.8. General principles for the glacial comminution of debris derived from a resistant coarse-grained bedrock in the glacial environment. Modified from Haldorsen, 1981.

Currently, conventional theory suggests that only in glacial environments can "rock flour" be produced – this is the comminution of debris to silt-size quartz and feldspars attributed to subglacial erosion processes (Smalley, 1966; Drewry, 1986; Sharp and Gomez, 1986; Bischoff and Cummins, 2001; though note the contradiction with the comment on rock avalanche rock flour of Heim, 1932). Because rock flour is commonly found in proglacial rivers and lakes it must be delivered there by the proglacial water flow. Correlations between abundance of the rock flour and increase in glacier activity (glaciations or glacier advances) were reported from studies of deposits in lakes (Bischoff and Cummins, 2001; Rosenbaum and Reynolds, 2004). These are used as a major argument in confirming that glacial erosion produces silt-sized particles of rock.

Basal erosion and entrainment of the resultant debris are primary controlled by the thermal regime at the glacier base (Drewry, 1986; Swift et al., 2002; Eyles, 2006). Eyles (2006) noted that the role of meltwater in glacial erosive processes is usually underestimated, because only with water present are glaciers able to erode and transport large quantities of sediment. Subglacial hydrology primarily controls basal sediment evacuation. Rapid removal of evacuated sediment from the ice-bedrock interface encourages ice-bedrock interaction (Swift et al., 2002). Flow velocities, physical characteristics of the sediment particles, their concentration in the flow and the flow pathway all contribute to basal erosion as a result of abrasion induced by the sediment load. It is also known that meltwater may chemically alter basal material, leading to increased rates of erosion and sediment transport (e.g. Sharp et al., 1995; Benn and Evans, 2010). In alpine terrains, evidence of vigorous mechanical weathering is widespread. Reynolds (1971) concluded that in maritime glacial environments, chemical weathering and clay mineral formation are significant influences on erosion rates and the type of sediment particles produced. Thus, sediment production by temperate mountainous glaciers may be as high as 2000 tonnes/km^2/year, which contrasts with the low precipitation, low erosion rates and less than 40 tonnes/km^2/year associated with polar glaciers (Eyles, 2006).

In conclusion, the variables that most influence erosion at the base of a glacier are: glaciology (basal shear stress and velocity, thermal regime and subglacial water pressure); substrate properties (grain size, lithology, weathering degree, structure); the topographic nature of the bed and landscape; and the duration of glaciations in the valley (Evans, 2002). Hallet et al. (1996) estimated rates of glacial denudation from sediment concentrations in proglacial streams, reporting that they vary globally from one glacier regime to another. The erosion rate calculated for polar glaciers and thin temperate plateau glaciers on crystalline bedrock was 0.01 mm/yr; for temperate valley glaciers on resistant crystalline bedrock in Norway 0.1 mm/yr; for small temperate glaciers on diverse bedrock in the Swiss Alps 1.0 mm/yr and up to 10-100 mm/yr for large and fast-moving temperate valley glaciers in the tectonically active ranges of southeast Alaska. Note however that these calculations ignore the possibility of fine sediment entering or leaving storages, instead assuming that all sediment measured came immediately from bedrock erosion.

Extraglacial sources

External sources include all sediment originating from the environment above the glaciers. In valley glaciers a high percentage of this material derives from mass movements (Kirkbride, 1995; Benn et al., 2003; Owen et al., 2003), including snow and ice avalanches containing sediment, debris flows, rockfalls, rock avalanches, and sediment discharge from alluvial processes operating in ice-free valleys that discharge onto or into a glacier (Kirkbride, 1989). Other sources of material, such as aeolian, volcanic and extraterrestrial inputs, contribute infrequently or to a usually smaller degree. It seems logical to include previously-supplied material entrained by basal processes as an external source of glacial sediment supply, which, once incorporated into the ice, will undergo glacial reworking.

The dominance of one source of denudation over another is conditioned by catchment topography, lithology, climatic factors and the level of tectonic activity in the region. Thus, in tectonically-active mountains, uplift will initiate and maintain the development of a steep topographic gradient leading to faster glacier ice flow and activity; further, the proportion of rock avalanche-generated material will be higher, because uplift of the slopes will lead to increased erosion. Bedrock lithology will also affect the rate of the erosion. For example, the east side of the Main Divide of the Southern Alps of New Zealand is composed mostly of Torlesse Supergroup rocks, or greywacke, which are intensively shattered sandstones and siltstones (Suggate, 1978; Fitzsimons and Veit, 2001). As a result, a high proportion of the sediment found in glaciers east of the Main Divide has originated from that source, by contrast with the steep topography associated with the highly resistant ancient gneisses and intrusive granites found in Fiordland and southern Westland (Kirkbride, 1989; Hambrey and Ehrmann, 2004). Similar contrasts in lithology occur between the crystalline rocks found in glaciated areas of central Norway and highly erodible limestones of the European Alps (Fitzsimons and Veit, 2001).

Climatic factors, such as the proportion of snow/ice input to debris supply, significantly affect the glacier sediment regime. Benn et al. (2003) compared and contrasted the concentration of debris-mantled glaciers and rock glaciers in areas of low precipitation (about 500 mm $year^{-1}$) in the Nepalese Himalayas with ice-dominated glaciers and an absence of rock glaciers in western Norway, which he concluded reflected the presence of highly resistant lithologies and high precipitation (2000-3000 mm $year^{-1}$) in the latter area. Similar glaciers in Westland, New Zealand, have a low supraglacial sediment component and high

turnover (Chinn, 1996) compared with glaciers east of the Main Divide which are thickly debris-covered.

2.3.3.2. Transportation

The bulk of the accumulating sediment load is incorporated into the glacier and then modified and transported by the flow of ice to areas of deposition often tens or even hundreds of kilometres from the source (Kirkbride, 1995). Boulton et al. (1985) view the glacial transporting system as a conveyor belt with material added by erosion and lost by deposition at any point along its length, with net discharge at the terminus. Thus, the sediment migrates among supraglacial (on ice surface of glacier), englacial (within the glacier ice) and subglacial (zone of contact with the substrate) pathways that are characterized by different transport processes. Modification and redistribution of the sediment occurs not only subglacially (Boulton, 1978), but en- and supraglacially as well, where glaciofluvial processes play significant roles in sediment transportation and modification, such as sorting and reshaping (e.g. Kirkbride, 1995; Kirkbride and Spedding, 1996; Hambrey and Ehrmann, 2004).

The variations of thermal regimes determine the ice flow of the glacier, the dominant glacial erosive processes, the water fluxes through the glacier and thus the debris transportation system. The high sediment supply rates and high rates of ice flow associated with warm-based glaciers can result in huge volumes of sediment being incorporated into and transported by the glacier. Another important sediment transport and reworking agent within the glacier body is water flowing within the ice that is derived from melting ice, precipitation or ice-marginal rivers. Therefore, an understanding of sediment sources, sediment transportation and deposition processes is required before any attempt to quantify sediment modification within the glacier sediment-transportation system is undertaken.

Subglacial transportation

Subglacially transported debris is derived from the substrate by basal erosion and from higher (englacial and supraglacial) levels within the transportation zone (Owen et al., 2003). Cold-based glaciers usually entrain limited amounts of the debris, while warm-based glaciers usually develop active basal sequences in which the majority of debris comminution and deformation occurs. Once that is achieved, grain-size differentiation and removal of fines by water occurs. The debris-layer thickness and concentration, basal sliding speeds and strain rates will determine transport rates in an active layer at the bottom of the ice sole (Benn and

Evans, 2010). It has been shown that the subglacial drainage network is able to transport significant bedload sediment, which in turn can affect glacier motion and produce short term but intensive sediment outbursts (Davies et al., 2003; Davies and Smart, 2007).

In valleys with rough terrain, high migration rates of material between transportation zones are common. The debris may reach the ice-bedrock interface as a result of falling into crevasses, via meltwater tunnels or by downward flow associated with basal melting (Drewry, 1986; Kirkbride and Spedding, 1996) and may remain in that location until it is deposited on the glacier bed or at the glacier snout. Alternatively, subglacial sediment may be transferred upwards as a result of glacial-tectonic deformation (e.g. by compressive deformation resulting in folding and thrusting of ice upwards along flow lines, Fig. 2.9; Benn and Evans, 2010) or by injection of turbid waters into basal crevasses (Ensminger et al., 2001).

Sediment transported basally is significantly comminuted under conditions of higher stresses and differs from that found in en- and supraglacial environments. Many studies (e.g. Andrews, 1975; Boulton, 1978; Haldorsen, 1978) suggest that the subglacial wear of sediment is quite distinct from crushing in other transportation zones. However, recent research (Owen et al., 2003; Hambrey and Ehrmann, 2004) has shown that the fine particles present, which were mostly deformed during entrance to the zone, could be derived from the supraglacial layer.

Englacial and supraglacial transportation

Englacial sediment can be derived from debris falling on to the glacier accumulation zone and being buried by accumulating snow, from the subglacial zone or from superimposed ice streams (Sharp, 1949; Rogerson et al., 1986). The englacial zone is characterized by minimal abrasion and usually an absence of crushing.

The supraglacial cover is a crucial factor in the modification of a glacier's response to atmospheric changes, and thus in the formation of glacial deposits. This cover results from the slope processes downvalley of the equilibrium line, and it will usually remain, and be transported, as a supraglacial deposit. The common extensive debris cover towards the terminus of many glaciers is usually formed by melt-out of englacial debris, which may itself be sub-, en- or supraglacially-sourced (Rogerson et al., 1986; Kirkbride, 1993; Hambrey et al., 2008). For example, in the Southern Alps of New Zealand, Hambrey and Erhmann (2004) determined that debris on five glaciers (the Tasman, Mueller, Hooker, Franz Josef and Fox) is

sourced from the valley slopes and emplaced by screes, snow avalanches and streams, and after being progressively incorporated sub- and englacially has been exhumed supraglacially in the ablation zone (Fig. 2.10).

Figure 2.9. Sediment delivery to the glacier surface by thrusting of subglacial sediment. The Fox Glacier terminus, the Southern Alps of New Zealand. Photo: Reznichenko N., February, 2011.

The thin melt-out debris blanket increases in thickness toward the terminus as a result of lateral displacement and the emergence of englacial debris, which may reverse the increasing rate of clear-ice ablation towards the terminus caused by the reduction in glacier-surface elevation. Medial moraines often occur on glacier surfaces, and the materials associated with such deposits are delivered by the emergence of ice at the glacier surface below the equilibrium line. Hence, as they travel down-valley below the ELA they widen non-linearly, steepen laterally and increase in relief (Anderson, 2000). Transport of this sediment is considered passive, as individual particles/grains do not show glacial abrasion marks (Dreimanis, 1990). Additionally, finer material is removed by melt water, and most of the remaining rock fragments are angular (perhaps enhanced by frost-shatter).

By contrast, rock avalanches leave a distinctly different type of debris cover. It is usually a one- to several-metre thick continuous blanket which, if emplaced on the ablation zone, will

be transported supraglacially towards the terminus without substantial thickness changes. Such rock avalanche blankets usually replicate surface topography (McSaveney, 1975). If the glacier surface is heavily crevassed, some of the deposit may be incorporated into the en- and subglacial sediment. While there are certainly intermediate members on debris-covered glaciers, the two types described above represent the majority of debris covers. Most of the area of debris-covered glaciers is covered by the first type of debris (melt-out). Rock-avalanche debris occurs less commonly, but is much greater in volume and thickness where it does occur. It is crucial to differentiate normal supraglacial cover from supraglacial rock avalanche deposits because the latter will significantly modify the glacier morphology and behaviour.

Figure 2.10. The Franz Josef Glacier's complex supraglacial cover derived from exhumed sub- and englacial debris, rockfall (at the foreground) and supraglacial debris from the subglacial conduit outburst at Black Hall rock (black line of debris in the middle). Photo: Reznichenko N., November, 2010.

2.3.2.4. Glacier with high sediment fluxes

Glaciers vary from the end members such as uncovered or "clean" glaciers with limited supraglacial debris at one end of the spectrum, to debris-covered glaciers at the other. Although rock glaciers represent different processes, some researchers identify them as a maximum possible end member for debris-covered valley glaciers (Ackert, 1998). The type of glacier may be defined by the role supraglacial sources play in the sediment budget; however, other characteristics such as flow velocities and fluvial water availability are also important in the determining the specifics of each glacial system (Fig. 2.11). In general, it is possible to identify the main controls leading to the development of each glacier type and the associated valley landforms (Benn et al., 2003). Firstly, the tectonics and erosional history of the valley will determine the mode of debris supply to the supraglacial environment. Ice and snow availability controls the redistribution of the delivered sediment its transport and finally its deposition. Subsequently, glaciofluvial processes transport the sediment from the glacier through the proglacial environment resulting in a significant modification of sediment distribution patterns in the valley. Glaciers with high flow velocities or insufficient supraglacial sediment usually have debris-free surfaces with some supraglacial cover, and respond rapidly and significantly differently to climatic fluctuations compared with debris-covered glaciers.

In tectonically-active areas where uplift and a high rate of slope failure lead to the delivery of large volumes of debris, and if the ice flow velocity of the glacier is not fast enough to transport the sediment away, the distal ablation zone will become covered by debris (e.g. Himalaya, Alaska, Andes, Southern Alps and some valleys of the European Alps). Debris-covered glacier snouts are usually very rough: the debris deposit several cm thick forms a mosaic with thin layers of debris, clear patches of the ice and exposed ice cliffs. Differential melting amplifies the topographic unevenness of the snout of the glacier and makes estimation of total melt rates under debris cover extremely difficult.

Debris-covered glaciers usually have very low ice-flow velocities in the ablation zone. The reduced ablation caused by the accumulation of debris in the ablation area results in "over-lengthening" (Kirkbride, 1995, p. 291) of the covered portion of the glacier. In order to achieve an equilibrium state the length of ablation area remains unchanged with AAR in the order of 0.2 - 0.5 (Kirkbride, 1989). The gradient of the debris-cover thickness increases towards the terminus; however, random rockfalls or rock avalanches onto glaciers may lead to variable debris distributions and thickness patterns (e.g. the 1991 Aoraki/Mt. Cook rock avalanche deposit on the Tasman Glacier, New Zealand). It has been noted that debris

mantles on glaciers have expanded as the glaciers have shrunk due to warming since the Little Ice Age (Kirkbride, 1993; Jansson and Fredin, 2002; Benn et al., 2003). A glacier terminus will often remain stable until prolonged downwasting causes proglacial lake formation leading to rapid retreat as a result of calving. Additionally, large terminal and lateral moraines may act as barriers to glacier advance, causing a glacier to react to mass balance disturbances first by thickening or by thinning rather than through fluctuations of the terminus position (Benn et al., 2003). Thus, large glaciers with extensive supraglacial debris cover, a wide valley and shallow slope have longer time lags (~100 years) in responding to climatic variations when compared to steep clean glaciers with high turnover that occupy neighbouring valleys (e.g. Tasman Glacier in contrast with Fox and Franz Josef Glaciers in New Zealand). Differential ablation caused by supraglacial cover leads to collapse and coalescence of englacial conduits, forming 'glacier karst', followed by lake formation (Kirkbride, 2000; Kirkbride and Warren, 1999; Quincey and Glasser, 2009).

The extensive sediment cover on glaciers with high sediment flux causes delayed response to fluctuating climatic conditions. In the Himalaya the longer-duration response to climate changes of some glaciers are controlled by the extensive sediment supply in the catchment of these glaciers (Scherler et al., 2011). In European Alps the Miage Glacier, Mt. Blanc, is heavily debris-covered and has responded much more slowly to 20th century warming than its less debris-covered neighbours (Deline, 2009). This fact has initiated the development of a number of hypotheses which attempt to account for the differential timing of the last Holocene advances of Himalayan covered glaciers when compared to those in Europe (Kick, 1989).

It is crucially important to differentiate between the slower responses of these debris-covered glaciers to climate changes from the short-lived alterations in glacier regime caused by individual large rock avalanches, which are independent of climate.

2.3.4. Debris deposition

Glaciers rework all available debris and deposit it in the valley. The landforms associated with glacial activity reflect the valley lithology, sediment delivery, intensity of glaciofluvial processes and the concurrent regime of the glaciers.

Clean and debris-covered glaciers differ in principle with respect to sediment deposition at their margins (Benn et al., 2003). Clean glaciers construct small (<10 m) moraines as a result of seasonal pushing, dumping of small volumes of supraglacial sediments and the squeezing of finer material available at the front of the terminus (Winkler and Nesje, 1999).

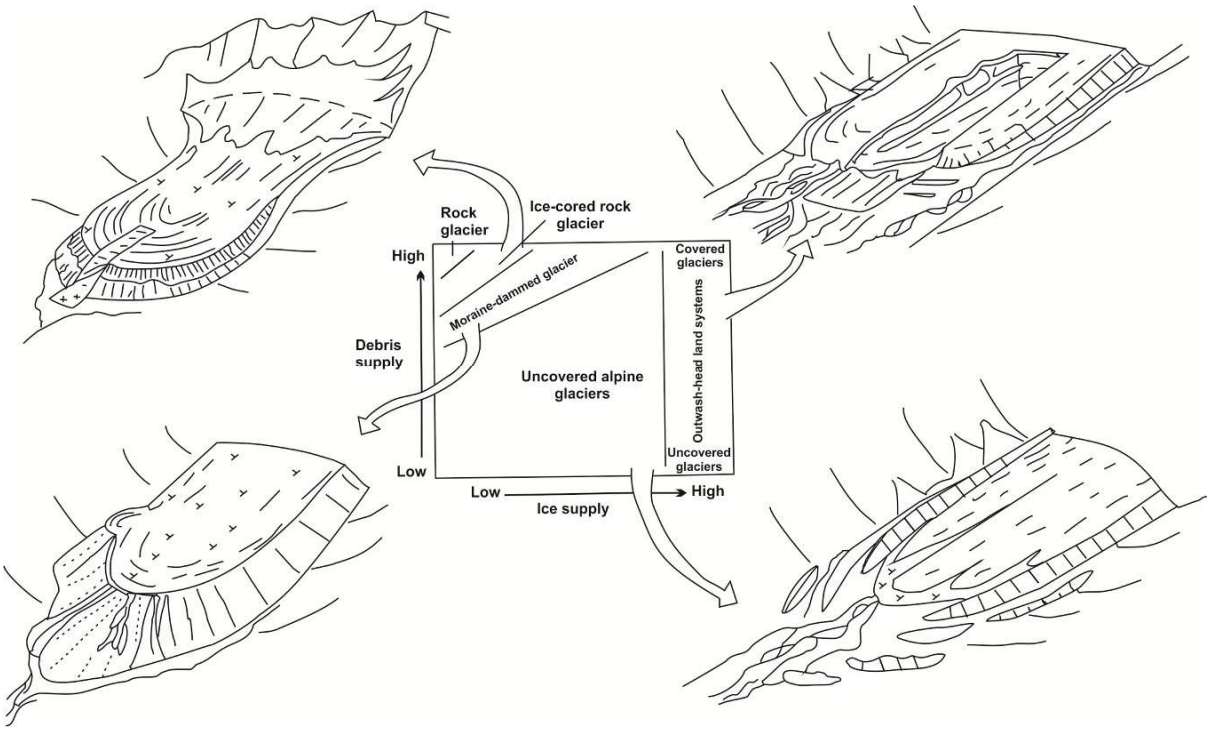

Figure 2.11. Proposed conceptual development of glacial valley landsystems due to the differential rates of debris and ice supplies. Modified from Benn et al. (2003).

Recent terminal moraines produced during the 1990s at the snouts of clean glaciers on the central plateau of Jostedalsbreen, Norway, have ridges resulting from annual frontal advances and periods of stationary fronts (Chinn et al., 2005). Existing terminal moraines are mostly the result of bulldozing of the sediment pile at the front of the terminus, with some occasional supraglacial contribution and from freezing-on and subsequent melting-out of slabs of subglacial sediment (Winkler and Matthews, 2010) (Fig. 2.12).

In contrast, an abundance of supraglacial sediment and relatively low ability of the proglacial sediment system to rework all material will lead to the formation of larger terminal moraines. These moraines (>100 m high) reflect the long still-stand positions of the glaciers and their slow responses to climatic fluctuations (Benn and Evans, 2010). However, for debris-covered glaciers with a very high glacial-fluvial activity deposition in the ice-contact zones will be dominated by quasi-fluvial processes (Shulmeister et al., 2010b). Thus, the large volumes of subglacial runoff and meltwater in these glaciers redistribute sediment away from the glacier

terminus and as a result, have a significant impact on the valley morphology (Swift et al., 2002). In the Southern Alps, newly accumulating or previously-deposited terminal moraines are reworked and modified (or buried) by dominant glaciofluvial processes to form extensive outwash plains. Thus lateral moraines in these systems are often considerably larger than terminal ones (Fig. 2.13). In these systems the outwash heads are the dominant landform, with ice-contact fans deposited at a stationary terminus, while meltwater channels and push moraines may be preserved during retreat accompanied by outwash head incision. Because of intense fluvial reworking, both ice-contact fans and push moraines are eventually reworked into the outwash head. Similarly the supraglacial material present on the majority of these glaciers is preserved only as a small dump component in the final moraines. The terminal moraines of some glaciers, such as the Lyell and Tasman Glaciers, did not develop until the onset of rapid thinning (Speight, 1940; Kirkbride, 2000). Kirkbride (1989) concluded that glacial advance/retreat deposits are often preserved as a result of being protected from glaciofluvial erosion.

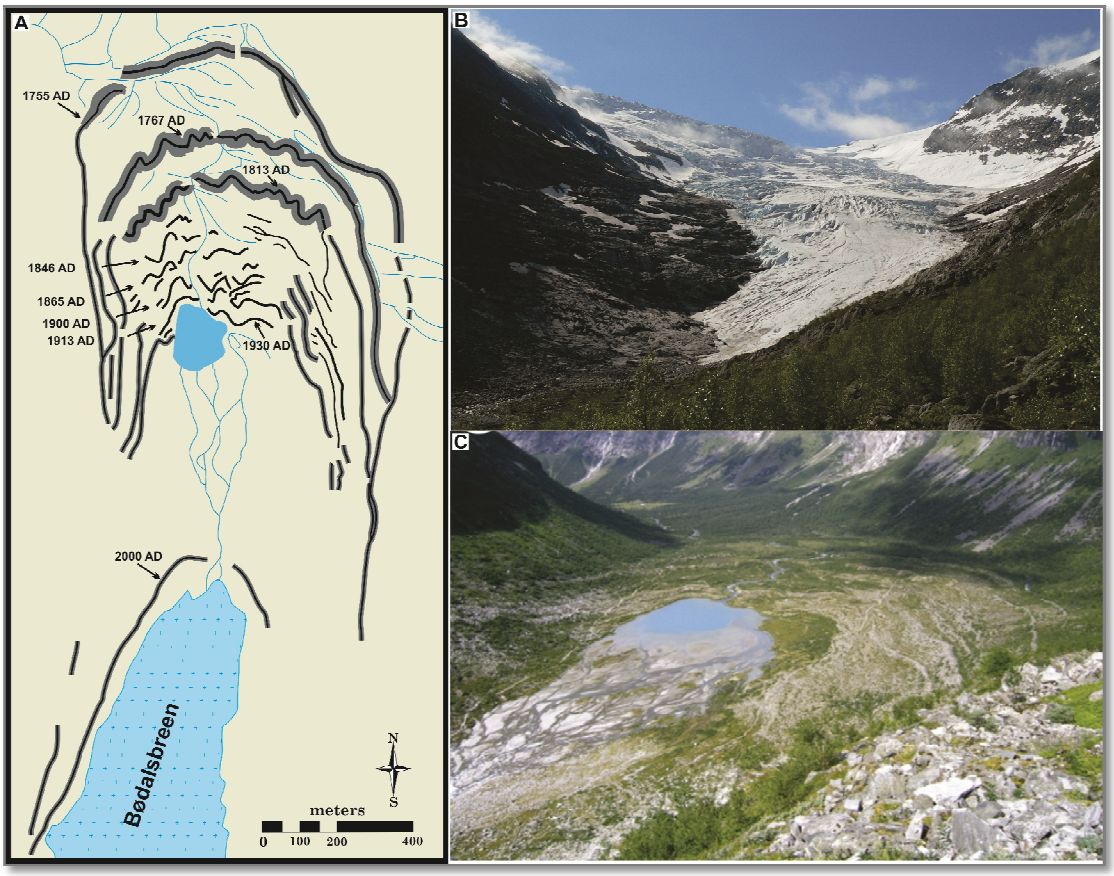

Figure 2.12. A. Schematic of the Bødalsbreen Glacier moraines ridges since LIA; ages obtained by lichenometry, modified from Burki et al. (2009a). B. The supraglacial-debris-free Bødalsbreen Glacier, looking south. Photo: N. Reznichenko, June, 2010. C. Overview of the "saw-toothed" moraines ridges and Lake Sætrevatnet at the Bødalsbreen Glacier proglacial area. Photo from Burki et al. (2009a).

Additionally, heavy rainfall events or the collapse of subglacial conduits (Davies et al., 2003; Goodsell et al., 2005) may change proglacial valley geometry significantly, with total reworking and/or removal of small moraines. This is certainly the case for small moraines recently deposited in front of the Franz Josef Glacier, which were interpreted as a result of passive melt-out and dumping from ice (Carrivick and Rushmer, 2009). Consequently, glaciofluvial activity in the proglacial valley significantly reworks the glacially-delivered sediment, and individual events can result in rapid redistribution of the sediment.

Figure 2.13. The rapidly calving debris-covered terminus of the Tasman Glacier. The intense outwash reworked all available sediment at the terminus, where a small dump moraine formed only recently after the proglacial lake formation. At the true right is preserved the large LIA moraine with Blue Lakes and a prominent lateral moraine. Photo: J. Thomson, GNS Science photo library, August, 2010.

Figure 2.14. The concise proglacial valley of the Fox Glacier, the Southern Alps, New Zealand, with intense glacifluvial reworking by Fox River, which destroying deposited terminal moraines. Photo: Reznichenko N., February, 2011.

2.4. SUPRAGLACIAL ROCK AVALANCHES

Rock avalanches occur commonly in glaciated valleys, and their associated deposits have a significant effect on the morphology of these valleys. Although rock avalanches have always been a feature of glacial landscapes in mountainous areas, it is only recently that researchers have recognized and described the effects of rock avalanches on glaciers (Hewitt et al., 2008). This review will focus on the emplacement of rock avalanches, and the effect this has on glaciers and the glacial sediment budget.

2.4.1. Background

Recognition of the influence of rock avalanches on glaciers first appeared in some of the earliest glaciological observations made in the European Alps, and was based on more general observations of material transport by glacier flow. One of the earliest expressions of the hypothesis, that large rock avalanches could affect glacier mass balance, was proposed by de Saussure (1786) (cited in Deline and Kirkbride, 2009), who suggested that rock avalanche debris cover caused the Triolet Glacier in the European Alps to advance as a result of reduced

ice ablation beneath the debris-cover. After more than a century it has been confirmed that the main and older morainic complexes of the Triolet Glacier were deposited in response to rock avalanches in AD 1000 and AD 1717 (Deline, 2009). Later, Agassiz adopted this idea when he described similar effects of reduced ablation under medial moraines on glaciers (Agassiz, 1840).

In first half of the 20th century several large earthquakes that resulted in rock avalanche deposits on glaciers reignited the debate on how glacial mass balance might be impacted by such deposits. As a result of field work in Alaska at the end of the 19th century, Tarr and Martin (1912, 1914) described the potential of rock avalanche deposits to have significant impacts on glacier mass balance. They proposed the "Earthquake advance theory", based on studies of the 1899 Yakutat Bay earthquake, as a result of which many landslides fell onto the glaciers in the area. The theory suggested that increases in the glacier mass resulting from additional snow, ice and rock materials associated with the earthquake-induced landslides, would lead to the advance of the affected glaciers in the years following the event. About fifteen glaciers advanced in the next ten years and then returned to their pre-earthquake conditions. Tarr and Martin (1914) pointed out that the size of the glacier affected the lag of the response, an observation confirmed by the fact that the Nunatak Glacier (the largest glacier in the study area at over 30 km long) was the last to advance 11 year after the event. Over a period of several decades this hypothesis found general acceptance amongst North America researchers (Field, 1968) until 1964, when detailed studies of glacial surges in the years following the 1964 Alaskan earthquake led to questions related to this idea. Post (1967) argued that Tarr and Martin's advances could have been surges initiated when an abrupt kinematic wave of ice in the upper glacier moved very rapidly down valley, supported by evidence of previous similar surges on these glaciers. The surging of the glaciers independently of seismic activity implies that there was no direct correlation between earthquakes and these events. However, more recent research provides evidence that the extra supraglacial debris mass resulting from earthquakes can also trigger glacier surges. A premature glacier surge may be the result of abrupt mass balance fluctuations caused by the additional loading of mass from the supraglacial debris cover, and from protected ice on the glacier which, in combination with the resultant modified glacial drainage system, may lead to an advance of the affected glacier (for example, the Bualtar Glacier surge after 1986 rock avalanche emplacement, Hewitt, 2009; and the McGinnis Glacier surge in 2006 after two rock avalanches in 2002, Truffer, unpublished data, 2006; cited in Shugar et al., 2011).

One of the best-observed and studied events, which has refocused attention on the impact of rock avalanches on glacier mass balance, was the 1964 Alaska earthquake (Tuthill, 1966; Post, 1967, 1968; Field, 1968; Johnson and Ragle, 1968; Reid, 1969). Alaskan glaciers are the largest valley glaciers in the world (Voight and Pariseau, 1978) and are also concentrated in one of the most seismically active regions. Field (1968) reported that in the previous 65 years in South-central Alaska, twenty-four major earthquakes of M > 7.0 occurred within 160 km of glaciated areas. The strongest (M = 8.5) earthquake in the 1964 sequence triggered 79 supraglacial rock avalanches (Post, 1968; McSaveney, 1978), including the well-documented Sherman Glacier rock avalanche (Shreve, 1966, 1968; Marangunic and Bull, 1968; Plafker, 1968; Tuthill et al., 1968; McSaveney, 1975, 1978). Fortunately, photographs of the affected glaciers prior to the earthquake were available, providing invaluable base-line data for an assessment of the effects of rock avalanches on the glaciers' behaviour. In a detailed study of the effects of the rock avalanche on the Sherman Glacier, McSaveney (1975) assessed the long-term response of the glacier to emplacement of a thick debris cover on its surface (Fig. 2.15). As a result of multiple observations of large rock avalanches on glaciers, Tuthill (1966) concluded that earthquake-triggered snow and rock avalanches are an important and effective mode of delivery of supraglacial debris and could cause non-climatic glacier responses.

Similar to the 1964 event, the M = 7.9 Denali earthquake (November, 2002) triggered thousands of rock avalanches, of which the largest (several km^3) were emplaced onto the Black Rapids, McGinnis and West Fork Glaciers of south-central Alaska and the Alaska Range (Jibson et al., 2006) (Fig. 2.16). However, investigations of the effect of these deposits on glacial morphology and dynamics have been only partially completed to date (Shugar, 2011).

These examples, together with observations of single rock avalanches on glaciers (e.g. the Brenva and other glaciers in the European Alps, the Netland Glacier in Alaska, the Bualtar Glacier in Karakoram, Himalaya), support the concept that catastrophic slope failures can alter glacier net mass balance without climatic changes. The frequent occurrence of rock avalanches during recorded history indicates a high possibility of similar effects on glacier behaviour and landscape development. Thus prehistoric moraines, which are conventionally considered as due solely to climate change, may now also be attributed either to advance, surge or as simply deposits from rock avalanches. This suggests a potentially significant change in the geomorphic interpretation of glacial deposits and their paleoclimatic implications.

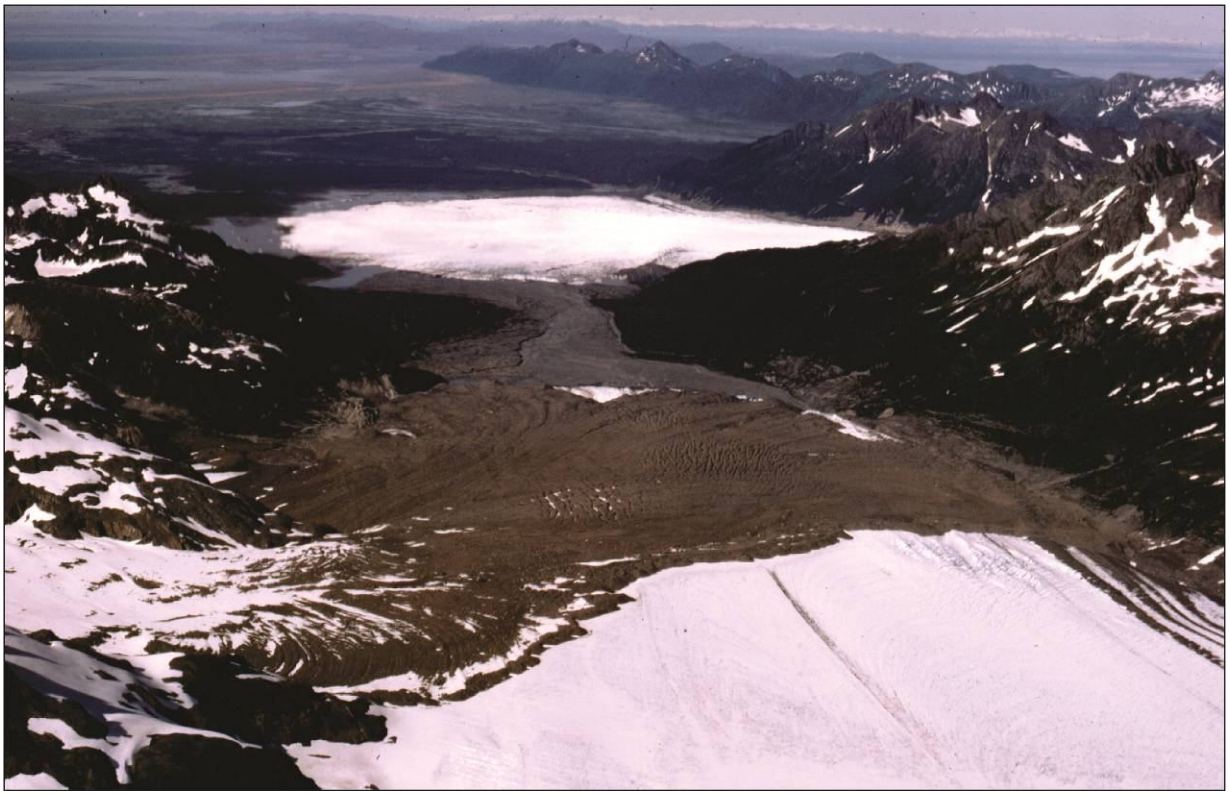

Figure 2.15. Downvalley view of the rock avalanche triggered by the 1964 M = 8.5 Alaska earthquake on the Sherman Glacier. In the background is the debris-free ice of the Sheridan Glacier. Photo by McSaveney, 1967.

2.4.2. Global occurrence and investigation

The emplacement of rock avalanches onto glaciers commonly occurs in orogens that are characterised by some of the highest known rates of tectonic uplift and denudation. Included are the Karakoram Himalaya of Asia (Hewitt, 1998; 2009), the high mountains along the coast of north-western North America (e.g. Post, 1968; Evans and Clague, 1994; Pelto, 2000; Jibson, et al., 2004; 2006), South America (Plafker et al., 1971; Petrakov et al., 2008), the European Alps (Noetzli et al., 2003; Deline, 2009) the Southern Alps of New Zealand (Whitehouse and Griffiths, 1983; McSaveney, 2002; Fort et al., 2009) and Iceland (Sigurðsson and Williams, 1991; Decaulne et al., 2010), or occasionally Greenland (Hewitt, 2009) and Norway (Owen et al., 2010). The infrequency of observations and published results of studies of similar events in many areas of the South American Cordilleras or the Caucasus and Asian mountain chains is probably a reflection of a lack of monitoring and research caused by the difficult access, low population density and economic and/or political instability in those countries.

Figure 2.16. Large rock avalanches on Black Rapids Glacier, triggered by the M 7.9 Denali, Alaska, earthquake of 3 November 2002. Photo reproduced from Department of Natural Resources, DGGS, 2002.

It is notable that the occurrence of rock avalanches on glaciers (Fig. 2.17) replicates the global distribution of debris-covered glaciers (Kirkbride, 1989). This is logical due to the large availability of debris in high relief areas that are usually formed at convergent plate boundaries, with well-developed systems of active faults. Clark et al. (1994) described the phenomena of the presence of continuous debris cover near glacial termini as a result of slow ice flow and high ablation rates. In these areas rock avalanches are source of a significant amount of debris being deposited onto the surface of the glacier. Such deposits arrive in a very short time rather than over long periods as a result of a prolonged ablation/ice flow/debris supply interaction.

The climate change debate has led to a significant discussion in the scientific literature about the relationship between ongoing deglaciation and rock-avalanche frequency in glaciated areas. The possible interactions of changing glacial and permafrost conditions with the frequency of slope failures have recently been studied (e.g. Evans and Clague, 1988; Harris, 2005; Deline, 2009; Fort et al., 2009; Allen et al., 2011). In New Zealand it has been estimated that late-Pleistocene- to Holocene-aged landslides covered 2% (414 km^2) of the area of the Southern Alps (Allen et al., 2011). Whitehouse and Griffiths (1983) studied 42 prehistoric rock-avalanche deposits and estimated the frequency of large ($\geq 10^6$ m^3) rock avalanches in the Southern Alps of New Zealand to be at the rate of one per century with larger (10^9 m^3) events occurring at a millennial timescale and being initiated by large earthquakes. However, McSaveney (2002) concluded that uplift and high erosion in Southern

Alps is balanced by frequent slope collapses of magnitudes > 10^6 that occur (based on historical records) every 20-30 year, taking into account rock avalanche deposits which were reworked by glaciers. By analogy, the long-term preservation of the 79 supraglacial rock avalanches from the 1964 Alaska earthquake is highly unlikely.

In order to estimate recent climate influences, Allen et al. (2011) analysed rock avalanche and other types of failures initiated during the past 100 years in the Southern Alps. Their results show that post-1949 there has been a higher proportion of smaller events (in the range of 0.02 to 0.25 km^2) than before 1949 interspersed with occasional larger avalanches. This confirms the fact that the larger events have a higher probability of preservation, whereas small avalanches occurring in prehistoric times are more likely to have been reworked. Since 1717 AD, there have been no large earthquakes on the Alpine Fault; but palaeoseismicity indicates that the frequency of the earthquakes with magnitudes higher than M = 8 on the Alpine Fault appears to be about once every 260-300 years (Bull, 1996; Rhoades and Van Dissen, 2002). Therefore, the probability of seismically-initiated large rock avalanches descending onto glaciers in the Southern Alps is high. It is notable that since 1991 there have been six rock avalanches of ~ 10^7 m^3 in the Southern Alps, none which was triggered by earthquake (M.McSaveney, *pers. comm.*).

The question of what triggers rock avalanches in mountainous terrains, and the relationship of such events to glacial recessions (e.g. Owen et al., 2003; Allen et al., 2011; McColl et al., 2010), leads to further discussion about the primary debris supply to glacial systems and the contribution rock avalanches may make to moraine formation (e.g. Porter, 2000; Larsen et al., 2005; Shulmeister et al., 2009). For example, Hewitt (1998; 1999) identified over 115 rock-avalanche deposits in the Karakoram Himalaya, the majority of which were interpreted as prehistoric (not including the rock avalanche deposits which were subsequently recycled by glacier activity). The presence of recent supraglacial rock avalanche deposits may appear to indicate an increased occurrence of these events; but almost certainly, equivalent events have occurred in the past at a frequency similar to that being experienced now. The majority of earlier rock avalanches travelling onto glaciers are now unrecognizable because they have been deposited in the valley and then reworked by other processes, or were recycled by glacial ice flow before deposition. However, some traces of older rock avalanches may still be preserved in old moraine sequences and, as a result, play a significant role in modern landscape geomorphology. Additionally, rock avalanche deposits that do survive glacial

modification often are misidentified as moraines (Heim, 1932; Porter and Orombelli, 1980; Hewitt, 1999; Blikra et al., 2006).

Figure 2.17. Global distribution of reported rock avalanches that travelled over glaciers (listed in Table 2.1).

2.4.3. Supraglacial rock avalanches: emplacement and transportation

In glaciated mountain ranges, large rock-avalanche deposits often fill valleys or spill onto glaciers in these valleys (e.g. Post, 1967; McSaveney, 1975, 2002; Gordon et al., 1978; Evans and Clague, 1988; Gardner and Hewitt, 1990; Jibson et al., 2006; Deline, 2009; Lipovsky et al., 2008; Hewitt, 2009; Shulmeister et al., 2009). The velocity of the supraglacial rock avalanche and the thickness of the resultant deposit are the result of interaction between the avalanche, and the glacier and after deposition the blanket of debris affects the glacial regime (Fig. 2.18).

At the same time, the glacier modifies the rock avalanche deposit by moving the debris to its margins where it may be deposited as moraines. In this section I summarize the main characteristics of the rock avalanches that have travelled over glaciers and identify their post-deposition interactions with glaciers.

Table 2.1. Major reported historic rock avalanches that travelled over glaciers grouped by the main mountain ranges where they occurred.

Mountains	Event	Rock Avalanche date	Source
European Alps:			
Italy	Brenva Glacier	1920, 1997	Porter and Orombeli (1981), Barla et al. (2000)
	Triolet Glacier	< 1000 BP, 1717	Deline (2009), Orombeli and Porter (1988)
	Miage Glacier	1945, 1991, 1988	Noetzli et al. (2003)
	Perazzi Glacier	1936	Bottino et al. (2002)
	Grandes Jorasses	2002, 2007	Deline (2009)
	Frébouge	1000-1150 AD, 1530 BP	Deline (2009)
	Becca de Luseney	1952	Noetzli et al. (2003)
	Monte Rosa	2001	Noetzli et al. (2003)
	Tronchey	2006	Deline (2009)
	Grapillon	2003	Deline (2009)
	Androsace	2002	Deline (2009)
Swizerland	Grosser Aletsh	1937	Alean (1984)
	Rossbode Glacier	1901	Noetzli et al. (2003)
	Tschierva	1988	Noetzli et al. (2003)
	Piz Serscen	1988	Noetzli et al. (2003)
	Gruben	2002	Noetzli et al. (2003)
France	Drus Glacier	2005	Deline (2009)
Iceland:	Morsárjökull Glacier	2007	Decaulne et al. (2010)
	Myrdalsjokull Glacier	1976	Sigurðsson and Williams (1991)
	Steinsholtsjokull Glacier	1967	Sigurðsson and Williams (1991)
Greenland:	Holsteinsborg	1600-1700 AD	Kelly (1980) in Hewitt (2009)
Caucasus:	Urukh	1959	Hewitt (2009)
Karakoram, Hymalaya:	Bualtar Glacier	1890s, 1986	Hewitt (2009)
	Barpu Glacier	2 prehistoric	Hewitt (2009)
	Chillinii Glacier	1991	Hewitt (2002)
	Aling Glacier	1992	Hewitt (2009)
	Marsherbrum Glacier	Late 1980s	Hewitt (2009)
	Pasu Glacier		Hewitt (2009)
	Ghulkin Glacier		Hewitt (2009)
	Charakusa Glacier	Prehistoric	Hewitt (2009)
	Panmah Glacier		Hewitt (2009)
	Kuto Glacier		Hewitt (2009)
	Ultar Glacier		Hewitt (2009)
	Baltura Glacier		Hewitt (2009)
	North Te-Rong Glacier		Hewitt (2009)
	Pasu & Ghulkin Glacier		Hewitt (2009)
	Chhateboi Glacier etc.	Prehistoric	Hewitt (2009)
North American Cordilleras:			
USA	Emmons Glacier	1963	Eisbacher and Clague (1984), Crandell and Fahnestock (1965)
	Carbon Glacier	1916	Driedger (1986)
	Lyman Glacier	1930	Pelto (2000)
	Sherman Glacier	1964	Marangunic and Bull (1968), McSaveney (1975)
	Schwan Glacier	-	Post (1968)
	Martin River Glacier	-	Post (1968)
	Bering Glacier	-	Post (1968)
	Steller Glacier	-	Post (1968)
	Slide Glacier	-	Post (1968)
	Johnson Glacier	-	Post (1968)
	Allen Glacier	-	Post (1968)
	Saddlebag Glacier	-	Post (1968)
	Fickett Glacier	-	Post (1968)
	Scott Glacier	-	Post (1968)
	Serpentine Glacier etc.	-	Post (1968)
	McGinnis Peak Glacier	2002	Jibson et al. (2006)
	Black Rapids Glacier	2002	Jibson et al. (2006)
	West Fork Glacier etc.	2002	Jibson et al. (2006)
Canada	Tim Williams Glacier	1956	Evans and Clague (1994)
	North Creek	1986	Evans et al. (1989), Evans and Clague (1994)
	Howson	1978, 1999	Evans et al. (1989), Evans and Clague (1994)
	Tweedsmuir Glacier	1979	Eisbacher and Clague (1984)
	Jarvis Glacier	-	Eisbacher and Clague (1984)
	Towagh Glacier	-	Eisbacher and Clague (1984)
	Frobisher Glacier	1990, 1991	Eisbacher and Clague (1984)
	Kshwan Glacier	1992, 1993	Eisbacher and Clague (1984)
	Kendall Glacier	1999	Eisbacher and Clague (1984)
	Melbern Glacier		Eisbacher and Clague (1984)
	Steel Glacier	2007	Lipovsky et al. (2008)
	Ice Valley Glacier	1997	Evans (2002)
	Fubar Glacier	1999	Evans (2002)
	Pandemonium Creek	1959	Evans et al. (1989), Petrakov et al. (2008)
South American Cordilleras:			
Peru	511 Glacier	30,000 BP, 1962, 1970	Plafker et al. (1971), Voight (1978), Vilímek et al. (2008)
Chile	Parraguirre	1987	Petrakov et al. (2008)
Argentina	SE Aconcagua		Hewitt (2009)
South Georgia, Antarctica:	Lyell Glacier	1975	Gordon et al. (1978)
Southern Alps, New Zealand:	Tasman Glacier	1873, 1991	McSaveney (2002)
	Maud Glacier	1991	McSaveney (2002)
	Mueller Glacier	1950s, 1996, 2002/4	McSaveney (2002), Cox et al. (2008)
	Merchison Glacier	1979	Whitehouse (1983)
	Hooker Glacier	2004, 2007	Cox at al. (2008)

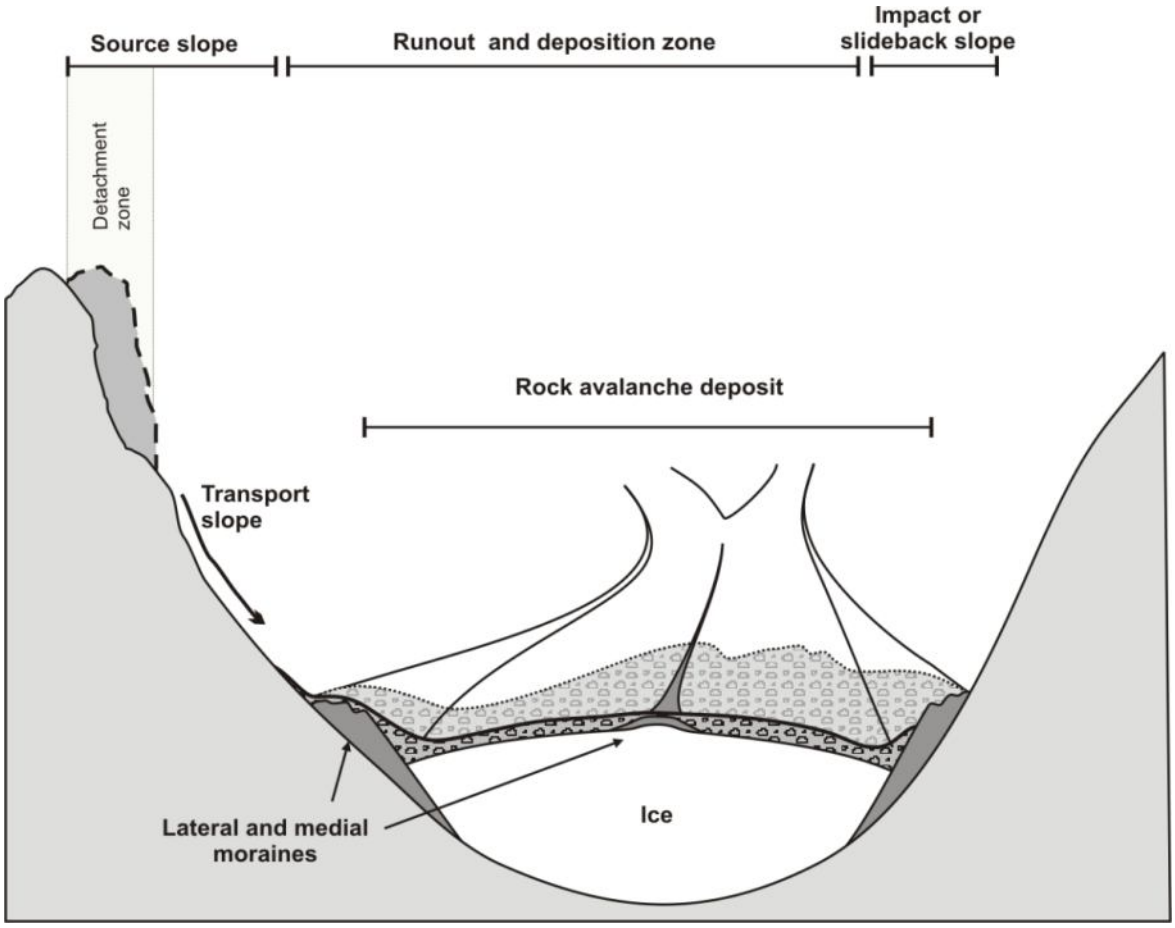

Figure 2.18. Schematic of a rock avalanche deposit emplaced onto the glacier surface. The thin and widely-spread debris blanket covers the main tongue of the glacier and overruns the lateral and median moraines. Usually the direction of the rock avalanche deposit is downvalley towards the glacier terminus, but not always as in the case of the 2007 Mt. Steele rock avalanche (Lipovsky et al., 2008).

2.4.3.1. Motion of rock avalanches over glaciers

One of the most important components of the emplacement of rock avalanche deposits into a glacial system is its supraglacial travel. The main features that characterise rock avalanches that have travelled over ice result from the basal friction of a rock mass moving over ice, rather than over a rock/soil substrate. Data from rock avalanches that have run over glaciers indicate several features that allow these to be distinguished from equivalent deposits found in non-ice environments.

Denudation and entrainment of snow and ice. As a rock avalanche crosses a snow field, it erodes snow/ice and incorporates it into the moving body of sediment. It is common in such cases that about 10% of the avalanche deposit volume is snow and ice. Often, this melts during the emplacement leading to the development of ponds on top of the deposit (Fig. 2.19). After a year or so the ice within the deposit will melt leaving crater-type topography on

the avalanche surface. Similar topography may also be as result of the development of karst-like features within the ice under the deposit.

Increased travel distance. The lower friction associated with rock avalanches that travel over snow and ice leads to an increase of mobility of up to 24 % (e.g. Gordon et al., 1978; Evans and Clague, 1988; Jibson et al., 2006). Once on the glacier, the avalanche head will melt or erode sufficient ice to eliminate relatively rough surfaces, allowing the moving body to decelerate more slowly. Other factors, such as pore pressures at the base of the debris from frictional melting, channelization and air-launching of debris by topographic irregularities such as moraines, have also been suggested as potential contributors to rock avalanche acceleration (Evans and Clague, 1994). During the emplacement of two rock avalanches after the Denali Earthquake, 2002, deposits were channelized by tributaries of the main glacier resulting in the formation of overlapping medial, lateral, and wave deposit features (Schulz et al., 2008). However, where a topographic barrier and rapid unconfined spreading of the debris combine, the travel distance may be relatively short in relation to deposit volume (e.g. the 2007 Mt. Steel rock avalanche, Lipovsky et al., 2008).

Thinner deposit. As a result of higher mobility and the fact that glacier surfaces are usually relatively flat, the debris from a rock avalanche is thinner than a corresponding deposit onto non-ice terrain. The thickness of the majority of reported non-supraglacial rock avalanche deposits varies between 10 m and 60+ m (Smith et al., 2006; Strom and Korup, 2006). On average the thickness of a supraglacial deposit that covers large area of a glacier is in the order of 1-10 m (McSaveney, 1978, 2002; Evans and Clague, 1994; Noetzli et al., 2003; Jibson et al., 2004; Geertsema et al., 2006). Often, supraglacial rock avalanche deposition is complicated by overlapping channel deposits, in such cases total deposit thicknesses in the order of tens of metres should be anticipated (Schulz et al., 2008). However, visual observations and interpolation of the deposit thickness from the lateral margins also probably results in an underestimate of total thickness (Reznichenko et al., 2011). Often the boulder carapace on the surface of a rock avalanche deposit prevents excavation to determine the deposit thickness.

Moraine overrun. The higher mobility of rock avalanches on ice allows the debris body to overrun or surround obstacles in its path. Because the main obstacles on the surface of a glacier are medial and lateral moraines with heights usually less than tens of metres, a rapidly moving rock avalanche will easily overrun such topographic highs. Schulz et al. (2008) give

an example of a 2 m thick deposit crossing a medial moraine; the deposit increased to 3 m thickness on the stoss side and reduced to 1-1.5 m thick on the lee side. McSaveney (1975) described the formation of transverse, compressional ridges on rock avalanche debris sheets as a result from buckling of the debris sheet as it came to rest, a concept supported by physical modelling (Dufresne and Davies, 2009). How rock avalanches modify moraines is not known, however from deposit topography it can be seen that the deposit often replicates underlying relief (Figs. 2.19 and 2.20). Additionally, due to its high mobility the deposit may also climb onto lateral moraines on the opposite slopes of the valley. Thus, during emplacement of the 1991 Aoraki/Mt. Cook rock-avalanche deposit, the Southern Alps of New Zealand, a portion of the avalanche climbed up to 300 metres onto the lateral moraine on the opposite slope (McSaveney, 2002).

Longitudinal features. Prominent ridges are commonly found on the surfaces of rock avalanche deposits. These are often oriented sub/parallel to the flow direction and aligned radially from the source as a result of debris spreading (Dufresne and Davies, 2009). The higher mobility of thin rock avalanches results in the "stretching" of ridges into flowbands which occur more commonly on glacier surfaces (e.g. McSaveney, 1975; Evans and Clague, 1998). It has also been noted that some ridges have large boulders at their starting points and large clasts at their distal ends (Evans and Clague, 1998; Dufresne and Davies, 2009; Shugar and Clague, 2011).

2.4.3.2. Transportation and modification of supraglacial rock avalanche deposits

Data on the emplacement of rock avalanches on glaciers are rare and inadequate, with only a few studies documenting the evolution of supraglacial rock avalanche deposits that have travelled supraglacially (McSaveney, 1975; Hewitt, 2009; Shugar, 2011). None of these studies, however, monitored the sediment until its final deposition by glacier ice.

Most studies of supraglacial rock avalanches have focussed on deposit travel patterns based on observations of ice flow, sediment fabric and surficial features (Marangunic and Bull, 1968; McSaveney, 1978; Dufresne and Davies, 2009; Hewitt, 2009; Shugar, 2011), which, however, do not provide information about the possible degradation and erosion of the sediment itself. The first detailed study was of rock avalanches on the Sherman Glacier, triggered by the 1964 Alaskan earthquake.

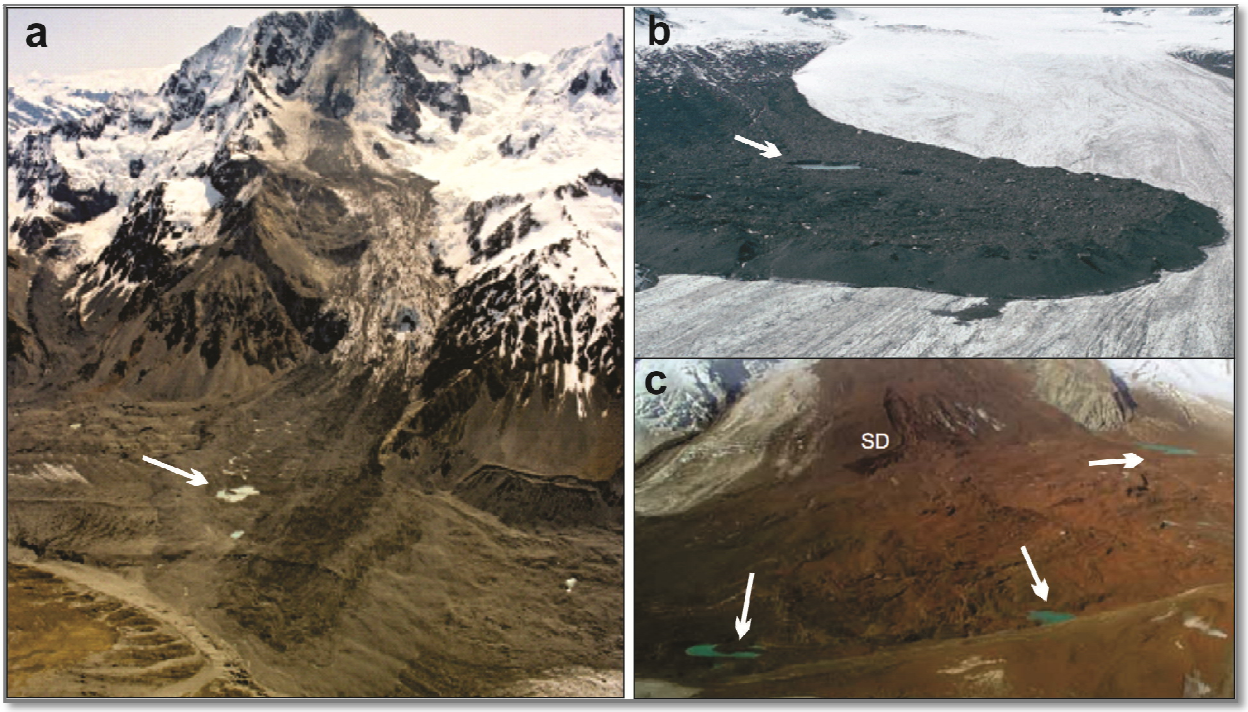

Figure 2.19. Ponds (indicated by arrows) formed from melting of incorporated snow and ice a) the fresh Aoraki/Mt. Cook rock avalanche, the Southern Alps, New Zealand. Photo: GNS, NZ; b) the rock avalanche on the Allen Glacier due to the 1964 Alaskan Earthquake. Photo: from U.S. Geological Survey; c) discontinuous debris of 2007 Mt. Steel rock avalanche, SD indicates secondary debris flow channel. Photo: from Lipovsky et al. (2008).

Figure 2.20. One of the rock avalanche deposits triggered after Denali 2002 earthquake overrun the medial moraine. Photo reproduced from Dept. of Natural Resources, DGGS, 2002.

The travel directions were reflected in the long axes of clasts (Marangunic and Bull, 1968), which paralleled the direction of glacier flow (also noted by Shugar, 2011). McSaveney (1978) suggested that longitudinal stretching of the deposit resulted in the clast orientation, caused as a result of the avalanche material travelling due to the ice-flow to the glacier margin and an associated ridge formation. Modification by ice flow will also contribute to the formation of transverse fissures and ridges, longitudinal flowbands, debris cones, and distal lobes or jigsaw blocks in the deposit. Twenty years after the emplacement of a rock avalanche onto the Bualtar Glacier, Himalaya, Hewitt (2009) concluded that the morphology of debris deposit had changed little. However, he noted the thinning of the rock avalanche debris sheet with time since emplacement. Nevertheless, the degree of thinning and how it was determined remains unclear. In a detailed study of three rock avalanches on the Black Rapids Glacier, Shugar (2011) described surface deposit characteristics, using terminology such as "jigsaw" brecciated blocks, clusters of large blocks and longitudinal flowbands. Shugar (2011) found that travel distance is determined by block size with larger blocks concentrated on the periphery (a pattern that might reflect less fracturing during deposition rather than a response to transport direction) and with time, elongate clasts usually tending to be re-oriented into a direction that parallels ice flow.

In these studies, removal of the fines from the supraglacial rock avalanche deposits has been suggested. Shugar (2011) determined that the finer fraction of the the Black Rapids and Sherman Glacier rock avalanche deposits had been removed and that they were significantly reworked. He also noted that the percentage of fines in the Sherman Glacier rock avalanche deposits increased, and the clasts in general were coarser, with distance from the source. However, it is important to highlight that laser particle size analysis indicates Shugar's fine fraction is 0.5 microns. By contrast, McSaveney (1975) indicated that the removal of fine (silt and clay-sized) material occurred only from the surface of the deposit on the Sherman Glacier, where degradation of the fines within the body of the deposit was not investigated. Hewitt (2009) also suggested that rock avalanche debris is modified by supraglacial processes that result in finer matrix material being selectively removed from the debris. However, the resultant finer material should either accumulate within or close to the bottom layer of the deposit simply because their transportation away by surface water is not feasible. Moreover, Hewitt (2009) gave little information to support his conclusions and provided no mechanism for the selective removal of those fines.

In conclusion, only a few studies present data that characterised sediment properties (McSaveney, 1975, 2002; Gordon et al., 1978; Hewitt, 2009; Shugar, 2011). None of these studies actively monitored changes in the sediment. The problem is compounded by the fact that studies of deposit emplacement and change through time are largely absent. In the Southern Alps of New Zealand, apart from one sampling of the Aoraki/Mt. Cook rock avalanche sediment the day after emplacement (McSaveney, 2002), no supraglacial rock avalanche deposit has ever been studied in detail. Therefore, the modification of rock avalanche sediment during supraglacial travel before final deposition, and whether rock avalanche sediment can be eroded during glacial transport, remain unclear.

2.4.4. The effect of rock avalanches on glaciers: alteration of mass balance

From observations of how a thick debris-cover insulates covered ice surface ablation it is evident that supraglacially-emplaced rock avalanches modify glacier mass balance primarily as a result of reduced ablation of sub-debris ice (Reznichenko et al., 2010). The reduced surface ablation under the rock avalanche deposit is analogous to the effect of the debris-cover, studies of which are more frequent simply because general deglaciation has increased the supraglacial cover. As a result, here the effects of debris-cover on ice-surface ablation will be extrapolated to thicker rock avalanche deposits.

2.4.4.1. Investigations of the impact of debris-cover on glacial ablation

The reduction of glacier ice melting rates under a thick debris cover was recognised in some of the earliest studies of glaciers by Agassiz (1840), who observed a reduction of ice melting under medial moraines and supraglacial clasts. In the 20th century, more detailed investigations of the effects of debris on surface ablation (Fig. 2.21) established that increasing debris thickness caused a corresponding decrease in the ablation rate (Mattson et al., 1993), which is usually calculated by heat conduction through the debris layer of known thickness and physical properties of the debris. The consensus was that a debris layer only 0.5 metre deep will result in about 75% reduction of melting. Sharp (1949) first identified the importance of sensible heat transfer through the debris to the ice below, and that moisture and air voids in the debris significantly influenced the efficiency of that transfer. Swithinbank (1950) concluded that heat transfer is not only dependent on the porosity and moisture content of the debris, but also on the thermal conductivity of the sediment. After a series of experiments examining supraglacial and ice-cored moraines at the Isfallsglaciaren and

Grasubreen, Sweden, Østrem (1965) concluded that a 40 cm thick layer of sand and gravel was sufficient to reduce ablation by up to 80% when compared with debris-free adjacent ice. But in ice-cored moraine, ice beneath 3.1 - 15 metres of debris cover lay in an area of permafrost that was not affected by summer thaw and was not melting at all.

Based on vertical temperature profiles which penetrated only half way through deposits associated with kame terraces in Alaska, McKenzie (1969) estimated that the conductive heat transfer continued down to the buried ice. He concluded that rainwater percolation, radiation and convection within gravel are important agents of heat transfer through the debris; however, he did not estimate the amount of heat transferred or the depth to which the transfer might take place. McSaveney (1975) argued that McKenzie could detect this effect during prolonged rainfalls, and that McKenzie greatly underestimated the role of the thermal conductivity and thermal gradient within the debris layer. As a result of studies of the effect of a rock avalanche on the surface ablation of the Sherman Glacier, McSaveney (1975) concluded that measuring the thermal gradient near the debris-ice interface was essential for the estimation of melting rates.

In more recent studies (Carrara, 1975; Driscoll, 1980; Kirkbride, 1989), measurements of thermal gradients through the debris have been used as an input to quantifying ice ablation under the debris. Nakawo and Young (1982) suggested that it should be possible to eliminate the need to measure the temperature gradient within the debris, based on the assumption that it has a linear function. However, based on the ablation calculations from the Djankuat Glacier, Caucasus, Bozhinskiy et al. (1986) concluded that the debris layer thermal gradient varied as a result of diurnal and seasonal fluctuations. They observed that diurnal fluctuations affected the upper 0.16 m, seasonal fluctuations the upper 1.5 m and annual fluctuations the upper 3.1 m, showing that melting will always occur if the debris-ice interface lies above the annual warm wave penetration. This indicates that the role of the debris cover as an influence on glacial behaviour is also dependent on the geographical location of the glacier.

The ability of debris to insulate or accelerate the underlying ice ablation has been studied on many glaciers around the world (e.g. Nakawo and Young, 1981; Kirkbride, 1989; Mattson and Gardner, 1989; Lundstrom et al., 1993; Mattson et al., 1993, Clark et al., 1994; Purdie and Fitzharris, 1999; Conway and Rasmussen, 2000; Mattson, 2000; Popovin and Rozova, 2002; Mihalcea et al., 2006; Yamaguchi et al., 2007; Hagg et al., 2008; Kellerer-Pirklbauer et al., 2008). Numerical modelling of ablation under a debris layer has also been carried out

(e.g. Nakawo and Young 1982; Bozhinskiy et al., 1986; Adhikary et al., 1997, 2000; Kayastha et al., 2000; Konovalov, 2000; Takeuchi et al., 2000; Haidong et al., 2006; Nicholson and Benn, 2006). Within the Soviet Union, one aspect of glaciological research was to investigate the effects of moraines and dust on ablation in glaciers, with the aim to control the runoff from glaciers used as a water source and for hazard assessment and mitigation. As a result of the availability of a large amount of data from research on Asian glaciers, researchers then attempted to calculate the relationship between debris thickness and underlying ice ablation in particular glaciers (Kamalov, 1967 (cited in Demchenko and Sokolov, 1982); Dolgushin et al., 1972; Khodakov, 1972; Demchenko and Sokolov, 1982).

All these studies showed that reducing ablation alters the mass balance of the glacier; in that it becomes more positive (or less negative), leading to a change of glacial regime.

2.4.4.2. The effect of reduced ablation under a rock avalanche deposit in contrast with other supraglacial debris

The influence of rock avalanche debris on glacier ablation is distinctly different from that of other supraglacial debris due to its different sedimentology and greater depth.

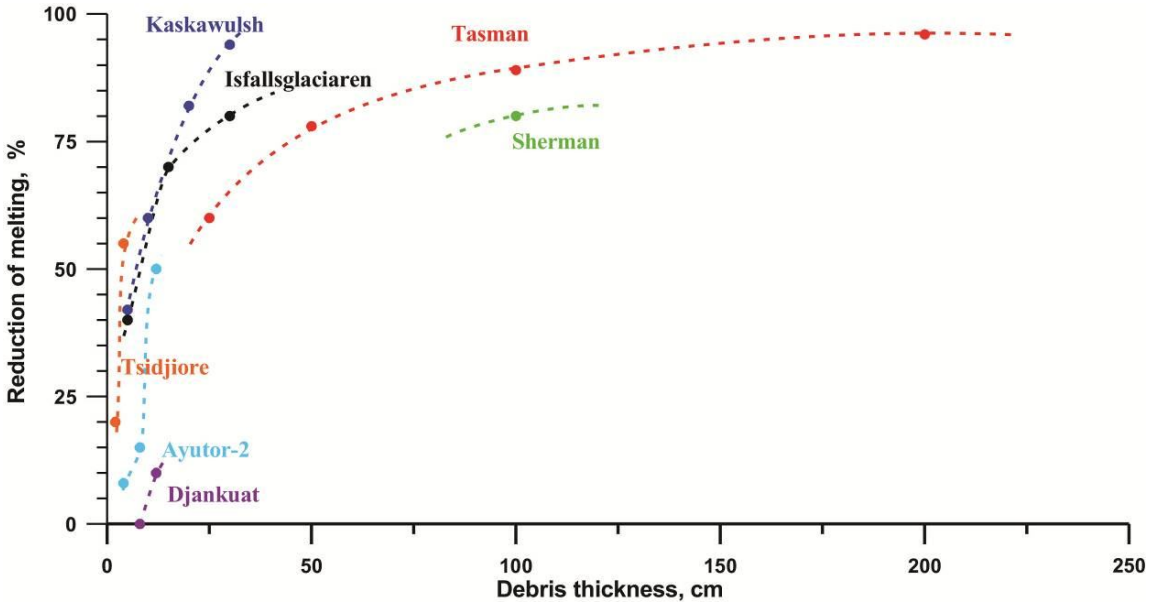

Figure 2.21. Estimates of the measured insulating effect of supraglacial debris cover. Isfallsglaciaren Glacier, Sweden (Østrem, 1959); Kaskawulsh Glacier, Yukon (Loomis, 1970 in Kirkbride and Dugmore, 2003); Ayutor-2 Glacier, Tien Shan (Glazyrin, 1975); Sherman Glacier, Alaska (McSaveney, 1975); Djankuat Glacier, Caucasus (Bozhinskiy et al., 1986); Glacier de Tsidgiore Neuve, Switzerland (Small, 1987); Tasman Glacier, New Zealand (Kirkbride, 1989). Modified from Kirkbride (1995).

Supraglacial rock-avalanche-deposited debris is distinguishable from other debris as a result of its genesis. During the fall and runout of a rock avalanche, much of the originally intact

rock travels long distances at high speed causing its rapid crushing and comminution. Rock avalanche deposits comprise a range of coarse material within a dominant matrix of finely-pulverized material (Dunning, 2004; McSaveney and Davies, 2007; Hewitt et al., 2008), characterized by angular clasts, minimum meter-scale thicknesses, absence of sorting and high bulk density. In contrast, melt-out debris is the result of the slow, gradual exhumation of englacial material of basal or rockfall origin that has been constantly reworked; it forms shallow deposits with small amounts of fine silt, low density and higher permeability.

The main difference between supraglacial and non-supraglacial rock avalanche deposits is the relative thinness of the former; nevertheless the deposit depth on ice is always of the order of metres. If the glacier surface is crevassed, part of the rock-avalanche deposit may enter the sub- and englacial transportation systems of the glacier (Hewitt, 2009). However, most of the debris remains supraglacial and will eventually be carried to the terminus by glacier flow (e.g. the Sherman Glacier, Alaska, Fig. 2.22). The quasi-continuous exhumation of melt-out debris-cover takes place over years or decades without adding mass to the system. It results in thinner deposits of the order of tens of cm up to a meter towards the terminus with patchy cover. Differential ablation and formation of supraglacial ponds (Röhl, 2008) often causes this cover to be extremely variable. In contrast with melt-out debris the rock-avalanche deposit instantaneously contributes an enormous mass of sediment to the glacier and covers part of an ablation zone with a layer thicker than a meter or two.

Another characteristic of supraglacial rock-avalanche deposits is the rapid development of vegetation. In places where there is not a thick carapace, sediment with high quantities of silt- and clay-sized particles favours growth of small bushes on relatively stable deposits. On the other hand, plants are unable to develop on supraglacial melt-out debris because it is too high in elevation or, because of insufficient and/or too mobile debris cover due to the differential ablation (Fickert et al., 2007). Although Veblen et al. (1989) describe forest growing on ice moving with velocities up to 22 m/year, any block of sediment with flora must be reasonably stable, travelling down-valley without disturbances at the surface. Mature forests are common on the debris-covered termini of glaciers in south-central Alaska (the Bering, Malaspina, Fairweather, Grand Plateau, Martin River Glaciers), some of which have records of supraglacial rock avalanches in the past (Post, 1968). Vegetation developed on the Carbon and other glaciers at Mount Rainier (Fickert et al., 2007), where several large rock avalanches are recorded (Driedger, 1986). In New Zealand, small shrubs are common on a fairly stable part of the 1991 Aoraki/Mt. Cook rock avalanche deposit on the Tasman Glacier (Fig. 2.23).

However, no vegetation is observed on the less stable part of this deposit emplaced onto the adjacent fast-moving Hochstetter ice-stream and on adjacent non-rock-avalanche debris-cover.

The ice surface ablation is reduced under a rock-avalanche deposit. This results in "ice thickening" under the rock-avalanche deposit from the reduced melting of the ice under the deposit in contrast with faster melting of the surrounding debris-free ice (Fig. 2.24). After a single melting season the avalanche deposit stands on an ice platform higher than the surrounding ice.

With increasing ice thickness under the deposit the growing side slopes suffer local collapses of sediment, and different slope orientations cause local ablation to vary. The sediment sliding on the growing slopes contributes to a widening of the area of ice covered by the deposit and increasing the buried surface area of the glacier. At the same time the deposit is constantly moving down the valley with the glacier ice flow, and may be distorted by the differential flow.

These large-scale features are commonly observed on glaciers with deposits of rock avalanches (e.g. Post, 1968; McSaveney, 1978; Jiskoot, 2011). In the second ablation season following its emplacement, the Sherman Glacier avalanche deposit stood on a platform more than 9 metres thick (Alaska; Post, 1968). A platform thicker than 30 metres formed under the rock avalanche deposit that occurred after 1951 on the Netland Glacier, Alaska, and at 1964 rested at its terminus position (Post, 1968) (Fig. 2.24 A). In New Zealand, 5 years after deposition of the Mt. Beatrice rock-avalanche on the Hooker Glacier an ice platform more than 30 metres thick had built up (Fig. 2.24 B), and at the Aoraki/Mt. Cook rock avalanche the platform was higher than 25 metres after 18 years. Recent investigation of the Morsàrjökull rock avalanche deposit on the Vatnajökull Glacier, South Iceland, shows that after a single year an average 5.5 metres thick deposit caused ice thickening of up to 22 metres, and in the third year it reached 29 metres (Fig. 2.24 C; Decaulne et al., 2010). The estimated glacier ablation is 8-10 m/year, which is in accordance with the non-ablated ice under the deposit after the two melting seasons in 2008 and 2009. Protected ice thickening under the deposit was about 7 metres per year - indicating almost complete cessation of ablation under the deposit.

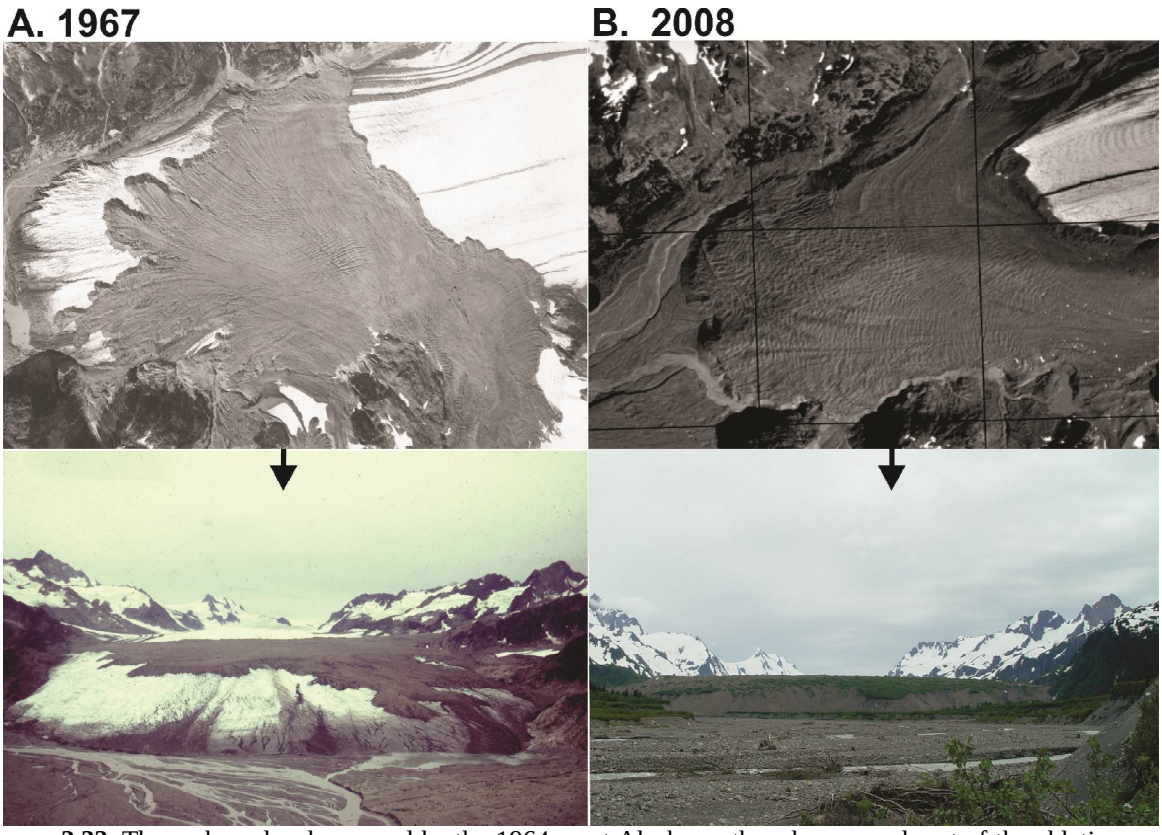

Figure 2.22. The rock avalanche caused by the 1964 great Alaska earthquake covered part of the ablation zone of the Sherman Glacier. A – the rock avalanche after its emplacement in 1967; B – the rock avalanche reached the terminus of the glacier in 2008. Photo: M. McSaveney.

Figure 2.23. Vegetation is growing on the stable part of the Aoraki/Mt. Cook rock avalanche deposit (left), whereas on the active part of the ridge zone, the rock avalanche deposit is too mobile for plant growth (right). Photos: N. Reznichenko, Feb, 2009.

If the avalanche deposit thickness exceeds 2-3 metres, the underlying ice-surface ablation reduces effectively to zero (Bozhinskiy et al., 1986). In this case the rate of relative thickening under the deposit equals the surface ablation rate of clear ice at that location. Because a rock avalanche deposit is by definition greater than about one million m^3 in

volume, it spreads a few metres thick deposit widely over the glacier and often causes almost total reduction of ablation beneath it. Thus, the area covered by this debris is large (~ km^2) and the reduction of surface ablation to zero over that area can have a significant effect on glacier mass balance.

2.4.4.3. The effect of supraglacial rock avalanche deposit on glacier mass balance

The protective effect of a thick covering of debris on the underlying ice, and the possibility that this might cause a non-climatic advance of debris-covered glaciers, was first described by Ogilvie (1904). As a result of his observations on the glaciers in the Canadian Rockies, British Columbia, he concluded: "It is to be expected that protected glaciers should advance farther down their valleys than if not so protected and that the retreat of protected glaciers would be slower" (Ogilvie, 1904, p.723).

Recently, several researchers have recognized the effect of thicker and larger rock avalanche deposits on the glacial regime. Thus, in recent literature, there has been a shift of emphasis towards documenting the contribution rock avalanches make to the debris-cover on glaciers and how that impacts on mass balance (e.g. Reid, 1969; McSaveney, 1975; Shulmeister et al., 2009; Decaulne et al., 2010; Vacco et al., 2010; Alexander et al., 2011; Shugar et al., 2011). Rock avalanches emplaced into the accumulation zone of a glacier are usually buried by the next season's accumulation of snow, subsequently being transported englacially down the valley and more deeply buried. If the deposit is eventually exhumed to the glacier surface, and depending on its volume, the meltout debris will blanket the ice surface, reducing or increasing ablation to a level determined by the layer thickness. When a rock avalanche deposit blankets a glacier surface in an ablation zone, by contrast, the associated alteration of mass balance and ice dynamics of the glacier are often evident within a year of emplacement. The degree of disturbance is determined by the location, size and run-out of the rock avalanche, and the area of the glacier mantled with rock avalanche deposit is critical (Hewitt, 2009; Shulmeister et al., 2009).

Shulmeister et al. (2009) proposed that if a rock avalanche deposit covers a large enough area of the ablation zone with debris of the order of metres thick, surface ice ablation will almost completely cease and, as a result, the dynamics of the covered glacier will be significantly affected. That the reduction of surface ablation under the rock-avalanche deposit may be 60-70% or more has already been documented (e.g. Reid, 1969; McSaveney, 1975; Alexander et

al., 2011) leading to the conclusion that if a significant area of the ablation zone is covered, the glacier net mass balance will be significantly altered. Vacco et al. (2010) modelled such an advance and although their deposit thickness estimates were exaggerated and model did not account for basal melting (Shulmeister et al., 2010a; Alexander et al., 2011), the calculations confirm that suppressed ablation will lead to glacier advance and further disintegration of the covered end of the glacier tongue when the clear part of the glacier reaches the pre-event terminus.

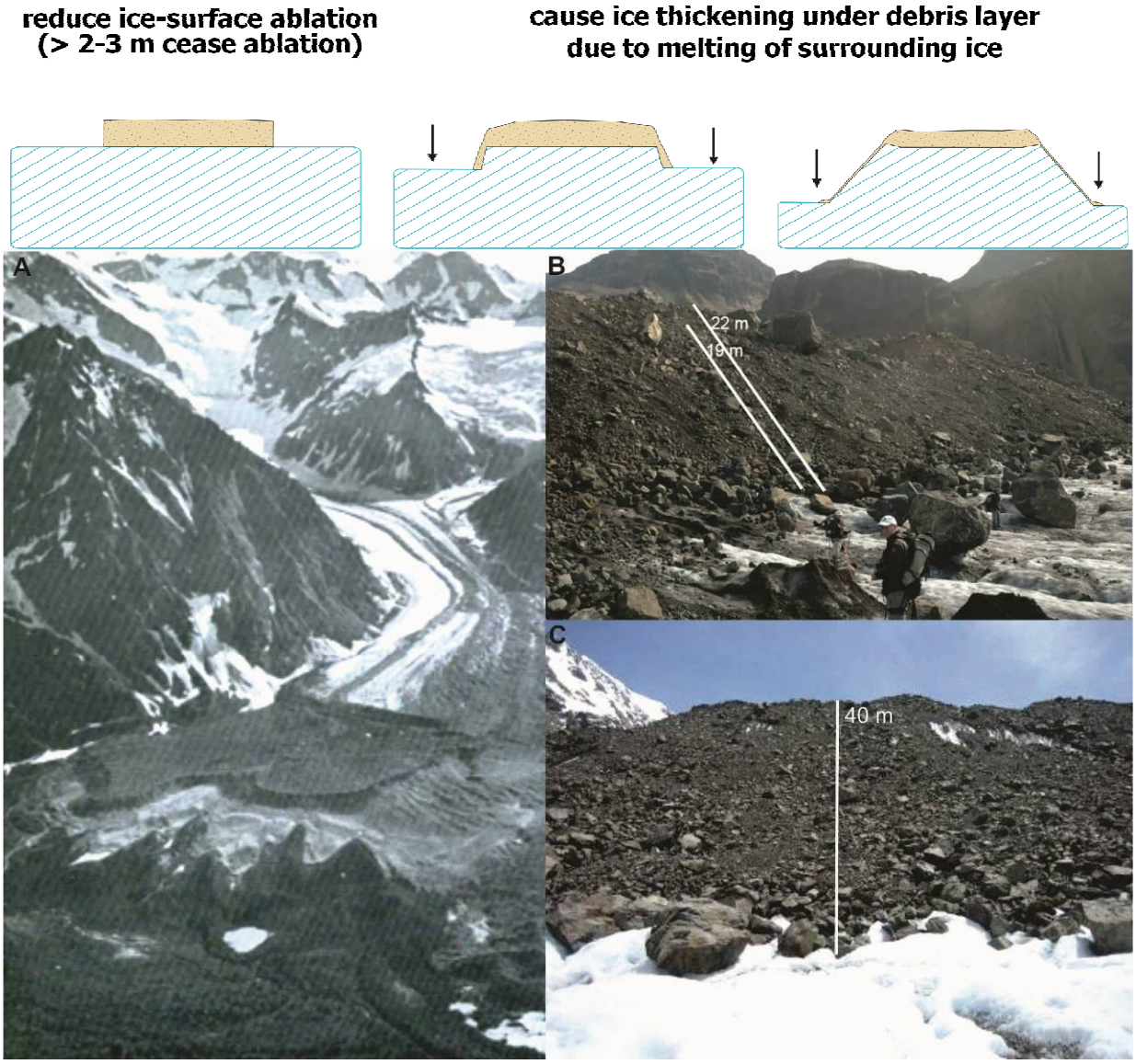

Figure 2.24. Ice platforms formed under supraglacial rock avalanches. Diagram showing ice thickening under the rock avalanche deposit in contrast with surrounding ice. A. Ice platform more than 30 metres under the rock avalanche deposit at the Netland Glacier, Alsek valley, Alaska. Photo: from Post (1968), August, 1964. B. Ice thickening under the Mt. Beatrice rock avalanche 5 years after deposition, the Hooker Glacier, NZ. Photo: Reznichenko N., December, 2009. C. Ice thickening under the Morsàrjökull rock avalanche 2 years after deposition, the Vatnajökull Glacier, South Iceland. Photo: from Decaulne et al. (2010).

Other studies have examined the effect of volcanic ash deposits on the mass balance of glaciers (Brugman and Meier, 1981; Driedger, 1981; Sturm et al., 1986; Kirkbride and Dugmore, 2003; Richardson and Brook, 2010), and all indicate that volcanic ash also suppresses surface ablation of the underlying ice. Depending on the magnitude and proximity of the eruption, volcanic tephra can cover clear or already debris-covered glacial ice with ash layers as thin as several cm (7,5 cm of ash, Mt. Ruapehu eruption, 1945, New Zealand; Krenek, 1958), and up to a several metres thick (5 m of sand and ash, Mt. Redoubt eruption, 1967, Drift Glacier, Alaska; Sturm et al., 1986). To estimate the insulation effect of the tephra, researchers usually based their calculations on the same physical parameters as those used for rock debris. Thus, measurements of tephra cover thickness and changes of terminus position showed that advances of some glaciers were a response to reduced ablation. For example, the Gigjokull Glacier, Iceland advanced 328 m in 7 years after a 1947 eruption (Kirkbride and Dugmore, 2003). Similarly, after the 1980 Mt. Helens eruption, the preserved Swift Glacier had an unusual positive mass balance (Brugman and Meier, 1981), as was also the case for the Knife Creek Glaciers on Katmai (Muller and Coulter, 1957). Consequently, the known pre-eruption mass balance and terminal position of affected glaciers when compared with the post-eruption fluctuations of those glaciers provides evidence of the impact of debris-cover on the mass balance of affected glaciers.

An understanding and integration of how rock avalanches effect glacial ablation and mass balance are necessary before we can reliably predict and assess glacier responses and depositional imprints of these often catastrophic events. Numerous documented examples, including the Triolet, Brenva, Bualtar and Sherman Glaciers, aid the continued investigation of the possible effect of rock avalanche deposits on glaciers.

Case studies

Glaciers in the European Alps are well studied and monitored. Deline (2009) described nineteen rock falls and rock avalanches 10^4-10^6 m^3 in volume that occurred between 2500 BP and 2007 AD, including short-runout rock avalanches on the Miage and Drus Glaciers, and the Tour des Grandes Jorasses, and long-runout events on the Brenva, Triolet, and Frébouge Glaciers.

The Triolet Glacier advanced after a 1717 rock avalanche as confirmed by geomorphological and sedimentological re-examination of the Haut Val Ferret deposit, Mont Blanc Massif, Italy (Porter and Orombelli, 1981; Deline and Kirkbride, 2009). The supraglacially-emplaced

deposit of 12 September 1717 covered the glacier surface and by preventing ablation over much of the glacier caused its advance over an older Little Ice Age moraine complex during the subsequent 10 years. This is shown in Fig. 2.25; that growth being followed by a slow retreat with disintegration of the stagnating debris-covered terminus, the remains of which persisted in the form of dead ice on the upstream valley floor until the 1980s. Until the 1930s some smaller advances occurred (Deline and Kirkbride, 2009). At the southeast part of the deposit an earlier rock avalanche deposit was found that was emplaced shortly before AD 1000 (Deline, 2009).

In November 1920 a rock avalanche fell from the base of the east face of the Grand Pilier d'Angle onto the Brenva Glacier and overtopped the large lateral moraines below. This glacier advanced 100 m in the first 2 years after the event, as were many other glaciers in the European Alps at that time. However, after 1925 most other glaciers ceased to advance, while the Brenva Glacier advance continued until 1941 totalling 500 m and ending close to its maximum extent of 1818 (Porter and Orombelli, 1980; Deline, 2009). After this advance the debris-covered tongue stagnated, and was reactivated by a climatic re-advance in 1970-1971. Although there is ongoing debate whether the advance resulted from increased precipitation or the rock avalanche deposit (Barla and Barla, 2001; Deline, 2011), Capello (1941) (cited in McSaveney, 1975) concluded that advance was independent of precipitation and caused by the deposit mass load and reduced surface ablation.

The rock avalanche deposited on the Sherman Glacier by the Alaska earthquake of 1964 (estimated average depth 1.5 m; McSaveney, 1975) covered about 30% of the ablation zone with an average thickness of 1.65 m and reduced underlying ice ablation by 80%. The areal net balance became less negative by about 35 Tg (1 Teragram = $1x10^6$ Tonne) than that which brought glacier into the balance (McSaveney, 1975). Before 1964 the glacier retreated for 15 years with rates 27 m/y, but from 1964-71 there was an overall average positive mass balance; the glacier flow velocities increased caused by the disruption of the equilibrium profile from the reduced ablation under the deposit; the stress field changed and there were small changes in the terminus. During the first two years after the rock avalanche emplacement the glacier terminus receded up to 10 m due to increased melting from the deposit; however, after 1966-67 the northern part of the terminus advanced by 20 m and next season the whole terminus was advancing (Bull, 1969; McSaveney, 1975). McSaveney (1975) reported the formation of different seasonal push moraines from slumped till, outwash deposits and reactivated buried ice, which due to their small size and the active glaciofluvial

environment were destroyed in the same or the next season. The resulting changes in the net mass balance caused the previously retreating glacier to reach an equilibrium regime (Post, 1968; McSaveney, 1975), and after 1979 it slowly re-advanced.

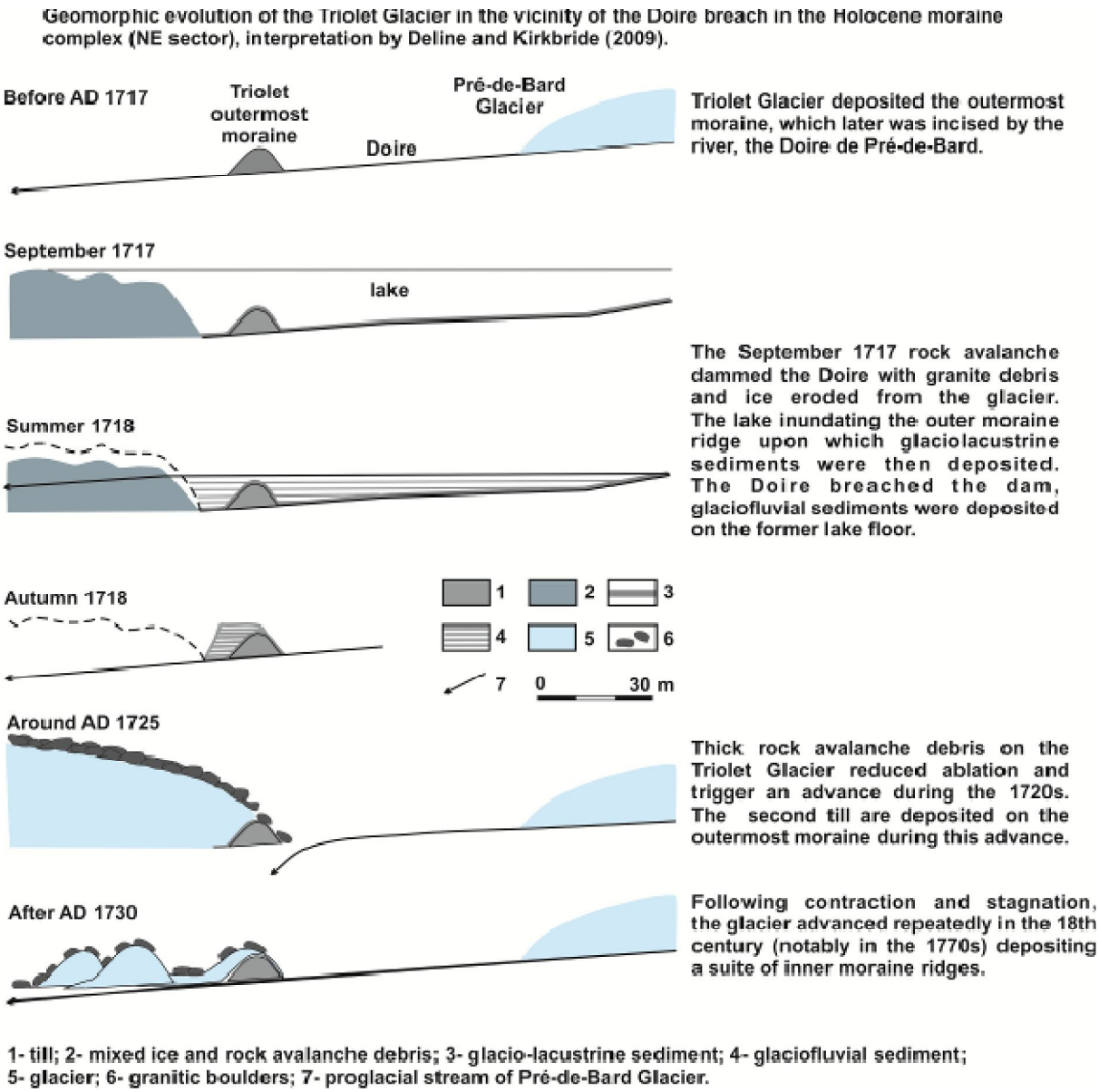

Figure 2.25. Reconstruction of geomorphic evolution for the Triolet Glacier Holocene moraine complex after 1717 rock avalanche emplacement. Modified from Deline and Kirkbride (2009).

Although there was no surge of about 50-100 m/y as Bull (1969) predicted in 1979-80, by 1979 the rock avalanche-covered area reached the terminus, and since then the terminus has advanced at about 10-12 m/y or 300-400 m in total (Fig. 2.26). This is explained by the slow response of the glacier to the event, and by strong proglacial fluvial activity. Additionally, the

rock avalanche deposit, in the processes of being transferred towards the terminus, was also affected by longitudinal compression forming ridges perpendicular to the glacier flow. Shugar et al. (2011) described the terminus in 2008 in an advancing position with some blocks falling down the steep terminal face and accumulating as a moraine. The distal part of the debris sheet now is vegetated and the whole debris sheet actively modified by ice flow.

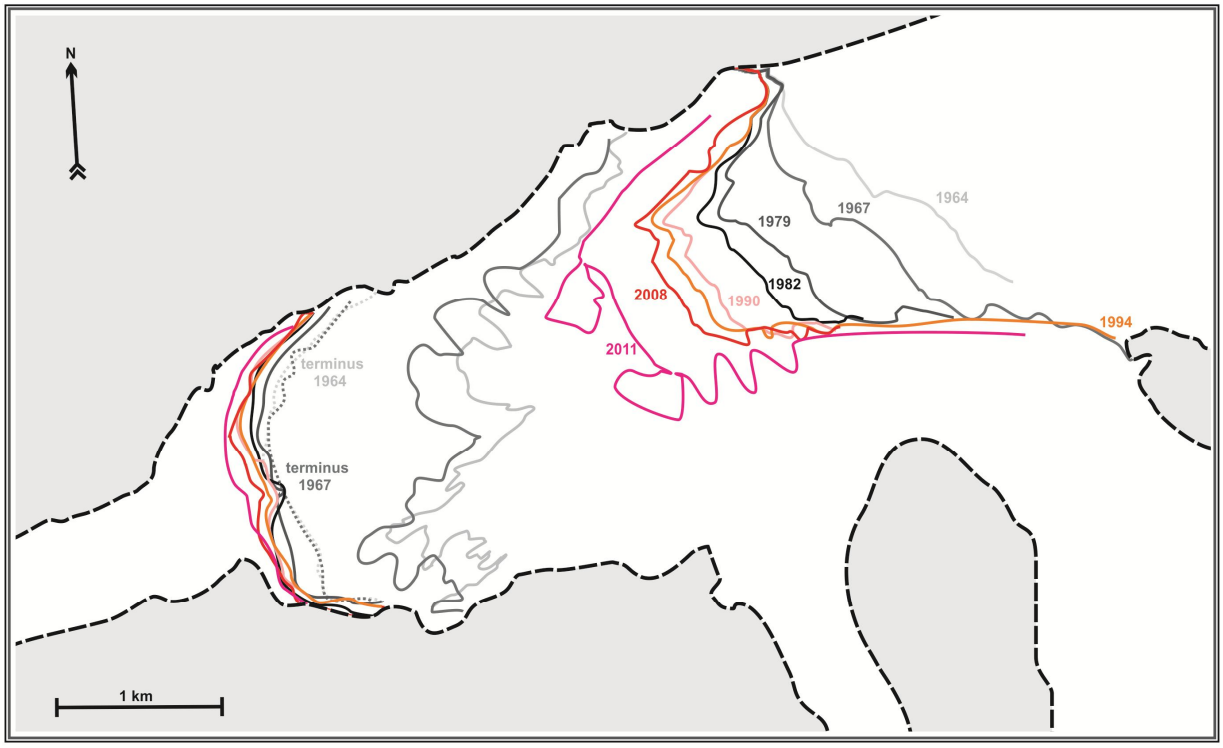

Figure 2.26. Changes of the Sherman Glacier rock avalanche deposit position since its emplacement, obtained from satellite and aerial images. In 15 years the deposit distal edge reached the terminus, while the upper ridge was moved 2 km downvalley by the ice flow and formed a high ridge platform from reduced ablation under the deposit.

The Slide Glacier (Sioux Glacier prior to 1964 earthquake) was extensively covered by a rock avalanche deposit in 1964. Before the earthquake, the glacier had shrunk as much as 35 m from the beginning of the 20th century and the lower part of the ablation zone was covered with medial moraine widening towards the terminus. The rock avalanche deposit caused the glacier surface profile to rise (up to 28 m in 2 years at some locations) with velocities of 175 m/y at the upper end of slide and 21 m/y near the terminus (Reid, 1969). The lower part of the glacier with moraine cover was not covered by rock avalanche deposits, but also thickened by 5 m from 1965-66, while the deposit-free upper part of the glacier during the same period of time become extensively crevassed and lowered by 8 m. Although the glacier response has not been studied since, Molnia's (2008) photographic record suggested the

glacier was in a state of equilibrium with a small amount of retreat along the debris-covered terminus.

Another example of glacier advance due to a rock avalanche is that associated with a deposit emplaced about 12 years before the 1964 earthquake on the Netland Glacier (Post, 1967). A photograph showed that rock avalanche deposit covered about a third of the ablation zone and a high ice platform had formed. Prior to the 1964 earthquake, the glacier had an unusual form of advance caused by this deposit, where a digitate terminal moraine and presence of high ridges on the later moraines upflow of the deposit, with excessive crevassing, could indicate the response of the glacier to the deposit (McSaveney, 1975).

A rock avalanche on the Bualtar Glacier, Karakoram, in 1986, resulted in relative ice thickening under rock-avalanche debris covering only 15% of the ablation zone, but the positive impact on mass balance was equivalent to a 20% increase in annual accumulation (Hewitt, 2009). The rock avalanche emplacement caused the glacier to surge prematurely. As a result, the Bualtar Glacier (which had been previously retreating for several decades) surged in the first 5 years and continued to advance during the following 12 years. The initiation of a surge is one possible response to mass load increases from rock avalanches on glaciers that are predisposed to surge (Tarr and Martin, 1914; Gardner and Hewitt, 1990; Hewitt, 2009), although the term “surge” implies large-scale, short-term glacier movement with or without a terminal advance (Post, 1967). Several examples of premature surges are reported (Reid, 1969; Röthlisberger, 1969; Orombelli and Porter, 1988; Gardner and Hewitt, 1990; Deline, 2009).

Study of a slide of rock, firn, and ice debris (volume $3.5x10^4$ m^3) that fell from Paulsen Peak (1877 m) in 1975 onto the Lyell Glacier, South Georgia, led Gordon et al. (1978) to conclude that active calving of the glacier along a wider front may preclude any marked advance from this rockfall as the bay in front of the glacier margin widens seawards. However, Gordon et al. (2008) showed that the calving front of the Lyell Glacier had changed little by 2000 since its advance position just before 1955. In comparison, the adjacent Geikie and Neumayer Glaciers retreated between 1973/4 and 2003 by ~1.6 km and 2.5 km, respectively.

A prehistorical example of rock-avalanche-induced glacier response is the Waiho Loop terminal moraine of the Franz Josef Glacier, the Southern Alps. This moraine has been correlated to the northern hemisphere Younger Dryas (YD) event (Denton and Hendy, 1994) or to the Antarctic Cold Reversal (ACR) about 13,000 BP (Putnam et al., 2010a); whereas

sedimentological research has showed that the moraine could have originated from rock avalanches (Tovar et al., 2008; Shulmeister et al., 2009). Evans et al. (2010) provide evidence of a rock avalanche in a Pleistocene moraine at nearby Gillespies Beach, which could have been deposited by the LGM extension of the Fox Glacier. Therefore, similar events are expected to be common in areas like the Southern Alps.

2.4.5. The effect of rock avalanches on glaciers: alteration of glacier motion

The mass added to the glacier both immediately (by rock avalanche debris) and gradually (by relative ice thickening) will tend to increase both the flow velocity and the basal sliding of a warm-based glacier. The rock avalanche material itself is equivalent to about double the weight of the same volume of ice (Shulmeister et al., 2009). Vacco et al. (2010) estimated an even higher density by assuming the rock avalanche bulk density to be about 2400 kg m^{-3}. The sliding velocity of a warm-based valley glacier is proportional to the square of the bed shear stress, which depends on the ice-surface slope and the mass of the ice per unit area of bed (Paterson, 2004). Thus 10% additional ice depth should increase flow velocity by 20% at a given location. In addition, extra sediment finding its way to the glacier base via crevasses and moulins may affect the subglacial topography, drainage and the basal water pressure, which in turn affects sliding (Turnbull and Davies, 2002; Davies and Smart, 2007), but the magnitude of this effect is difficult to determine.

Accelerated ice flow was first observed after the St. Elias earthquake by Tarr and Martin (1914) on seven glaciers. But only the effects of a few rock avalanches on glacier motion have been estimated, among which are the Slide (Sioux), Sherman, Bualtar and Black Rapids Glaciers. The Slide Glacier surface ice velocities increased up to 10% (Bull and Marangunic, 1968), where now the glacier is in a state of the equilibrium or slight advance. The Bualtar Glacier prematurely surged in 1987 and 1989 after rock avalanche deposition in 1986 (Gardner and Hewitt, 1990). Similarly, the McGinnis Glacier was reported to be surging in 2006 after two rock avalanches triggered by the 2002 Denali earthquake covered the majority of both its tributaries (Truffer, unpublished data, 2006; cited in Shugar et al., 2011). However, for three extensive rock avalanches onto the Black Rapids Glacier, Shugar et al. (2011) described a significant but short initial speed-up of the surface velocities in the area of the rock avalanche debris sheets, followed by a gradual slowdown to pre-earthquake values. A similar pattern was observed on the Bualtar Glacier, where, firstly, in the 10 months after

rock avalanche emplacement ice near the downglacier edge of the debris sheet moved four times faster than ice near the upglacier edge; however, this behaviour subsequently reversed. These measurements were confirmed by a full-Stokes numerical ice-flow model for Black Rapid Glacier (Shugar, 2011), which indicated surface velocity changes due to mass balance disturbance, surface slope and a switch from compressional to extensional flow caused by rock avalanche deposits.

In principle, the addition of this mass must alter the glacier dynamics, and this will be evident in proportion to the percentage of the ablation zone affected and the ice depth. An equilibrium glacier may advance; a retreating glacier may retreat more slowly, or come into equilibrium, or advance; and an already advancing glacier may advance more rapidly or prematurely surge. In the latter case the Bualtar Glacier adjusted to mass balance and drainage disturbance by surging and rapidly transporting the avalanche deposit down the valley (Hewitt, 2009). However, usually the ice flow acceleration from rock avalanche deposits was hard to estimate, but changes were often observed in mass balance caused by reduced ablation beneath the deposit, resulting in elevation increase of the glacier profile, changes in the surface topography from differential ablation of the deposit edges and changes of the vertical velocity under the debris resulting from extending flow (e.g. Reid, 1969; McSaveney, 1975; Gardner and Hewitt, 1990).

2.4.6. Palaeoclimate reconstructions from rock avalanche deposits on glaciers

The correct identification of rock avalanche deposits in a glaciated valley has significant implications for the reconstruction of the palaeoclimate in that area. Deposits associated with prehistoric rock avalanches could easily be mistaken for moraines caused by climatically-driven advances, which have similar surface features (Chinn, 1979; Orombelli and Porter, 1988; Hewitt, 1999). Recently-identified rock avalanche deposits were previously described as being a late-glacial kame field, for example those studied by Hewitt (1999; 2009) in the Karakoram Himalaya, and the Fernpass (Prager et al., 2009) and Flims (Ivy-Ochs et al., 2009) rock avalanches in the European Alps were previously identified as moraines. In the central Southern Alps of New Zealand the “kame” deposit in the Dart River valley, Otago, known as “The Hillocks” has been reinterpreted as a rock avalanche deposit by McColl and Davies (2011). In the reverse sense, glacial till has been described as having a non-glacial origin in the Macaulay River valley deposit (Grant-Taylor and Rafter, 1971; Beck, 1972;

Burrows, 1972; McSaveney and Whitehouse, 1989). McSaveney and Whitehouse (1989) used morphologic evidence, such as the morainic topographic surface of the deposit slopes and the lack of rock avalanche diagnostic features, to support their observation that the overlying deposit is of glacial origin. By contrast, a recent geomorphological and topographical re-assessment by Putnam et al. (2010b) concluded that this deposit resulted from a large debris flow.

Secondly, the observed effects of large rock avalanches on glaciers has led to a reinterpretation of the origin of some moraines that were traditionally assumed to be deposits reflecting responses of glaciers to climatic change (e.g., Röthlisberger, 1969, Orombelli and Porter, 1988; Porter, 2000; Larsen et al., 2005; Tovar et al., 2008; Deline and Kirkbride, 2009; Shulmeister et al., 2009). Some studies have suggested this contribution is significant (e.g. Deline, 2009), while others have proposed that formation of some particular moraines is entirely the result of such events (Röthlisberger, 1969; Orombelli and Porter, 1988; Hewitt et al., 2008). Porter (2000) highlighted the fact that dated Holocene glacial advances may not always represent a response to climate change, and that some tills and moraines may have a non-glacial origin. Because of the very large volume of debris involved, rock-avalanche–driven advances can generate substantial terminal moraines, which may be completely unrelated to climatic change. Even if a rock avalanche deposit does not cause a glacier to advance, the eventual arrival of a large volume of supraglacial debris at the terminus may result in the rapid formation a large moraine. In contrast, to form the same size of moraine without rock avalanche debris (i.e. with only a thin debris cover and en-and sub-glacial debris) would require the terminus to remain in one position for a relatively long time. Similarly, surge-type and tide-water glaciers often record non-climatic ice-front fluctuations (Yde and Paasche, 2010). The Triolet rock avalanche deposit in Val Ferret, on the Italian flank of the Mount Blanc massif, could be as classical an example of a rock-avalanche-induced moraine as a climatic one (Orombelli and Porter, 1988).

Continued debate of the origin of some moraines has resulted in important reassessments of the impact of variations of paleoclimate on those deposits. However, many more unidentified moraines could potentially be the result of catastrophic events in glaciated mountains. To date, the assumption that all moraines owe their existence to climatically driven advance-retreat sequences is still prevalent among palaeoclimatologists (e.g. Denton and Hendy, 1994; Schaefer et al., 2009; Kaplan et al., 2010). However, the continued development of a more accurate climate-change history requires a more realistic interpretation of glacial

chronologies, which are driven by global and intra-hemispheric atmospheric circulation patterns. For example, any purely rock-avalanche–generated moraine whose date is assigned paleoclimatic significance will generate an error in the inferred paleoclimate record. Clearly this situation is compromised when the rock avalanche event coincides with a climatically driven advance-retreat. Therefore, *moraines used as paleoclimatic indicators must be of known, solely climatic, genesis.*

Any misinterpretation of the origin of morainic deposits will lead to a corresponding incorrect assessment of paleoclimatic conditions at the time. In the Southern Alps of New Zealand there are numerous moraine-like ridges, the origins of which are open to debate: are they solely rock avalanche deposits that were emplaced into the valley after glacier retreat; or did they originate when the glacier was depositing moraine during an advance caused by supraglacial rock avalanche deposit; or do they reflect regional climate fluctuations?

The Waiho Loop terminal moraine of the Franz Josef Glacier has received much attention with respect to correlating southern hemisphere deposits with the northern hemisphere Younger Dryas (YD) event (~11000 BP; Denton and Hendy, 1994; Ivy-Ochs et al., 1999; Barrows et al., 2008; Applegate et al., 2008) or as more recently proposed, to the Antarctic Cold Reversal (ACR) about 13,000 BP (Putnam et al., 2010a). However, Tovar et al. (2008) attributed its formation to a catastrophic rock avalanche, an event that is common in mountains of high tectonic activity such as the western flanks of the Southern Alps (Larsen et al., 2005). Hence, the Waiho Loop can no longer be cited as a reliable datum for palaeoclimatic interpretation without recognition of the fact that rock avalanches have had a significant impact on associated deposits. Shulmeister et al. (2009) have also highlighted another rock avalanche in a Pleistocene moraine at Gillespies Beach, which may have been deposited by the LGM extension of the Fox Glacier. Due to the frequent occurrence of large-scale mass movements in the Southern Alps (e.g. Whitehouse and Griffiths, 1983), it seems very unlikely that Waiho Loop is an isolated exception.

To date, however, there are no reported detailed investigations of this topic. Significantly, neither have techniques to differentiate climate-independent, rock-avalanche-generated moraines from climatically-induced moraines been developed. Moreover, all terminal moraines are assumed *de facto* to result from climatic variations. Given the crucial contemporary importance of palaeoclimatology in understanding climate change, this is potentially a serious deficiency. The various difficulties outlined herein can only be resolved

when the processes of formation of both climatically-driven and rock-avalanche–driven moraines are much better understood, and criteria can be developed for distinguishing them in the field.

2.4.7. Identification of rock avalanche deposits

In the majority of studies, landform genesis is identified by the approach of multiple working hypotheses (Haines-Young and Petch, 1983). This method is used when explaining the same phenomenon by formulation of several hypotheses and by testing those against each other to eliminate less likely options. Thus, landform genesis and development should be established as a result of finding evidence and developing theories of how they were formed so that they can be tested against each other. “Only then, through the process of experiment and observation, can the geomorphologist hope to eliminate any false conjecture” (Haines-Young and Petch, 1983; p. 466).

Several criteria are proposed in an attempt to identify rock avalanche deposits of past geological events (Laznicka, 1988; Hewitt, 2002; Abdrakhmatov and Strom, 2002; Dunning, 2004). Hewitt (2002) reported more than 180 rock avalanche events in glaciated valleys of Karakoram, Himalaya, and proposed a checklist of diagnostic features for rock avalanche deposits for both identification and to allow differentiation from other diamictons or “coarse fragmentise”. However, supraglacial rock avalanche deposits will be partially reworked by differential topography, ablation and crevasses on glacier surface and the deposit remnants will be eventually attributed to heavy supraglacial cover on these glaciers (Hewitt, 2002). The final rock avalanche sediment deposited by the glacier will be reformed as a moraine, albeit one with rock-avalanche sedimentology. In the following section, I have summarized some known geomorphological and sedimentological characteristics of rock avalanche deposits that could be used to recognise them after reworking and re-deposition by glaciers.

2.4.7.1. Geomorphology

The morphologically, the depositional landforms created by rock avalanches share many characteristics with glacial landforms. Steep margins, ridges, conical hills and coarse boulder carapaces could be misled with hummocky moraines or rock-glacier tongues. These deposit features are often confused with other landforms of entirely different origins; examples

include the hummocky terrain of glacier deposits, glacier kame landforms (Fig. 2.27) (Hewitt, 1999; McColl and Davies, 2011), and rock glacier remnants (Owen et al., 2010).

Post-depositional processes could erode the rock avalanche remnants and further modify/complicate the morphology. Nevertheless, rock avalanche deposits can be distinguished from glacial features by their thickening against the impact slopes and topography-confined and substrate-induced forms (Hewitt, 1999). For example, rock avalanches deposits have a steeper angle than landforms constructed by glaciers and the ability to climb several hundred metres up a valley wall (Rondu A, Gol-Ghoro, Katzarah, Gannissh Chissh and others rock avalanches in Karakoram; Hewitt, 2002).

Rock avalanches moving over a non-glacial terrain usually form boulder lobes (Hewitt, 1999; Strom, 1999; Owen et al., 2010). When the travel path of rock avalanche runout zone is entirely on a glacier surface the possibilities of finding evidence of such an event will be much reduced. It is suggested that supraglacially-moved rock avalanche deposits are transported and then re-deposited by ice in the form of aligned boulders of common lithology. Thus, the trains of "Darwin's Boulders" at Bahía San Sebastian and west lobe at Bahía Inútil, east of Patagonia, are now suggested to be glacially-transported detritus of alpine rock avalanches rather than ice-rafted blocks (Evenson et al., 2009). Rock avalanches of Beagle-type granite from the Cordillera Darwin spilled onto glacial ice flowing during LGM into the Bahía Inútil–Bahía San Sebastian lobes, which elongated the deposits into boulder trains during transport and then deposited them onto moraines. In similar way the Sherman Glacier, Alaska, is currently slowly depositing the 1964 rock avalanche which ice flow is transporting supraglacially towards the terminus. Thus, the rock avalanche deposit is also concurrently reworked by meltwater at the terminus with only large clast accumulation (personal communication, M. McSaveney, 2011). The Wilberg rock avalanche in Westland, New Zealand, was reworked by the Wanganui River rather than ice, but similar elongate clusters of large, dark boulders of a distinctive lithology of known source in the catchment indicate the rock avalanche origin (Chevalier et al., 2009).

Additionally, determining the source area could help to verify the origin of the deposit from rock avalanche event (Tovar et al., 2008; McColl and Davies, 2011). In a valley the detachment scar of rock avalanche is preserved for thousands of years (Turnbull and Davies, 2006), the deposit of which will replicate the source lithology (Hewitt et al., 2008; Tovar et al., 2008). Dating of the scar could determine the event age. However, the sources are located

at high elevations with steep rock slopes have frequent rockfalls and snow avalanches eroding their surface additionally may be occupied by small cirque glaciers or icefalls, which complicate their genesis (Turnbull and Davies, 2006).

2.4.7.2. Sedimentology

The identification of rock avalanches deposits is primarily supported by sedimentological approaches (Hewitt et al., 2008).

The first determinant of a rock avalanche deposit is that the sediment lithology exactly matches the source lithology, which can then be used to distinguish it from glacial deposits that reflect the mixture of the lithologies available in the entire catchment (Hewitt, 1999). Based on its monolithology and high angularity, Orombelli and Porter (1988) linked a moraine at Triolet Glacier to a rock avalanche. Similarly, Tovar et al. (2008) demonstrated that the sediments in the Late-Glacial Waiho Loop at Franz Josef Glacier must originate from a rock avalanche because of the dominance of angular clasts of a rock type found only in the upper part of the catchment.

Secondly, the conditions during the rapid fall and runout of a rock avalanche deposit at speeds up to hundreds of m/s and for distances in the order of 10 km produce a high proportion of extremely finely crushed material (McSaveney, 2002). It is uncertain if these fines diffuse throughout the deposit; however, commonly reported preserved stratigraphy and jigsaw clasts indicate deposition of the sliding mass as a single unit.

Finally, the rapid comminution of rock under enormously high stress conditions during rock avalanche emplacement (McSaveney and Davies, 2007) results in sediment bodies that are densely compacted, highly-fragmented, and poorly sorted with an observed crude inverse grading from a sand grade interior to a boulder rich surface that is often topped with a coarse carapace.

The grain size distribution curves have been used to describe the rock avalanches deposits (Dunning, 2006), but this analysis is not always reliable. I consider grain size analysis alone as a tool of spurious precision for the identification of rock avalanche deposits based on inconsistencies where the particular method of sieving, dispersing technique and equipment used can lead to variable results (e.g., Wilson et al., 2005). However, the microsedimentology of rock avalanche sediment is characteristic of debris produced under conditions of high stress and high strain rate and can be used for distinguishing it from deposits of other origin.

Figure 2.27. Top: hummocky topography of the Round Top rock avalanche, Westland, South Island, New Zealand, composed of elongate ridges aligned radially from the bottom of the source scar (the rock avalanche travelled away from the camera). Photo Reznichenko N., September, 2010. Bottom: the hummocky terrain known as the moraine at the north east of Mt. Alfred, Lake Wakatipu, South Island of New Zealand. Photo Reznichenko N., February, 2010.

2.5. SUMMARY AND SYNOPSIS

This literature review in combination with data from unpublished reports on the impact of slope instability on glaciers not only establishes the research goals of this thesis, but also highlights key targets for research in the future.

1. Rock avalanches are rapid, large-volume catastrophic events with long, fast runout and high flow mobility. They are caused by fracture propagation through the rock mass from seismicity, oversteepened slopes and climate changes. In glacierized valleys these events are common. Because many deposits are reworked by valley glaciers, the frequency of these events has been significantly underestimated in terms of their contribution to glacial sediment-transportation and associated depositional systems.

2. In high-relief tectonically active valleys, erosive slopes and high ice-flow rates condition the glacier transport large amounts of debris. The sources of the debris are external (from the surrounding slopes) and internal (from basal erosion and incorporation the sediment deposited in the valley previously. During the last few hundred years with global temperatures rising, the number of glaciers with extensive debris-cover and proglacial lakes has increased. Supraglacial debris cover suppresses surface ablation rates in comparison with clean glaciers, and increases the response times of these glaciers to climate fluctuations, but initiates exponential calving retreat following proglacial lake formation. Glaciofluvial debris redistribution plays a crucial role in moraine deposition and preservation, and in areas like the Southern Alps of New Zealand destroys evidence of previous glacier fluctuations.

3. The deposits from large-volume catastrophic events disturb the valley landscape and as a result, should be evident. Many reported rock avalanches that travelled over glaciers incorporated snow and ice on the way, had longer runout due to the lower basal friction (with snow and ice) and formed thinner and spatially larger deposits on the glacier surface, compared with non-supraglacial deposits. The debris-cover from supraglacial rock avalanches is much thicker than that of melt-out debris, so it suppresses surface ablation and alters glacier net balance. Some glaciers respond to these disturbances by altering their flow regime, the evidence of which is found in form of glacial deposits containing high proportions of rock avalanche sediment.

4. Globally, many morainic deposits are assumed to reflect glacial responses to climatic fluctuation, despite the fact that some have been proved to be of rock avalanche origin or deposited by a glacier as a non-climatic response to a catastrophic event. The knowledge of possible glacial responses to rock avalanches, with particular reference to the glacier transporting significantly increased amounts of the debris and the deposition of non-climatically driven moraines, is important for correct understanding of regional and, hence, global palaeoclimates. However, reliable methods must be developed which allow the

reconstruction of the history of a glacier's behaviour that include not only identification of rock avalanche sediments but take into account the impact such deposits will have had on the glacial record.

This chapter has outlined the general effects of the rock avalanches on glaciers. The fact that the relationship between glaciers and rock avalanches is not fully understood leads to the conclusion that more detailed study of these events must be undertaken. This in turn has significant implications for the interpretation of landforms and for palaeoclimatic reconstructions based on glacial advances and retreats. At the same time, it provides an indication as to how glaciers responded in the past and might be expected to behave during rapid, anthropogenically-induced climate change. Once that is achieved then the results should be incorporated in current glaciology, glacial geomorphology and sedimentology knowledge.

3. Description of study sites

3.1. NEW ZEALAND

3.1.1. Physical settings

The Southern Alps of South Island, New Zealand are the result of oblique collision of the Indo-Australian and Pacific plates, with mountains running south-west north-east along the South Island. The plate boundary Alpine Fault developed in the early Neogene (Cox and Barrell, 2007), and was accompanied by continued widespread faulting and folding, where the major active dextral fault lies at the north-western margin of the Southern Alps with a total displacement of 470 km (Fig. 3.1). East of the Alpine Fault a sequence of steeply dipping regional schists (Haast Schist Group) is of decreasing metamorphic grade eastward and passes into metamorphosed sands and argillite, greywacke that belong to the Torlesse Supergroup (well-indurated sandstone and mudstone that form the greywacke and argillite 'rotten rocks'), of Permian to Jurassic age (Cox and Barrell, 2007). These detrital sediments were eroded from the Gondwana supercontinent and deposited about the Middle Cambrian against the western side of the ancestral New Zealand landmass (Kamp, 1992). Active tectonics result in a general uplift that varies from up to 10 mm/yr near the Main Divide and decreases to 0.5-3 mm/yr in the eastern mountains foot hills (Stevens, 1990). The Aoraki/Mt. Cook area has the highest mountains of the range (including Aoraki/Mt. Cook itself; 3754 m) with uplift rates from 2.5 to 7.5 mm/year (Stevens, 1990). The prevailing westerly wind belt brings humid maritime air masses from the Tasman Sea onto the western side of the Southern Alps. The high mountain belt forms a barrier to winds and causes very high precipitations on western side up (to 13,000 mm; Griffiths and McSaveney, 1983) with much lower amounts to the east (typically <2000 mm).

Rock avalanche deposits are widely distributed across the Southern Alps, with Whitehouse (1983) suggesting that the rock avalanches deposits are more common in the Torlesse Supergroup rocks east of the Main Divide. The volumes of rock avalanche deposits were up to 500 x 10^6 m^3 with runouts up to several km (for example, 3.2 km for the Falling Mountain rock-avalanche). Whitehouse and Griffiths (1983) estimated that rock avalanches occur at a rate of one per 100 years in the Southern Alps, while near the Main Divide rates increase to one per 20-30 years (McSaveney, 2002).

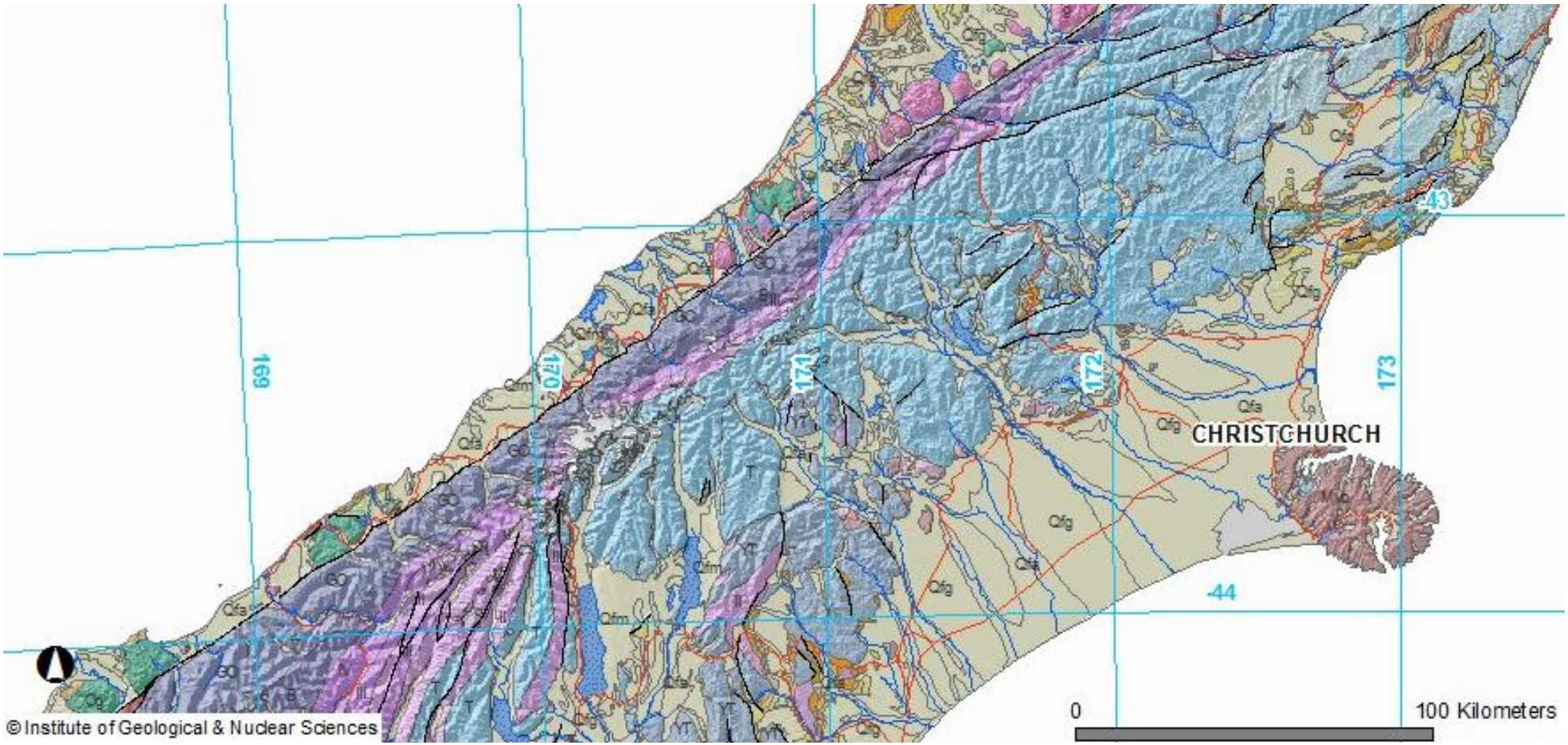

Figure 3.1. Geological map of the central part of the Southern Alps (South Island, New Zealand) and the Alpine Fault trace on the West Coast with geological legend (next page). Image source: online Qmap series of the Institute of Geological and Nuclear Sciences, New Zealand, (http://maps.gns.cri.nz/website/geoatlas/viewer.htm).

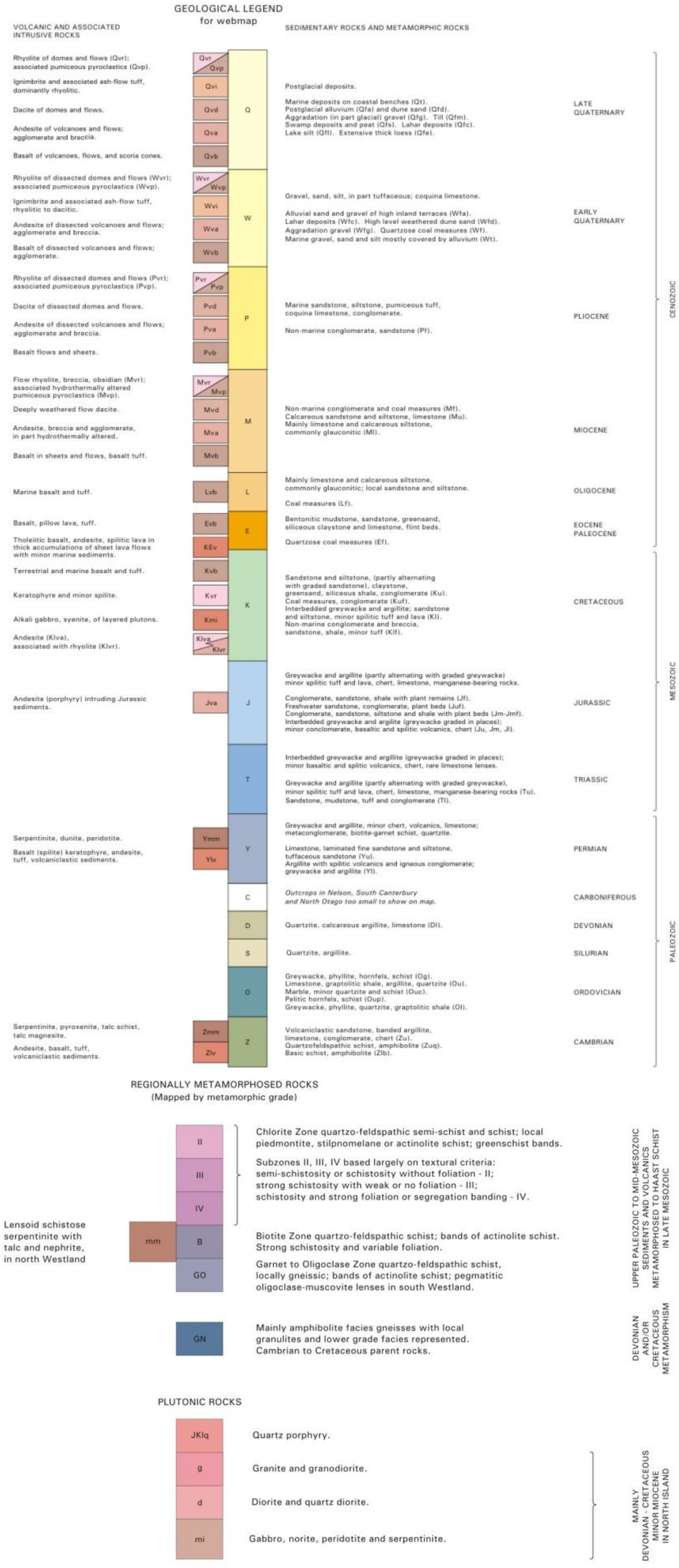

Fig. 3.1. (continued).

The Southern Alps experienced many glaciations during the Quaternary and these were reviewed by Suggate (1990), Fitzsimons (1997) and recently mapped in detail from surface exposure dating obtained for several glaciated valleys (Schaefer et al., 2009; Kaplan et al., 2010; Putnam et al., 2010a). Since the Little Ice Age (between about 1750-1890 AD) all glaciers have undergone a general recession with minor re-advances and loss over last century in the order of 23-32% of glacierized areas (Chinn, 2001). Sequences of moraines throughout the South Island mark the last position of the ice in the valleys (e.g. Sara, 1968; Burrows, 1973; Wardle, 1973; Chinn, 1996).

In total, glaciers of the Southern Alps (>3100) presently cover about 1100 km^2 with an estimated volume of ice of 53.29 km^3, that is about 20% of the mountain glacier ice in the Southern Hemisphere (Chinn, 2001). Half of this volume is concentrated in the largest valley glaciers: the Tasman, Murchison, Franz Josef, Fox, Mueller and Hooker Glaciers. The glaciers are maritime temperate and are sensitive to changes in atmospheric circulation (Shulmeister et al., 2004; Chinn et al., 2005). Many of the larger glaciers have extensive supraglacial debris cover on the lower tongues with rapidly developing proglacial lakes. These glaciers are characterised by large lateral moraines and relatively small terminal moraines developed at the margins of the lakes.

3.1.2. Rock avalanche deposits

The effect of two supraglacial rock avalanche deposits on the debris-covered Hooker and Tasman Glaciers was studied (Fig. 3.2; Chapter 5).

The Aoraki/Mt. Cook rock avalanche originated from the High Peak of Mount Cook (3754 m) during the night of 14 December 1991. This rock avalanche, the volume of which was originally estimated at $11.8 \pm 2.4 \times 10^6$ m^3 (McSaveney, 2002), travelled across the Grand Plateau, down the Hochstetter icefall and spread onto and across the Tasman Glacier (Fig. 3.2 and 3.3). In 2 minutes it fell 2720 m and travelled about 7.5 km with an average speed of 60 m/s and generated a magnitude $M = 3.9$ earthquake (McSaveney, 2002).

Shortly after its deposition, the Hochstetter ice stream deformed the original avalanche deposit into two main parts. The northern-eastern part of the deposit was on the much slower-moving ice from the upper Tasman valley, while the south part is moving downvalley on much more rapid ice-flow sourced from the Grand Plateau and the Hochstetter icefall. In those areas where the deposit makes contact with surrounding debris-covered ice the large

boulders (carapace) are aligned along the flow lines. On the upstream and downstream edges of the deposit large boulders slid down the margin slopes. From aerial and satellite images it is evident that already after first year the Hochstetter ice had modified the deposit, and by 1997 clean ice was present on the whole icefall area (Fig. 3.4). The debris volume delivered to the glacier surface represents approximately 180 years of the annual average debris flux of the icefall (Kirkbride and Sugden, 1992).

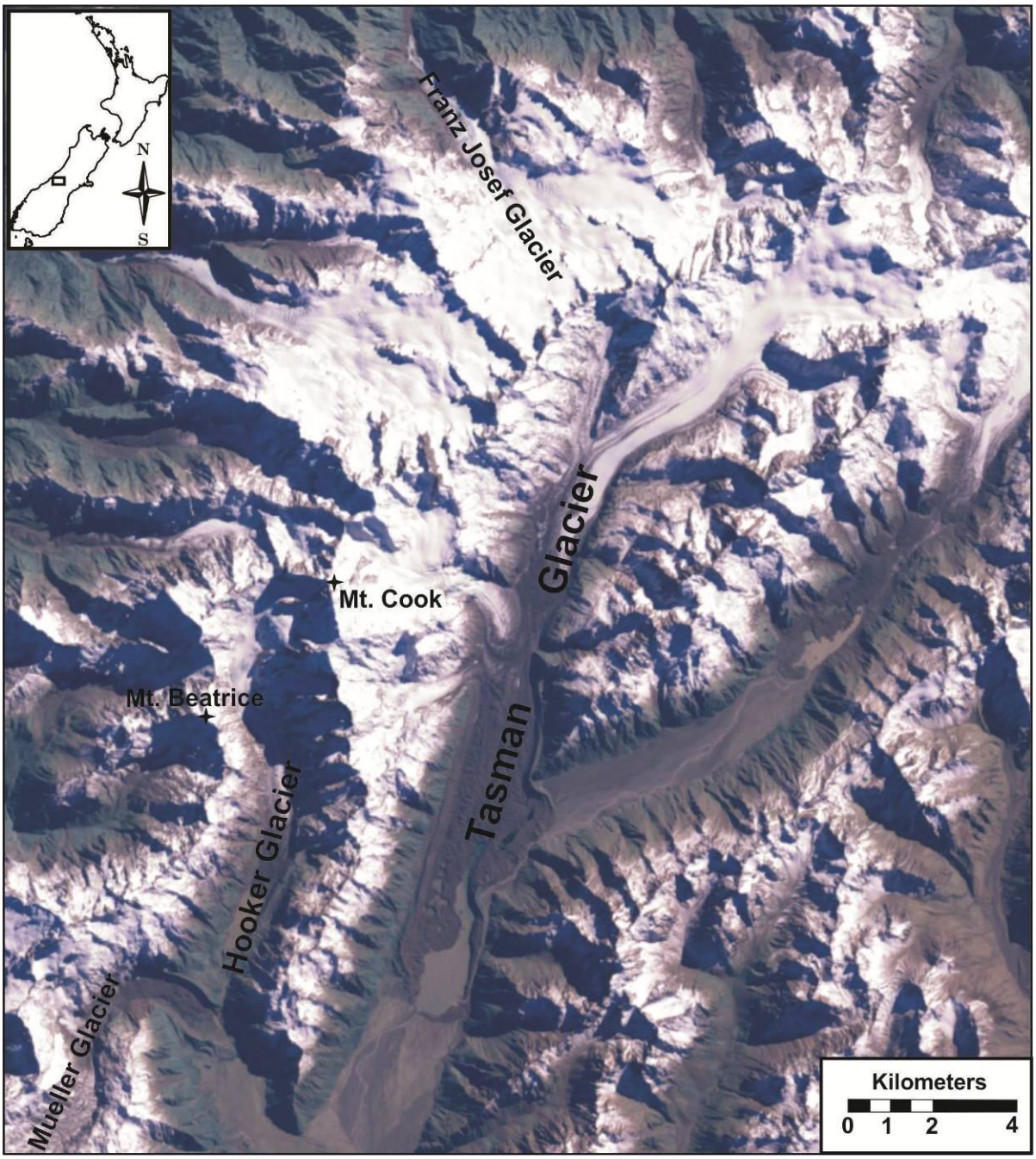

Figure 3.2. Location of the Hooker and Tasman Glaciers, Aoraki/Mt. Cook National Park with Mt. Beatrice and Aoraki/Mt. Cook indicated. Photo: satellite image, LandSat, 2001.

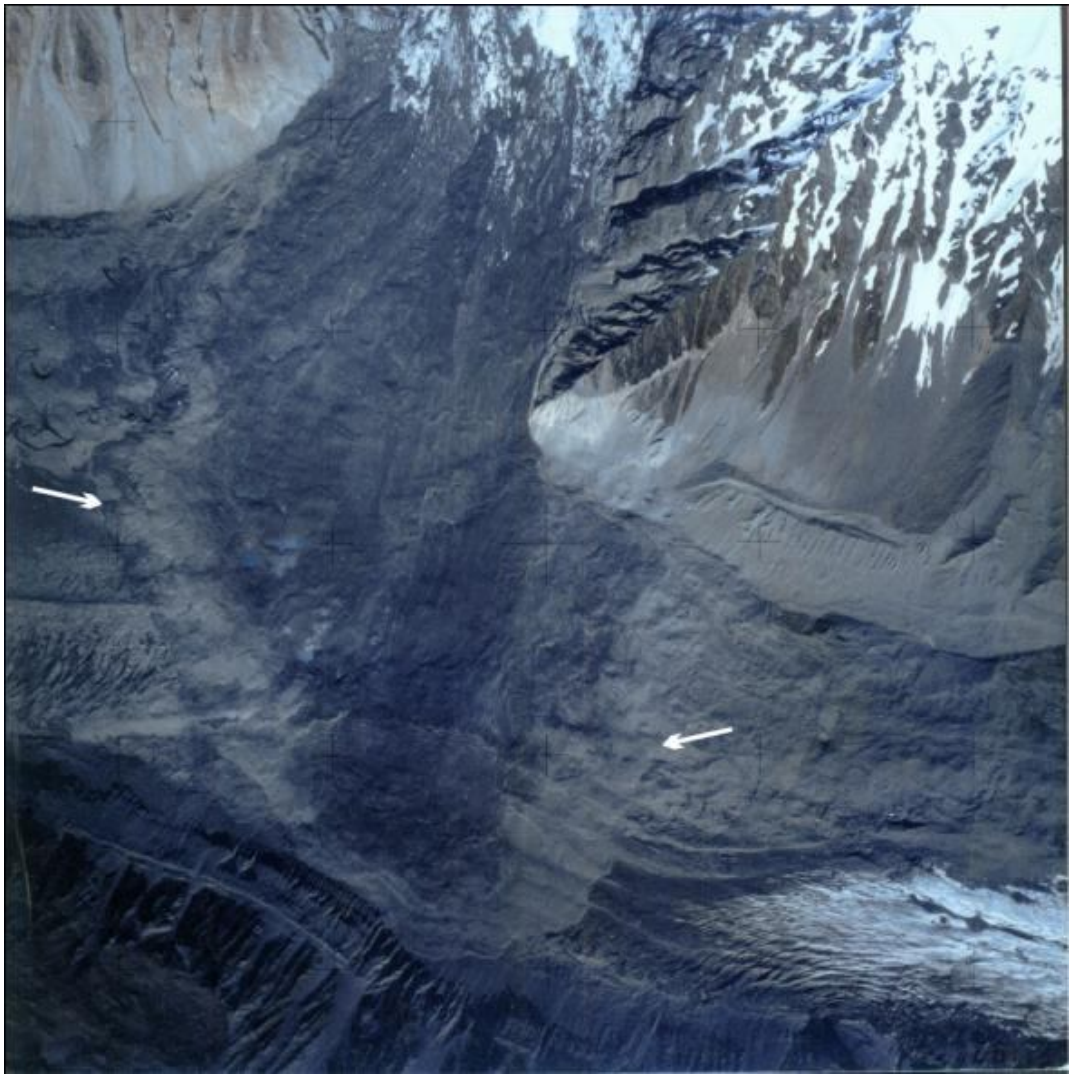

Figure 3.3. Aerial photo of the fresh Aoraki/Mt.Cook rock avalanche deposit taken several days after its emplacement. Arrows indicate edges of the deposit. The deposit climbed more than 100 metres up the opposite side lateral moraine (at the bottom of the picture). Photo: M. McSaveney, December, 1991.

On 23 November 2004 a rock avalanche from Mt. Beatrice (2528 m) was emplaced onto the debris-free part of the ablation zone of the Hooker Glacier, close to a previously deposited rock avalanche that presumably originated from the same source (Fig. 3.5). Tim Billington's diary (witness), cited by Cox et al. (2008), describes the event: "A huge plume of dust was kicked up over the glacier and the land slide tumbled across the glacier like a wave on the beach". The Mt. Beatrice rock avalanche fell from an elevation between 1620 and 1700 m, from a 60º east-facing area from which small rockfalls had been observed previously. The avalanche fell 440 m and spread across the middle of the Hooker Glacier. According to Cox et al. (2008) the first deposit lobe covered an area of 87,000 m^2 and the second 90,000 m^2; in the present study the second lobe is estimated to cover ~47,800 m^2 (2011).

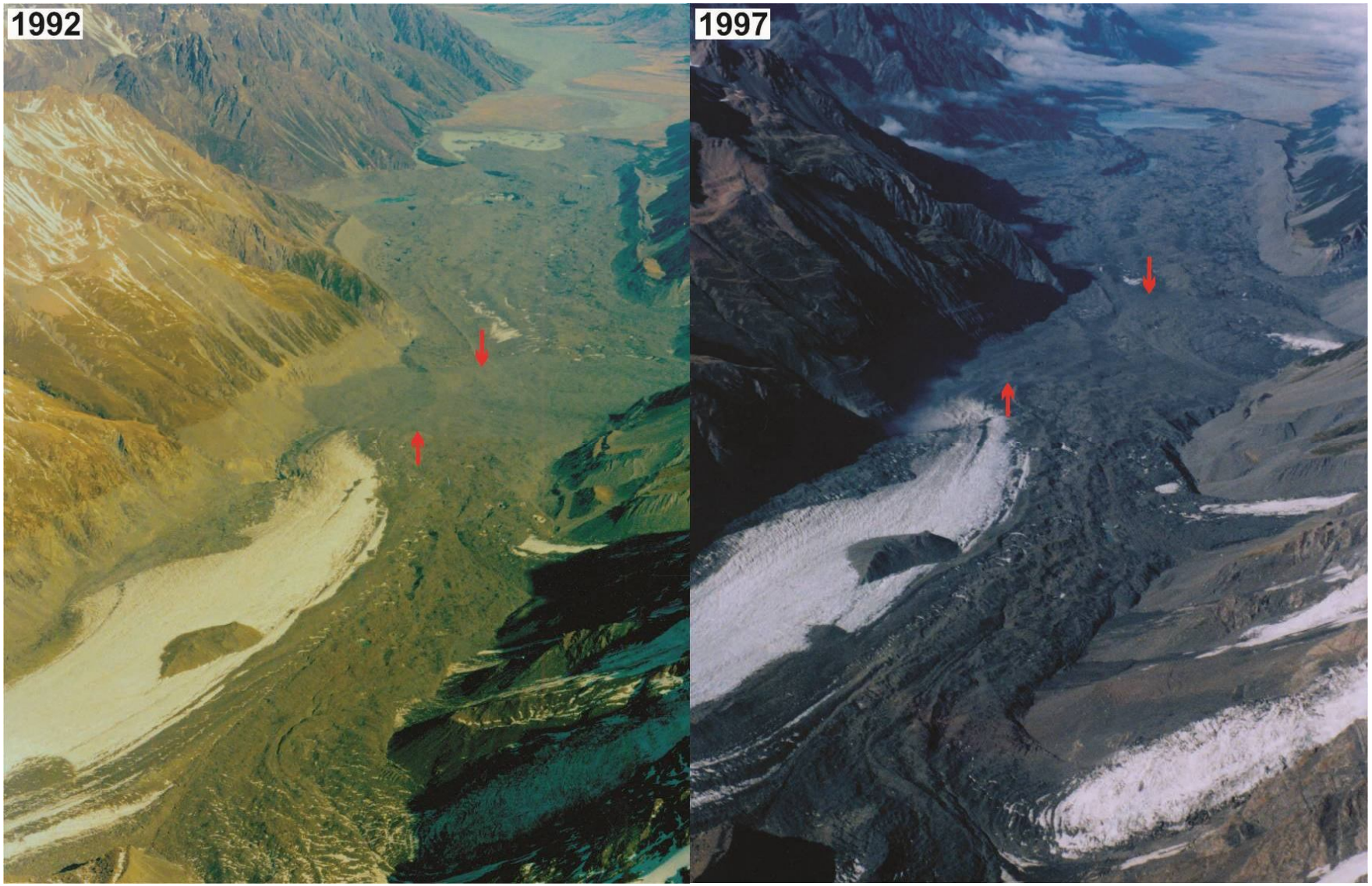

Figure 3.4. Changes of Aoraki/Mt. Cook rock avalanche from 1992, at the same season as the event occurred (on the left), to 1997 (on the right). The southern part was moved downvalley by the Hochstetter icefall. Note the rock avalanche deposit high on the true left lateral moraine in left picture. Photo: T. Chinn, 1992 and 1997.

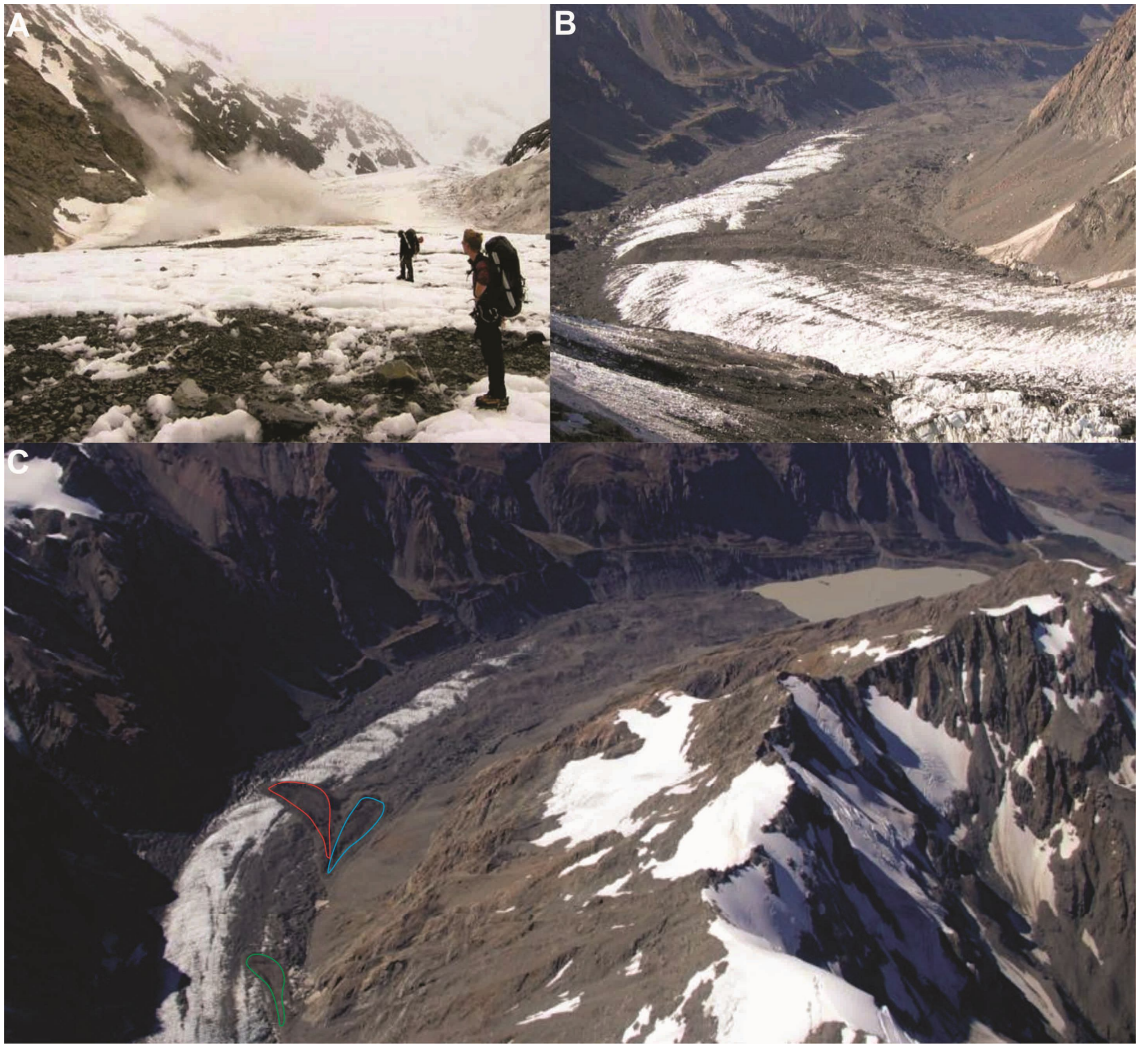

Figure 3.5. Mt. Beatrice rock avalanche. A. Photograph of the event, 23 Nov 2004 by Neil Monteith. B. Two-lobe deposit in 2007. Photo: S. Allen, 19 Jan 2007 from Cox et al. (2008). C. Location of the Mt. Beatrice rock avalanche deposit (2004) on the Hooker Glacier (red line). The small rock avalanche on the right (blue line) was emplaced before Beatrice; up the valley is located another recent smaller rock avalanche (green line). Photo: S. Winkler, February, 2009.

Sediment from other rock avalanches in the Southern Alps was sampled (Fig.3.6).

The **Acheron** rock avalanche deposit lies in greywacke sandstones east of the Main Divide (Fig. 3.1). The 1100 year old rock avalanche with a volume of 10 x 10^6 m^3 and a runout distance in 3.5 km was emplaced from Red Hill (1641 m) into the upper catchment of the Acheron River at the southern end of the Cragieburn Range, Canterbury, New Zealand (Smith et al., 2006). The rock

avalanche is believed to have been triggered by earthquake along the Porters Pass-Amberly Fault (7 km west) and has a deep-seated source scar.

The **Coleridge Lake** rock avalanche represents three events from a single source area composed of Torlesse Supergroup 'greywacke': one at 9 750 yr BP and two at about 700 yr BP (Lee et al., 2009). The total deposit about of 10^7 m^3 in volume covers an area of 23 x 10^4 m^2 with average thickness of 20 m and crosses the course of the Ryton River.

The **Round Top** rock avalanche originated from range front, schist and schist-derived mylonite, and from the deep-seated failure scarps at a height of 550 m on Round Top, Westland. The rock avalanche was probably triggered by seismic shaking of the Alpine Fault at AD 930 ± 50 yr (Wright, 1998; Dufresne and Davies, 2009). The deposit consists of three lobes, with the Round Top lobe having a volume of about 45 x 10^6 m^3, spread over an area of more than 5.5 km^2; the Southern Deposit has a volume of about 10 x $10^6 m^3$ and covers an adjacent area of 1 km^2. A third unnamed lobe of similar size is nearby (Wright, 1998; Dufresne and Davies, 2009). All deposits rest on an alluvial surface and have a hummocky topography.

3.1.3. Glaciers

The Hooker, Mueller and Tasman Glaciers are the largest glaciers of the Southern Alps (Table 3.1) located in the Aoraki/Mt. Cook national park. They lie in Triassic to Jurassic age Torlesse Group greywacke and less indurated argillite. At the climate station at Mount Cook Village in 2001 the annual precipitation was 3020 mm, mean air temperature 8.08 ºC, mean wind speed 5.0 ms^{-1} and mean daily global radiation total 13.7 MJm^{-2} (Röhl, 2008). The annual rainfall varies from 3000–4000 mm/year at the terminus up to 7000 mm/year on the upper Tasman Glacier.

The glaciers terminate about 3 km north of the township of Mount Cook at elevations of about 730 and 760 m a.s.l. for the Tasman and Mueller Glaciers, respectively, and about 870 m a.s.l. for the Hooker Glacier (Chinn, 1996). The high, steep slope activity in this area conditions the large sediment delivery to the glaciers. During the last century these glaciers had negative mass balance mostly by downwasting with stationary terminus positions. In the 1980s proglacial lakes were formed by the coalescence of ponds, and since the 1990s the glaciers termini have retreated mostly as a result of calving (Warren and Kirkbride, 2003). Numerous ponds developed

supraglacially due to the glacier down-wasting and debris-cover. These ponds and proglacial lakes are frozen for up to 2 months in winter, and at any season surface ice can occur during the night (Röhl, 2008).

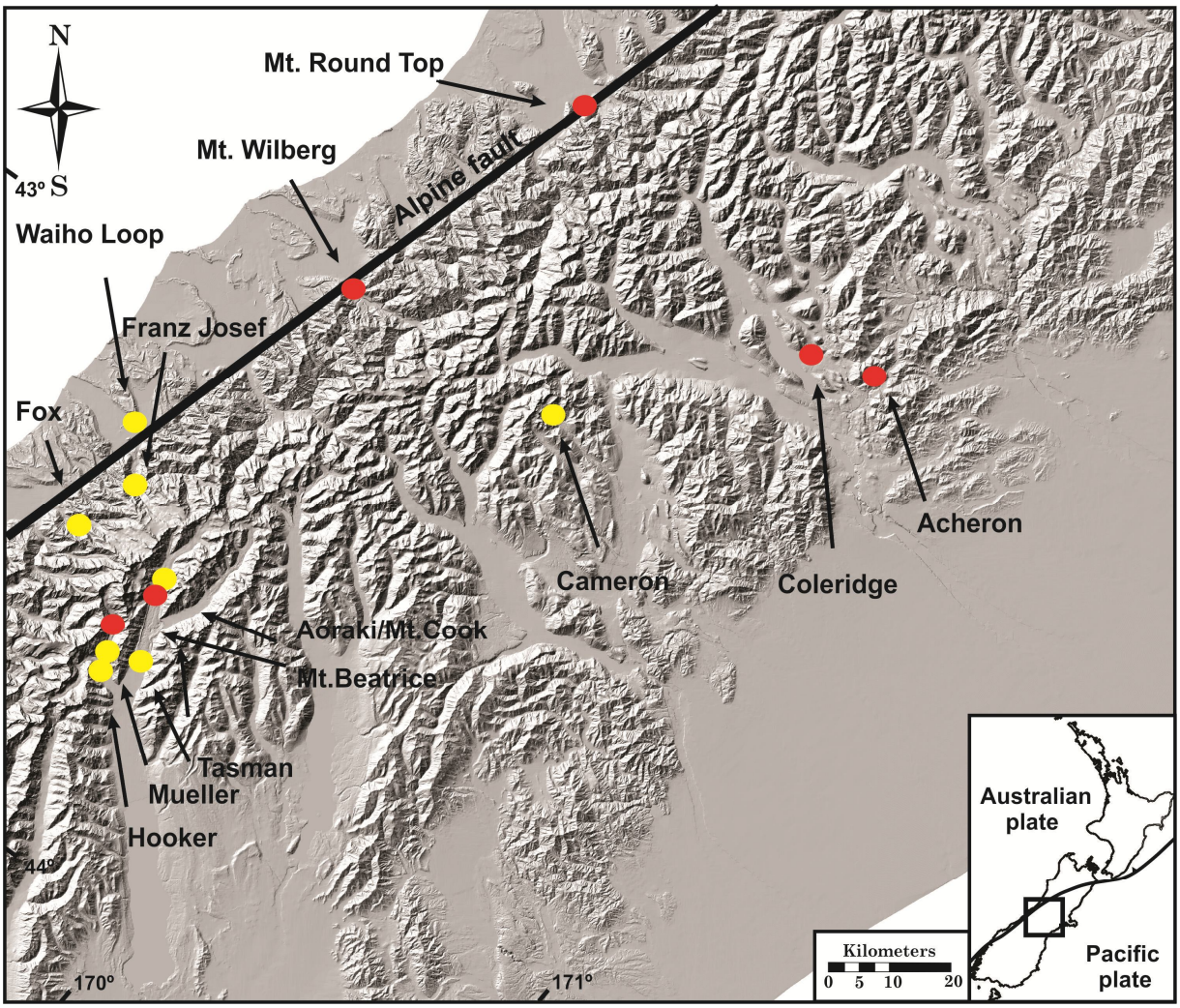

Figure 3.6. Location of sampled rock avalanche deposits (red) and the sediment from glacial environments (yellow), the Southern Alps, New Zealand.

A number of tributary ice streams flow into the main trunk of the Tasman Glacier (Ball, Hochstetter, Haast, Rudolf, Darwin Glaciers and others). The lower 9 km of the glacier is covered with debris, the thickness of which increases down-glacier from the clean-ice interface

to an average of 1-2 m at the terminus (Fig. 3.7A; Kirkbride, 1989). Among 25 tributary glaciers (Anderton, 1975) the Rudolf Glacier contributes to the debris cover supply, whereas Hochstetter icefall is the largest tributary source with high flow rates and mostly debris-free surface. The size, low gradient and extensive supraglacial debris cover of the ablation zone causes the glacier to respond slowly to climate warming. High lateral moraines (presently up to 200-300 metres above the ice surface) indicate rapid glacier recession during the last century. The negative mass balance was reflected by down-wastage with a relatively stable terminus at the LIA limit until the proglacial lake formed; since the 1980s a rapid calving retreat has been prevalent. During the last 10 years the glacier terminus has receded >4 km at the western margin by calving (Dykes et al., 2011).

Table 3.1. Data for studied glaciers in New Zealand.

	Area				Elevation (m)			Length				
Glacier	At 1996 (km^2)	Debris (%)	LIA (km^2)	ΔA (%)	At 1996 (min)	LIA (min)	Δ mean	At 1996 (km)	LIA (km)	ΔL (km)	ΔL (%)	Rate (m/a)
Tasman	99.35	31.86	109.29	9.10	730	730	0	28.5	28.50	0	0	0
Franz Josef	35.70	1.43	40.92	12.76	425	220	103	10.25	13.20	2.95	22	29.50
Fox	34.69	0.93	38.77	10.52	306	250	28	13.2	15.70	2.50	16	25.00
Mueller	22.54	37.22	24.71	8.80	760	760	0	13.87	14.85	0.98	7	9.80
Hooker	17.32	25.08	20.76	16.57	870	870	0	12.3	13.08	0.78	6	7.80
Cameron	2.68	5.23	4.36	38.60	1380	1234	73	3.1	4.50	1.40	31	13.99

Modified from Chinn (1996), where LIA data from various sources; AA - glacier area change; AL - length change; Rate - mean annual retreat rate.

The Hooker Glacier flows almost due south within the narrow Hooker valley. The east side of valley is the Aoraki/Mt. Cook Range, to the west is the Main Divide and the south is bounded by the lateral moraines of the Mueller Glacier. The upper Hooker Glacier catchment includes Permian to Triassic rocks of the Haast Schist Group. The Hooker is fed by hanging glaciers from the flanks of Aoraki/Mt. Cook, and by the Empress, Sheila, Noeline and Mona Glaciers and ice cliffs on the western wall of the valley. The glacier tongue is covered with debris that originates englacially and from rockfall and rock avalanche deposits descending from steep cliffs of the valley sides. Some rock avalanche deposits can be seen on old photographs. During the last 10 years at least three rock avalanches (or large rockfalls) have fallen from Mt. Beatrice. The proglacial Hooker Lake is surrounded by a series of Holocene moraines (Burrows, 1973;

Winkler, 2005), which indicate increased downwasting of the glacier during the last century (Fig. 3.7B). The outer faces of lateral moraines are vegetated, whereas the inner slopes are unstable and periodically collapse onto the glacier.

The Mueller Glacier is confined along the narrow upper Mueller valley, with Holocene moraine systems surrounding the proglacial lake and an outwash plain to the south. The Mueller Glacier is fed from the Huddleston, Frind, Bannie, and Welchman Glaciers, and by ice avalanches from steep east face of Mt. Sefton. The tributary glaciers and avalanches from the steep faces supply debris that has resulted in an extensive cover towards the terminus. Rock avalanches (Cox et al., 2008) significantly contribute to the supraglacial sediment. The thick cover towards the terminus is presumably comprised of rock avalanche sediment from older events. The lake is bounded by latero-frontal moraines and younger frontal moraines along the southern margin.

In South Westland, the Franz Josef and Fox Glaciers have steep gradients and insignificant supraglacial cover. They are about 10 and 12 km long, respectively, and descend from about 2700 to 3000 m a.s.l. to about 250 to 270 m a.s.l. The catchment areas of Fox and Franz Josef Glaciers are 68 and 47 km^2, respectively. The Fox Glacier is characterised by steeper gradient at 1100–1900 m a.s.l. than the Franz Josef Glacier (Carrivick and Rushmer, 2009). In both catchments the underlying bedrock is variably metamorphosed schist and gneiss, and tectonic uplift and denudation (12 mm/year) have been estimated to be similar (Hovius et al., 1997). The climatic conditions, radiation cycle and precipitation up to 14,000 mm/year are comparable as well, with, however, slightly different ablation zone orientation (westerly direction for the Fox Glacier and north-northwesterly for the Franz Josef). These create fast turnover (ice velocities about 1 m/day) and rapid response times: 5-25 years for the Franz Josef Glacier and 6-26 years for the Fox Glacier, depending on the calculation technique used (Oerlemans, 1997; Purdie et al., 2008). The glaciers terminate in valley-confined outwash plains about 400 m wide with discontinuous small terminal moraines. They feed the Waiho and Fox Rivers. Both glaciers have been oscillating between advance and retreat over the last 50 years (Suggate, 1990; Sara, 1968).

The Cameron Glacier lies in the Cameron valley of the Arrowsmith Range, western Canterbury. This relatively high group of mountains with peaks >2,500 m located 15 km east of the Main Divide is composed of undifferentiated hard sandstone (greywacke) and argillite of the Torlesse

supergroup bedrock (Warren, 1967). The glacier is located in a confined valley, which opens into the Lake Heron Basin, ~760 m a.s.l. (Fig. 3.6; Burrows, 1975). The terminus of the glacier is a steep face of ice at ~1,550 m a.s.l., from which the Cameron River flows downvalley in a south-eastward direction. The glacier elevation is 1500-2300 m a.s.l. with its source in three distinct névés located on the slopes of Mt. Arrowsmith (2,795 m), Couloir Peak (2,644 m) and Jagged Peak (2,720 m) (Burrows, 1975). The seasonal temperature fluctuates from -5° to 30°C at the nearby Mt. Hutt skifield (1600 m a.s.l.) that is situated 46 km southeast of Cameron Glacier (NIWA CliFlo, 2007).

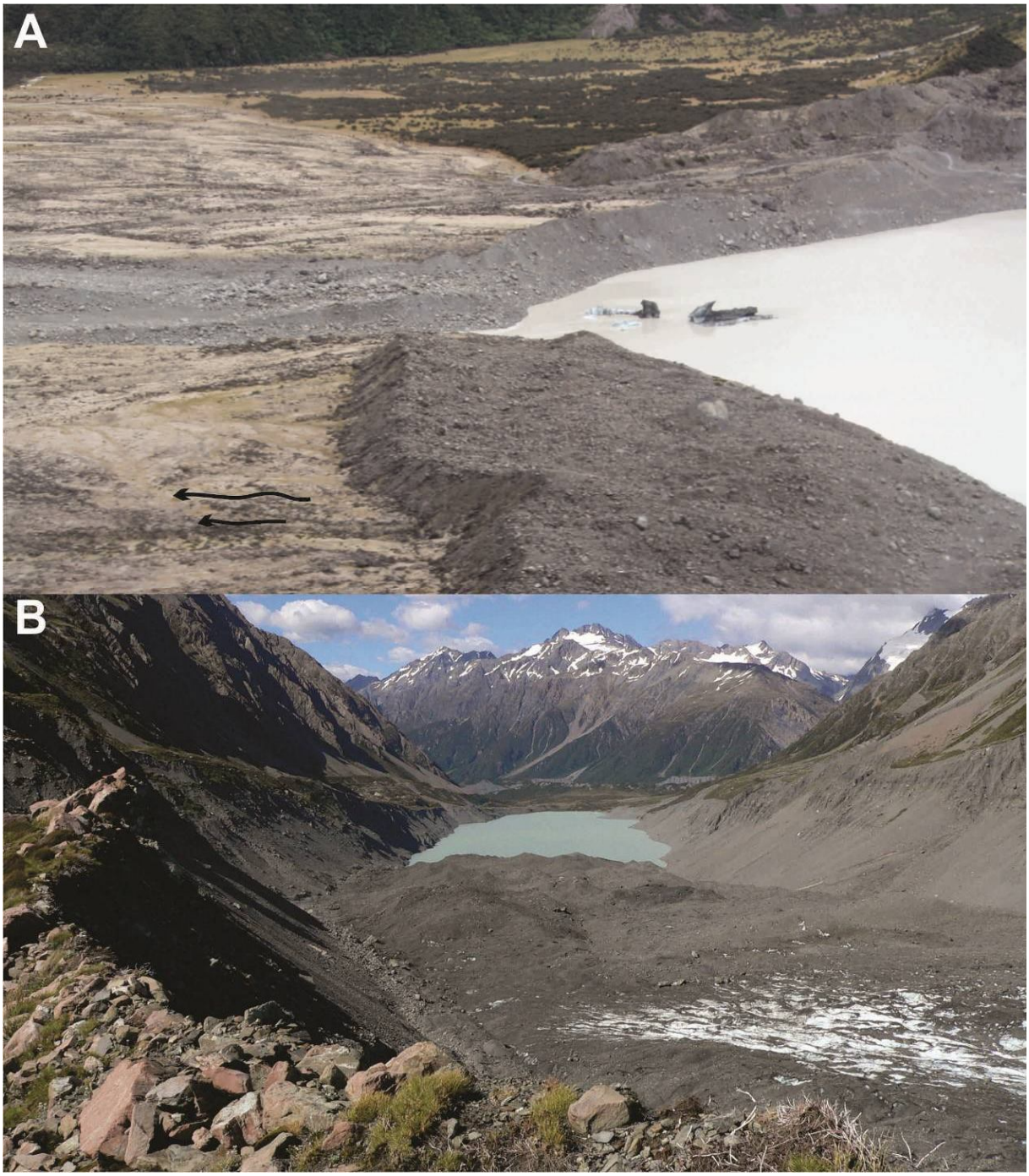

Figure 3.7. A. Tasman Glacier lake front; this was the glacier terminus before the proglacial lake development in the early 1990s. Note the outwash plain (black arrows) with small dump moraines developed after glacier retreat from this position. Photo: J. Shulmeister, February, 2009. B. Downvalley view of the Hooker Glacier with prominent steep lateral moraines that periodically collapse and contribute to supraglacial sediment. The glacier terminus is calving into the Hooker Lake which is bounded by a sequence of Holocene terminal moraines. Photo: N. Reznichenko, December, 2010.

3.2. NORWAY

3.2.1. Physical settings

Norway extends from c. 58°N to over 71°N and longitudes 4° and 32° E with extensive high terrain and mountains with peaks up to about 2500 m a.s.l. The country was heavily glaciated during the Quaternary, and glaciers still exist in Western Norway. The southern and western part of Norway is composed of Precambrian crust forming the Fennoscandian (Baltic) Shield, which mostly consists of re-sculptured Precambrian erosional surfaces. Northern and western parts of Norway are composed of rock from Caledonian orogens, mostly granite and gneiss that were formed from folding and metamorphism of marine Cambro-Silurian sediments during Silurian and Devonian (Fig. 3.8; Donner, 1995). The mountains underwent morphological changes as a result of glacial erosion during the Quaternary with preferential overdeepening of the river valleys and fjord formation, to depths of up to 2 km (Ramberg et al., 2008). Modern Norway is still rising at rates from 1 mm/year in the west to 3.5 mm/year in the east (Olesen et al., 2004) as a response to the isostatic rebound after the last glaciations, with no tectonic uplift component (Ramberg et al., 2008).

The North Atlantic westerly winds create a maritime humid climate in Norway. The North Atlantic Current warms the westerlies that cause mild winter temperatures and a strong gradient with decreased precipitation eastwards from the Main Divide. The annual precipitation ranges from 3500 - 5000 mm at the foot of west coastal mountain regions to eastern interior totals of <400 mm (Chinn et al., 2005).

1627 individual glaciers cover an area of ~2,600 km^2 of Norway, with 714 glaciers covering 1,592 km^2 in southern Norway (Nesje et al., 2008). The glaciers have been classified into two main groups based on climate influence. The first group are western maritime outlet glaciers that usually descend from large ice plateaus into the surrounding valleys, such as Jostedalsbreen (487 km^2), Svartisen (in total 369 km^2) and Folgefonna (in total 219 km^2). These glaciers are considered to be warm-based glaciers. The second group are continental glaciers (Jotunheimen, Lyngshalvøya), which are mostly small cirque glaciers located in the eastern part of the southern Norway (Chinn et al., 2005). The eastern glaciers are retreating rapidly. For example, Jotunheimen which is at highest elevation in Norway and has a continental climate has decreased

in ice volume (Nesje et al., 2008). In contrast, the Jostedalsbreen ice cap is influenced by a western maritime climate and is the largest ice body on continental Europe (Winkler and Matthews, 2010).

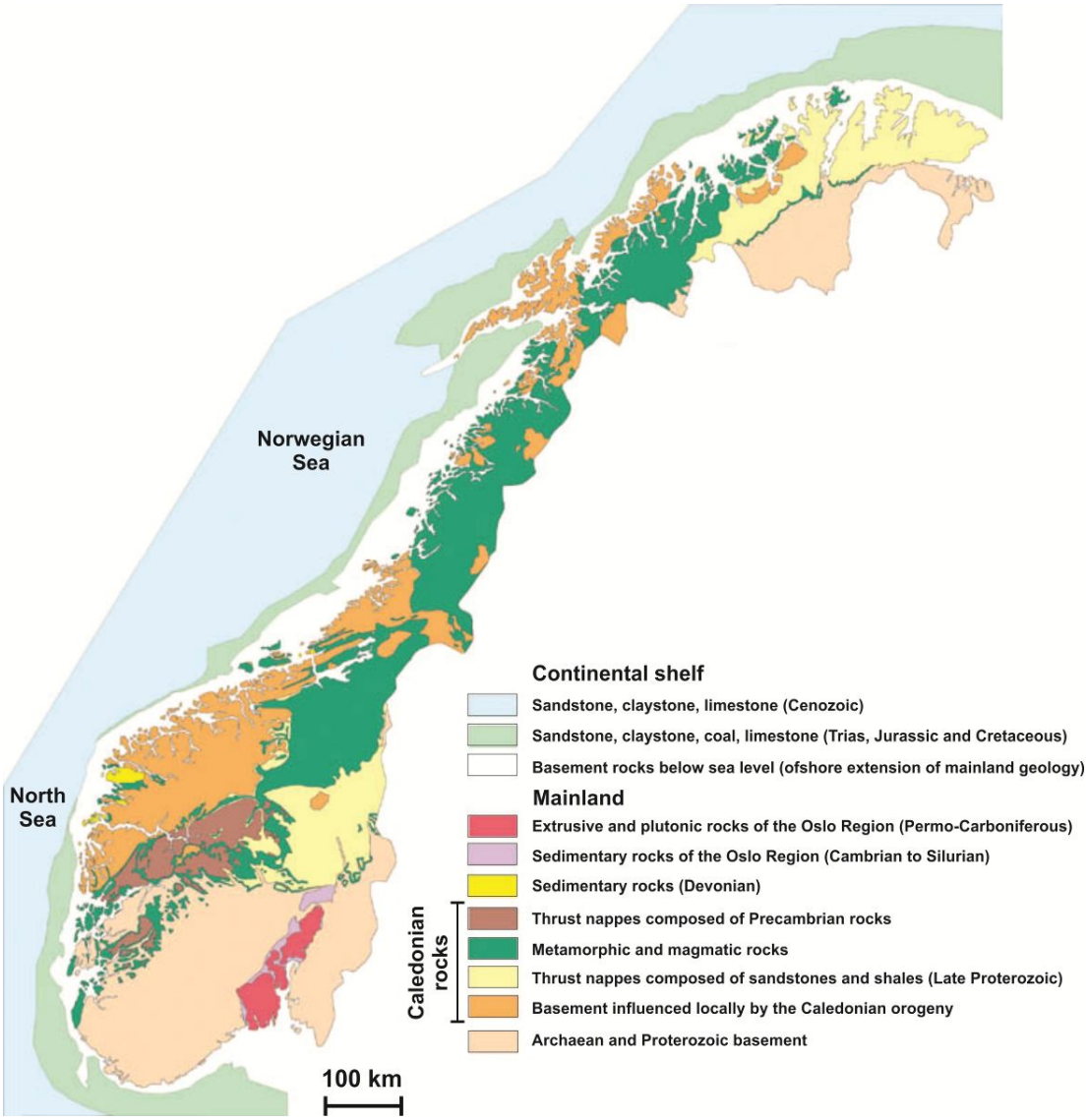

Figure 3.8. Simplified geological map of Norway (Ramberg et al., 2008).

Rock avalanches are common in most regions of Norway. The relief of the Norwegian fjords and valleys conditions rock-slope failure and the development of rock avalanches. Prehistoric and historic deposits of these events are found in mountainous regions, such as the counties of

Troms, Møre og Romsdal, and Sogn og Fjordane (Braathen et al., 2004). Numerous rock avalanche deposits studied on land and in the fjords are characterised by boulder lobes, mounds and intervening ponds and extensive debris flows (Braathen et al., 2004). Up to 200 rock avalanches are registered by the Geological Survey of Norway. Concentrations of events are common in the inner fjord areas, while on land Romsdalen valley in West Norway is covered with 15 large rock avalanches (Blikra and Anda, 1997). In Tafjorden, there are more than 10 rock-avalanche deposits that have been mapped on the bed of the fjord over a distance of less than 7 km.

The reported deposits (NGU Report, 2009) suggest a high frequency of rock avalanches in the earlier Holocene after deglaciation, during or before the Younger Dryas period (13 000 – 11 500 years BP). For example, in the inner part of Storfjorden 25 rock avalanches occurred during the deglaciation (12 500-10 000 ^{14}C years BP), while after the final deglaciation 10000-9000 ^{14}C years BP the number of events decreased to 5-8 for the whole fjord system (Table 3.2).

Table 3.2. Rock-avalanches number, volumes and average frequencies per 1000 years per fjord for the last 9 000 ^{14}C years BP.

Fjord	Total number of events	Total volume 1 x 10^6 m^3	Number of Holocene events	Holocene volume 1 x 10^6 m^3	Average frequency since 9000 ^{14}C years BP
Geirangerfjord	56	40,6	44	19.1	1/350 years
Sunnylvsfjord	17	363.3	12	22,2	1/1300 years
Tafjord	20	144,8	16	18,4	1/650 years
Nordalsfjord	4	6,6	4	6,6	
Storfjord	11	31,7	6	22,9	1/3000 years

Holocene numbers cover the period after 10 000 ^{14}C years BP. Modified from NGU Report (2009).

3.2.2. Rock avalanche deposits

Because in Nordfjord, Western Norway, many deposits rest on the bottoms of the fjords, few are available for sampling; only the Mt. Vora rock avalanche deposit was sampled in the present research. This deposit consists of a number of rock avalanche lobes from the northern slope of the 1435 m high Mt. Vora located in Myklebustdalenin valley, Breim, inner Nordfjord, Norway

(Fig. 3.9), which were studied in detail by Aa et al. (2007). The source area of the avalanche consists of banded gneiss, coarse-grained quartz monzonite with feldspar grains and some biotite, with fractures close to parallel with the valley side. The deposit fills the valley to the east of Byrkjelo town over an area of 3 km^2. Its thickness varies from 17 m at the avalanche margins to 62 m at the outlet of Lake Sandalsvatnet, with a mean thickness of about 35 m. The minimum total volume of the deposit is estimated to be 100×10^6 m^3 (Aa et al., 2007).

Through the Holocene minimum a total of 11 large rock avalanches have occurred from Mt. Vora. According to Aa et al. (2007), the average frequency of rock avalanches during the Holocene was about 1 per 1000 yr, and during the period 7100–3600 BP it was about 1 per 700 yr, but after 3600 BP no rock avalanches have been recognized. Between 6920–7170 and 5090–5440 cal. yr BP glaciers were absent from the area (Myklebustbreen) and silt laminae in a 5.5 m deep bog basin are interpreted as primary sediments from dust clouds generated by rock avalanches.

3.2.3. Glaciers

Jostedalsbreen is the largest ice field in continental Europe. It is situated at the eastern end of the Nordfjord in Western Norway with about 20 outlet glaciers flowing down from the central ice plateau (Fig. 3.9; Table 3.3). The bedrock mostly consists of meso- and Neoproterozoic granitic to granodioritic gneiss, with some unmetamorphosed sandstone and shist, and phyllite (Ramberg et al., 2008). The glaciers descend into the valleys and at some places their termini reach to below 350 m a.s.l. (Winkler and Matthews, 2010). Precipitation on the glacier forelands is more than 1500 mm. Mean annual temperatures range from 2.5 to 5.0 °C (for Kjenndalsbreen, Briksdalsbreen, Bergsetbreen, and Bødalsbreen) based on the mean annual temperatures at Bjørkehaug in Jostedalen (3.7 °C; 324 m a.s.l.) and Olden-Vangsberg (5.9 °C; 78 m a.s.l.) with a mean adiabatic lapse rate of 0.6 °C/100 m (Winkler and Matthews, 2010).

During the Last Glacial Maximum (LGM), the Scandinavian ice sheet (Ramberg et al., 2008) reached the outer limit of the continental shelf, from which it retreated only at 12.5k 14C yr (Mangerud et al., 1979). Since the LGM two significant ice advances have occurred: during the

Younger Dryas (about 11-10 ka ^{14}C yr BP (Denton and Hendy, 1994) and at the Preboreal/Boreal transition (the Erdalen-Event about 9 ka yr BP; Dahl et al., 2002). From 9 - 5 ka yr BP increased summer temperatures and/or less winter precipitation resulted in the melting of the majority of the glaciers in Norway. The glaciers of Jostedalsbreen ice field probably disappeared completely for about 1000 years until 6 ka BP (Nesje et al., 2008). The next period is characterised by growth of the Jostedalsbreen ice field until a maximum during the LIA, the timing of which varied from the beginning of 18th to the end of 19th century in different parts of southern Norway (Nesje, 2005). Since LIA glaciers have generally retreated, but had positive mass balances in the 1990s with smaller advances in 2000/2001 and general retreat during the following years (Nesje, 2005).

Bødalsbreen, Kjenndalsbreen, Brenndalsbreen and Briksdalsbreen are outlet glaciers descending from western Jostedalsbreen. From 1990s until 2001 the Bødalsbreen advanced but has subsequently retreated ~200 m (Winkler and Matthews, 2010). The proglacial area of the glacier is framed by steep rock faces up to 700 m high with Holocene debris cones. The glacier foreland consists of outwash plain that grades into the delta of Lake Sætrevatnet and nine moraine ridges dated at between AD 1755 and AD 2000 are recognised (Burki et al., 2009a and 2009b). These recessional moraines formed by thrusting and bulldozing, and consist of sandy diamicton, whereas older deposits have a “saw-toothed” shape. A few lateral moraines are composed of boulders (Burki et al., 2009a and 2009b). The smaller Kjenndalsbreen advanced from 1990 until 1997. Previously deposited small (< 3 m high) moraines were overridden in 1995 with the formation of larger moraine that incorporated soil and vegetation. The smaller moraines of 1998, 1999 and 2000 were formed during the general glacier retreat since 1997 (Winkler and Matthews, 2010). The Brenndalsbreen descends into the valley of Oldevatnet. This glacier advanced rapidly over 4-5 km during LIA between AD 1650 and 1700 with an average advance rate of 90m/yr (Nesje, 1994). Two recent re-advances at AD 2000 and AD 2001 formed 3 m high moraines. Briksdalsbreen is a steep glacier adjacent to Brenndalsbreen. Briksdalsbreen has had many periods of advance and recession due to its rapid response to changes in the mass balance of the plateau glacier (Andreassen et al., 2005). Briksdalsbreen reached its LIA position around AD 1760-65 and then started to retreat. During the 1930s and 1940s the glacier front rapidly

retreated and formed Briksdalsvatn Lake (Nesje, 2005). The readvance in 1997 resulted in formation of a push moraine (Winkler and Nesje, 1999).

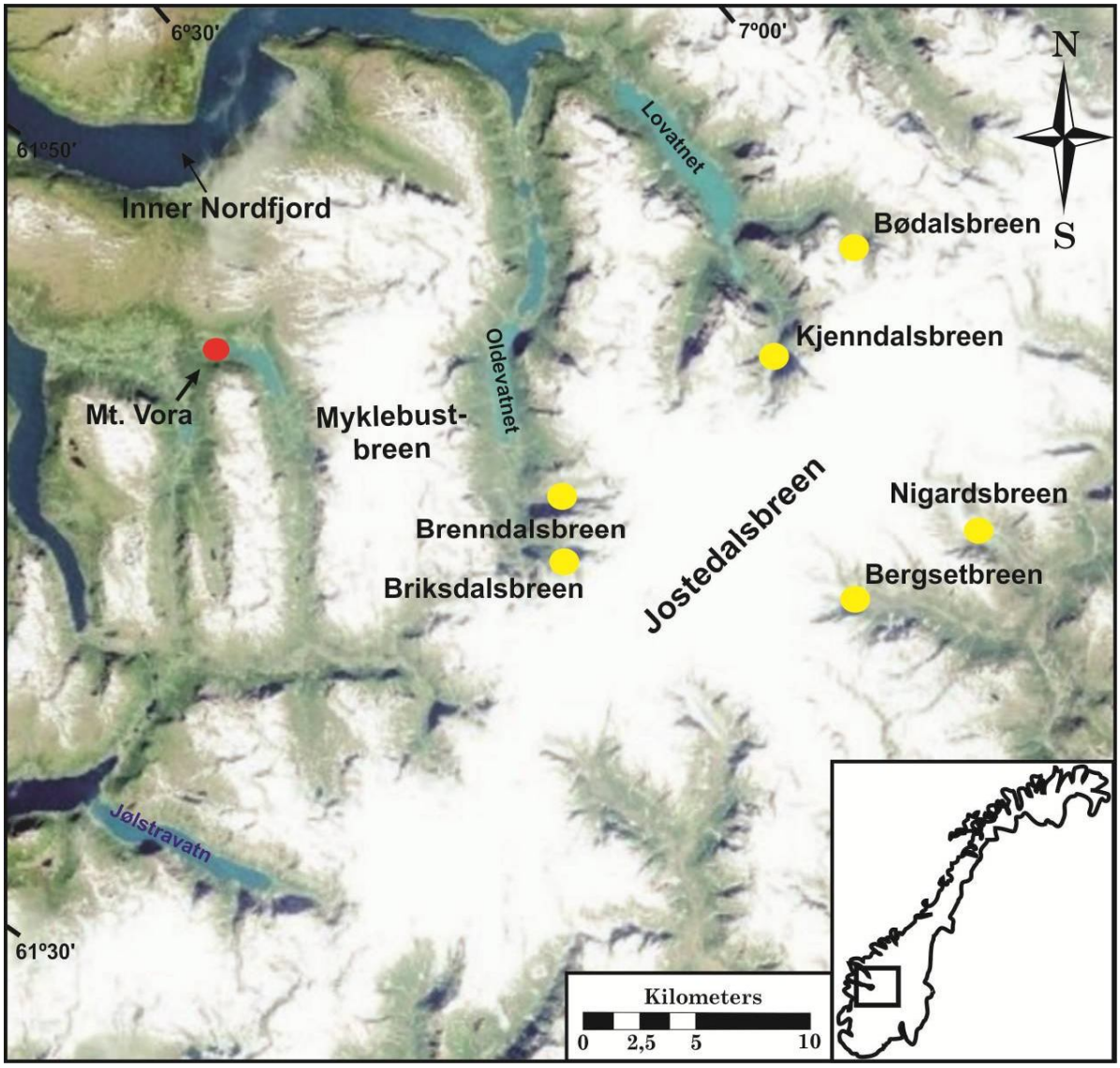

Figure 3.9. Location of sampled rock avalanche deposits (red) and the sediment from glacial environments (yellow), Jostedalsbreen, Norway.

Bergsetbreen and Nigardsbreen are outlet glaciers descending from eastern Jostedalsbreen and have similar patterns of the advance and retreat to the other glaciers. The Bergsetbreen re-advanced in 2000 partially overriding a 1997 moraine and producing a double-ridged lateral

moraine (Winkler and Matthews, 2010). The proglacial area inside the year 2000 moraine is mostly an outwash plain. In 2010 the lower tongue was not connected to the main glacier body hanging from the steep cliff. Dead ice was covered with debris and the remains of snow avalanches. Nigardsbreen is the largest of the glaciers I studied in the area. This glacier retreated from the lake formed within the early 20th century moraine and is currently about 1600 m long. Below the lake there are numerous moraine ridges since the 1748 LIA. Historical data suggest that the glacier was rapidly advancing during LIA from AD 1710 till 1735 at rates of 112 m/yr (Nesje, 2005). The moraines of 1845, 1873, 1909, 1937 and 1950 are preserved, and the 1873 moraine is the largest in the valley. Nigardsbreen currently shows the most positive net balance in Norway. It had had a general positive mass balance from 1964 to 2000 (Andreassen et al., 2005), caused by its high altitude accumulation area (Chinn et al., 2005).

Table 3.3. Topographic data of studied glaciers, the data taken from Andreassen et al. (2005), which since has been modified.

Glacier	Area in km^2	Length in km	Altitude in m asl	Coordinates N	E
Bødalsbreen	8.2	6.5	740-1990	61 47	007 06
Kjenndalsbreen	19.1	6.9	380-1960	61 44	007 01
Brenndalsbreen	18	9.6	510-1960	61 40	006 51
Briksdalsbreen	11.9	6	350-1910	61 39	006 51
Bergsetbreen	10.5	4.8	560-1960	61 38	007 06
Nigardsbreen	48.2	9.6	355-1950	61 40	007 12

3.3. KALININGRAD REGION, RUSSIA

3.3.1. Physical settings

Kaliningrad region is the western State of the Russian Federation and is located in the South-eastern Baltic between Lithuania to the north and Poland to the south. Palaeozoic sedimentary rocks of the East European Platform border the Fennoscandian Shield to the east and south, and are exposed along the shores of the Baltic Sea, while to the south-east (south of the Baltic Sea)

lies a zone of younger Palaeozoic, Mesozoic and Cretaceous sedimentary rocks (Donner, 1995). On top of this sequence rests Quaternary sediment from the last glaciation, the effects of which during LGM reached central Poland and Germany. The Kaliningrad region lies in south-eastern part of the Baltic Syneclise, a depression in the platform basement, where only Quaternary and Cenozoic sedimentary rocks are exposed. Over most of the area, the Weichselian continental glacier eroded away Cenozoic rocks and the glacial sediments (till and end moraines) resting directly on the Cretaceous rocks. Only on the Sambia Peninsula is the recessional moraine ridge cover preserved on top of Cenozoic rocks.

A thick layer of till covers the Kaliningrad region. It varies from 4-5 m along the coast to a depth of up to 100 m inland. Three phases are distinguished in Late Vistulian ice sheet limits in nothern Poland (south from Kaliningrad region) (Marks, 2010): at 24 kyrs BP (Leszno Phase), 19-20 kyrs (Poznan Phase) and 16-17 kyrs (Pomeranian Phase) with ice sheet retreats between these re-advances. There are no dated LGM continental moraines in the Kaliningrad region, but data from adjacent moraine ridges in Lithuania and Poland allow that to be interpolated to be about 13.5-14 kyrs BP (Fig.3.10; Donner, 1995; Kalm, 2010; Marks, 2010).

3.3.2. Glacial deposits

The sediment is a sandy-silt with some clays and gravel, while erratics that originated from north of the Baltic trench, Latvia and Lithuanian, also occur. Three samples were collected from moraine outcrops on the coast of the Baltic Sea in an area of an anthropogenically produced series of terraces in the cliff near Primor`e and from a beach outcrop 2 km east from Primor`e (Appendix E).

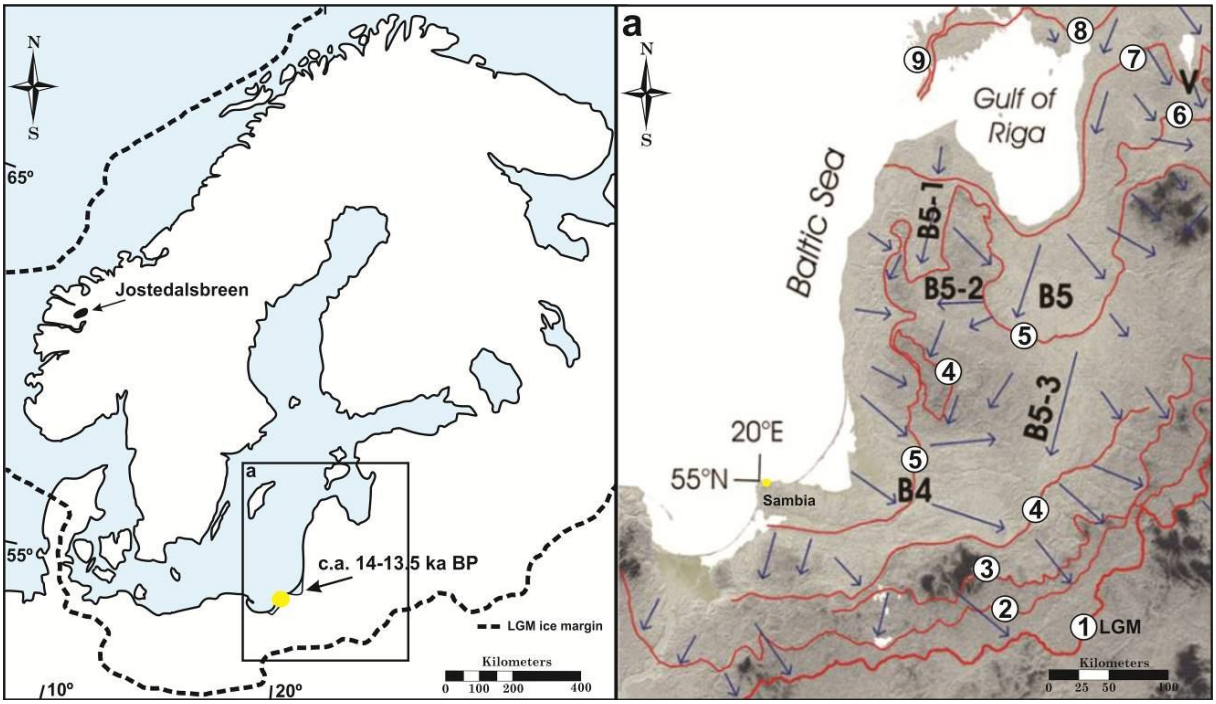

Figure 3.10. Location of the samples taken from basal moraines of the continental glaciation, Weichselian ice sheet over Fennoscandia, South-East Baltic, of the post-LGM deglaciation (according to the Donner, 1995) with respect to the Jostedalsbreen ice cap, Norway, where a) represents the ice lobes and marginal position of the last Scandinavian Ice Sheet southeast of the Baltic Sea, modified from Kalm (2010) with indicate ice streams complexes: the Baltic ice stream complex (B) with Neman (B4) and Riga (B5) ice-streams and Usma (B5–1), Vadakste (B5–2) and Zemgale (B5–3) sub-ice-streams and Võrtsjärv ice stream (V); and ice marginal zones: 1 – LGM; 2 – Baltija (Pomeranian); 3 – South Lithuanian; 4 – Middle Lithuanian, 5 – North Lithuanian; 6 – Otepää, 7 – Sakala; 8 – Pandivere; 9 – Palivere.

4. Laboratory studies: the impact of debris-cover on ice ablation

4.1. INTRODUCTION

The main impact that supraglacial rock avalanche debris has is to reduce or halt ice-surface ablation and thus cause a shift of net mass balance; the additional weight of rock debris also results in a change of glacier motion. The response of affected glaciers will lead to non-climatic changes in the valley morphology. However, because there are few detailed case studies and a resultant lack of appropriate models which predict how a glacier might respond to rock avalanche debris deposition, debate continues within the scientific community about the impact of rock avalanches on the glacial record.

In this chapter I test the hypothesis that a thick cover of rock avalanche debris on the surface of a glacier will reduce its ablation, alter its mass balance and, as a result, alter its behaviour. This chapter focuses on the impact of debris-cover on glacial ablation, and results from the first laboratory experiments conducted on the effects of debris of different thicknesses and properties on ice ablation are presented. The experimental results and their implications are discussed.

4.2. THEORY

4.2.1. Acceleration and inhibition of ice ablation under debris cover

A thin debris cover accelerates the melting rate of the underlying ice due to increased absorption of solar energy by the low-albedo debris and transmission of that heat to the ice (Clark et al., 1994). Østrem (1959) suggested that the layer of debris must be of a thickness equivalent to the mean particle diameter in the cover to increase ice ablation in comparison to adjacent debris-free ice. Other studies (e.g. Nicholson and Benn, 2006) have suggested that accelerated ablation occurs below thin debris layers, not as a result of the ability of the debris to absorb more radiation, but rather because the debris layer is discontinuous, with clean ice patches melting faster due to the re-radiation of heat from numerous, surrounding patches of debris. Although this mechanism is not disputed, it is apparent that uniformly thin debris layers indeed do have the ability to accelerate ablation of underlying ice by low albedo of the debris layer that increases ablation rates (‘rising limb’). In contrast, scattered aggregations of

particles (formed during melting) occurring as a dust cover “have a negative feedback on melting” (Adhikari et al., 1997, p.92). The problem of estimating the effect of thin debris layers on melt-rates relates to the irregular topography and constantly changing surface of the glacier that make measurement of a continuous 1 cm debris layer inaccurate if not impossible.

Debris covers that are thicker than a critical depth reduce heat transfer from the debris surface to the ice and, with increasing debris thickness, lead to a reduction of the total ice ablation. Not only the thickness but also the debris properties alter absorbed incident radiation (thermal conductivity, porosity, permeability, and colour) and its transmitted downwards resulting in altered ablation rates under the debris.

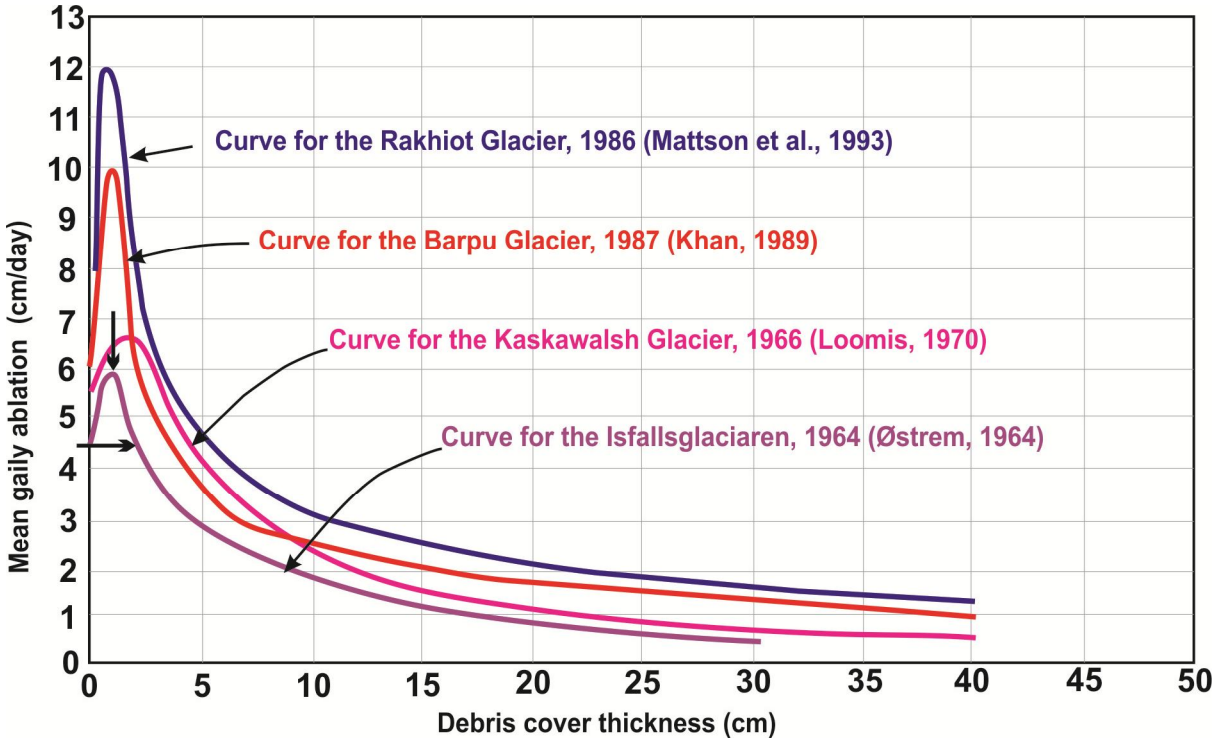

Figure 4.1. Relationships between debris-cover thickness and ablation rate under debris layers on glaciers. Vertical arrow indicates the effectiveness thickness and horizontal arrow indicates the critical thickness (see definitions in text). Adapted from Mattson et al. (1993).

Very small debris thicknesses in all cases show ablation rates higher than for bare ice, however, once the specific thickness associated with maximum ablation rate is passed (at which point, increased solar absorption by low-albedo debris is offset by reduced heat conduction through thicker debris) the ablation decreases to a point where ablation rates are equal to that for bare ice under the same conditions (“critical thickness”; Adhikary et al.,

1997; Nakawo and Rana, 1999). Beyond this point, ablation decreases exponentially and under a 2-3 m thick debris layer, surface melting practically ceases (Bozhinskiy et al., 1986) (Fig. 4.1). Thus, the critical thickness represents a comparison between debris-free ice and sub-debris melt rates under the same conditions, where variations in bare ice melt rate are implicit in the critical thickness.

4.2.2. Heat flow and thermal conductivity within the debris layer

Heat flow through a substrate will occur when temperature differences exist across it. In the case of a debris layer, it is impossible to isolate and determine all the physical properties and characteristics of individual components making up that deposit, thus calculations of the contributions made by each of the variables to heat flow are always estimates. Heat transfer within the debris layer occurs as a result of both conduction and advection. McSaveney (1975) suggested that the heat flow is a response to a temperature gradient normal to the plane of the debris layer, and that the debris layer may be treated as a uniform aggregate of isotropic thermal conductivity. The heat flow (h) through the debris layer will depend on the temperature (T) variation with vertical thickness (x) and the thermal conductivity (k) of the debris:

$$h = - k \frac{dT}{dx} \qquad (4.1)$$

Thermal conductivity of the debris can be estimated since the thermal conductivity of the debris layer parent rock, the porosity of the debris layer and its moisture content are all measureable. If the debris layer is lithologically uniform, then the thermal conductivity may be obtained from published data or by laboratory measurements. In the case of multiple lithologies, the percentage contribution from each lithology gives the average thermal conductivity (McSaveney, 1975). The porosity is not usually measured *in situ*, but rather is an estimate based on the theoretical conditions of the particle sorting and packing (Kirkbride, 1989; Table 4.1). High water content increases the thermal conductivity of the debris (Nakawo and Young, 1981), although McSaveney (1975) showed that the porosity has a larger impact on thermal conductivity than the water content. Additionally, during the melting the debris in contact with ice will be continuously saturated, whereas moisture levels in the surface layer will depend on weather conditions, which may periodically lead to wetting, drying or freezing from the surface downwards. The advection of heat by air flow or water

percolation will contribute to heat transfer through the debris layer and this will depend on either the permeability of the debris, or its voids volume. McSaveney (1975) observed that although thermal conductivity is unaffected by permeability, the presence of the pore passages within the debris will accelerate water percolation and heat-transfer. He concluded that low permeability inhibits advection at the base of the debris layer, whereas factors that contribute to the advective heat flow are important in the upper part of the debris.

Table 4.1. Published estimates for thermal conductivities (K) of coarse aggregates (adopted from Kirkbride, 1989).

K debris ($W m^{-2} deg$)	K parent lithology ($W m^{-2} deg$)	Porosity %	Moisture content %	Source
1.50	1.50 Ottawa sand	-	-	McKenzie (1969)
1.80	2.30 Greywacke	30 ± 20 assumed	100	McSaveney (1975)
0.79	-	-	-	Driscoll (1980)
2.23	Otawwa sand	-	17 - 22	Nakawo and Young (1981)
1.46	Otawwa sand	-	8 - 17	Nakawo and Young (1982)
1.60	2.80 Granite	40 ± 45 assumed	0	Bozhinskiiy et al. (1986)

The thermal gradient within the debris layer will also vary diurnally, seasonally and annually as a response to surface temperature fluctuations. Instantaneous temperature profiles within the debris layer are not linear, but constantly change in response to fluctuations of the energy available at the surface (Benn and Evans, 2010). It is also known that there is a lag in terms of heat flow through the debris during the day, when during colder periods, surface temperatures may go below zero, while within the debris layer heat will still be being transferred. However, equivalent lags occur after a switch from the cold to the warm part of the diurnal cycle, in which cooling continues at the base resulting in a decreased rate of heat transfer from surface to the base (Fig. 4.2). During a 24 hour cycle, depending on the surface cycle of the temperature and debris thickness, there could be small changes at the base of the debris layer, which determine the melting of covered ice (bottom 3 cm in Fig. 4.2). Seasonal and annual energy changes on the surface of the debris cover will result in a similar pattern, confirming

the importance of location and debris layer characteristics with respect to heat transfer, and their impact with respect to the debris cover and the underlying ice.

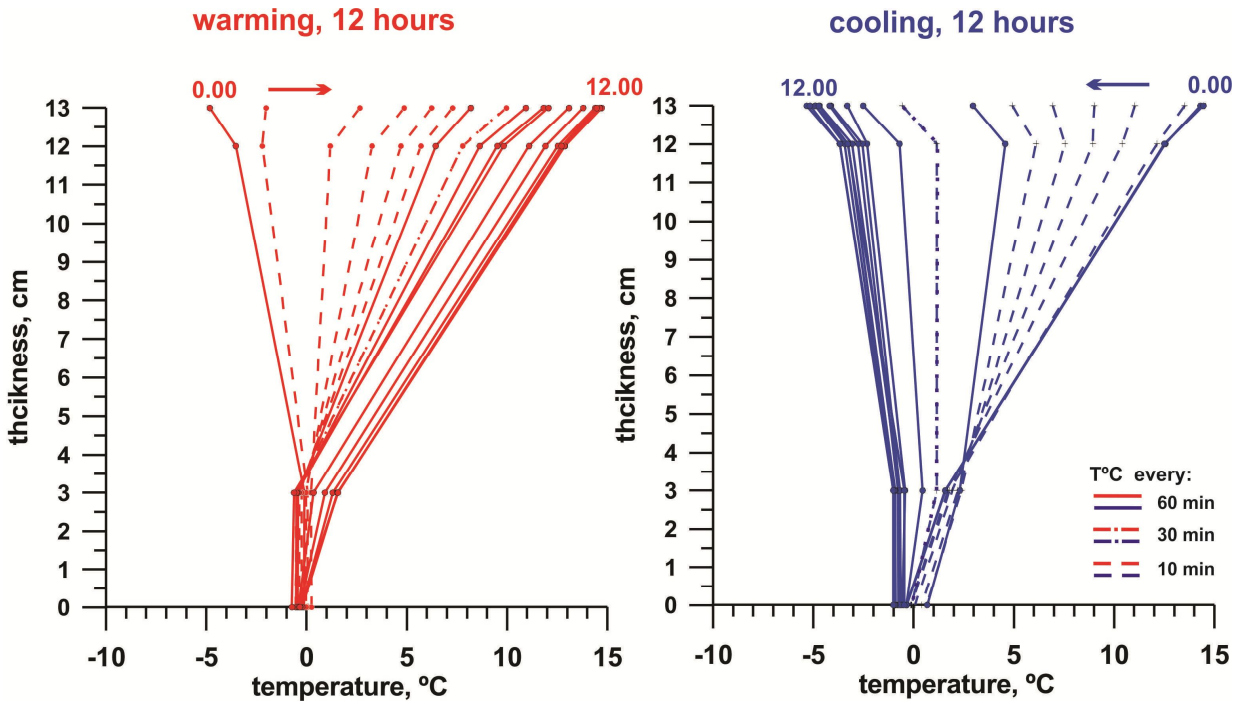

Figure 4.2. Diurnal temperature oscillation at different depths in a 13 cm debris layer obtained during laboratory experiments in this study. Left graph shows the temperature gradient changes during 12 hours of the positive part of the cycle in 12 hours, where right graph shows the changes during next 12 hours cooling, where the surface temperatures reached -5ºC.

4.2.3. Modelling ablation beneath the debris cover

In order to estimate the reduction of ice melting under a debris layer, the heat transfer by conduction and advection through the layer must be determined. McSaveney (1975) and Kirkbride (1989) both concluded that the primary controls are:

- the thickness of the debris layer;
- the thermal conductivity of the debris, which varies with physical properties of the debris;
- the thermal gradient through the debris layer, which varies with daily and seasonal air temperature cycles.

Although the thickness and properties of the deposit are critical contributors to the reduction of ice ablation, radiation cyclicity in the region controls the heat that is available to transfer through the debris. In cold environments with short ablation seasons and mostly negative

temperatures, thin debris layer will prevent ice from melting (Dry Valley in Antarctica; Trevor Chinn, *pers. comm.*, 2010). In contrast, debris layers will reduce ablation less in areas with higher average temperatures and longer periods of ablation. As a result, similar thicknesses of the debris may have significantly different effects on ablation simply as a result of variations in seasonal and annual heat budgets at different locations. This explains variations of melting rate reduction recorded for the same debris thicknesses from different glaciers, and of different critical thicknesses for these glaciers (Fig. 4.1 and Table 4.2).

Table 4.2. Measured critical thicknesses on glaciers, where critical thickness is thickness at which sub-debris ablation rate equals ablation of adjacent bare ice.

Glacier	Country	Latitude °N	Elevation m a.s.l.	Critical thickness mm	Source
Khumbu	Nepal	27.57	5400	50	Kayastha et al. (2000)
Lirung	Nepal	28.13	4400	80	Tangborn and Rana (2000)
Rakhiot	Pakistan	35.21	3400	30	Mattson and Gardner (1989)
Barpu	Pakistan	36.11	4000	25	Khan (1989)*
Kul'dgilga	Kyrgyzstan	39.30	5000	115	Demchenko and Sokolov (1982)
Djankuat	Russia	42.12	2700	70	Popovin and Rozova (2002)
Eliot	USA	45.23	2200	40	Lundstrom et al. (1993)
Peyto	Canada	51.41	2600	15	Nakawo and Young (1981)
Dome	Canada	52.12	2200	20	Mattson (2000)
Athabasca	Canada	52.12	2200	20	Mattson (2000)
Bilchenok	Russia	56.10	700	40	Yamaguchi et al. (2000, 2007)
Kaskawulsh	Canada	60.46	1000	35	Loomis (1970)*
Isfallsglaciären	Sweden	67.54	1200	30	Østrem (1965)

*from Kirkbride and Dugmore (2003)

Calculations of ablation under a debris-cover are based on variations of heat conduction through the debris layer as a function of thickness and physical properties of the debris, or on comparisons of surface ablation of adjacent bare ice under the same conditions (Nakawo and Young 1981, 1982; Bozhinskiy et al., 1986; Kayastha et al., 2000; Konovalov, 2000; Nicholson and Benn, 2006). In general, the melting of the ice under the debris layer (M) can be calculated as:

$$M = \frac{h}{\rho L}, \tag{4.2}$$

where h is downward energy flux at the base of the debris layer (W m^{-2}), ρ is the density of ice (900 kg m^{-3}) and L is the latent heat of fusion (334 kJ kg^{-1}) (Nicholson and Benn, 2006).

Incorporation of the thermal conductivity (k) of the debris layer and temperature differences within a debris layer of thickness x results in the modified equation:

$$M = k\frac{(Ts - Ti)}{x}, \quad (4.3)$$

where T*s* is the steady-state surface temperature and T*i* is the ice temperature.

However, this equation does not take into account diurnal or annual temperature variations and, as a result, produces errors when compared with actual melting under the debris layer. Fujita and Sakai (2000) pointed out that the air temperature at the base of the debris layer on a glacier cannot be simply estimated using a constant lapse rate as in previous studies (Rana et al., 1997; Nakawo et al., 1999). Many recently proposed models use daily mean surface temperature (Conway and Rasmussen, 2000; Nicholson and Benn, 2006) or a degree-day factor (DDF) appropriate for the glacier being studied (Singh et al., 2000; Mihalcea et al., 2006; Zhang et al., 2007; Hagg et al., 2008), and debris thermal resistance rather than thermal conductivity (Kayastha et al, 2000). Nicholson and Benn (2006) suggested that the daily mean temperature gradient is linear, which is relevant for the ablation season of alpine debris-covered glaciers because ablation under the debris can then be calculated by using mean daily meteorological data. However, Haidong et al. (2006) noted the importance of diurnal heat and cold storage within the layer and then calculated ablation under the debris by obtaining the temperature gradient in debris layer based on measurements of heat flow exchange between 3 zones within the debris layer (Fig. 4.3).

4.3. LABORATORY EXPERIMENTS

4.3.1. Debris cover as an insulator

To determine the effects of rock avalanche deposits on glacier behaviour in general the effect of a thick rock avalanche deposit on ice-surface ablation must be understand. Laboratory experiments of the effect of debris cover on surface ice ablation were conducted in the Department of Geological Sciences, University of Canterbury, New Zealand. This appears to be the first laboratory study to directly measure the effect of a debris cover with known physical properties on ice melt rates under controlled conditions. The results provide a crucial insight into the effects of debris on ablation rates, and how these vary in differing insolation regimes.

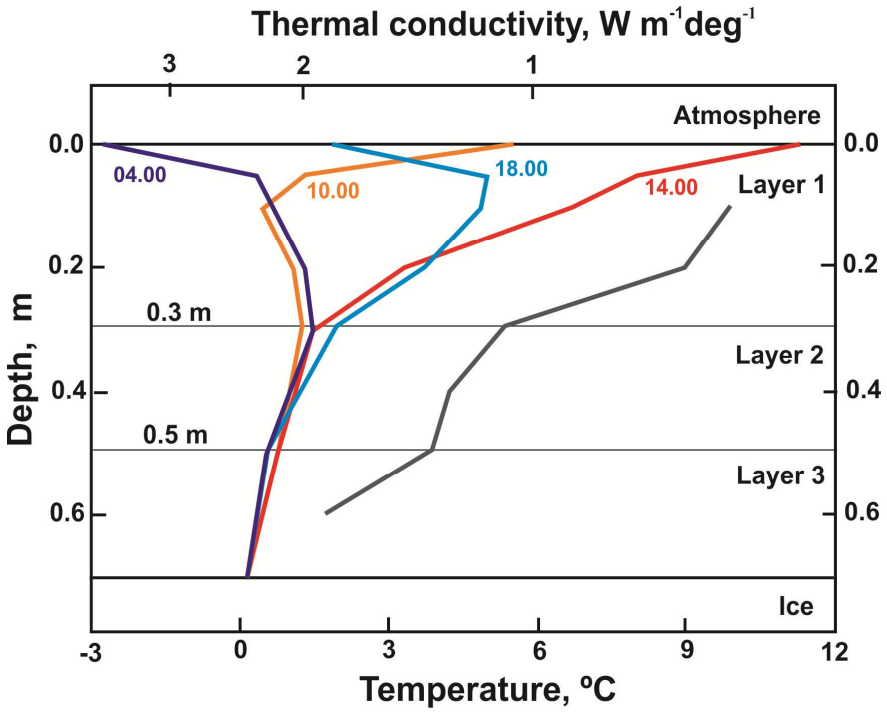

Figure 4.3. Debris temperature profiles and estimated thermal conductivities (gray line) on the Koxkar Glacier, Tien Shan, China, where variations occur according to a three-layer classification scheme based on varying thermal gradient and thermal conductivity. Modified from Haidong et al. (2006).

4.3.1.1. Aims

The experiments were designed to improve understanding of the processes by which debris-cover alters ablation of the covered ice. The relatively simple experiments focussed on melting rates of debris-covered ice in comparison to debris-free ice under the same controlled laboratory conditions, with the specific aim of establishing the basic physical dependencies and dynamic inter-relationships of the processes (Fig. 4.4). It is difficult to arrive at the same endpoint using field observations, since, besides the diurnal cyclicity, there are uncontrolled local spatial and temporal variations of a range of parameters.

Several formulae have been proposed for the calculation of ablation melt under debris cover using thermal conductivity and available heat. However, all previous data describing such ice ablation rates are based on field measurements involving site-specific physical parameters that cause variations in the estimated ablation rates. These observations are in addition primarily based on relatively thin debris layers, where the debris was greater than critical thickness and the influences of altitude and latitude have not been interpreted. Furthermore, the resulting models were based on measurements obtained from field observations often adjusted for the site conditions at the time of measurement (e.g. cloudiness, rainfall, shadows from slopes and

roughness of the glacier surface). As a result, it is extremely difficult to quantify accurately the relationship between debris thickness and ablation in the field and its influence on a glacier's mass balance using field data.

Laboratory experimentation has an added advantage with respect to investigating thin debris cover influences on ablation, because as a result of surface roughness, continuous thin, debris layers on glaciers are rare if not non-existent. In this laboratory study it was not considered necessary to specify the debris properties, such as albedo, humidity, porosity, thermal conductivity and detailed radiation characteristics, as long as the ambient conditions during all experiments were identical. It is important to highlight that the main objective of the experiments was not to reproduce conditions on a glacier, but to study the processes by which the presence of overlying debris affects ice-surface melting under the influence of incident radiation. Thus, in these experiments the insulation behaviour of the debris cover was examined under arbitrary "x"- conditions in comparison with bare ice under same "x"-conditions.

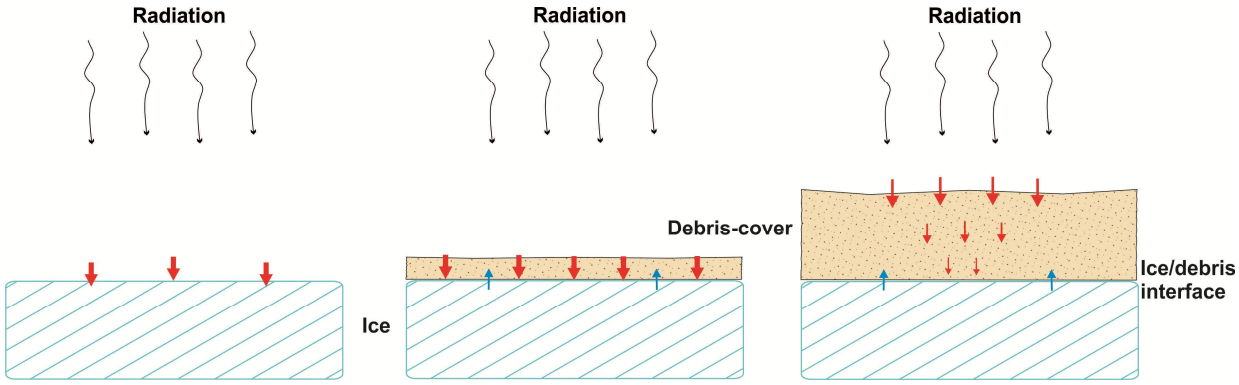

Figure 4.4. Scheme of the ice melting for debris-free ice, accelerated melting under thin debris layer and retarded melting under the thick layer of the debris.

4.3.1.2. Method

To examine the influence of debris cover on ablation rates, debris-free (bare) ice melt rates were compared with those under debris thicknesses by exposing identical blocks of bare ice and ice covered with debris to identical exposure levels of radiation. Two main sets of experiments were conducted:

1. In the first set of experiments, debris-free and debris-covered ice blocks were exposed to identical steady inputs of continuous radiation until melting was complete. This is

referred to as the "steady-state" experiment, the main objective of which was to determine the extent to which debris may act as an insulator;

2. The second set of experiments focussed on the effects of diurnal temperature and radiation cycles, which were generated by alternately cooling the ice in chest freezers for half of the cycle and exposing it to radiation for the same length of time (12 hours.)

The ice blocks (approx. 450 x 350 x 260 mm) were made by freezing approximately 35 litres of water in insulated containers ("chilly bins"), which have insulated walls that minimize ice melt near the sides and base, leading to increased confidence that surface ablation is accurately recorded (Fig. 4.5). To eliminate the effect of melting associated with the accumulation of meltwater on the floor of the container, the bases of the containers had a series of ribs which directed any water to a drainage tap located at the end of the container. Each experimental run was initiated only after the rate of meltwater drainage had stabilized in order to eliminate concentration of the meltwater on the surface. As a result of the very effective insulation of the containers, the water channels remained active during the cooling periods and thus the drainage system remained open, ready for the next period of heating.

To simulate solar radiation, incandescent and warm-white bulbs with different light spectra were used simultaneously; together these produced radiation with a wavelength range of approximately 350 to 750 nm. The incandescent bulb has high radiant power from 500 nm for long wave spectra while the warm white bulb has a peak at 400 to 450 nm which covers the short wave spectra. In order to introduce diurnal cyclicity the radiation was constant for 12 hours followed by constant cooling for the next 12 hours with the lights switched off. Thus, the "day" (up to 20ºC) and "night" (down to -5ºC) parts of the cycles were each maintained for 12 hours. The temperature range was chosen because this allowed for efficient recording of the physical processes rather than the development of a data set appropriate for comparison with published field data. Although one could argue that not all glaciers experience freezing during the night, in high mountains many glacier ablation zones are exposed to negative temperatures during most nights of the year. It is important to emphasize again that the objectives of this study were not to simulate daytime variations of radiation appropriate to 'field' conditions, but rather, to expose the ice to well-constrained cyclically-changing conditions. It would be almost impossible to replicate radiation changes experienced in the field, including constantly changing meteorological condition (clouds, different radiation

duration and intensity that change every day according to latitude and sun angle), valley slope exposures, shadows and roughness of the glacier surface.

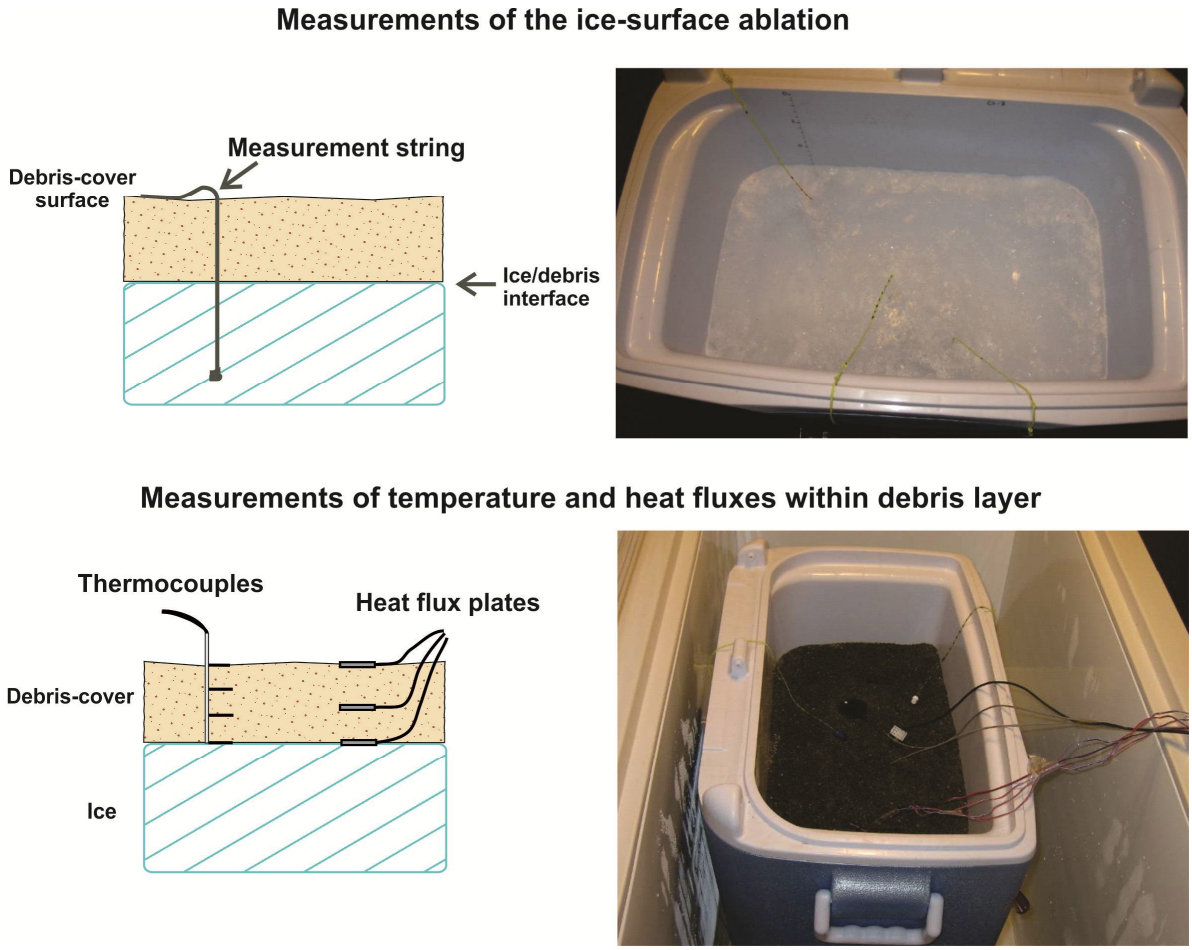

Figure 4.5. Experimental data acquisition system: measurement strings within the ice block accurately record of the ice surface ablation. Thermocouples and heat flux plates record temperature and heat flow at various levels within the debris layer.

Ablation rates of the ice surface were measured at intervals of 12 hours with 0.5 mm accuracy by a system of vertical measuring strings that were frozen inside the ice blocks to avoid side and bottom melting. Additionally, water discharges (ml/hour) of the melting ice blocks were recorded. The sediment representing a normal melt-out supraglacial debris-cover was uniformly spread on the ice surface in layers 10, 50, 90 and 130 mm thick. Normal melt-out supraglacial debris occurs commonly as a thin, fines-poor englacially-sourced deposit with high permeability and low thermal inertia on the glacier surface in the ablation zone. Greywacke sand of 0.5 mm mean diameter was chosen to represent this type of debris-cover because its insulation properties (grading, permeability and thermal inertia) were considered

comparable. This sediment provides a qualitative contrast between these materials and the debris of rock avalanches which is much thicker (of the order of metres), fines-rich, of lower permeability and high thermal inertia. Specific debris properties (porosity, moisture content etc.) have not been measured for the experiments due to comparative method of the experiments.

Because the objective was to compare melt-rates between bare and debris-covered ice under identical conditions, it was not necessary to monitor or control ambient conditions in the laboratory; however measured debris-surface air temperatures provided a good indication of variations of ambient temperature. During these experiments data of constant temperature profiles measured by temperature sensors, or thermocouples, and heat fluxes (local heat flow W/m^2) through the debris layer (at debris surface, within the debris layer and at the ice-debris interface) were collected and recorded by using a datalogger (Campbell Scientific 21X micrologger) connected to a computer (Fig. 4.6). All data were recorded at 10 minutes intervals and loaded into the PC for analysis.

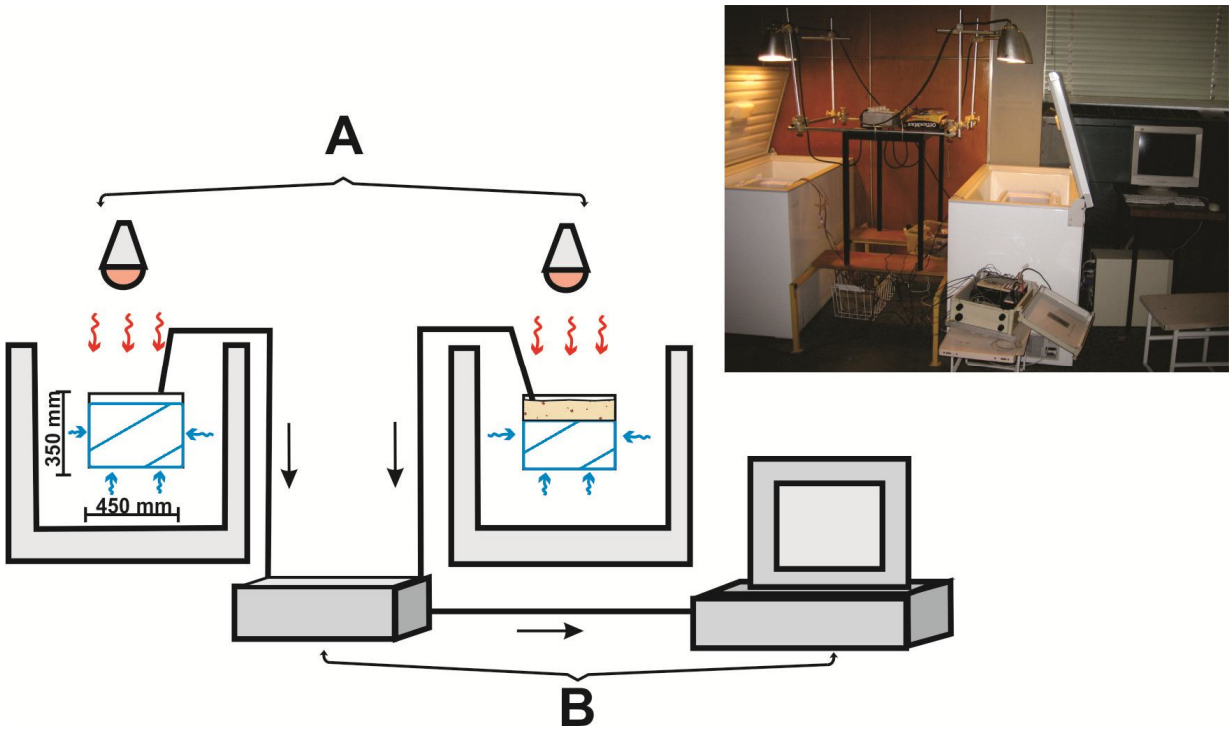

Figure 4.6. Experimental arrangement for tests with diurnal cycles: A - blocks of bare and debris-covered ice exposed to identical radiation during the 12–hour ablation period (attained by two electric bulbs with short and long wave radiation, shown by red lines) and cooling by freezer during the 12-hour night (shown by blue lines); B - Campbell Scientific 21X data logger and PC, which recorded temperature and heat fluxes profiles.

4.3.1.3. Results

Experiments under steady-state conditions

Five identical pairs of bare ice blocks and ice blocks under 10, 50, 90 and 130 mm of debris were exposed to constant levels of radiation until all of the ice melted. This series of experiments with constant radiation and narrowly-graded sand matched previously reported rates of ice ablation as a function of debris-cover thickness (e.g. Østrem, 1965; Lundstrom et al., 1993; Mattson et al., 1993), in the sense that the laboratory data showed that initially, ice under 10 mm debris-cover melts accelerated and under a $\geq$ 50 mm layer reduced. Complete melting of the ice block with a debris cover of 10 mm took about 120 hours, while the block with a cover of 130 mm needed more than 175 hours (Fig. 4.7). Debris-free ice melted about in 140 hours, and ice blocks under 50 and 90 mm required approximately 150 and 160 hours respectively.

The reduction of melting rate of the ice under the thicker debris-cover was primarily caused by the absorption of heat by the initially cold debris cover at the beginning of the experiment. Once heat conduction through the debris achieved a steady state, and the melting rate became constant, ice ablation rates were similar under each of the debris-cover thicknesses. In Figure 4.7 the parallel trend of the ablation rates is apparent after different trends during the stabilization periods (12 hours for clean ice and ice under thinner thicknesses, and more about 30 hours for ice under thickness in 130 mm). The melting rate with clean ice was consistently about 10% less than with 10 mm of debris, this presumably was an albedo effect.

The effect of the debris in slowing the melting rate prior to stabilization varied in direct relationship to its thickness. Thicknesses greater than 90 mm delayed the onset of melting significantly. The onset of ice melting under 130 mm of debris was delayed more than 12 hours and melt-rate stabilization occurred only after 60 hours (Fig. 4.7). The duration of retarding of the melting rates is dependent on the initial condition of the system; influences such as debris thickness, physical properties and initial debris temperature, and radiation intensity are all contributing factors. It can be concluded that with steady-state heat transfer, the rate at which energy enters the debris (after albedo effects are overcome) must equal the rate at which energy is transferred to the ice-surface. Because some energy has already been consumed in heating the debris layer, subsequently all available heat will be transferred to the debris-ice interface.

After reaching a peak value, water discharge steadily declines in the case of all ice block melting experiments (Fig. 4.8). This is due to the increasing distance between the radiation source (light bulbs) and the surface of the ice (debris-cover), as the ice melts. In contrast with real glaciers, where this increase is negligible, in the laboratory the ice surface lowering played a more important role and was noticeable when the distance exceeds 5-10 cm (5-10% changes of original bulb-ice surface distance of 1 m).

These results show that, under constant radiation, significant debris cover delays the occurrence of steady-state ablation, but once this occurred, the ablation rate is independent of debris depth. It should be noted that under steady-state conditions, it took over 12 hours to establish constant heat conduction and to achieve the same ablation rates as those for bare ice covered by a debris layer ≥50 mm (Fig. 4.8). This suggests that under diurnally-cyclic radiation, steady-state heat transmission may never be entirely achieved throughout the entire vertical section of that cover. This observation suggested further experiments aimed at investigating the effect of diurnally-cyclic radiation on ice ablation beneath debris layers.

Experiments under diurnal cycles

Under exposure to diurnally-cyclic radiation, the time-averaged melt rate was slower. As a result it took longer to melt the ice than under steady-state conditions (Fig. 4.9). Overall, experiment duration was more than 430 hours (about 3 weeks), which represents a 3-fold increase when compared to melting of the same amount of ice under steady-state radiation. In comparison, melting of 10 cm of debris-free ice under constant radiation took about 70 hours, but the same amount of melt under 12 hour heating and cooling cycles took about 150 hours (the actual melt occurred during the 12 hours heating part of the cycle). Therefore, the melt rate for debris-free ice was the same in both situations.

Under cyclic radiation the ablation retardation increases with the thicker debris layers. Thus, in about 390 hours 250 mm of debris-free ice melted, but under 50 mm of debris only 150 mm, under 90 mm of debris 115 mm and under 130 mm of debris only 85 mm of ice melted. In a further experiment with cyclically varied radiation levels, with a debris layer of 200 mm only 35 mm of ice was melted in 390 hours, representing an 86% reduction of ablation (Fig. 4.10). It appears that under diurnal radiation cycles a stable heat-conduction profile was never achieved within debris layers ≥50 mm thick.

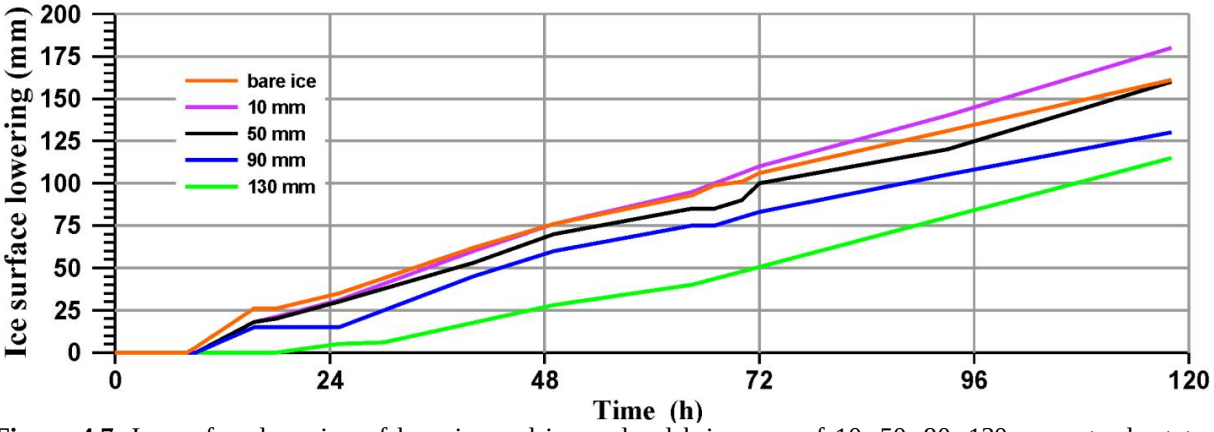

Figure 4.7. Ice-surface lowering of bare ice and ice under debris-cover of 10, 50, 90, 130 mm; steady-state conditions. The almost parallel lines after the initial period of stabilization and almost constant melt rates indicate the similar effect of different thicknesses of debris cover on ablation rates.

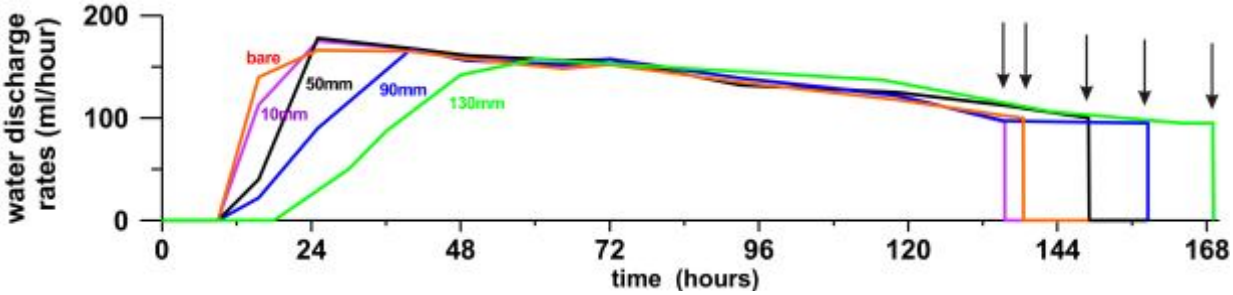

Figure 4.8. Water discharge rates for bare ice and ice under 10, 50, 90, 130 mm of debris-cover in steady state conditions, where the arrows indicate the end of melting for bare ice and ice under debris of different thicknesses (note also the different initial rates of melting under different thicknesses of debris). The decrease of melt rate with time is caused by the increasing distance of the ice or debris surface from the radiation source as melting proceeds.

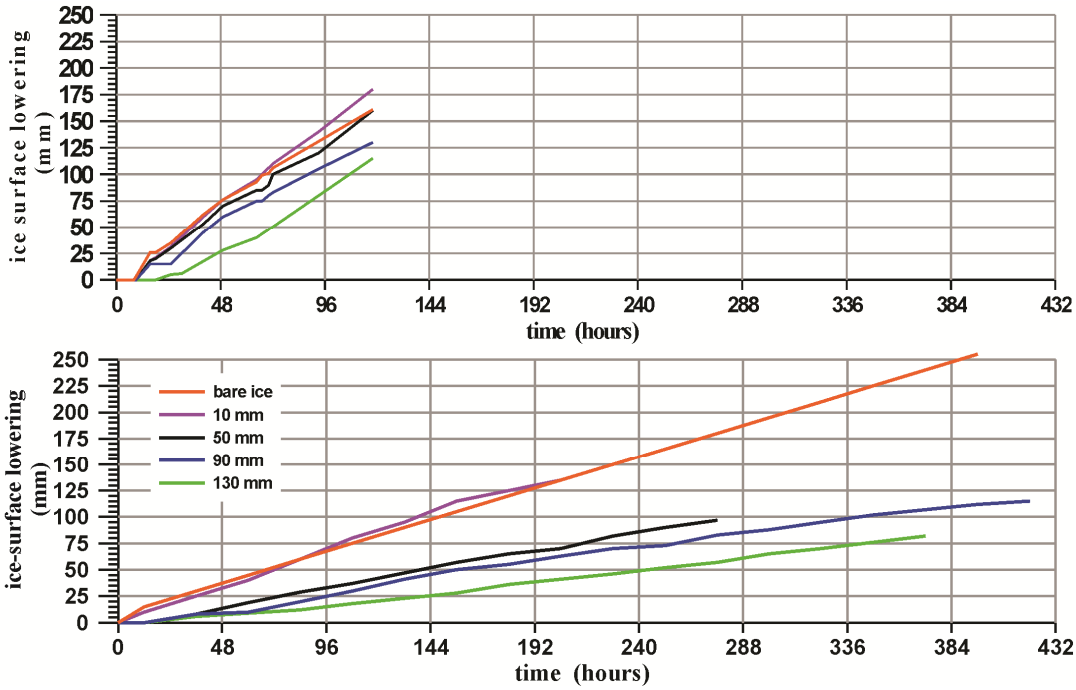

Figure 4.9. Ice-surface lowering of bare ice and ice under debris-cover of 10, 50, 90, 130 mm under diurnal-cyclic conditions (bottom); note the duration of the experiments and different slopes of the ice-surface elevation reduction lines in comparison with steady-state conditions (top). In both sets of experiments the initial ice volumes were equal; however the diurnal-cycle experiments were not all run to complete melting.

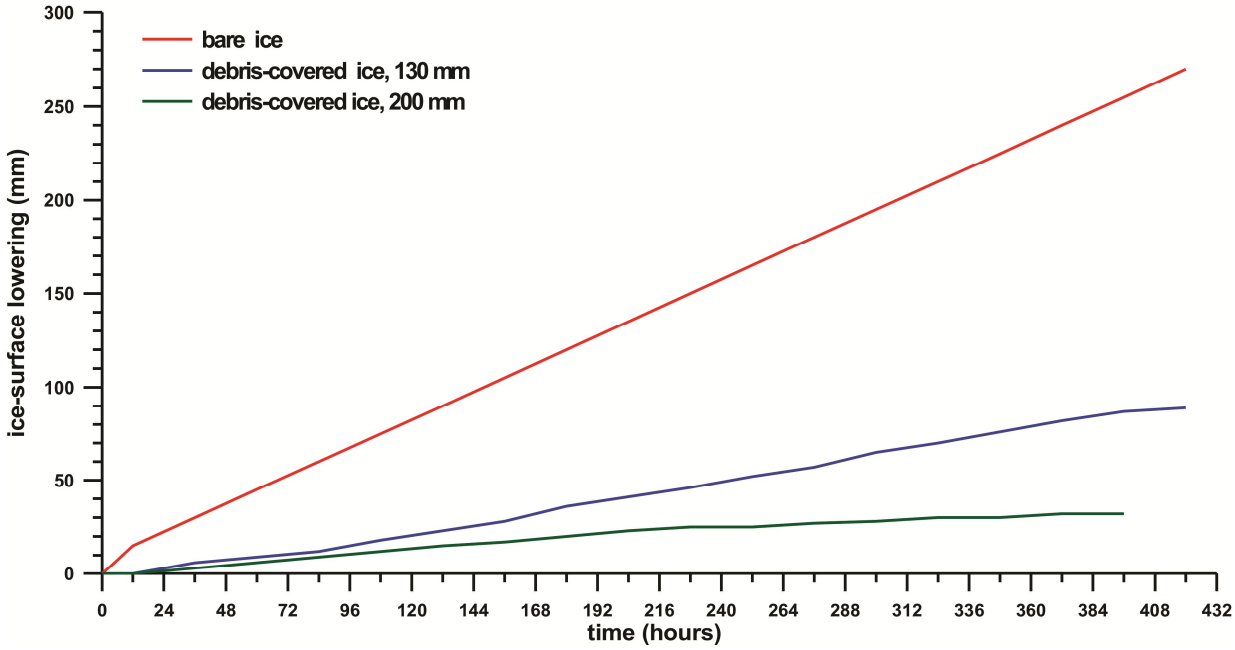

Figure 4.10. Surface level reduction of bare ice without any debris-cover (red line), of ice under 130 mm of debris (blue line) and of ice under 200 mm of debris during about 400 hours with exposure to diurnally cyclic radiation.

Heat flux and temperature-profile changes through the debris layer clearly show the effect of the debris layer on heat conduction (Fig. 4.11). After the ablation period of the cycle, when radiation ceases and cooling begins, the system temperature decreases. However, due to the heat capacity of the debris, it takes longer than the cooling part of the cycle to fully cool the debris. With every cycle these processes recur and consequently the system never reaches a steady state. Figure 4.12 shows examples of the temperature profiles and heat fluxes for one cycle through different debris thicknesses in comparison with non-cyclic experiments, where with 90 and 130 mm of debris layer the overall melting of ice is significantly slower under diurnal conditions.

During all experiments the basal part of the debris layer consistently became saturated with meltwater; and in steady-state experiments, depending on the debris thickness, the whole debris cover became saturated after a time (Fig. 4.13). In the diurnal-cycle experiments this processes was significantly retarded and it took of the order of days to saturate the debris layer to more than 50 mm from the ice surface.

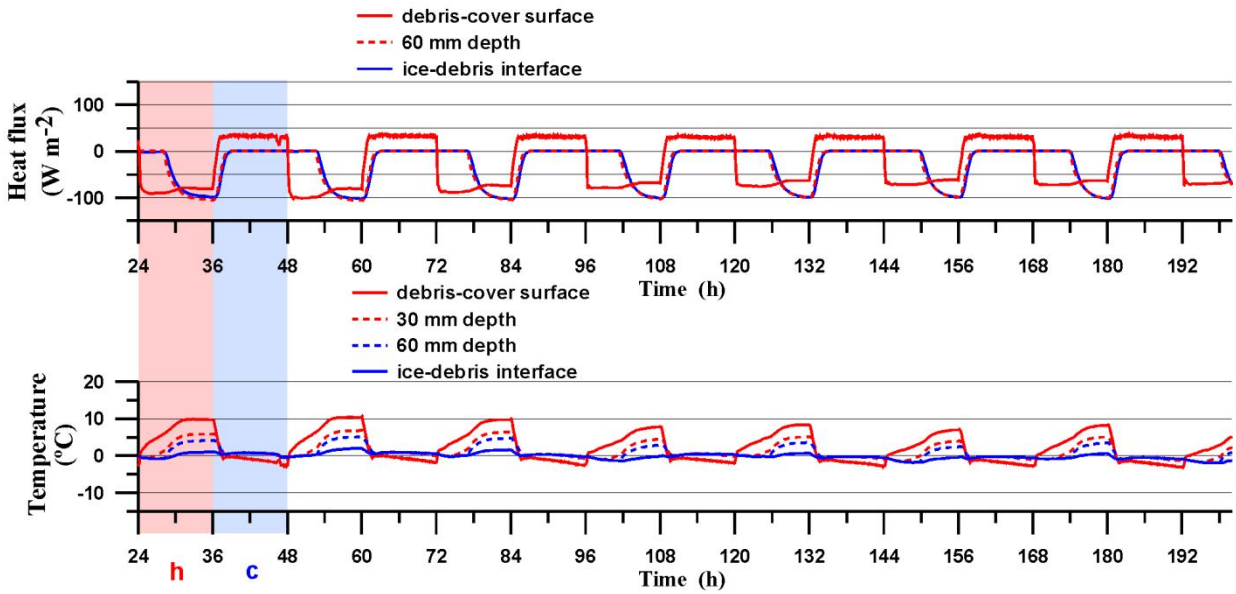

Figure 4.11. Examples of heat fluxes and temperature profiles through a 90 mm thick debris layer (at the debris surface, at depths of 30 and 60 mm and at the ice-debris interface) under diurnally-cyclic radiation. "h" indicates the heating part of the cycle with radiation exposure, and "c" indicates the cooling part of the cycle. Heat flux profiles show the delayed response of the deeper layer of the debris to radiation exposure during the ablation period of the cycles, where it takes more than 6 hours (half the period) to start heat conduction through the whole layer. Note the same trend in the temperature profiles, where as a result the temperature variation decreases towards the ice-debris interface.

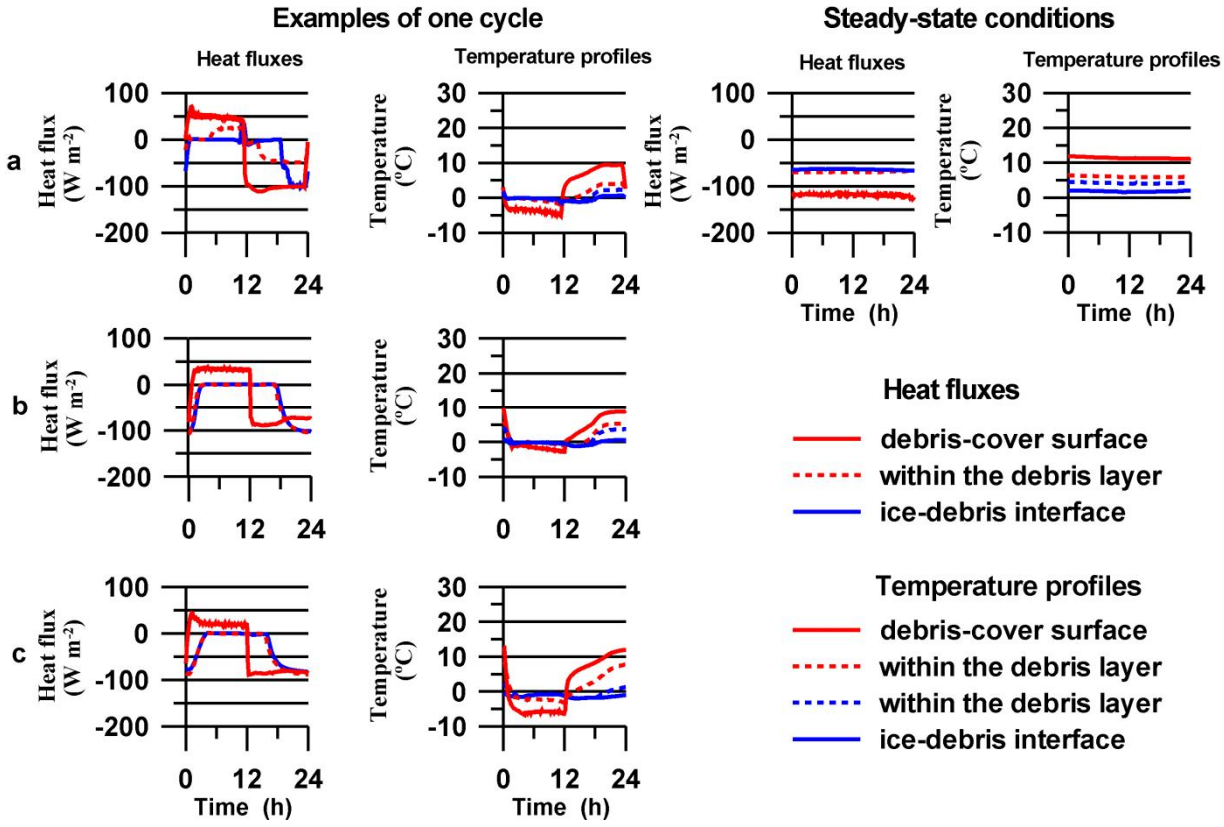

Figure 4.12. Examples of one cycle (24 hours) of temperature profiles and heat fluxes through debris-cover thicknesses of 50, 90 and 130 mm (the first 12 hours of the cycle is a cooling part), in comparison with the steady-state temperature profiles and heat fluxes through 50 mm debris-cover thickness. Note the constant heat transmission through the layer under steady radiation in comparison with changes under diurnal cycles.

Figure 4.13. Saturation of the 50 mm debris layer under diurnal-cycle conditions. At left the sediment is patchily saturated during first several days of the experiment, at right the debris is almost totally saturated after the fifth day of the experiment.

4.3.1.4. Discussion

The data collected are presented as graphs of coefficient of ice surface melting ratio (k) against time, for each debris-cover thickness k was defined as ratio of the melting rates of debris-covered ice and bare ice:

$$k = V_d/V_b \tag{4.4}$$

where V_d and V_b are the melting rates of the debris-covered ice surface and the bare ice surface respectively; $k < 1$ indicates reduced ablation rate; $k > 1$ indicates ablation increased by debris cover (Fig. 4.14). For each experiment the average coefficient of ice surface melting ratio (k) was calculated and plotted against the debris layer thicknesses (Fig. 4.15). Although the average k for the steady-state conditions was calculated from data after the heat flux through the debris and melting rates had stabilised, the average k for the ice under cyclic conditions remains significantly lower.

The steady-state experiments showed that debris cover delayed the onset of steady melting, but did not affect overall ice melting rates once stabilization of the heat conduction profile through the debris layer was achieved. Therefore, the debris depth had a minor effect on ice-surface ablation. In contrast, under diurnal cycles, when the system is constantly exposed to changing environmental conditions, these delays – repeated daily – result in the insulating effect of the debris cover on the glacier ice. Thus, the steady-state tests were crucial in quantifying the delay in heat transfer to the ice-surface as a function of debris depth. However, when the delay in heat transfer exceeded the length of a radiation period of the

diurnal cycle, the thermal inertia of the debris was sufficient to prevent steady-state heat transfer from occurring.

This leads to an understanding of the role of amplitude and duration of the positive (heating) and negative (cooling) parts of the cycles (or the role of the temperature amplitude as a function of the total radiation intensity) in controlling the thermal effect of the debris cover. The ablation rates of ice under debris will vary with the relative amplitudes of the positive and negative parts of the radiation cycle. Ablation is also affected by the length of time that the system is exposed to positive and negative radiation during each cycle. The interaction between these two variables will determine the degree of insulation afforded by the debris cover. In effect, a given depth of debris has a particular thermal inertia; the duration and intensity of the cycles, relative to that inertia, determine the dynamics of energy transfer to the underlying ice and thus the melt rate.

The experiments show that with more than 50 mm of debris-cover the retardation of ablation in comparison with debris-free ice is linear (Fig. 4.16). Therefore, in the diurnal-cycle experiments, 50 mm of debris cover is the threshold thickness above which ablation reduction is linear. There is similar linear dependency of increase in the melting duration (in times) of the ice under debris thicknesses > 50 mm for experiments with diurnal-cycles in comparison with steady-state (Fig. 4.17). A similar trend can be seen from the graphs of ablation melting rates under diurnal-cycle condition (Figs. 4.9 and 4.10). Evidently, the melting reduction under the debris-cover re-occurs every new cycle and total melting rates decrease with increasing numbers of cycles for more than several melting days. In contrast, the melting rates of debris-free ice are stable irrespective of the time after the experiment starts. Therefore, the melting rates of ice under the debris at different periods of the experiment will be different that will be controlled by debris thicknesses and cyclicity. Variation of k during the experiment reflects this trend, k decreasing from > 0.5 at the beginning of the experiment to about 0.3-0.4 at the end.

This phenomenon could be explained as follows:

- Firstly, by the increasing distance between the radiation source and the surface of the debris-cover as ice melts, that was also apparent in the experiments under the constant radiation. However, it is not the preferred explanation because the melting rates of the ice under 130-200 mm of the debris are very low and the surface elevation changes during the time could be negligible (in order of 10-30 mm).

- Secondly, the saturation degree of the debris layer with time could have affected the changes of the ablation rates. After several cycles the debris layer becomes saturated with water from the ablation of the underlying ice (Fig. 4.13), whereas for steady-state experiments saturation occurred in the stabilization period (the first 12-36 hours depending on the debris thickness). The debris-ice interface is never more than 0 Cº, and as a result, the thermal gradient due to the water saturation of the debris affected the ablation rates of the ice. Under cyclic radiation, the saturated debris layer was affected during the cooling part of the cycle by freezing the water from the surface, which then needed more energy to heat it up during next positive part of the cycle. However, if the cooling part of the radiation cycles is not below 0 Cº (or is for a shorter period of time), the thermal gradient of the debris layer will have a different effect on ablation of the underlying ice.

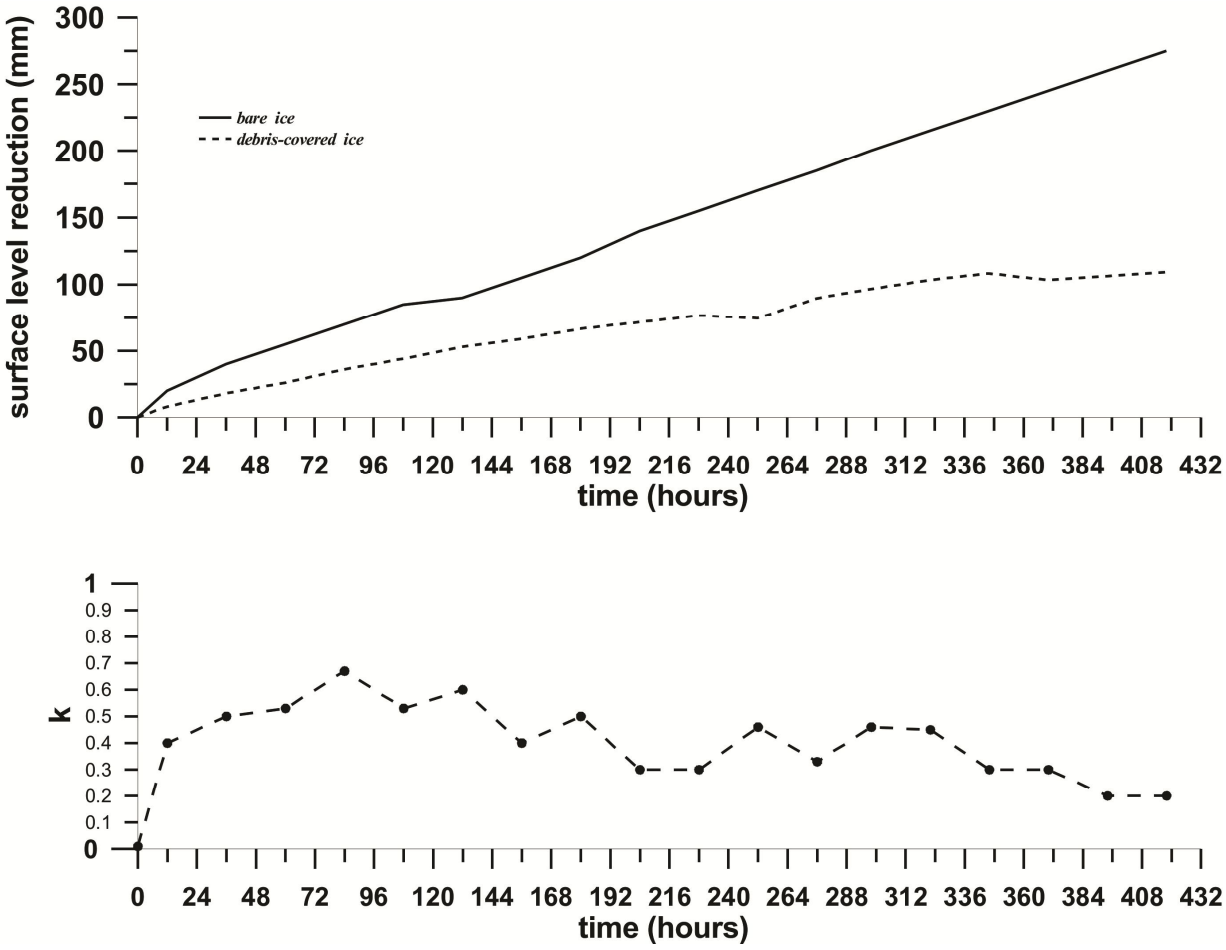

Figure 4.14. Coefficient of ice surface melting ratio (k) for 90 mm debris-cover under diurnal cycle conditions: a) surface level reduction rates for 90 mm debris-cover ice and bare ice; b) coefficient of ice surface melting ratio (k) for ice covered with 90 mm debris.

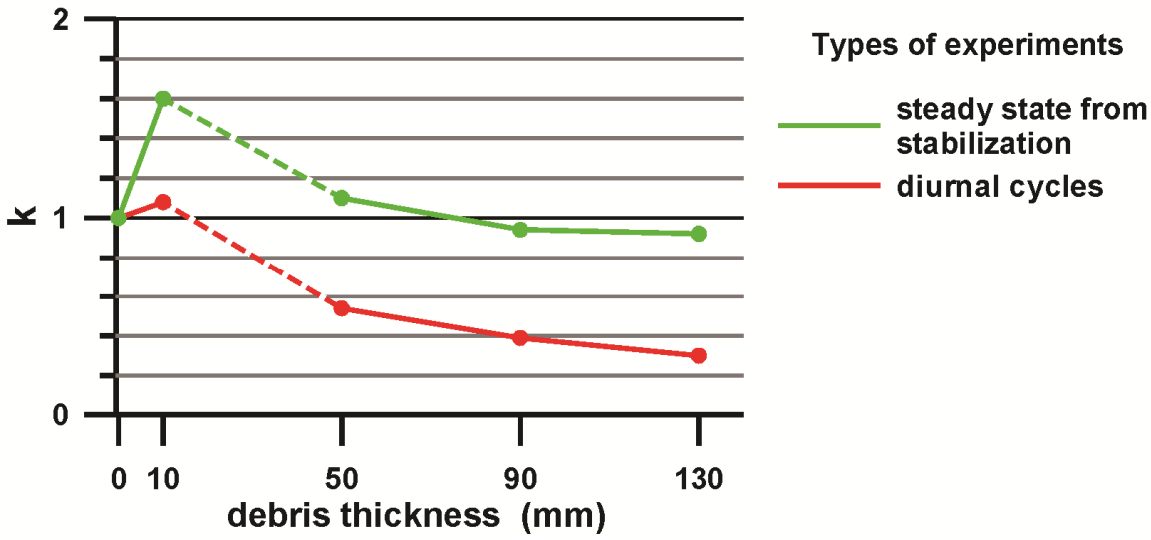

Figure 4.15. Average coefficients of ice surface melting ratio (k) for bare ice and ice under 10, 50, 90 and 130 mm of sand debris-cover. Green points - steady-state experiments after the heat flux through the debris layer stabilized; red points - cyclic experiments. The small increase in steady-state ablation with 10 mm of debris is an albedo effect.

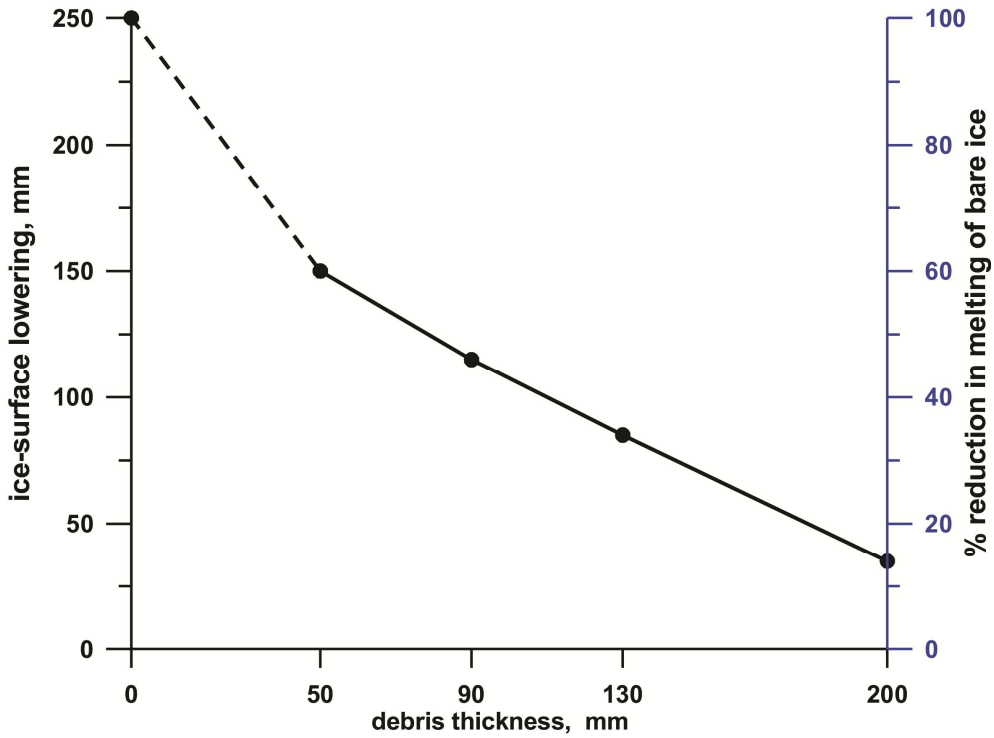

Figure 4.16. Melting rates of bare ice and ice under 50, 90, 130 and 200 mm debris under diurnal-cycle conditions during 396 hours after the start of the experiment. The right ordinate shows the melting reduction due to the debris-cover as a percentage of the bare ice melting rates (100%). The dotted line covers the lack of data for debris thicknesses < 50 mm.

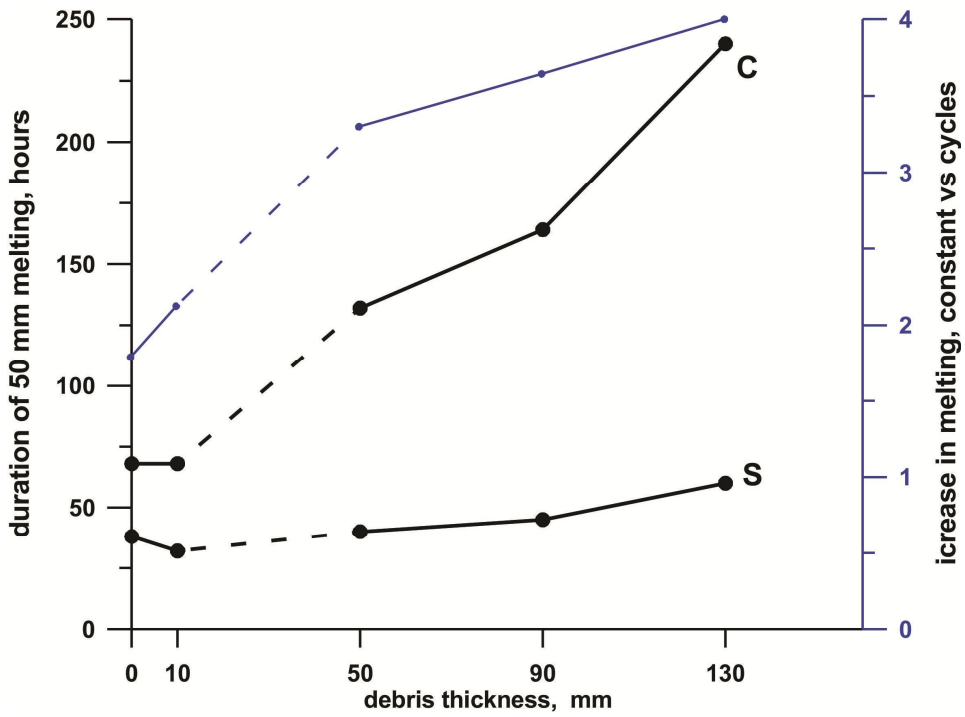

Figure 4.17. Time required to melt 50 mm of ice for bare ice and ice under 10, 50, 90 and 130 mm debris during steady-state (s) and diurnally-cyclic (c) conditions. The blue line shows the increase in the melting duration (in times) of the ice under diurnal-cycles in comparison with steady-state (right ordinate), where 1 means the same melting rates. The dotted lines represent data not available for debris thickness 11-49 mm.

We now come to the third set of experiments: we compared the insulating effects of rock avalanche debris to those of greywacke sand, in the presence of rainfall.

4.3.2. The impact of rainfall on insulating qualities of debris cover

4.3.2.1. Aims

The effect of rock-avalanche debris on ablation in the absence of rainfall was considered to be similar to that of sand, but the higher thermal inertia of the thicker and more fines-rich rock avalanche debris would be expected to increase the insulating effect. The average thermal conductivity of a rock-avalanche deposit of same lithology as a melt-out normal supraglacial cover would be higher due the compaction, presence of clays and lower air and water contents. The rock-avalanche deposit also has lower permeability than normal supraglacial debris. Additionally, rock avalanche deposits on glaciers are rarely less than 1 m thick (Shulmeister et al., 2009), therefore using small depths of material (up to 130 mm) would have been very unrealistic. The much larger pore passages within the melt-out debris will accelerate water percolation and heat-transfer advection towards the debris-ice interface

(McSaveney, 1975). At the same time, the smaller average thicknesses of the supraglacial melt-out debris allow faster percolation of warm air and rainwater through the debris compared with the much thicker rock-avalanche deposit. Considering the depth of rock-avalanche debris, it can be expected that in reality dry rock-avalanche debris would effectively cause ice-surface ablation to cease.

Only in a few studies has the effect of rainfall on ablation rates been considered (McSaveney, 1975; Bozhinskiy et al., 1986; Kirkbride, 1989). It was established by Paterson (2004) that rain and snowmelt introduce negligible heat to debris-free temperate glaciers, and the same must be true for debris-covered glaciers. McSaveney, (1975) estimated the contribution of advective heat flow by rainfall interacting with the thermal gradient through the debris layer within the Sherman Glacier rock avalanche. He showed that in a thick debris cover the advective heat flow from rainfall will be important in the upper part of the debris, but near the base the low permeability of the debris will inhibit advection. Similar conclusions were obtained by Bozhinskiy et al. (1986) when the percolating water through the thick debris mantle of the Djankuat Glacier in the Caucasus increased the seasonal ablation rates only 2%; the thick consolidated debris layer completely insulated the underlying ice from melting. Consequently the main pattern of the heat advection contribution by rainfall with a different debris cover still needs detailed elaboration.

Taking into consideration that the effect of rainfall on ice melting under debris-cover is controlled by debris permeability, debris thickness, temperature and quantity of the rain, the impact of these parameters was included in experiments by comparing the effect of sandy debris-cover with that of lower permeability rock-avalanche material.

4.3.2.2. Method

This set of experiments was conducted to determine the influence of rain on ice ablation under debris cover of different thicknesses and of different materials: normal debris cover (sand) and real rock avalanche material. These tests were conducted in a similar manner to the cyclic experiments (section 4.3.1.2), but with rain. The contrasting materials used were: narrowly-graded medium sand with a high permeability, 1.6×10^{-3} m/s (greywacke river sand), and rock avalanche deposit material with lower permeability of 1.8×10^{-7} m/s. Because the rock avalanche deposit thickness on glaciers is usually of the order of 1 to 5 m, the effects noted

during the experiments would be reduced by the much smaller depth (≤ 90 mm) used in the experiments.

The amount of the rain for the experiments was chosen as 10 mm per day. The rain water was at room temperature (the water container was left in a room for 12 hours). 10 mm depth of water was sprayed onto the experiment each day over the course of one hour during the radiation part of the cycle (6 hours after the start of the heating). During the rainfalls only the short-wave radiation bulbs were used in order to eliminate long-wave heating and to replicate the cooling effect of cloud-cover.

Four main types of experiment were conducted:

1. Rain percolation effect on ablation rates of the ice covered by greywacke sand 90 mm thick in steady state (non-cyclic conditions) with 10mm (1144 ml) and after 24 hours 20 mm (2300 ml) of rainfall (Fig. 4.18 A).
2. Comparison of ablation rates of the ice covered by greywacke sand 90 mm thick under cyclic condition (24 hours cycles) both with rain (10 mm per day) and with no rain.
3. Rain percolation effect on ablation rates of ice covered by greywacke sand 90 mm thick and debris-free ice under cyclic condition (24 hours cycle, 10 mm of rain per day).
4. Rain percolation effect on ablation rates of ice covered by greywacke sand 90 mm thick and debris-free ice under cyclic condition (24 hours cycle, 10 mm per day) using the rock avalanche material as debris-cover.

4.3.2.3. Results

During the experiment with rainfall under constant radiation (steady-state conditions) the rain advected heat towards the debris-ice interface and contributed to melting but only in the first hours; then the system after 2 hours came back to the previous conditions (Fig. 4.18 A). Similar effects occurred in the experiments on rain percolation under diurnally-cyclic conditions (Fig. 4.18 B). The results show that when the rain percolating through the sand debris-cover reached the debris-ice interface in a short period of time (about one hour) it enhanced ice melting under the debris-cover.

Melting rates under the debris were higher than those with no rainfall because percolating rain advects heat from the warm debris to the ice. The sand used in the experiments is intended to

represent thin supraglacial material with a high permeability on glacier, and rain will have same effect as observed in the laboratory. Because rainfall accelerates the ablation of debris-free ice to almost same degree as with debris cover (Fig. 4.19), the rainfall has the same effect on a debris-free ice as on ice with thin supraglacial layer of highly-permeable debris cover.

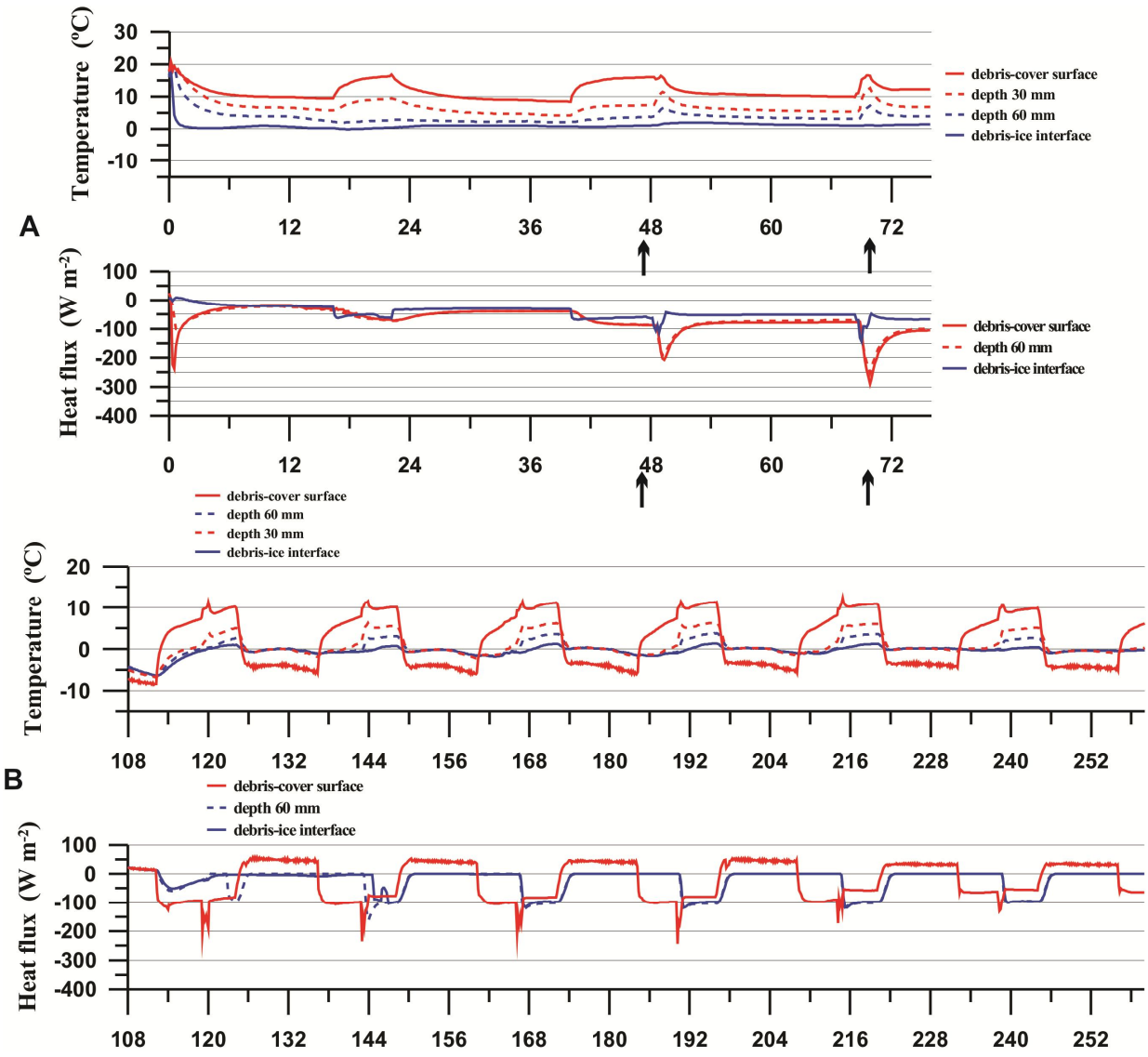

Figure 4.18. A. Temperature (upper) and heat flux (below) for experiments of rain percolation on ablation rates of ice covered by debris 90 mm thick in steady state (under constant radiation). Arrows indicate when rain was applied. B. Temperature (upper) and heat flux (below) profiles within ice covered by debris 90 mm thick for experiments of the effect of rain percolation on ablation rates under diurnally-cyclic conditions (24 hours cycle). Rain was applied to the debris-covered ice for one hour in the middle of every heating cycle.

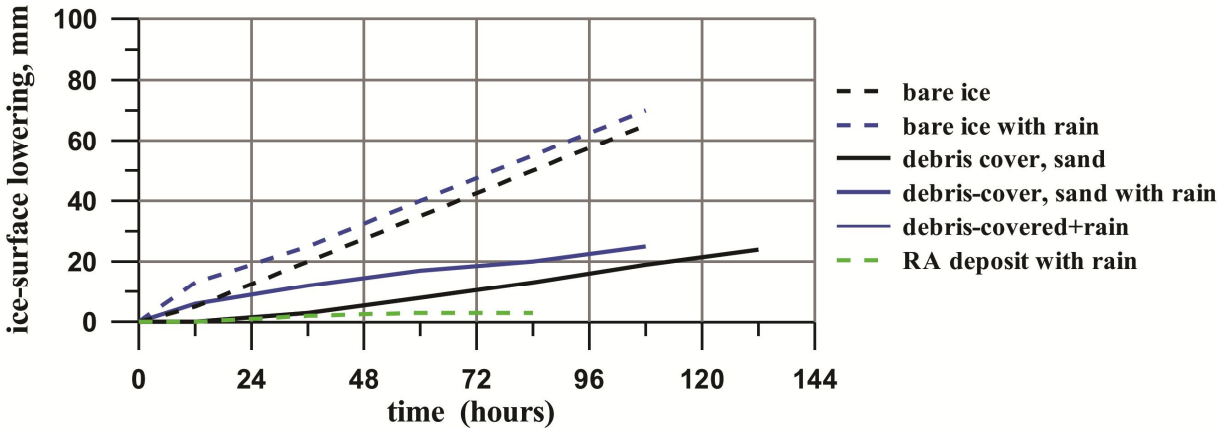

Figure 4.19. Ice surface level lowering beneath 90 mm of sand and with bare ice under diurnally-cyclic conditions with no rain (black lines), with bare ice and with ice covered with 90 mm of sand with rainfall of 10 mm (blue lines); water was sprayed onto the surfaces daily over 1 hour in the middle of the ablation period.

For better interpretation, data from rain percolation through the sand debris experiments were compared with data of the same experiments but without rain, which had been conducted previously. To some degree conditions were different (different room temperature); however, comparison of some cycles gives insights in understanding the effect of rain on ablation processes in debris-covered ice. Two almost identical cycles were plotted on the same graph for comparison (Fig. 4.20). The graph shows that the rain-percolation delivery of heat happened in the hour after the rainfall and contributed to temperature increases of 1 or 2 ºC (at 60 mm depth), and overall the effect of increasing temperature had the same pattern as in the case of non-rain conditions. Similarly, in the heat flux profiles the input of the rain changes fluxes only during the hour, and there are no significant changes in heat flux during the rest of the cycle. It can be concluded that rain percolation through the debris-cover will have same effect on the ice ablation rates under debris as it has on debris-free ice.

When the same system, but with rock-avalanche deposit material cover, was exposed to rainfall under cyclic conditions, the cycles played a crucial role in heat advection by rain through the debris. Because of the very low permeability of the rock-avalanche deposit the saturation of the debris layer requires much more time. Even at the end of the ablation period water is unable to percolate to the debris-ice interface. When this did eventually happen, the debris layer froze during the non-ablation period of cycle and consequently during the next cycle prevented normal heat percolation through the debris layer (Fig. 4.21). This effect may be described as an extra radiation demand for the saturated debris to bring the system to the condition it was in before the rainfall. In this case the commencement of ice ablation under the rock-avalanche debris-cover was significantly retarded or, in our case, never even started.

As a result, during this set of experiments there was almost no ablation under the rock-avalanche debris-cover in contrast to the accelerated ablation rates under the sand cover of the same 90 mm thickness (Fig. 4.18).

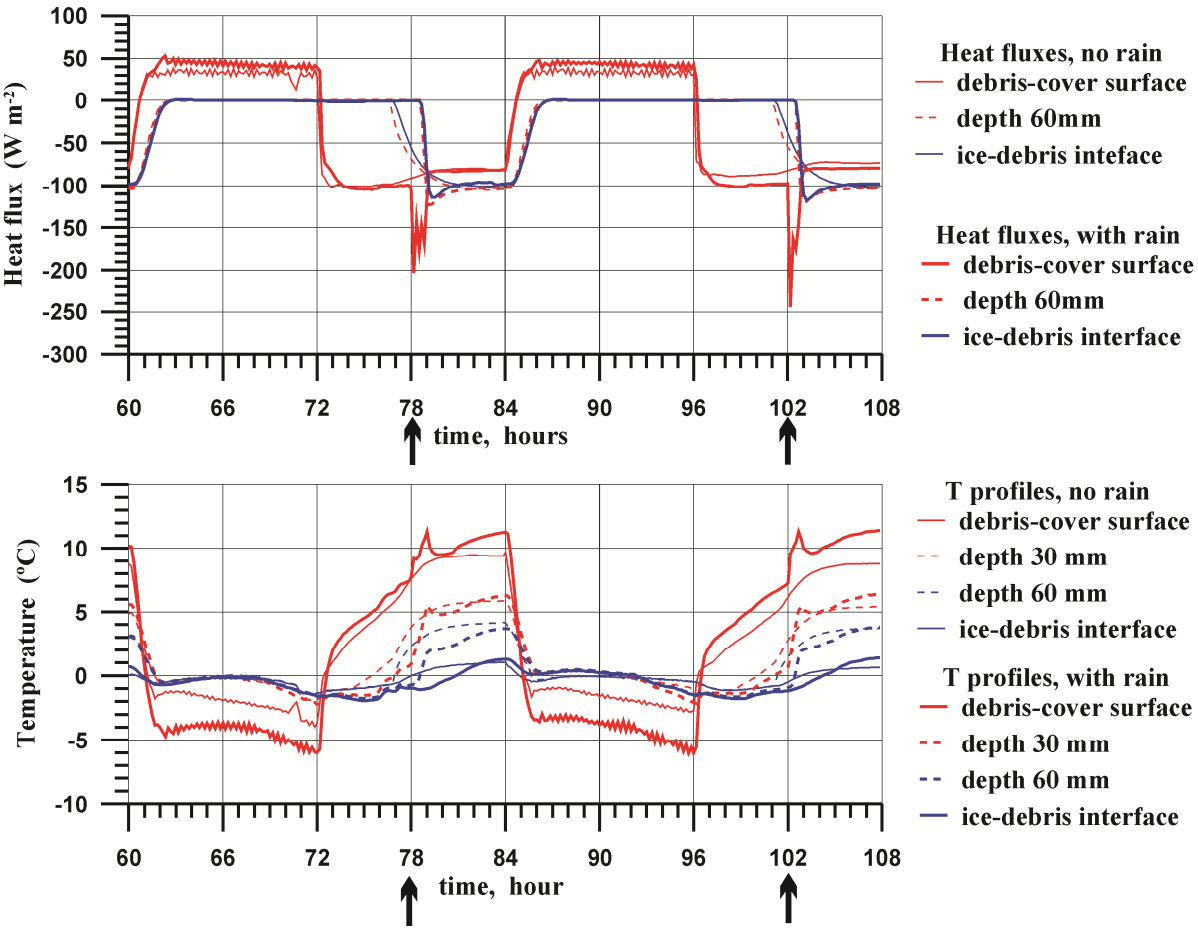

Figure 4.20. Comparison of two cycles of heat flux (upper) and temperature (below) within the 90 mm thick debris-cover in under diurnal-cycle conditions without (thin lines) and with rain percolation effect (bold lines).

4.3.2.4. Discussion

During the experiments, the difference of permeability between the two types of debris played a crucial role in the ablation rate under rainfall conditions. The thin layer of angular debris covering most debris-covered glaciers is rockfall material that has been redistributed through the englacial system and been exposed at the surface by thrust-faulting and melt-out. If the thickness of debris is small (several cm), it may be saturated by rainfall, however, some thin high-permeability debris covers cannot be saturated. In contrast, the rock avalanche debris is

much less common on glaciers than melt-out debris; but if it is present, debris from a large rock avalanche will cover a substantial area of glacier and potentially affect mass balance.

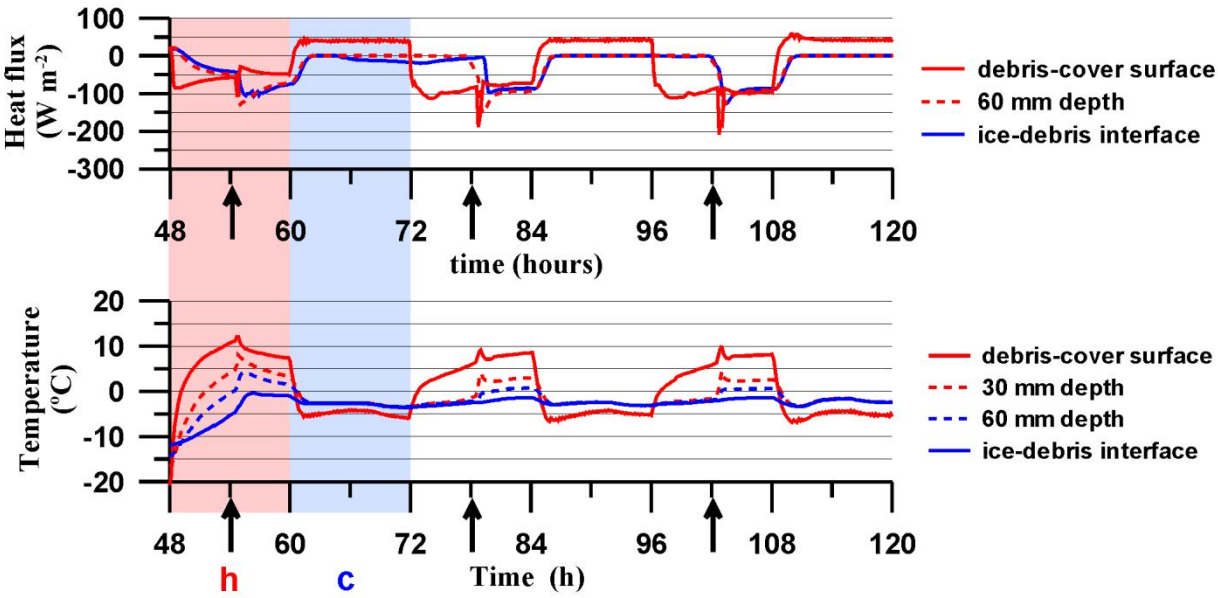

Figure 4.21. Heat fluxes and temperature profile changes through 90 mm of rock avalanche debris material under diurnal cycle conditions with rain of 10 mm/day. Temperature at the ice-debris interface (blue solid line) during the experiment remains negative and does not reach melting-point due to very slow heat conduction through saturated frozen rock avalanche debris. "h" indicates the heating part of the cycle with radiation exposure, "c" indicates the cooling part of the cycle and arrows indicate the occurrence of rainfall during the cycles.

The experiments show that, as expected, the water percolating through the thin highly permeable debris layer supplies the ice surface with extra heat and increases ice melting. On glaciers this acceleration of the melting effect will be of same magnitude as for the adjacent debris-free ice. In the case of rock-avalanche debris-cover (i) the percolation of the water is very slow and (ii) water within the saturated debris can refreeze during the night and slow down the heat percolation to the ice-debris interface during the next ablation period of the cycle. Thus, the experiments showed that deposit permeability is a crucial debris parameter that either accelerates or drastically reduces ablation during rainfalls, and the direction and intensity of these processes depend on the strength of the diurnal cycles in a particular region. The extra energy input to the system due to rainfall above 0°C on debris-free ice was pointed out by Paterson (2004), but he considered these effects insignificant in mass balance changes of the glacier. However, in the case of thick debris-cover with higher thermal capacity, this

extra heat storage capacity has a major effect in retarding rainfall-generated ice-surface ablation.

Rain falling onto sun-warmed surface debris can in principle advect heat from the debris down towards the ice surface. With rock avalanche debris some m thick, basal saturation can occur either due to rain percolation or by capillary rise from the ice-surface (recall that rock avalanche debris has a high content of very fine material; McSaveney and Davies, 2007). To fully saturate some m of dry rock avalanche debris with rain requires of the order of some hundreds of mm of precipitation (assuming a voids ratio of about 20%) so a very large precipitation event will be needed to fully saturate such a deposit. Supposedly, in long-duration rainfall water will leave the rock avalanche debris cover surface by surface runoff or collect in ponds in depressions of the uneven debris-cover surface; thus advection of heat to the debris-ice interface will be lower.

Evidently, freezing of pore water may not be a universally-occurring effect, depending on debris depth and permeability and cycle characteristics; however it indicates that radiation intensity and duration (cyclicity) and permeability need to be included in the estimation of ablation rates under debris cover, rather than using daily average values of radiation as is common.

In conclusion, the effect of the rainfall on ice melting under a debris-cover is controlled by debris permeability, debris thickness and, to a lesser extent, deposit density and consolidation. Rain temperature and rainfall duration will have a short-term effect on the ablation, but as the experiments show, don't have a significant effect on ice ablation. However, in the case of rock avalanche material with lower permeability and greater thickness the rainfall has the opposite effect on the underlying ice melting, which indicates that the radiation cyclicity must be considered in estimations of ice-surface ablation rates under debris-cover.

Implication for global patterns

The physical function of the debris-cover in reducing surface ice ablation under the debris is controlled by the properties of the debris and the diurnal and seasonal cyclicity. The above results show the importance of not just the average energy available for passage through the debris layer, but also of the parameters of these cycles. Thus, a cycle with high positive temperatures and high negative temperatures will have much less total ablation than one with lower positive temperatures but no or only slightly negative temperatures. In other words, ablation will not occur during the average duration of all the positive temperatures (>0ºC), or

the degree-day factor (DDF), but only when positive temperature at the base of the layer allows melting to start. For debris-free ice, estimation of the ablation using DDF is practical because radiation directly affects the ice, whereas with debris-covered ice radiation has to alter the thermal state of the debris before ice melting can be changed. As a result, in estimating the ablation under debris-cover this factor must be included and it depends on the geographical location of the glacier.

For estimating the effect of debris cover on the mass balance of a particular glacier, the critical thickness (defined as the thickness at which the underlying ice ablation equals that of adjacent bare ice in section 4.2.1) has to be determined. The global distribution of critical thicknesses demonstrates the variability of the effect of debris cover on ice-surface ablation. From numerous field experiments on snow-melt under dust it is evident that critical thickness increases with increasing solar energy input rate (Adhikary et al., 1997). Therefore, it is important to understand the spatial distribution of the measured critical thicknesses and, as a result, the different effects of the debris cover on glaciers in different parts the world.

The important role of diurnal cycles on the insulating effect of debris cover correlates well with the available field data on the spatial distribution of critical thicknesses (Table 4.2). Although local factors cause differences in ablation rates, the general trend is that the critical thickness decreases with increasing latitude and elevation (Fig. 4.22). The decrease of the critical thickness with latitude is explained by the decreasing amplitude of the diurnal cycle moving from low and middle latitudes towards the poles, and the corresponding gradual reduction of the average positive temperatures (Barry, 2008). The diurnal amplitude also increases with increasing altitude, due to enhanced radiation (Oerlemans, 2000) and lower temperatures during the night. The intense absorption of short wave radiation by the low-albedo debris cover during the day exceeds its absorption by bare ice (Slaymaker and Kelly, 2009); however, the increase in negative amplitude of the cycle during the night significantly cools the debris cover. Thus, according to observed data, in a given mountain region there is trend of a slight decrease (of order of 10 mm) of the critical thickness with increasing elevation, because factors such as significantly reduced atmospheric and vapour pressure, humidity, and the frequency of below-freezing temperatures will outweigh the effect of enhanced daytime radiation. This corresponds with the decrease of annual mean ablation rate with increasing latitudes and elevation found by Budd and Allison (1975) (Fig. 4.22).

Another factor that influences the intensity of the diurnal cycles is the degree of continentality of the climate. Continental climates are characterized by less cloudiness and consequently greater shortwave radiation in the glacier-surface heat budget than maritime climates (Oerlemans, 2000). Under these conditions the debris cover on the ice surface absorbs more radiation and the debris-cover insulation properties are reduced, which may explain high critical thickness at the Kul`dgilga Glacier in Pamir mountains where very little cloud occurs and annual precipitation is low (Table 4.2).

Therefore, the effect of debris cover on ice-surface ablation rates depends on geographical location due to variation in diurnal cycle intensity: debris cover retards ice-surface ablation when its thickness exceeds the critical thickness for a given glacier; and the critical thickness generally decreases with increasing latitudes and with increasing elevation.

These results suggest that debris cover should have a greater effect on ablation in regions with strong diurnal cycles, such as the Karakoram Himalaya, compared with regions of lower diurnal variability at higher latitudes. In a similar analysis of data from four glaciers Mattson et al. (1993) concluded that the location of the glaciers will affect the intensity of the ablation (or the quantity of melted ice) with differences in debris cover thickness, where glaciers located at low latitudes or high elevations will receive more energy per unit time. However, this will affect debris-cover thicknesses in order of less than a meter, whereas under rock avalanche deposits the ablation is dramatically reduced.

4.4. CONCLUSIONS

From the laboratory experiments comparing ablation from debris-free ice with that from debris-covered ice it was found that:

1. The strength of the diurnal cycle plays a significant role in controlling the rate of melting beneath debris. In the absence of diurnal variability of radiation, the primary role of debris cover is to delay the onset of steady ice surface melting; once melting rates stabilize, the debris has no further significant effect. With diurnal cycles of radiation a long-term reduction in surface ablation occurs. Therefore, the rate of reduction of ablation depends on both the radiation cyclicity and thickness and properties of debris-cover.

2. Geographical location significantly affects the impact of debris on glacial melting rates. Because debris cover retards ice-surface ablation when its thickness exceeds the critical

thickness for a given glacier, the critical thickness generally decreases with increasing latitude and with increasing elevation. Thus, the effect of debris cover is magnified at high altitude and in lower latitudes.

In the experiments comparing the effect of normal melt-out debris with thick rock avalanche sediment the effects of debris permeability and of rainfall were investigated:

1. The effect of rainfall on ice ablation under debris depends both on diurnal cyclicity and on the permeability of the debris cover. Thus, thin high-permeability supraglacial debris cover accelerates ablation from the ice surface to a similar degree to that from debris-free ice under rainfall; whereas relatively impermeable rock avalanche sediment has the opposite effect.

2. The effects of the two main types of supraglacial debris on glacier behaviour are dramatically different, so distinguishing melt-out debris from rock avalanche debris needs to become a primary requirement in studies of debris-covered glaciers. This is particularly the case where the studies involve mass balance changes, and also where the formation of glacial deposits (e.g. moraines) is important.

The effects of rock avalanche deposits on glacier mass balance appear unarguable in principle, but it is unfortunate that no field data exist to test these inferences, because no rock avalanche has yet fallen onto a glacier whose mass balance has previously been studied.

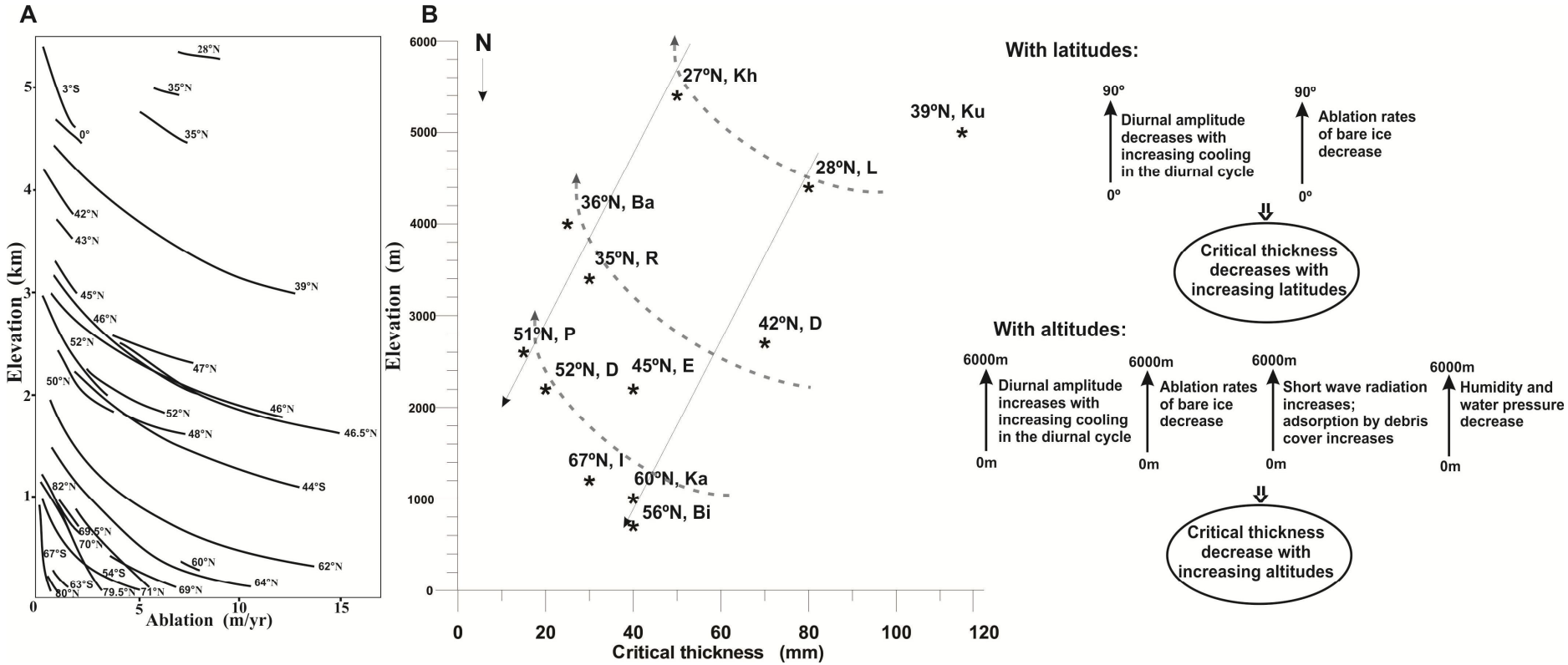

Figure 4.22. A: The pattern of decrease of annual mean ablation rate (for bare ice) with increasing latitudes and elevation. Modified from Budd and Allison (1975**).** B: Critical thicknesses (mm) varying with altitude (m a.s.l.) and latitude (Northern hemisphere) from the available observed data (Table 4.1). The critical thickness of the equivalent latitudes (dashed lines) decreases with increasing elevation. Kh – Khumbu Glacier (Kayastha et al., 2000), Ku - Kul`dgilga Glacier (Demchenko and Sokolov, 1982), L – Lirung Glacier (Tangborn and Rana, 2000), Ba – Barpu Glacier (Khan, 1989 in Kirkbride and Dugmore, 2003), R – Rakhiot Glacier (Mattson and Gardner, 1989), D – Djankuat Glacier (Popovin and Rozova, 2002), E – Eliot Glacier (Lundstrom et al., 1993), P – Peyto Glacier (Nakawo and Young, 1981), D – Dome and Athabasca Glaciers (Mattson, 2000), I – Isfallsglaciaren Glacier (Østrem, 1965), K – Kaskawulsh Glacier (Loomis, 1970 in Kirkbride and Dugmore, 2003), B – Bilchenok Glacier (Yamaguchi et al., 2000, 2007).

5. Field investigations of ablation under modern rock avalanches on glaciers

5.1. INTRODUCTION

A rock avalanche deposit emplaced onto the ablation zone of a glacier immediately reduces surface ablation beneath the deposit. In the long term this will result in changes of the local and net glacier mass balance. In this chapter the function of the debris cover on subsurface ablation investigated in laboratory will be supported by geophysical field surveys during 2009-10 on two modern (1991 Aoraki/Mt. Cook and 2004 Mt. Beatrice) rock avalanches on the Tasman and Hooker Glaciers, respectively, in the Southern Alps of New Zealand. The surveys show deposit geometry and geomorphology, and the effect on the underlying ice of the ablation zone of the glaciers. The process of ridge formation, the effect of these rock avalanches on the glacier net balance and motion are discussed. From these field studies and laboratory experiments the glaciological and geomorphological implications of rock avalanche emplacement on glaciers are discussed in the context of glacier regime disturbances and resultant moraine formation.

5.2. FIELD INVESTIGATIONS

5.2.1. Aims

The Aoraki/Mt. Cook rock avalanche on the Tasman Glacier was surveyed immediately after its emplacement with visual estimation of its thickness and one surface rock sample collected (McSaveney, 2002). The size of the 2004 Beatrice rock avalanche deposit on the Hooker Glacier has been estimated only visually (Cox et al., 2008). No other field surveys have been reported on these supraglacial rock avalanches or any others in the Southern Alps of New Zealand. Because during a visual investigation the actual thickness of the rock avalanche deposit and the underlying ice could not be known, and the digging through a thick (> 1m) rock avalanche deposit is almost impossible, geophysical investigation is required. The aims of the geophysical surveys on two modern rock avalanches at Aoraki/Mt. Cook National Park, the Southern Alps of New Zealand, were to investigate the deposit geometries and geomorphologies, detect the border with underlying ice and estimated the ice thickness developed under the deposit in comparison with the surrounding clean ice. Therefore, two perpendicular Ground Penetrating Radar (GPR) profiles were obtained across the Aoraki/Mt.

Cook (1991) rock avalanche deposit and uncovered ice on the Tasman Glacier in February of 2009, and two perpendicular profiles on the Mt. Beatrice (2004) rock avalanche deposit on the Hooker Glacier in December of 2009.

5.2.2. Method and field location

GPR is a non-destructive near-surface geophysical technique that propagates electromagnetic energy (radar) into the subsurface and measures the echoes returned to yield profiles of the physical property variations in the subsurface (Nobes, 2011). A GPR system usually comprises a set of two antennas, one that transmits a pulse of radio-frequency (10-1000 MHz) electromagnetic energy into the ground and the other that detects the subsequent echoes that return from subsurface layers and structures. The electromagnetic pulse is partially reflected at interfaces with dielectric contrast. The time it takes for an echo to return can be converted to the depth or distance to the reflecting surface if, and only if, the average radar velocity is known. The signal is transferred through a console into a visual display and recording device (Fig. 5.1).

The dielectric coefficient ε, or relative permittivity (ε_r), of the medium determines the velocity of a radar wave. In the absence of any significant amounts of magnetic material, the radar velocity, v, is equal to:

$$v = c/\sqrt{\varepsilon_r}, \quad (5.1)$$

where c is the speed of light in air, 300 m per microsecond (m/μs) (Nobes, 2011).

Because the penetration of the wave depends on the conductivity of the medium, the low conductivity of ice allows high penetration, whereas penetration into the rock avalanche deposit is much lower. The water found on glaciers has a high dielectric coefficient (Table 5.1), the changes of amount of which will cause the reflective interface. Lower frequencies (50 MHz or lower) can be used for penetration through thick ice layers and the base of a glacier usually can be detected (Hochstein et al., 1995). Thus, the boundary between rock avalanche debris and ice can be successfully obtained. Because the rock avalanche deposit is not very thick, low frequency antennae (50 MHz or lower) could detect the interface with the underlying ice. GPR survey is thus one of the best non-invasive ways to determine the thickness of a supraglacial rock avalanche deposit.

Table 5.1. List of the relative dielectric permittivity and radar velocities for some common materials, in particular water, snow and ice. Note that these material velocities are for "pure" materials, which in nature usually mixed with others.

Material	Relative dielectric permittivity, ε_r	Velocity, m/μs
Air	1	300
Water	~80*	~33
Snow	2 - 3	200
Ice	3 - 4	160
Dry sand	3 - 5	150
Wet sand	20 - 30	60
Dry salt	5 - 6	130
Granite	4 - 6	130

*The dielectric properties for water are temperature-dependent.

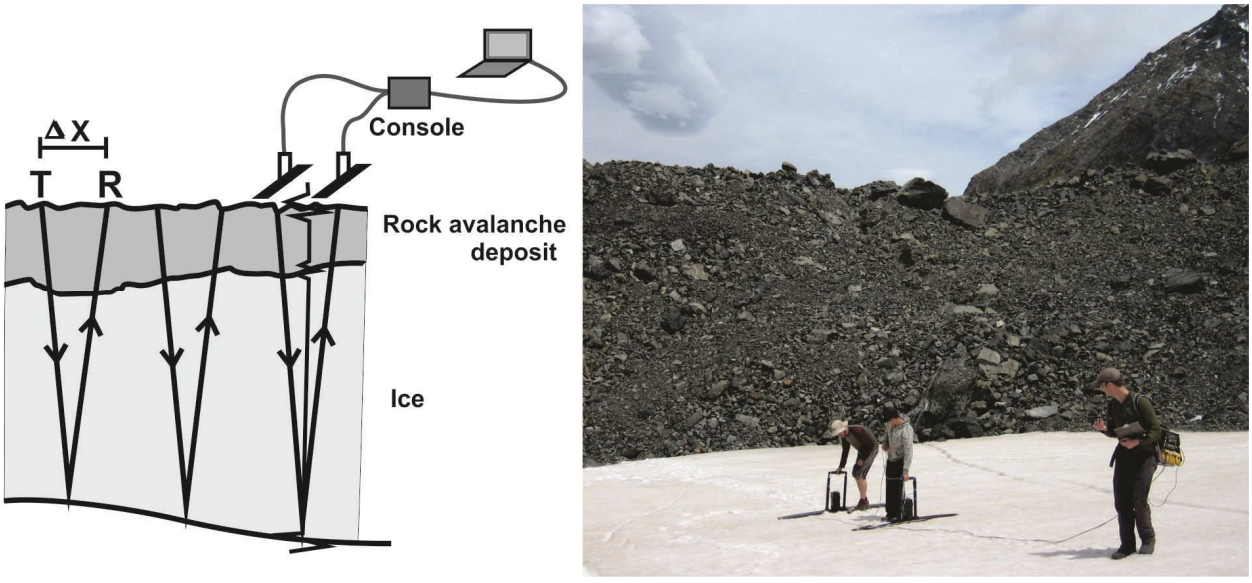

Figure 5.1. On the left is a schematic of a GPR system, showing the transmitting-receiving antenna pair (T-R) with the electronics used to generate and measure the signal and its echoes; the cables connecting to the control console and the storage and display unit. T-R pair is shown stepped along at constant step sizes, or offset Δx. At each location (deposit surface, deposit/ice interface and bottom of the ice) a record of the radar echoes is obtained. On the right is a GPR survey adjacent to the Mt. Beatrice rock avalanche deposit on clear ice of the Hooker Glacier.

For the Aoraki/Mt. Cook rock avalanche deposit, 100 MHz antennae were used with separation of 2 m and 1 m offset. For the Mt. Beatrice rock avalanche deposit 50 MHz antennae were used with separation of 2 m and 0.5 m offset. The row data were analysed by standard procedure of

the traveltime of direct and reflected radar waves through the medium. The boundary between rock avalanche deposits and underlying ice was clearly identified in both cases.

Since its emplacement the 1991 Aoraki/Mt. Cook rock avalanche deposit has been modified by ice flow mostly from Hochstetter icefall. Quincey and Glasser (2009) estimated that the Tasman ice flow has velocities of about 150 m/year at the junction with the Rudolf Glacier, but downvalley at the northern edge of the deposit the speed is negligible. At the toe of the Hochstetter icefall velocity increases from the large icefall input, and then decreases towards modern terminus. As a result, Hochstetter iceflow had moved the northern part of the deposit more than 2200 m down the valley by 2007 (on average ~137 m/year), and another 300 m downvalley in the next 3 years, whereas the deposit on Tasman ice had moved only 500 m by 2007 (on average 30 m/year), and there has been small movement of the ice (several m) in last 3 years (Figs. 5.2 and 5.3). The velocity of the ice from Hochstetter icefall decreases down valley, so the flow velocity of the deposit during its first 10 years must have been much higher (up to 160 m/year), decreasing in the last 3 years to 100 m/year. Similar the north part of the deposit moved 500 m in the first 10 years and is now almost stationary.

With the exception of visual description, there has been no investigation of the 2004 Mt. Beatrice rock avalanche since emplacement. From satellite images it is estimated that between 2004 and 2009 the deposit moved about 800 m down the valley, indicating an average ice-flow velocity of ~160 m/year (~0.5 m/day) at that location. Between Dec 2009 and Dec 2010 the deposit moved ~145 m down the valley. During the supraglacial travel down the glacier the shape of the avalanche deposit and underlying ice were modified by differential ice-flow across the glacier and by collapse of its sides. The main deposit is surrounded by two smaller deposits: one on the right that was emplaced before 2004 and from the same source as Beatrice (according to Cox et al., 2008) and one up the valley that was deposited before 2009 (Fig. 3.5).

5.2.3. Results

The GPR images of two perpendicular profiles along the Aoraki/Mt. Cook and Mt. Beatrice rock avalanche deposits and adjacent clear or debris-covered ice provide information on the current thickness of the rock avalanche deposits, the elevation of the underlying ice surfaces, the modification of the deposits since deposition and the interaction of the rock avalanche deposits with clear or debris-covered ice.

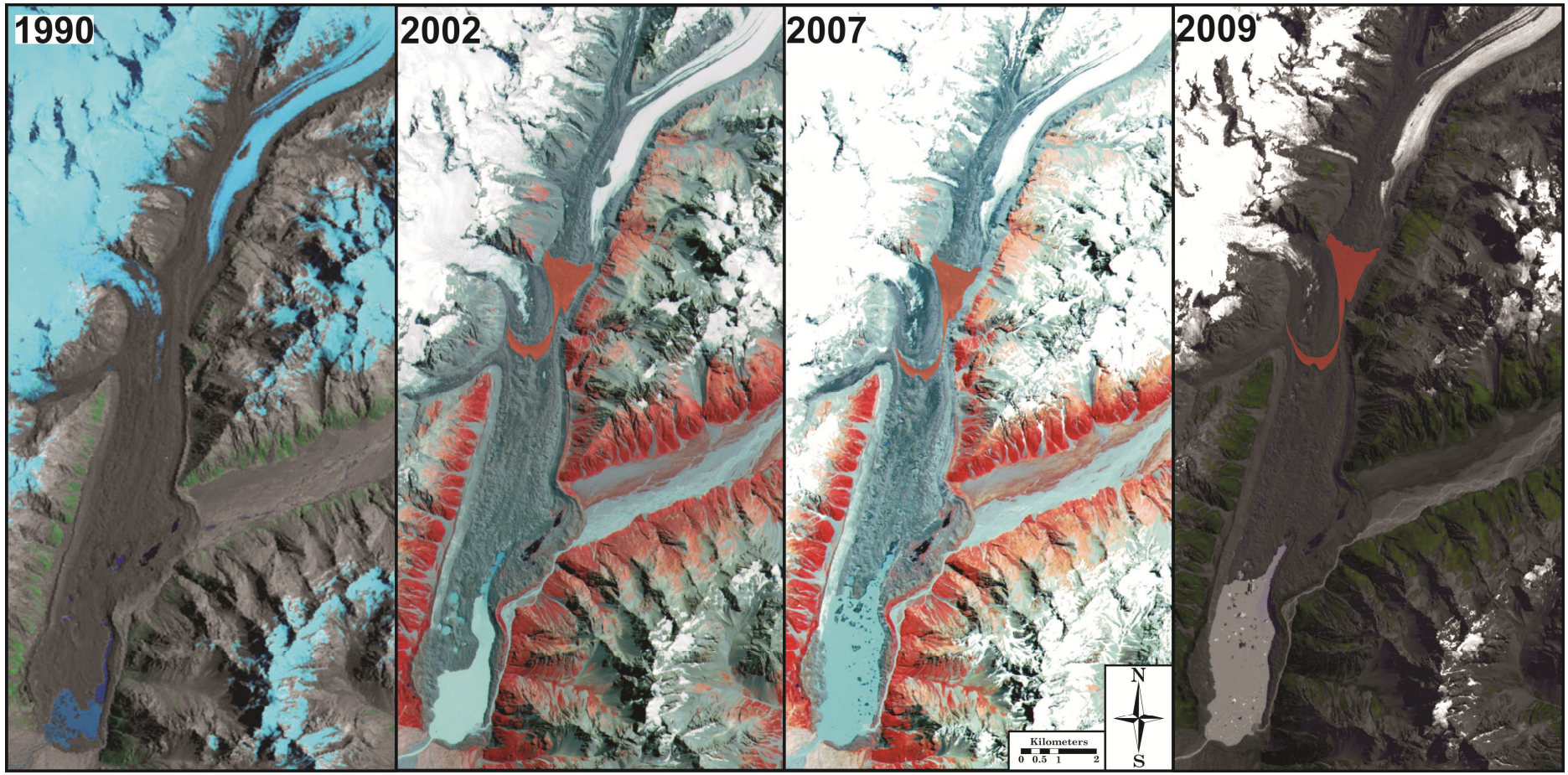

Figure 5.2. The history of the Aoraki/Mt.Cook rock avalanche deposit changes (indicated by red) modified by the active Hochstetter icefall. Photo: ASTER Satellite images, images 2002 and 2007 modified from Quincey and Glasser (2009).

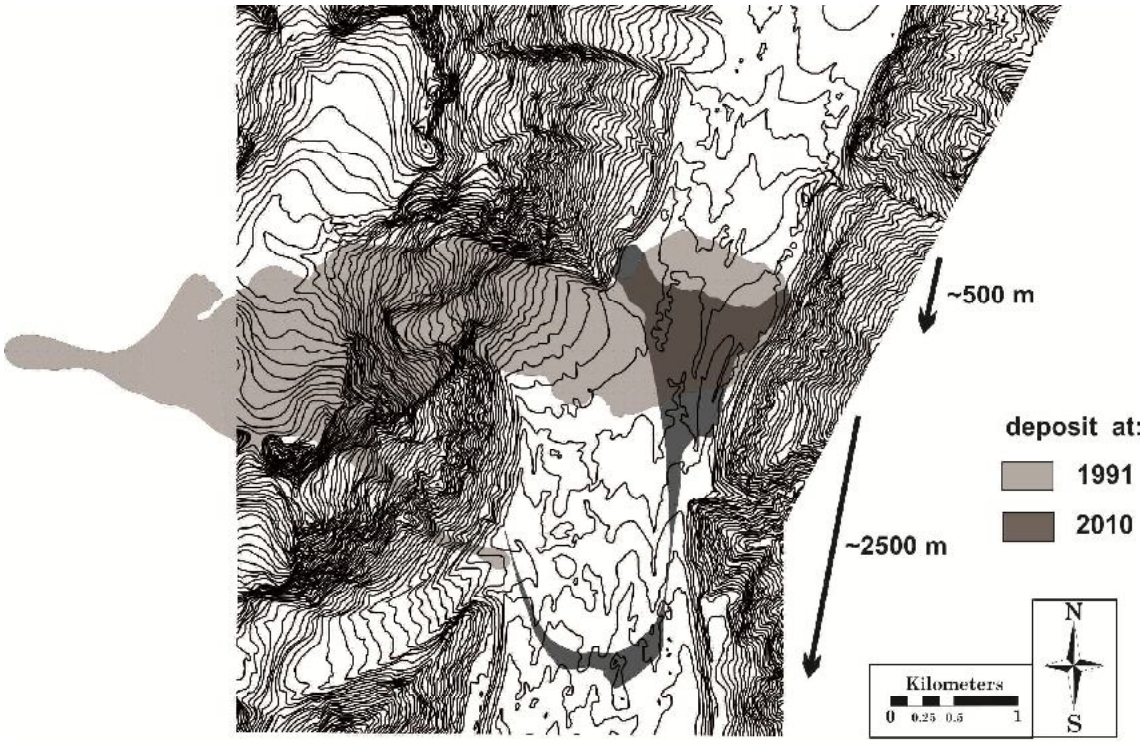

Figure 5.3. Position of the Aoraki/Mt. Cook rock avalanche deposit after emplacement (1991) and in 2010. The deposit was split into two parts by ice-flow from the active Hochstetter icefall.

5.2.3.1. Aoraki/Mt. Cook rock avalanche deposit

Both GPR images clearly showed the thickness of the deposit with high diffraction, and the underlying ice. The longitudinal profile at the edge of the deposit and one cross-profile (Fig. 5.4) revealed that the Aoraki/Mt. Cook rock avalanche deposit is up to 10 m thick, and a 25 m high ice-ridge had formed at the upstream edge of the deposit at February 2009 (Fig. 5.5). This ridge was not present immediately after emplacement (McSaveney, 2002), where the day after the event only a 1.5 m thick deposit was observed at the edges. This indicates the difficulties in estimating the actual debris thickness without drilling or geophysical observations. The edges of supraglacial rock avalanche deposits are usually thin (~1 metre), but within the main body of the deposit the thickness could reach ≥10 m.

The GPR cross-profile through the deposit shows some internal ice features attributed to the presence of water within the ice (Fig. 5.6). Englacial water channels would almost certainly have been present before the rock avalanche; they could also develop after deposition when the surface and englacial water channelized in order to find way through the ice. These channels may develop seasonally or over longer periods of time. On the platform of the deposit in places

are formed large (tens of metres diameter) craters of presumably locally-collapsed ice beneath the deposit.

From 1986 to 2007 the Tasman Glacier surface was lowering over the majority of its area, with the exception of almost no reduction over a 6 km long zone downstream of the Hochstetter ice fall (Quincey and Glasser, 2009). Under the rock avalanche deposit the actual ice thickening is difficulties to estimate due to the differential ice flow velocities and complications from tributary ice flow and local debris collapses. In 18 years the 25 m ice platform grew with a minimum rate of ~1.4 m/year. This estimation correlates with average ice-surface lowering rates of ~1.9±1.4 m/year in this area recorded by the multi-temporal elevation data (Quincey and Glasser, 2009). It could be concluded that the ablation under the deposit has been reduced to almost zero, however subsurface ablation still would occur from melting within the ice.

5.2.3.2. Mt. Beatrice rock avalanche deposit

Since 2004 the Mt. Beatrice rock avalanche deposit travelled supraglacially on the originally almost debris-free part of ablation zone. The GPR investigation revealed that an elevated platform, varying between 20 m and 30 m above the adjacent upstream and downstream ice surfaces respectively, was present under the 3 - 7 m thick rock avalanche deposit (Figs. 5.7, 5.8 and 5.9). The thickness of the deposit increases towards the south from ~3 m to 5-7 m on average, and from ~2.5 m at the west deposit edge to >5 m towards the east, or source slope. This thickness distribution must reflect the original debris thickness after emplacement. Originally the total Beatrice avalanche deposit volume was inferred to be between 10^5 and 10^6 m^3 (Cox et al., 2008); however, the estimated deposit thickness of 10 m did not include the relative ice thickening under the rock-avalanche debris during the three years following emplacement. The 2009 GPR survey showed an average rock avalanche debris thickness of 3-5 m, giving a volume about 1.4-2 x 10^5 m^3.

The ice thickening indicates an average reduction of ice ablation rate of 4 m/year under the deposit. Taking into the account that the deposit thickness is a minimum 3 metres, the ablation must be reduced under the deposit in comparison with adjacent clear ice by >90%. Consequently, the ablation of the surrounding ice must be around 4 m/year. After a year (in Dec 2010) the highest point on south-west end of the deposit was 51 metres higher than adjacent ice level in 2010 (Fig. 5.10) where that for the northern edge the difference did not exceed 30 m.

In contrast with the Aoraki/Mt. Cook rock avalanche, the elevated ice platform under the whole

deposit of the Mt. Beatrice rock avalanche remained intact, but its movement downvalley can indicate some peculiarities of supraglacially-travelled deposits. As debris is moved down the glacier by ice flow, the increasing relative ice thickness causes steep slopes to form along the sides of the deposit. These steep slopes constantly grow in height and backwaste due to melting of thinly-covered or exposed ice on the sides. The falling debris from the south slope covers more ice and increases the area with reduced ablation. The GPR data indicate a fault developed through the ice under the deposit due to the differential ice movement within the glacier, where the eastern part of the glacier moves faster than the western part (Fig. 5.7).

The northern platform edge is now much smaller and steeper that growing gentle south slope. The ablation rates of the surrounding ice upvalley from the deposit are smaller than those downwalley and after 5 years this causes the increasing differences in platform geometry. Also, I would suggest that the prevailing sun exposure during the day and katabatic wind also contribute to the edge evolution; the south edge remains in shadow from direct radiation, and therefore, the melting rates are smaller there and the edge is gentle.

As a result of all the modifications during passive transport of the deposit, the area affected by a supraglacial rock avalanche deposit slowly increases with time at its edges, whereas the main body of the deposit on top of the platform is modified (reduced in area) to a smaller degree.

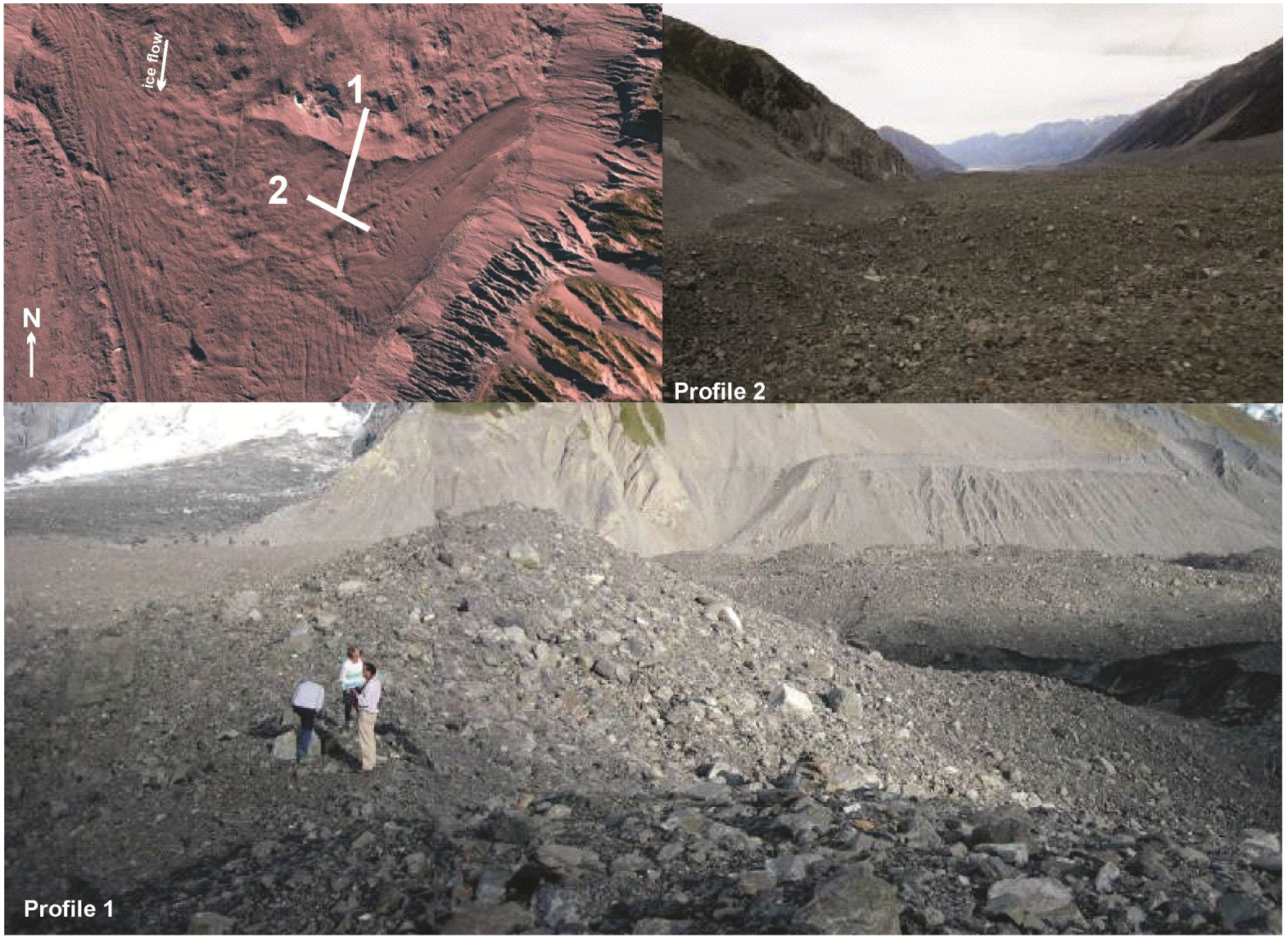

Figure 5.4. Location and views of two profiles on the edge of the Aoraki/Mt. Cook rock avalanche deposit on the Tasman Glacier. Photos: N. Reznichenko, February, 2009.

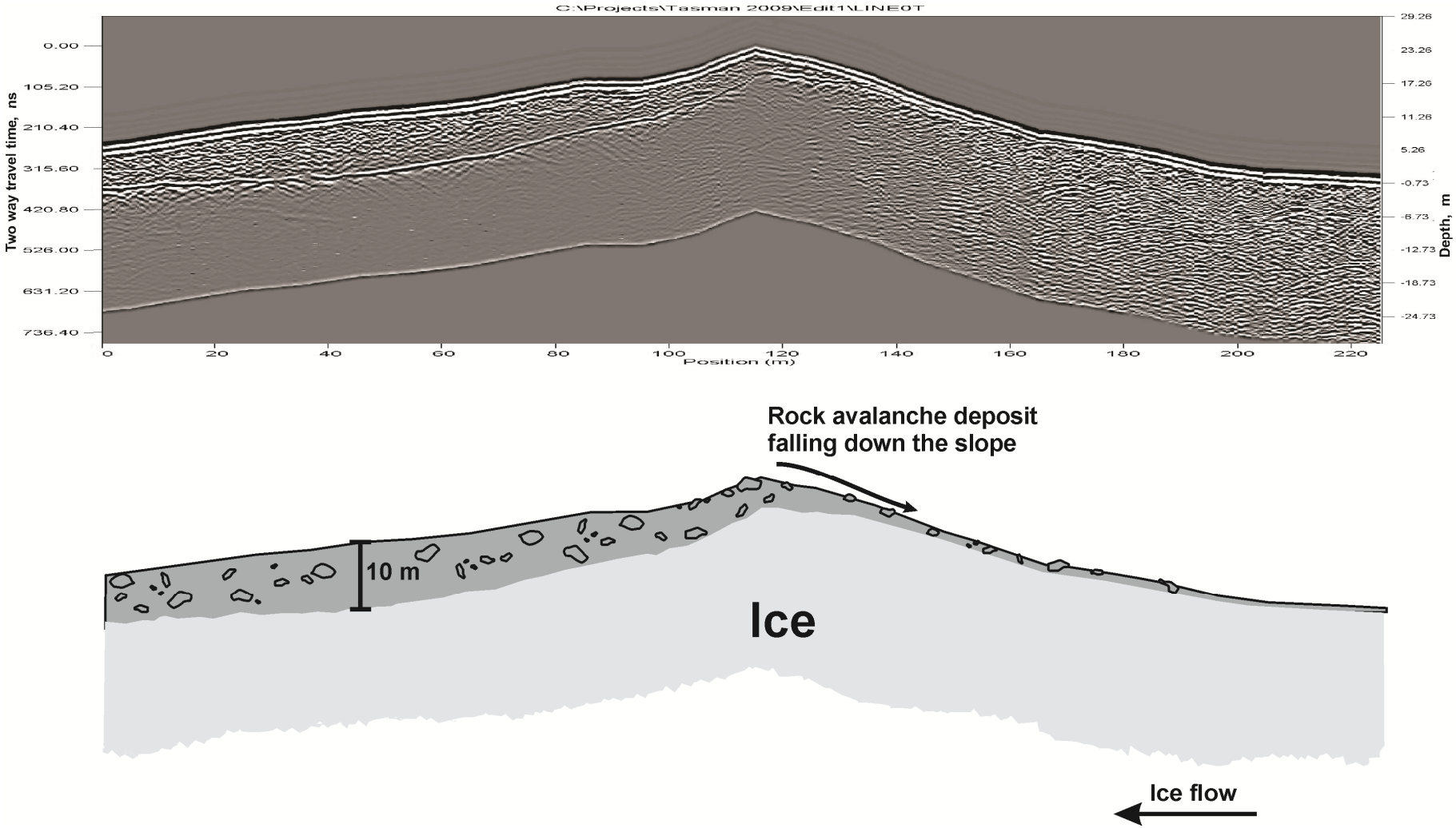

Figure 5.5. Processed GPR profile 1 on the edge of the Aoraki/Mt. Cook rock avalanche deposit and adjacent debris-covered ice.

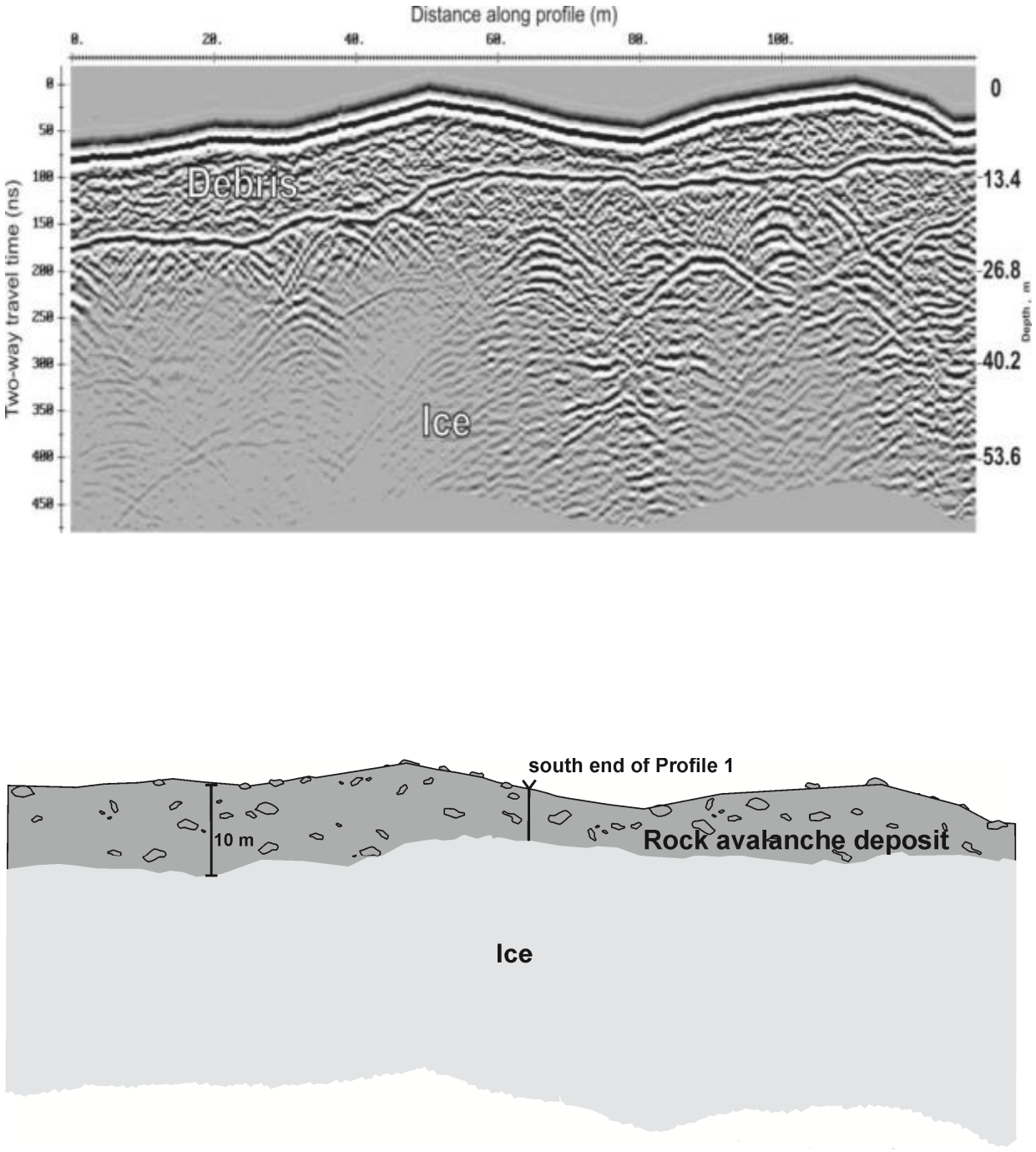

Figure 5.6. Processed GPR profile 2 perpendicular to the profile 1 of the Aoraki/Mt. Cook rock avalanche deposit.

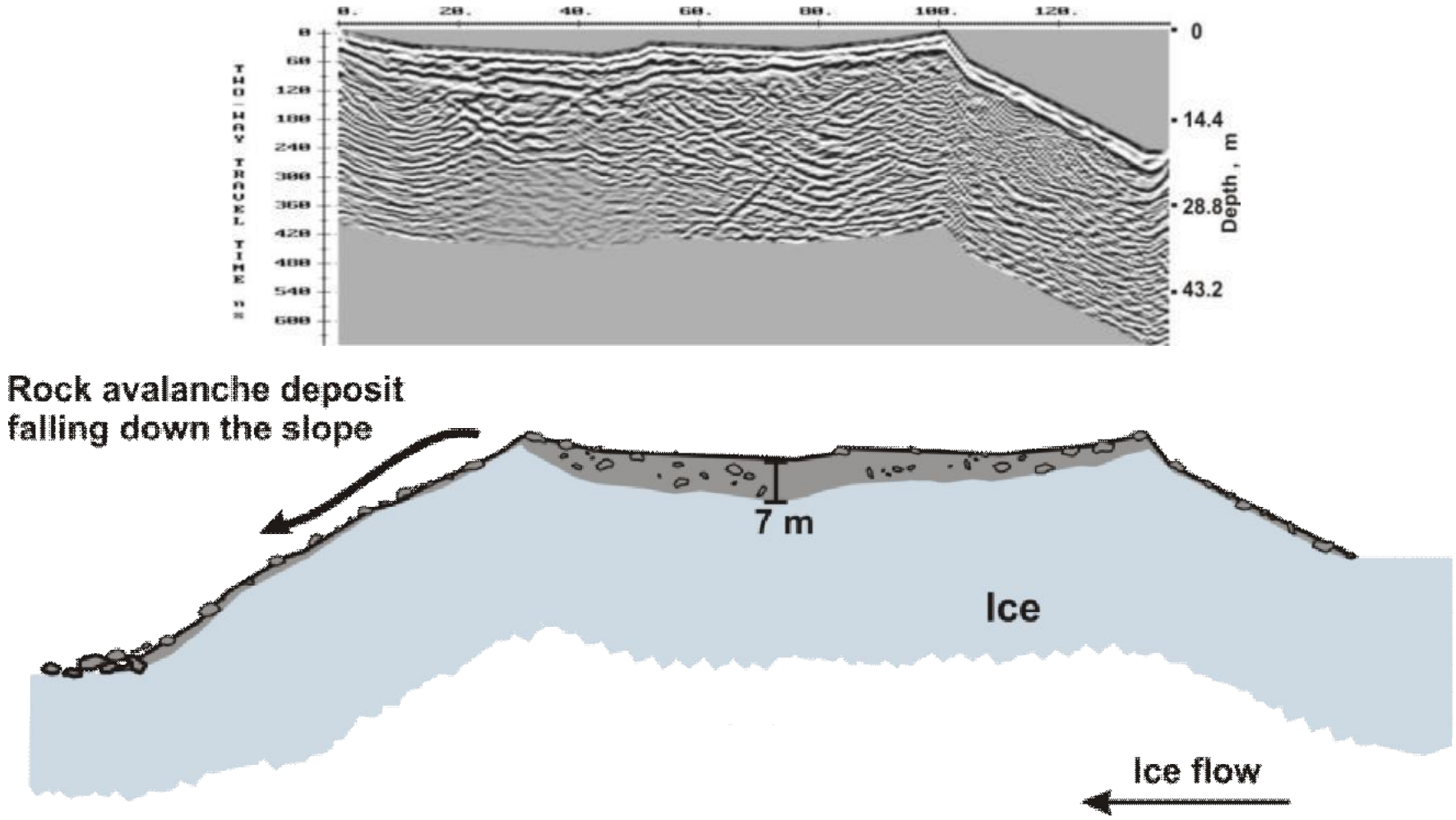

Figure 5.7. Processed GPR profile through the Mt. Beatrice rock avalanche deposit on the Hooker Glacier and its reinterpretation (below).

Figure 5.8. Panorama of the survey of the Beatrice rock avalanche, view from up valley, with clear ice up stream. Photo: N. Reznichenko, December, 2009.

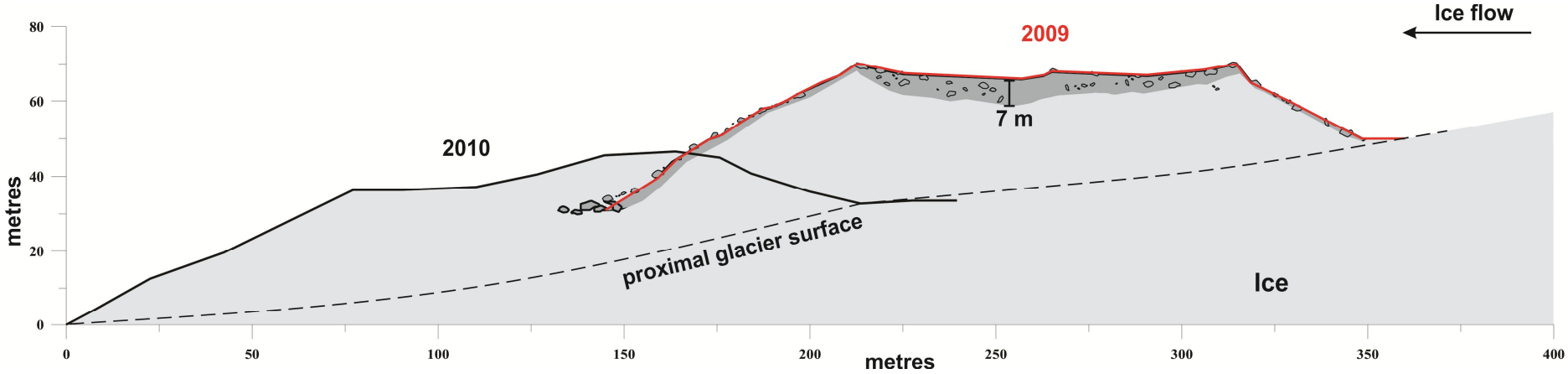

Figure 5.9. Changes of the Mt. Beatrice rock avalanche from Dec 2009 to Dec 2010. The deposit with elevated ice underneath moved down valley about 145 m with changes of the shape of the ice platform and deposit.

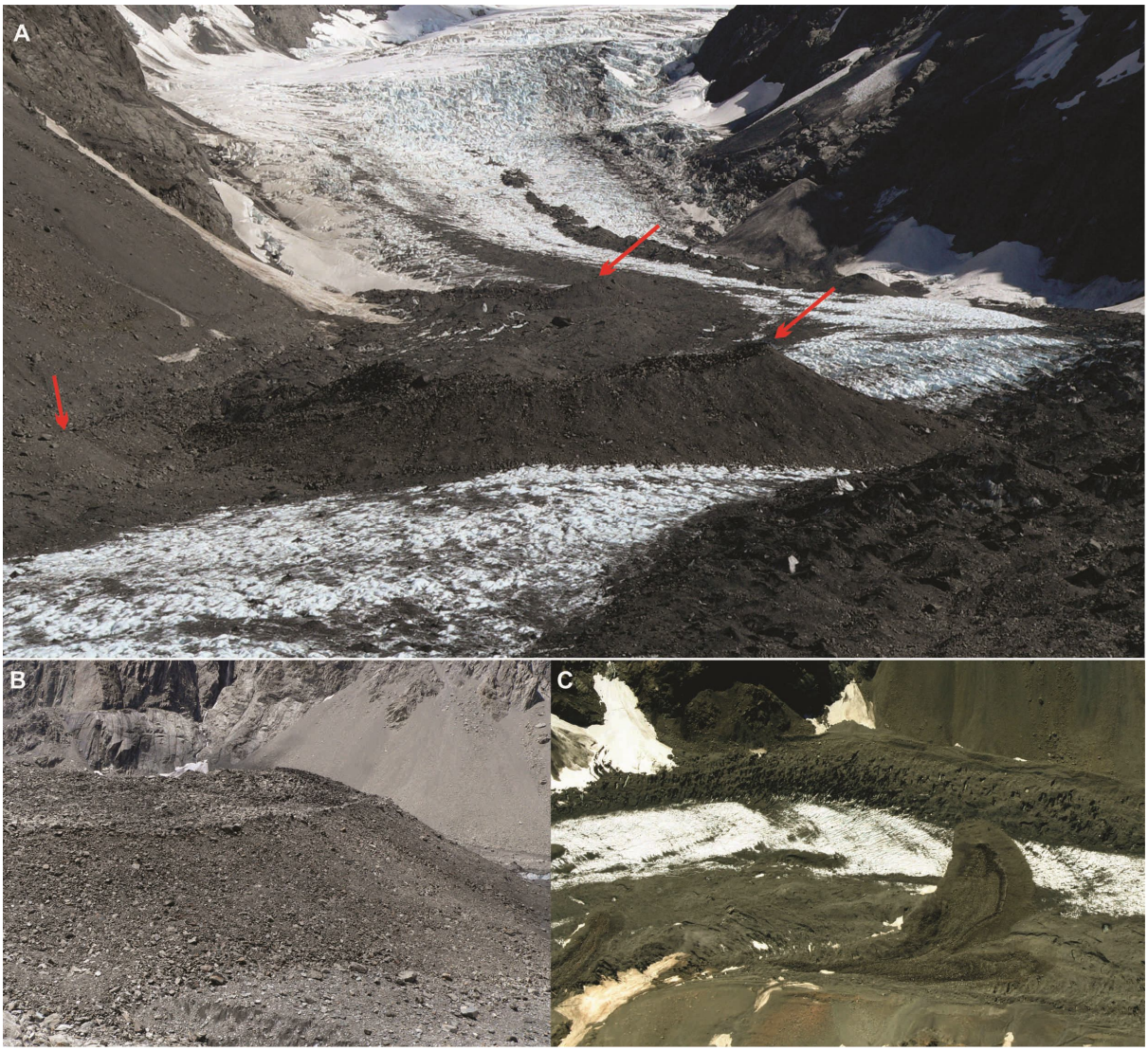

Figure 5.10. A. Overall view of the Mt. Beatrice rock avalanche deposit with arrow indicating the highest point (right), the smaller rock avalanche at the back (top arrow) and older rock avalanche at the front from the true right of the glacier (left arrow). Photo: N. Reznichenko, December, 2010. B. Closer view of the elevated platform, view from downvalley. Photo: N. Reznichenko, December, 2010. C. Aerial view of 3 deposits, with clear features of the edges and side slopes of the deposit. Photo: Stefan Winkler, January, 2011.

5.3. INTERPRETATION OF FIELD OBSERVATIONS

5.3.1. Effect of the debris cover on the mass balance of glaciers

GPR surveys on the Aoraki/Mt. Cook and Mt. Beatrice rock avalanches show that both rock avalanche deposits became elevated on platforms in contrast with the surrounding ice, and the deposit thicknesses are both greater and smaller than previously estimated (up to 7-10 m). Surface ablation under the deposits effectively ceased, and ice platforms several tens of m high develop. The Aoraki/Mt. Cook rock avalanche deposit split into two parts due to the active Hochstetter iceflow, the northern part is more stable and has moved little since

emplacement. The total thickening of up to 10 m could have been due to the compressional flow of the originally-covered area; however, there are no characteristic features on the surface of the deposit to suggest this (Fig. 5.4 B), and the amount of compression is inadequate to explain the difference in thickness estimated by McSaveney (2002) and measured in the present work. The southern part of the deposit will be eventually transported by Hochstetter ice towards the terminus of the glacier, where it will be deposited. The Mt. Beatrice rock avalanche deposit built up an ice platform 30-40 m high with expansion of the affected area by propagation of the edge slopes onto clean ice. Similar ice thickening under rock avalanche deposits has been reported on all glaciers with such deposits (Post, 1968; McSaveney, 1975; Decaulne et al., 2010; Jiskoot, 2011). Shugar (2011) pointed out that the 2-m-thick west debris sheet on the Black Rapids Glacier has reversed surface slope at the upglacier end and the slope at the downglacier end has steepened every season similarly to the Mt. Beatrice deposit.

With smaller deposits, the glacier may experience local dynamic effects from the additional supraglacial load, but the overall mass balance will not be significantly affected. The Aoraki/Mt. Cook avalanche deposit covered originally about 1.7 km^2, less than 4% of the ablation zone of the Tasman Glacier (about 45 km^2; Kirkbride, 1989); the deposit has since been redistributed by Hochstetter ice flow. The Mt. Beatrice rock avalanche covers about 0.05 km^2 of the roughly 7 km^2 of the ablation zone for the Hooker Glacier - less than 1% of the area (0.7% of ablation area, the total glacier area is 17.32 km^2, and ELA about 1800 m a.s.l.; Chinn, 1996). Therefore, apart from local disturbances of the mass balance, these two avalanches are not expected to affect total glacier behaviour noticeably. Another important factor is that these debris-covered glaciers are rapidly downwasting and calving into proglacial lakes, and so already have very negative mass balances, so a significantly larger event would be needed to trigger noticeable regime changes of these glaciers.

From the two studied examples it is evident that such events can significantly contribute to the glacier sediment fluxes. In future the southern part of the Aoraki/Mt. Cook rock avalanche deposit will be slowly transported downstream by the Hochstetter ice flow. If the Tasman Lake calving continues with same speed as for the last 4 years, the southern part of the rock avalanche deposit will reach the calving terminus in about 7-8 years. Similar future development is expected for the Mt. Beatrice rock avalanche deposit. The calving terminus of the Hooker Glacier has retreated about 400 m in the last 4 years. The downvalley movement rate of the deposit (145 m/year for 2010) will decrease with decreasing flow rates toward the

terminus. With a rate of 100 m/year for both the deposit and for calving, the deposit will reach the lake in 15 years; or, if the calving rates increase up to 400 m/year, this could happen in about 7-8 years.

From laboratory experiments (Chapter 4), these investigations and other reported examples it is concluded that after the emplacement of a rock avalanche deposit on the glacier surface two main changes will occur in the glacier system:

1. The net mass balance becomes less negative by reduction of ice-surface ablation in the ablation zone, assuming there is no change in accumulation rate.

2. Additional mass is provided (i) immediately, by the rock avalanche deposit, and (ii) gradually, by the increasing relative ice thickness caused by reduced ablation under the rock avalanche deposit.

The reduction of total ablation under a rock avalanche deposit is larger than 50% and usually >70-80% (Reid, 1969; McSaveney, 1975; Alexander et al., 2011; this study). Ice-surface ablation usually reduces to close to zero beneath a rock avalanche deposit. Sub- and englacial ablation by melt-water heat flow, heat conductivity and other processes will be unaffected by the surface debris; they contribute only in a minor way (~ 10-20%; Alexander et al., 2011) to total ablation. Thus, if a sufficient area of the ablation zone is covered, the glacier net mass balance can be significantly altered. Because the clear-ice ablation rate increases toward the terminus (Schytt, 1967) and the rock avalanche deposit will be progressively carried downglacier, the reduction in surface ablation per unit area will increase as the debris approaches the terminus. At the same time, the upglacier limit of the debris cover is moving downvalley and clear-ice ablation thereby increasing, so the net variation of mass balance with time is not simple and will depend on the rock avalanche deposit geometry and local conditions. However, it is suggested that when the rear of the debris cover has been advected downvalley to the original terminus position, the glacier mass-balance is re-established and the debris-covered ice downvalley thereafter behaves independently of the glacier (Vacco et al., 2010; this study).

The effects of rock avalanche debris on glacier behaviour can be predicted quantitatively. Alexander et al. (2011) developed a simple steady-state mass balance model, calibrated on the modern (1999-2010) quasi-steady-state conditions of the Franz Josef Glacier and successfully tested against its LIA terminal moraine positions and trim lines. This was used to test the hypothesis of Tovar et al. (2008) that a catastrophic rock avalanche could have caused

the advance of the Franz Josef Glacier (western Southern Alps, New Zealand; Fig. 5.11) to the location of the Late Pleistocene/Early Holocene Waiho Loop moraine. The modelling shows that a steady-state terminus position at the Waiho Loop requires mean temperatures about 4-5°C cooler than present-day. Anderson and Mackintosh (2006), using an ice flow/mass balance model, found that an advance to the Waiho Loop required 3-4°C cooling from present-day. The results from both studies contradict proxy data, which indicate temperatures no more than ~ 2.5°C cooler than present-day during the last glacial-interglacial transition (LGIT) about 12,000-13,000 YBP (Carter et al., 2003; Turney et al., 2003; Barrows et al., 2008). Direct dating of the Waiho Loop moraine by Barrows et al. (2008) yielded an age of about 10,500 YBP, corresponding to significantly warmer temperatures than those that occurred during the LGIT and making a climatically driven advance even less likely.

To explain the advance of the Franz Josef Glacier from an equilibrium position close to Canavan's Knob to the Waiho Loop position during a time without any cooling (but ~ 2° cooler than present), Tovar et al. (2008) suggested, based on the sedimentology of the Loop moraine, that the ablation zone of the glacier was covered with debris by a rock avalanche. Alexander et al. (2011) showed that 65% reduction in total ablation (or a gradual reduction from 20-80% along the glacier) is needed to cause the required 3 km of advance from near Canavan's Knob to an equilibrium position at the Waiho Loop moraine (Fig. 5.11), assuming constant climate; based on the above data this appears reasonable. A coseismic rock avalanche of the required volume in the Waiho valley is certainly possible; Tovar et al. (2008) provided evidence of sufficiently large deep-seated, source-area scars in the correct location to match the dominant Loop lithology. Similar events have been reported elsewhere (e.g., Post, 1967; McSaveney, 1975, 2002; Gordon et. al., 1978; Evans and Clague, 1988; Orombelli and Porter, 1988; Gardner and Hewitt, 1990; Jibson et al., 2004, 2006; Lipovsky et al., 2008; Deline, 2009; Hewitt, 2009). Vacco et al. (2010) recently presented a one-dimensional numerical model of the Franz Josef Glacier. Though approximate, it confirmed that a debris-driven advance could reach the Waiho Loop under certain circumstances and, significantly, that the resulting deposition would have a prominent, high end moraine with an extensive blanket of ablation moraine to its rear, as appears to be the case at the Waiho Loop based on available evidence (Shulmeister et al., 2010a).

In summary, there is substantial evidence that a rock avalanche deposit covering a sufficient proportion of an ablation zone can cause glacier mass balance fluctuations and result in a non-climatically driven advance.

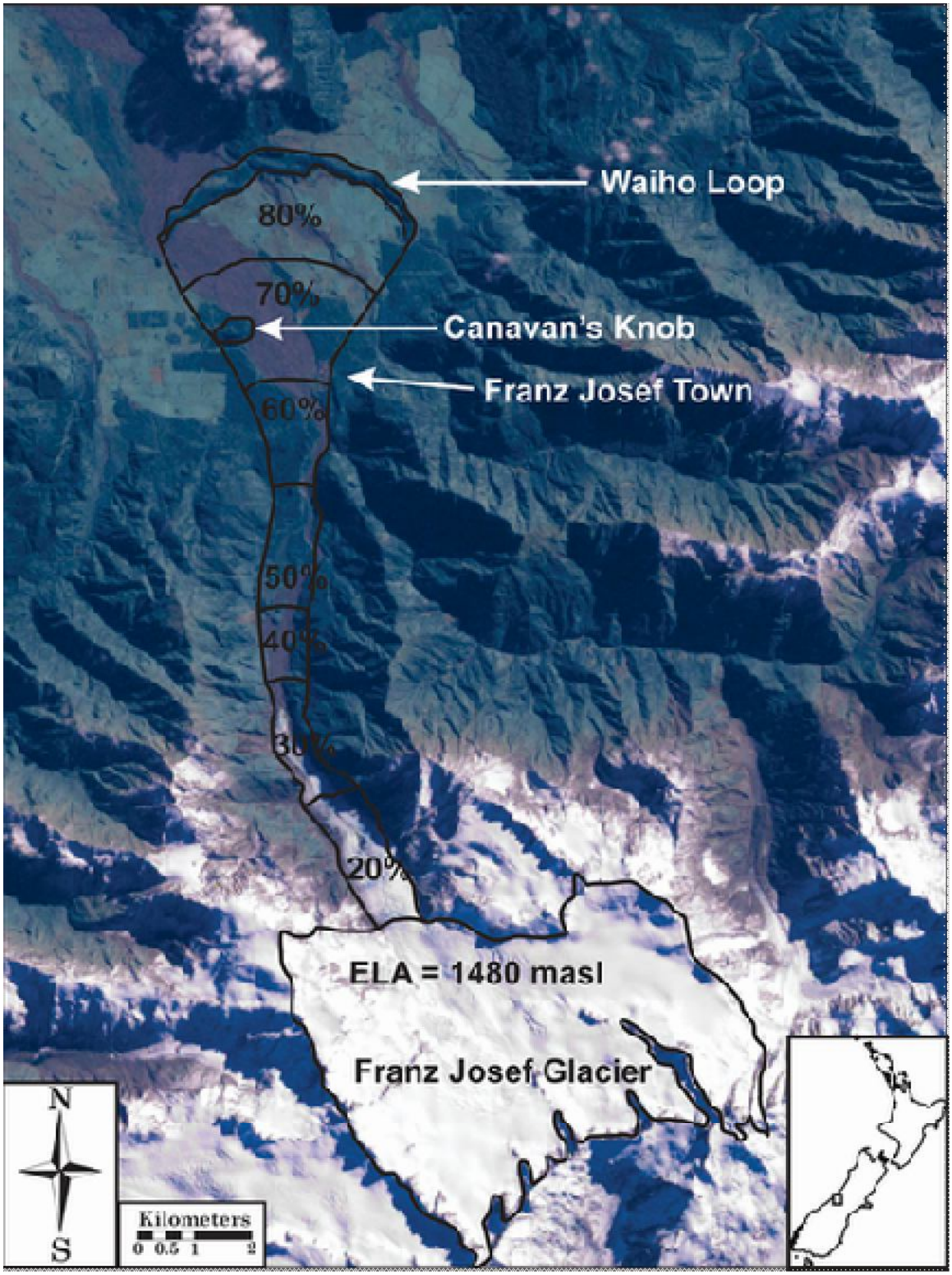

Figure 5.11. An example of the modelled rock avalanche debris cover on the Franz Josef Glacier, NZ, showing percentage of ablation reduction, which is staggered below the ELA to a terminus position at the Waiho Loop, assuming temperatures 2°C less than the present-day, with an ELA of 1480 m a.s.l. Photo: satellite image, LandSat, 2001. The staggered levels of ablation reflect the accumulation of high quantities of debris towards the terminus, while in the upper-ablation zone, ablation rates will return to those of cleanice once the debris has moved down-valley.

5.3.2. Effect of the rock avalanche on glacier motion

The formation of thick ice platforms beneath rock avalanche deposits must in principle affect the flow of the glacier (Shulmeister et al., 2009), to an extent dependent on the proportion of the ablation area covered with debris and on the depth of the glacier ice. The Tasman Glacier ice thickness in the area of the 1991 rock avalanche deposit is about 300-400 m, while gravity and GPR surveys in 1993/94 estimated that that the maximum ice thickness was 560 m in the Ball Hut area with average thickness varying from 300 - 400 m at the west and east, respectively, resting on gravels (basal moraine) about 50-100 m thick. The same basal moraine 100 m thick was found in the Malte Brun area (opposite the old Malte Brun Hut), where the maximum depth to bedrock is 500 m with an average 300 m of ice thickness. The average melting rates from 1974 to 1994 (geophysical investigation by Broadbent, 1974) were about 0.8 m at Malte Brun and 1.5 m at the Ball Hut area; if minimum melting rates had remained at these values until 2010, 25 m of ice would have melted at Ball Hut area and 13 m at Malte Brun. However, the small areas of disintegrated Aoraki/Mt. Cook rock avalanche, with ice thickening up to 30 m, are not large enough to influence the ice flow velocities of the Tasman Glacier, because the main flow in the area is generated by Hochstetter ice flow. Additionally, the main body of the avalanche is deposited on a glacier area with very low ice flow velocities (Fig. 5.12).

This study shows that the area of glacier covered by the Mt. Beatrice rock avalanche 5 years after emplacement has the equivalent of about 2 x (1.4-2 x 10^5) m^3 additional ice weight from the rock avalanche deposit plus about 13 x 10^5 m^3 of ice (if the average additional ice thickness is 27 m), which is increasing annually. In total it is equivalent to an extra 17 x 10^5 m^3 of ice on an area of about 5 ha, or 34 m of ice-depth. This additional mass must alter the local glacier dynamics by increasing ice flow and basal sliding. However, on the Hooker Glacier the ice depth beneath the rock avalanche deposit is unknown, but could be inferred to be in order of 300 m (by analogy with the Tasman Glacier at a same elevation of 1200-1300 m a.s.l.; Watson, 1995). If the area covered by the Mt. Beatrice rock avalanche was larger, it would cause larger glacier flow disturbances. Because the flow velocities for the Hooker Glacier are unknown, it is uncertain if the measured 145 m/y ice flow velocity is the normal in that area or whether it is accelerated due to the additional load from rock avalanche deposit and thickened ice.

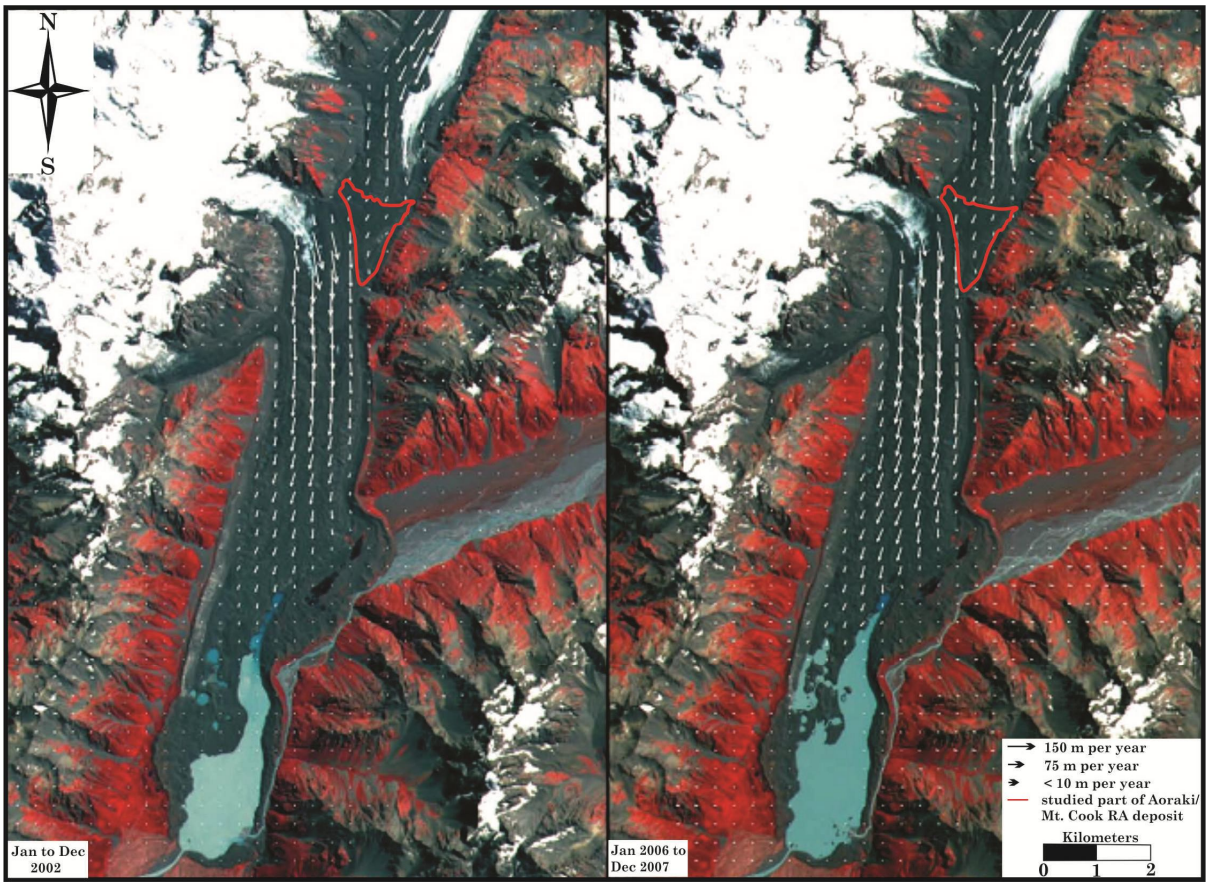

Figure 5.12. Ice flow velocity fields for the Tasman Glacier for January to December 2002 (on the left) and for January 2006 to December 2007 (on the right) superimposed on orthorectified ASTER data, modified from Quincey and Glasser (2009). Note the almost zero ice flow velocities in location of the Aoraki/Mt. Cook rock avalanche deposit (indicated by the red lines).

5.3.3. Ice platform formation under rock avalanche deposits

From close examination of these two deposits and comparison with other studied deposits a model of their development could be suggested (Fig. 5.13), which illustrates the development of edge ridges and extension of the platform with time as it is carried downvalley by ice flow. A rock avalanche deposit thicker than 1 m significantly suppresses ablation of the underlying ice. To a first approximation one can assume zero ice-surface ablation beneath the debris, with varying ablation of the adjacent clean ice. The ice flow is carrying the deposit platform downvalley into higher-ablation areas. The steep platform side slopes become less steep by gravity sliding of debris, differential ablation and slope orientation to the radiation source. The maximum slope of the sides is usually not more than 30-35° (Anderson, 2000), and becomes smaller with time. At the edges of the platform the ice tends to flow outwards and forms slightly raised edges. The downvalley ice-flow with differential surface flow velocities and resulting surface topography modify the shape of the deposit and platform, again with

potential sediment redistribution. The ongoing spread of the debris-cover around the deposit influences the platform growth rates and produces features like supraglacial ponds and cliffs.

This model was tested in the laboratory using the apparatus for investigating ablation beneath debris (Chapter 4), by covering half of surface of an ice block with rock avalanche material 25 cm thick, (the maximum possible with this apparatus). After several cycles of ablation a ~25º sloping profile developed in the contact zone (Fig. 5.14).

Anderson (2000) modelled the ablation-dominated formation of medial moraines that increase in relief down-glacier from the equilibrium line, considering the feedback of these moraines on glacier mass balance. This feedback resulted in larger down-valley glacier extents than meteorology alone would suggest, caused by suppressed ablation under increased medial moraine cover. His analytical and numerical modelling shows that as medial moraines travel downglacier over time, they widen and develop parabolic crests and linear slopes. In this model the debris thickness increases due to constant exhumation of englacial sediment, whereas in the case of a rock avalanche the deposit volume remains the same and changes only at the developed slopes. However, a similar slope developed in both cases. Anderson (2000) emphasised the higher debris thickness at the edges of the moraines, which he associated with the sharp slope break at the contact with clean ice and divergence of debris discharge. However, in the case of the large slopes several tens of metres high this effect is negligible.

It is commonly accepted that the platform of protected ice builds up to about 30-50 m height. There is no current explanation for this limit, however, I suggest that higher platforms can develop if other limiting factors do not prevail. The ice platform beneath the south part of the Mt. Beatrice rock avalanche deposit has reached >40 m thickness. On the Sherman Glacier in 2000 the debris-covered ice was about 35 m higher than the bare ice immediately upglacier from it (Molnia, 2008).

Thus, even small rock avalanches relative to glacier size dramatically reduced ice surface ablation and modified the glacier surface relief. The rock avalanche sediment input is several orders of magnitude greater than the annual sediment delivery to the glacier and its deposit traveled mostly passively with little change apart from the very edges of the deposit.

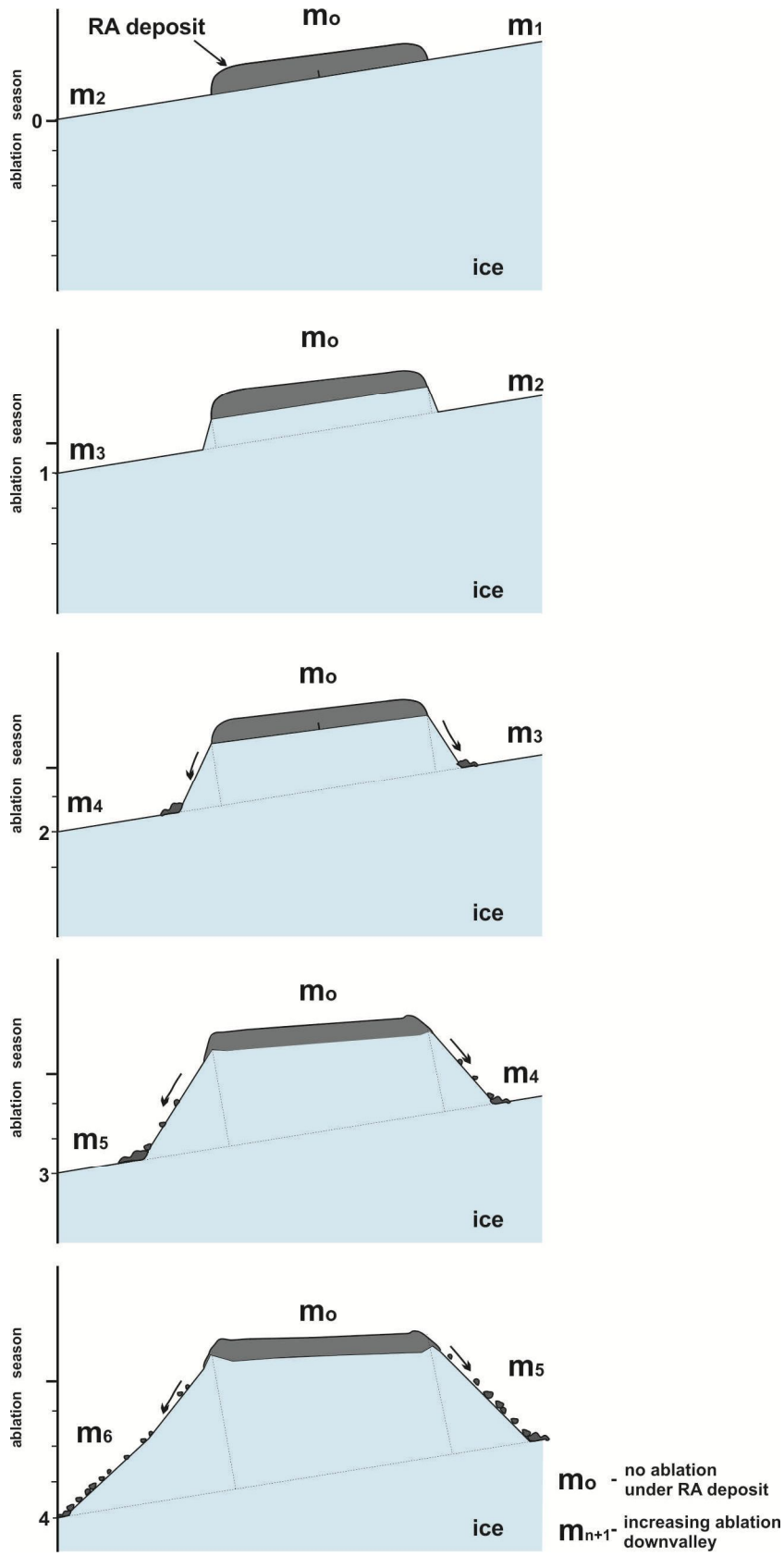

Figure 5.13. Model of platform development under the supraglacial rock avalanche deposit with each following ablation season during travel of the deposit downvalley.

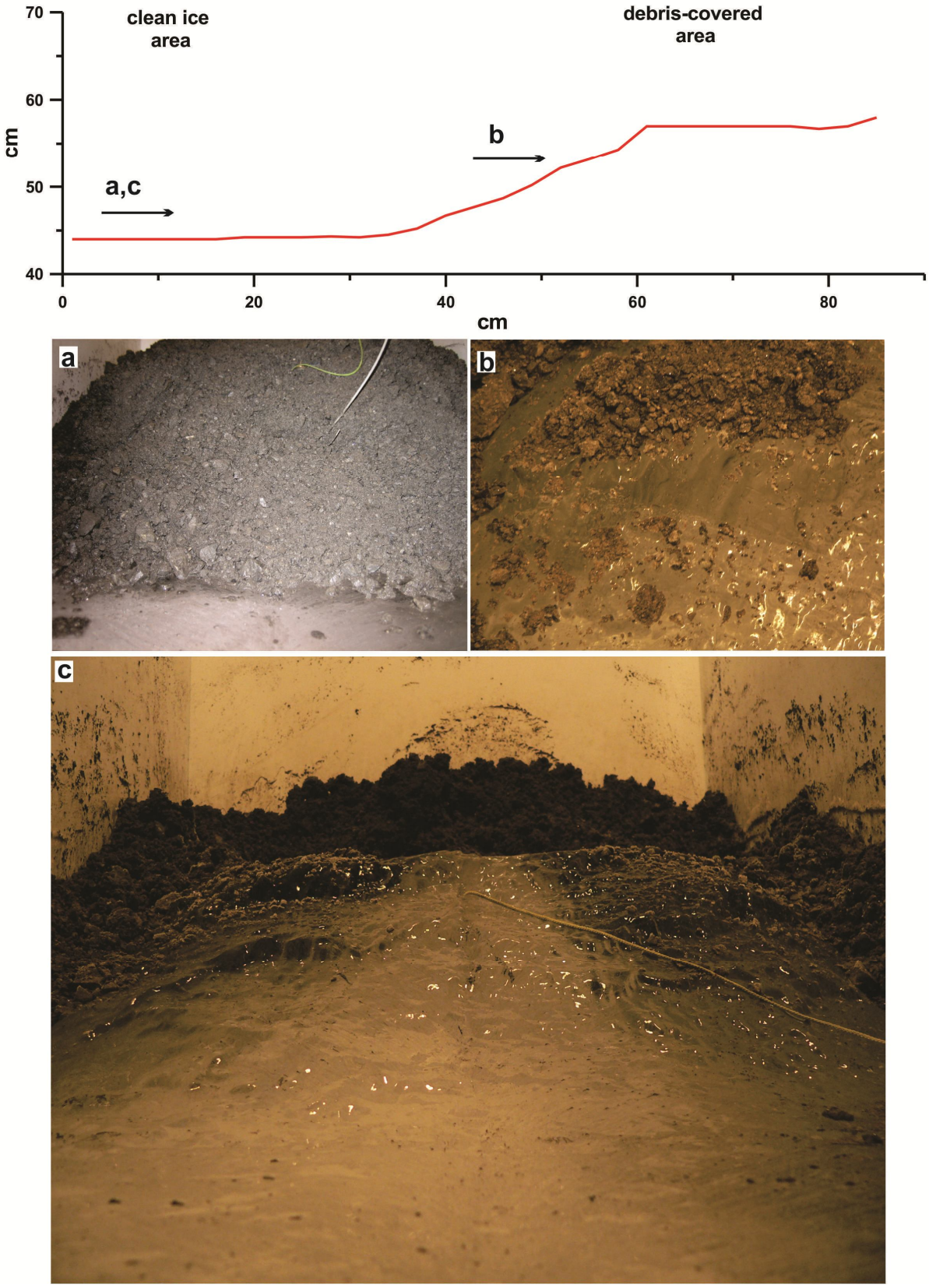

Figure 5.14. Experiment on ice platform formation. The ice profile shows the ridge at the contact between melted clean ice and ice beneath debris. A and c depict this ridge with and without deposit, respectively (note the "broken" rather than smooth type of the slope); b is a close-up view of the slope.

5.4. GLACIOLOGICAL AND GEOMORPHOLOGICAL IMPLICATIONS

Because sediment deposits found in the valleys of glaciers are commonly used to monitor modern and past climate fluctuations, it is essential that past and present sediment delivery, transport and deposition processes onto and within the glacier are well documented, constrained and understood. The present study gives a clear indication that rock avalanches have the potential to make a significant contribution to both sediment supply and its deposition in glaciated mountain ranges. The effects of a rock avalanche deposit on a glacier surface will result in:

1. Large loads of rock avalanche sediment contributing to the supraglacial sedimentology with disturbance of the supraglacial meltwater and sediment transportation.

2. The rock avalanche deposit alters glacier regime by reduction of the surface ablation and by alteration of the glacier basal, internal or surface ice flow velocities caused by load of rock avalanche debris and protected ice under the deposit.

3. The glacier responses to these changes.

4. Following glacier regime changes, alteration of the glacial sediment deposition.

However, the degree of these changes in the glacial system will vary and depend on the rock avalanche and glacier magnitudes and the glacier regime at the time of a rock avalanche emplacement. The possible glacier changes from rock avalanche events and a proposed classification of the consequences according to the glacier regimes are described below.

5.4.1. Contribution to the glacial sediment transport

In general, rock avalanches have tended to have been ignored or undervalued as an input to glacial sediment budgets. However, the erosional significance of the rock avalanches must be acknowledged. The total volume of sediment contributed by a single rock avalanche is such that a single event may exceed quantities considered normal for a glacial sediment budget of decades, or even up to several hundred years. For example, the rock avalanche from Paulsen Peak (1877 m) on the Lyell Glacier, South Georgia (total volume of rock, ice and snow estimated as 3.3×10^6 m^3) has been calculated to represent a minimum of 93 years of normal subaerial erosion (Gordon et al., 1978). Similarly the Aoraki/Mt. Cook rock avalanche of

1991 delivered in a single event, a total equivalent to 200 years of the annual average debris flux associated with icefall to the Tasman Glacier (Kirkbride and Sugden, 1992).

As a result, sediment incorporated into a glacier or deposited by glacial action should not be considered solely as material that originated from glacial erosion and small rockfalls. The fact that a portion of that load may also be the result of rock avalanche emplacement must also be given consideration. Based on studies of two glaciers in the Nanga Parbat Himalaya region, Owen et al. (2003) concluded that the widely held concept that the basal traction zone is the only major source of fine sediment production for glaciers is wrong, concluding instead that fine-grained sediments on glaciers in high-altitude environments were supplied by erosion occurring on the ice surface (Chapter 2). However, it is still uncertain how rather weak supraglacial forces might produce a higher proportion of finer sediment than those derived from traction forces underneath the ice. Owen et al. (2003) overlooked the possibility that frequent rock avalanche events in Himalaya (Hewitt et al., 2008) may also be a contributing factor, such that the fine material is a consequence of primary deposition and not erosion. Given the enormous quantities of fines generated by rock avalanches (McSaveney and Davies, 2007) this factor appears to be significant.

The concept of glacial fine sediment production being restricted to the basal parts of a glacier (Boulton, 1978) is widely accepted. This leads to the question about the input rock avalanches might make to glacial sediment load and the current research. The aim is to a) identify rock avalanche sediment on glaciers, b) trace its travel path through the glacier and its modification (or not) by glacier processes during that journey and c) determine how rock avalanche materials contribute to the overall sediment budget of the glacier.

5.4.2. Possible glacier responses to rock avalanche deposit

From observations and historical examples of rock avalanches on glaciers it can be concluded that the size of the rock avalanche and the current glacial regime (the glacier ‘regime’ is defined as the state of the glacier in respect to concurrent climate and includes seasonal and annual mass balances, mass turnover, equilibrium-line altitude (ELA), and accumulation-area ratio (AAR); Dyurgerov, 2003). Therefore, three scales of rock avalanche and their potential effects on a glacier can be distinguished.

1. A small rock avalanche deposit (relative to glacier size) would be reworked by the glacier ice flow and will contribute to en- and supraglacial debris transportation. For this to occur the glacier needs to be large, bearing in mind that a "small" rock avalanche has a volume $\geq 10^5$-10^6 m^3 (Davies et al., 1999), and, given an average depth of say 5 m, covers an area of up to 0.2 km^2. Today such large glaciers are found only in the Andes of South America, the northwest mountain ranges of North America and in Arctic and Antarctic areas. Several rock avalanches onto the large glaciers in Alaska after the 1964 Great Alaskan Earthquake were small in comparison with the glacier ablation zone areas and eventually became entrained by the glacier flow and incorporated into medial moraines. Traces of rock avalanche sediment could be found in lateral and terminal moraines, but the degree of its preservation is questionable.

2. The occurrence of a rock avalanche that is not large enough to cover > 10% of the ablation zone will affect mass balance of the glacier only locally (Shulmeister et al., 2009), but the glacial flow will be unable to disperse the deposit totally before it reaches the terminus. These deposits usually do not have significant effects on glacier behavior; however, their volume may be equivalent to many years of conventional sediment delivery, so the resulting moraines may be prominent (Gillespies Beach moraine; Evans et al., 2010). Numerous recent rock avalanches in the Southern Alps are examples of this. In the Aoraki/Mt. Cook area this type of event occurs every 10 to 100 years (Cox et al., 2008; Allen et al., 2011); with a stable terminus position, these deposits will reach the terminus and eventually dump or stagnate there contributing to a large moraine. Mt. Beatrice and Aoraki/Mt. Cook rock avalanches covered 1% and less than 4% of the ablation zones respectively, with no noticeable change of glacier behaviour, but contribution of several decades-worth of sediment delivery to the glaciers. Several superposed rock avalanche deposits from Mt. Vampire are found on the Mueller Glacier (Cox et al., 2008). The sediment from these rock avalanches contributes to moraine deposition due to the normal (climate change-driven) glacier activity and locally thickened ice; however, the existence of these moraines depends mostly on the rock avalanche sediment.

3. The rock avalanche deposit covers a large enough proportion of the ablation zone to change the total glacier mass balance significantly, causing glacier behavior to change noticeably; when it reaches the terminus the deposit could cause formation of a non-climatic terminal moraine. Among historical examples are the Triolet, Brenva, Bualtar Glaciers (Porter and Orombelli, 1981, Barla et al., 2000, Hewitt, 2009, Deline and Kirkbride, 2009),

and in New Zealand the Waiho Loop moraine was identified as the result of such an event in the early Holocene (Tovar et al., 2008). All these glacier mass balances were altered and the rock avalanche material was eventually deposited at the front of the glacier. The type of glacier response to the deposit, such as cessation or slowing of retreat, or re-advance, or surge, depends on the glacier regime, configuration and rock avalanche relative size and location; and the type of response is likely to affect the type of moraine formed.

The individual glacier configuration, response time and particular regime at the moment of and following the rock avalanche result in a particular response that will be complicated by concurrent climate changes. In some cases, however, end members of the glacier response to the catastrophic event are possible, such as faster adjustment than to the climatic fluctuations and retarded response due to climate changes before/after the event. The conceptual model of glacier responses and consequent deposition due to supraglacial rock avalanche emplacement is shown in Figure 5.15. Between pre-event glacier conditions to the return to this condition (according to the constantly changing climate) the glacier could have four main reactions:

- no significant changes in mass balance;
- mass balance disturbances (localized);
- net mass balance change (change of glacier pre-deposition regime);
- dramatic changes in net balance (immediate response).

Glaciers will respond by moving to a less negative net mass balance. Thus, an equilibrium glacier may advance; a retreating glacier may retreat more slowly, or come into equilibrium, or advance; and an already advancing glacier may advance more rapidly and/or surge. A surge-type glacier may surge prematurely (Hewitt, 1988). Therefore, the knowledge of the current mass balance of the glacier before, at the moment and after the rock avalanche deposition should be included in estimation of the glacier response to this event.

From the recorded events it could be concluded that the magnitude of the response will depend on the proportion of rock-avalanche-covered ablation zone of glacier and the concurrent regime of the glacier. As a result of reduced ablation caused by the rock avalanche deposit the AAR changed, implying that glaciers need to increase their entire surface area in order to adjust the area to present climate conditions by increased thickness in the ablation zone and possibly an advancing terminus position. Because of the number of conditions which will affect the response, each glacier must be considered individually; however, the minimum proportions of the covered ablation zone to the glacier with specific AAR and

regimes could be estimated. Thus, from observations on some glaciers and theoretical approximation I suggest the minimum proportions of the rock avalanche covered areas (%) that will cause net balance changes according to the main glacier types, grouped by their main types of regimes and AAR (Fig. 5.16).

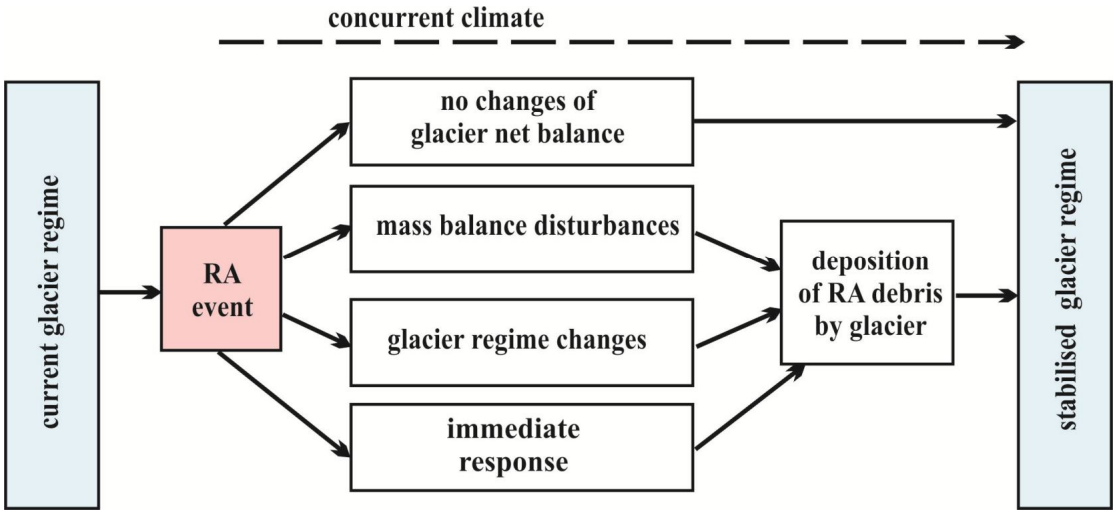

Figure 5.15. Schematic representation of the possible glacier responses and consequent deposition to the supraglacial rock avalanche event.

Surge-type glaciers (ice flow fluctuates strongly at decade-to-century intervals; AAR=0.6-1 and maximum during onset of surge) will require ≥10-15% of the ablation zone covered by rock avalanche deposit to have and advance/surge response. The Bualtar Glacier is the best example of such behavior, where the rock avalanche that covered only 15% of its ablation area caused glacier to surge and then advanced for 20 years after the deposition (Hewitt, 2009).

Advancing/equilibrium glaciers (high ice flow; AAR=0.5-0.8) will require ≥15% of the ablation zone to be covered by rock avalanche deposit to respond by advance or accelerated advance. The 1920 rock avalanche deposit on the Brenva Glacier ablation zone resulted in its continued advance for 20 years (Deline, 2009). However, depending on the size of the rock avalanche deposit this advance could occur irrespective of the concurrent climate to accelerate advance and possibly cause the glacier to surge – i.e. to immediately and catastrophically respond to the event (see Surge glaciers).

Retreating glaciers (high ice flow; AAR=0.4-0.6) will required ≥40% of the ablation zone to be covered by rock avalanche deposit to respond by achieving equilibrium or by advancing. The Sherman Glacier is example of the effect of rock avalanche covering 60% of the ablation zone by rock avalanche deposit; it responded by bringing the glacier from retreat state to the equilibrium and then to a small but definite advance (McSaveney, 1975), while the adjacent and similar Sheridan Glacier has continued to retreat.

Retreating glacier with ablation zone mostly debris-covered (slow ice flow; AAR=0.4-0.2) will require ≥60% of the ablation zone to be covered by rock avalanche deposit to cause a response by shifting the glacier regime.

Debris-covered glaciers with supraglacial lakes (ice flow almost ceased at the ablation zone; AAR=0.4-0.2) will required 60-100% of the ablation zone to be covered to cause the glacier to change its regime, although it will depend on the glacier flow rates and configurations. The Aoraki/Mt. Cook rock avalanche that covered <4% of the ablation zone did not trigger any change of the glacier regime, but caused local mass balance changes.

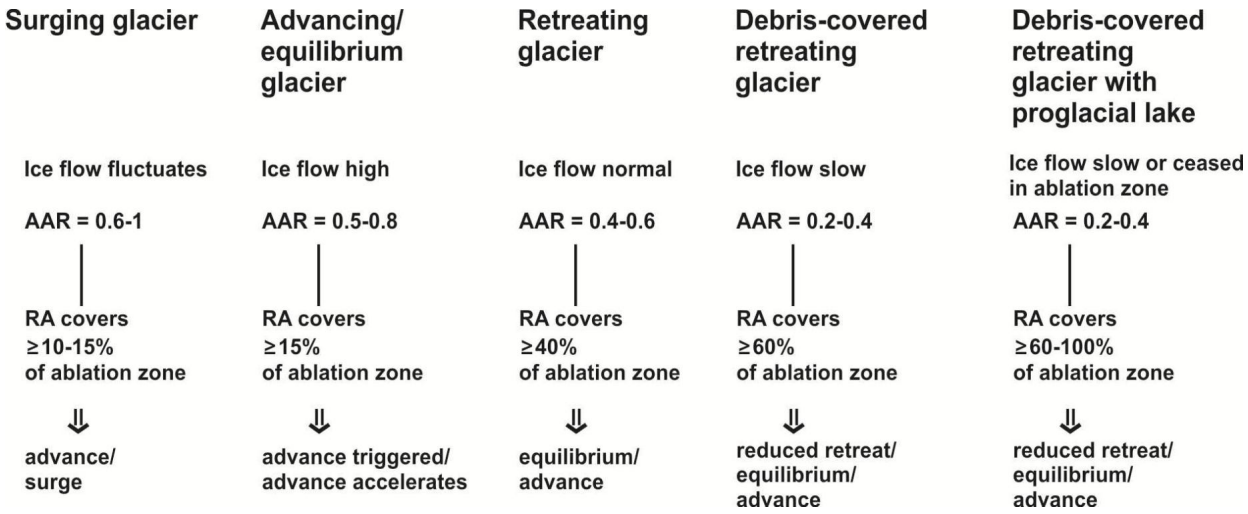

Figure 5.16. The minimum proportions of the rock avalanche covered areas (%) of the glacier ablation zones required to cause net balance changes according to the main glacier types, grouped by their main types of regimes and AAR.

5.4.3. Contribution to the moraine formation

From current research it is evident that large rock avalanches have a significant effect on glaciers and that this provides additional sediment for moraine formation that is unrelated to climate variation. In the next section of this chapter, the current understanding of moraine

formation resulting from climate triggers will be discussed, leading to an assessment of the research and its implications with respect to the development of a theoretical model for the formation of rock-avalanche-induced moraines.

5.4.2.3. Formation of moraines from climate fluctuations

During periods of positive glacier mass balance, terminal moraines are generally formed by the advance of the ice front into the valley resulting in the bulldozing of small "push" moraines or thrust moraines (commonly in permafrost conditions), "dumping" of supraglacial debris, often resulting in high and steep lateral moraines (Benn and Evans, 2010) or stratified "outwash" terminal moraines normally associated with large volumes of water (Evans et al., 2010). Typical lateral moraines associated with mountain glaciers are usually the result of the dumping of supraglacial debris. The 'style' of this dumping may result in the formation of different moraine morphologies (accretion-mode or superposition-mode), the sedimentology of which is influenced by variations in slope processes on the adjacent valley flanks (Benn and Evans, 2010), or through interactions with glaciofluvial deposition (Iturrizaga, 2001). The marginal landsystems for highly debris-covered glaciers in general are characterised by ablation moraines, glaciofluvial depositional features and hummocky moraines; however, the genesis of terminal moraine ridge formation remains somewhat uncertain (Benn et al., 2003; Benn and Evans, 2010).

Push moraine formation is well documented as a result of observation of the process during seasonal glacier front oscillations and at stationary glacier fronts. These moraines are usually formed as a result of the direct pushing of sedimentary material by advancing ice front during short-term re-advances or seasonal advances (Winkler and Nesje, 1999), which under some circumstances may be accompanied by ice-marginal squeezing (Evans and Hiemstra, 2005). Usually, such moraines are several metres high and form in front of glaciers with a minimal supraglacial cover. The presence of supraglacial load on glaciers leads to a more complicated process of moraine formation. During a glacial advance, the supraglacial component of the debris cover will be dumped at the ice front and will then be incorporated and mixed by further pushing in the case of an advance, or remain in place unless it is further reworked by outwash. Some dumped, terminal push moraines have a higher percentage of angular (and very angular) clasts when compared to push moraines without this component (for example, the Franz Josef Glacier moraines in New Zealand *versus* Jostedalsbreen moraines in Norway in this study).

In areas with high volumes of fluvial water (e.g. the Southern Alps of New Zealand) where the glacier often advances through its own outwash, the terminal moraines usually comprise steep-fronted, ice-contact outwash fans (generated by fluvial processes) and small surface dump moraines (Evans et al., 2010). Evidence of glaciotectonic deformation of the fan beds is often weak and localised (e.g. Shulmeister et al., 2009). During advances, these glaciers do not usually produce large moraines because the proglacial river is recycling most of the sediment. As a result, any large ridges are mostly composed of dumped supraglacial material that accumulated during glacier stillstand. In cases where the glacier is trapped behind an outwash fan head, the terminus remains in this position for prolonged periods of time. As a result, if formed, the moraine mostly consists from supraglacial material that has accumulated over periods of decades or more (the Tasman Glacier; Speight, 1940; Kirkbride, 2000).

Therefore, the mode of formation type of terminal moraine will depend not only on the glacial regime and the volume of supraglacial material, but also on post-depositional preservation conditions, fluvial activity and the rate of glaciofluvial incision into the outwash, sediment availability at front of the glacier, and non-climatic effects such as the presence of supraglacial or rock avalanche debris.

5.4.2.4. Rock avalanche-induced moraines

The impact of rock avalanche deposits on glacier behaviour will be determined by local factors such as the size of the event relative to the glacier size, the location of that event (above/below equilibrium line, or both), the regime (mass balance situation) of the glacier prior to the event and concurrent climate affects.

Rock avalanche deposits will often add a very large volume of sediment to the supraglacial debris load. Except for a small proportion of the avalanche material that is ‘lost’ via crevasses, the majority of the debris will be transported supraglacially. As a result of the increased supraglacial debris thickness and composition, the debris-covered ice surface is likely to reduce in elevation more slowly due to reduced ablation with a corresponding alteration to the profile of the glacier surface as the debris is transported down-glacier. As a result, large quantities of supraglacial debris will move to the frontal margin of the glacier and potentially be deposited there by dumping. The dumping of supraglacial debris, resulting in very high and steep moraines seems to be the most likely cause of very large, steep-fronted terminal moraines such as the Waiho Loop (Shulmeister et al., 2010a). A rock avalanche in

the order of 10^6 m^3 in volume would create a very prominent feature in the landscape. The large volumes of supraglacial debris required to achieve such an outcome suggest that a rock avalanche as the most likely cause of such moraines.

A glacier which has been impacted by a significant rock avalanche will produce moraines which will contrast with those associated with 'normal' climatic moraine formation simply because the latter will contain much less supraglacial material. The difference will be determined by the glacier regime at the time of deposition and the response of the glacier to the avalanche event. In a situation where the rock avalanche induces the glacier to advance, the rock-avalanche deposit will be carried further downvalley than the pre-event terminus position. In general, this will result in the partially compressed and thickened supraglacial deposit being dumped or remaining stationary at front of the maximum terminus of the glacier (Fig. 5.17).

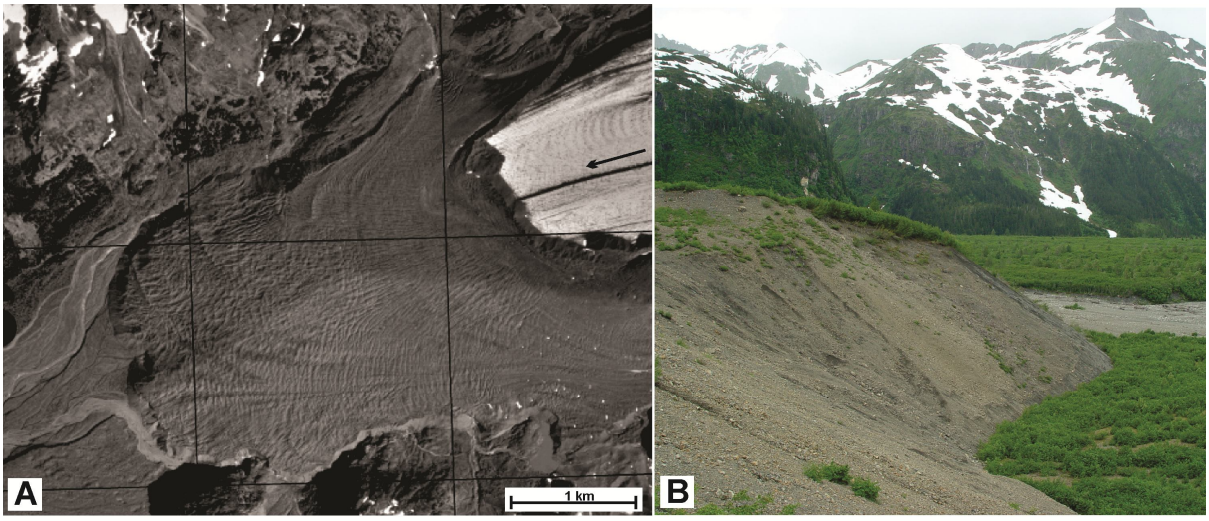

Figure 5.17. The 1964 Sherman Glacier rock avalanche deposit 44 years after emplacement: (A) the rock-avalanche cover travels supraglacially, arrow indicates ice flow direction; and (B) and is carried to the terminus by glacier flow, where it is dumped to form a moraine. Photos from M.J. McSaveney, 2008.

A conceptual model showing how rock avalanches may cause a glacial advance and frontal moraine formation is displayed in Figure 5.18. A rock-avalanche–driven glacier advance will be short-lived in comparison with climatic advances and will be about as long as the glacier response time. The ice covered with rock avalanche material reduces in elevation less slowly than the clean ice to its rear because of suppressed melting with respect to rates appropriate for clean or thinly-covered ice, and as a result the ice flows more rapidly (ice flow depends

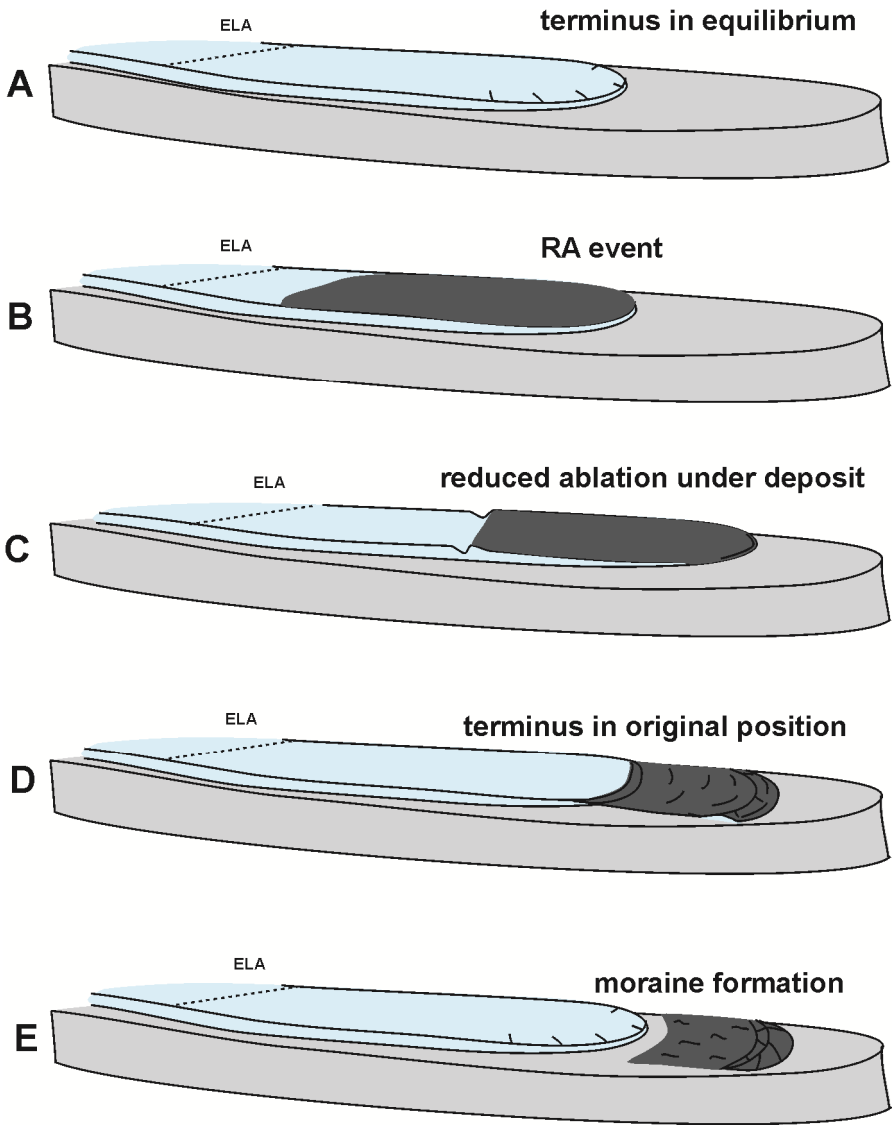

Figure 5.18. Response of a glacier to rock avalanche debris covering the ablation zone: (A) glacier in equilibrium prior to rock avalanche; (B) rock avalanche emplaced; total ablation reduced by~70%; (C) the lack of melting increases ice depth and sliding velocity; the rock-covered reach reduces in length caused by relative differences in velocity and ice thickens; (D) the now debris-free glacier re-attains its original terminus; debris-covered ice continues to flow and slowly melt, forming terminal moraine by dumping RA deposit; and (E) all ice has now melted, a new terminal moraine remains.

on ice depth and surface slope; Paterson, 2004). As the debris-covered ice moves downvalley it will tend to compress as the rear of the rock avalanche covered area detaches from the ice behind while the front slowly over-runs cleaner ice ahead. In addition, ice at the terminus has compressive flow which is less rapid than that farther upvalley, this results in a further reduction of the length of debris-covered ice with a corresponding increase in thickness. Eventually the original glacier ablation zone will become debris-free as progressively all the debris will be carried beyond the original terminus (Fig. 5.18 D). The debris-covered ice downvalley is now no longer fed by ice from the glacier and continues to flow increasingly

slowly under its own surface gradient while slowly melting, forming a terminal moraine; it eventually becomes stationary and slowly melts to form a sheet of ablation moraine to the rear of the terminal moraine (Fig. 5.18 E).

This moraine formation mechanism is similar to that generated by the model of Vacco et al. (2010). Whether a broad hummocky topography forms (claimed to be formed by Vacco et al., 2010) will be determined by the magnitude of the rock avalanche event, the glacier regime at the time of deposition and the post-depositional preservational regime. Thus, if the glacier had been retreating, a large rock avalanche may result in a temporary cessation of retreat but will still generate a distinctive terminal moraine. The rock-avalanche-deposit-buried ice will become stationary because the glacier will re-equilibrate to pre-event mass balance levels more rapidly, in a manner similar to a glacier surge and rapid advance. Therefore, the faster the glacier response to the rock avalanche emplacement and faster it returns to the pre-event conditions the larger the hummocky moraine that should form.

Sedimentologically, in contrast to the usually polylithological sediment in the moraine of a climatically-driven advance, a rock avalanche-induced-moraine will usually be dominantly monolithological as most of the sediment is usually sourced from a single rock avalanche scar (though note that a large earthquake can cause more than one rock avalanche in a catchment; Jibson et al., 2004; 2006). The sediment will have more angular material in contrast with a moraine from a sub-glacial source. Additionally, because rock avalanches contain very large proportions of very fine material and agglomerates (Reznichenko et al., 2012), a rock-avalanche generated advance moraine may be characterized by a much higher proportion of very fine particles and presence of agglomerates when compared to ‘normal’ climate-driven moraines.

All terminal moraines are likely to be removed by subsequent re-advances. For preservation of those moraines formed as a result of climatically-driven ice advances, a consequent glacier retreat is required to preserve the moraine. As a result, only the youngest moraines, rather than those of the entire Holocene, will be preserved (Kirkbride and Brazier, 1998). A rock-avalanche-driven advance (or decreased retreat) will usually be followed by a retreat resulting in moraine formation and a subsequent return to pre-avalanche conditions. Therefore each rock avalanche-driven advance moraine has a higher chance of preservation than a climatic moraine which is preserved only if it reflects a maximum cooling or a recessional position (e.g. Shulmeister et al., 2005; 2010a).

Given the potential for rock avalanches to generate terminal moraines, further work is needed to understand how the enhanced sediment delivery is related to final moraine form, but in the case of the Waiho Loop, it appears that a pronounced ridge will be one consequence (Tovar et al., 2008; Vacco et al., 2010; Shulmeister et al., 2010a).

5.5. CONCLUSIONS

1. GPR investigation on two supraglacial rock avalanche deposits on Tasman and Hooker Glaciers in the Southern Alps of New Zealand showed that the debris on the Mt. Beatrice rock avalanche deposits are 1.4-2 x 10^5 m^3 and covered the glacier with a 3-7 m thick layer; the northern part of the Aoraki/Mt. Cook rock avalanche deposit is up to 10 m thick. In the prevailing humid and temperate conditions ablation almost ceased and ice under the deposit thickened as much as 30-40 m (by 2010) for the Mt. Beatrice and 25 m (by 2009) for the Aoraki/Mt. Cook rock avalanches. These rock avalanches are small in comparison to the glacier ablation zones (<1% for the Hooker and <4% for the Tasman Glaciers) and, although they contribute to the less negative mass balance of the glaciers, there was no observable alteration of the glacier regimes. However, the sediment load from these two rock avalanches is equivalent to decades of normal input of debris into the glacial systems and is considered as a potential contributor to glacial moraines.

2. The GPR surveys were based on a distinct material contrast between rock avalanche debris and the underlying ice. This method is the most reliable available for identification and estimation of supraglacial rock avalanche deposit volumes.

3. The presence of rock-avalanche debris several metres deep affects the mass balance, and thus the motion, of a glacier. Based on these findings, observations of historical rock avalanches and simple calculation of changes in the net balance of the glaciers, the minimum rock avalanche sizes required to cause glaciers to respond are estimated based on simple classification by the glacier AAR and five main glacier regimes. A conceptual model of rock-avalanche-induced advance of the glacier is proposed. The glacier response to a rock avalanche is likely to result in the formation of a terminal moraine which will not necessarily reflect climate change.

Understanding the role of supraglacial debris on mass balance is crucial in distinguishing terminal moraines which reflect climatic change from those caused by debris-cover induced advance.

6. A new technique for identifying rock avalanche sediments in glacial sediments

6.1. INTRODUCTION

6.1.1. Concepts underpinning the need to differentiate rock avalanche material in glacial sediments

In order to identify rock avalanche sediment in moraines, a new methodology is proposed here. This method is based on the microsedimentological (< 63 μm size fraction) differences between rock avalanche deposits and glacially-derived sediment.

Rock avalanche deposition occurs under extreme conditions with intense comminution of the material resulting from high runout velocities (up to 100 m/s) combined with the depth (10-100 m) of the flowing rock mass (Davies and McSaveney, 2009). As a result, a large proportion of these deposits are composed of very fine fragments (< 10 μm) produced as a result of high-stress and high strain-rate conditions imposed during the fall and run-out of the deposit (Hewitt et al., 2008; Davies and McSaveney, 2009). After deposition the avalanche material is subjected to localised lateral redistribution and modification (Dunning, 2004; Aa et al., 2007), while the main body of the deposit remains unaltered. The fine material, however, remains essentially intact within the deposit, offering an opportunity to further understand emplacement dynamics and the potential to discriminate these sediments from deposits attributable to valley glaciers and associated meltwater processes.

In contrast, valley glaciers deposit sediment under comparatively low-stress conditions and in temperate regions with a strong contribution from meltwater processes. Glacial deposits are composed of sub- and englacially-sourced sediment that is gradually produced under low strain rates. As a result, only a small volume of very fine particles will be produced. In temperate glaciers, meltwater will constantly modify/rework the sediment such that fine material will be transported from the production zone to the proglacial environment or beyond. As a result of these processes, sediment in glacial deposits should have much smaller quantities of very fine (< 4 μm) particles and, as a result, be distinguishable from rock-avalanche-generated sediment.

Supraglacial rock avalanche deposits travel passively on the ice with localised reworking of the sediment along the glacier margins. Therefore, it is expected that the sediment will retain

the fine component until it is deposited by ice into a moraine. Consequently examination of the fine sediment found in moraines may indicate the presence of rock avalanche material.

6.1.2. Rationale

In this chapter the hypothesis that the presence and nature of fine particles in rock avalanche and glacial sediments will indicate the origin of the sediment is tested. The particle size distribution of fine sediment from rock avalanche deposits is compared with a variety of glacially-derived sediments that are known to lack rock avalanche material (from the Southern Alps of New Zealand and Jostedalsbreen of Norway). Initial work was carried out using a Laser Sizer. The results indicated that many fines are present in rock avalanche deposits but that the size distribution was remarkable uniform (platykurtic) with an improbably high percentage of coarse grains. This suggested some problems with the Laser Sizer results. Consequently, I examined grains under a stereo microscope to investigate this observation. This work demonstrated that rock avalanche grains were obscured by adhering particles or were possibly a range of smaller particles clumped together. After examination of whole grains under the Scanning Electron Microscope (SEM) it was decided to examine rock avalanche sectioned and polished grains in detail also using the SEM. This led to development of the new approach for the examination of very fine sediment on the SEM. As a result this chapter presents the particle size and composition work in the sequence that led to the polished grain mount work, where the key findings were made.

6.2. FIELD DATA COLLECTION

Samples used for this study were collected from rock avalanche deposits in the Southern Alps, New Zealand, and Jostedalsbreen, Norway, as a result having contrasting lithologies, ages and local environmental conditions. Sediments from deposits of rock avalanches, and numerous moraines and glacial sediments, have also been sampled in the central area of the Southern Alps of New Zealand, Jostedalsbreen, Norway and Southern-West Baltic Sea, Kaliningrad region, Western Russia. A summary table of the site descriptions and images are presented in Appendix E.

The aim of the sampling was to collect the most representative material for the deposit, and hence was restricted to rare naturally exposed sections in which contamination from erosional

features was unlikely. Samples of about 300-400 g of finer-fraction sediment were recovered from a minimum depth of 0.5 m below the surface of the outcrop and, where possible, from several metres below the top of the section to eliminate soil and down-washed colluvial contamination. For recent rock avalanche deposits on glaciers the samples were recovered by digging into the deposits, which were mostly homogenous except for a very coarse surface carapace. A variety of moraine environments (lateral moraines, terminal moraines, ground moraines) were sampled. The recent (10-20 year old) moraines in Norway and on the west coast of New Zealand are well exposed and loose, fresh deposits that are easy to dig into are common. Coarse clasts (> 60 mm) were manually removed and left in the field with only the finer material being collected, then sealed in plastic bags and taken to the laboratory for further analysis. Additionally, outcrop descriptions, general lithology and pebble roundness were recorded for each sample and completed in the field.

Clast roundness indicates the transport environment, whether clasts are passively, actively or glacifluvially transported has a significant influence on their roundness (Benn and Evans, 2010). Rock avalanche sediment is dominated by very angular and angular clasts produced as a result of comminution during the rock avalanche emplacement and perhaps accentuated by frost shattering during the non-active resting stage of the deposit. In contrast, during active transport within and beneath glacial systems, fracturing and abrasion increases edge-rounding and creates polished facets of glacial sediment (Evans and Benn, 2004). Thus, actively transported sediment in the basal zone of glaciers has mostly subrounded and rounded grains. Roundness was measured for 50 clasts from each sampled deposit.

6.2.1. Rock avalanche sediments

The **Acheron rock avalanche** deposit was sampled from a section where a stream has cut through the deposit. The outcrop is ~ 10 m high and the sample was recovered from about 1 m above the basal zone of the rock avalanche deposit (S 43º19’18’’; E 171º39’54’’). The sediment is a matrix supported angular greywacke gravel with a ‘jigsaw’ (Dunning, 2004) texture. The matrix is composed of crushed greywacke and is clay to sand sized. [Note that in these descriptions, clay implies size only, not chemistry].

Samples of the Lake **Coleridge** rock avalanche were taken from a 5 m high outcrop where the Ryton River has cut through the deposit adjacent to the eastern shore of Lake Coleridge (S 43°16'35.58"; E 171°32'12"). The sample was recovered from about 3 m above the base.

Lee et al. (2009) identified three rock avalanches in this area, and the outcrop is attributed to the second event which is ca 600 years old. This is capped by sediments of the third (youngest) event. The sediment is a matrix-supported angular greywacke gravel with the matrix being composed of crushed, clay- to sand-sized greywacke particles. There is crude inverse stratification in the deposit (Lee, 2004; Lee et al., 2009).

The **Round Top** deposit is composed of highly crushed, angular mylonitic schist with varying degrees of foliation. The original lithological bands have been preserved. Two samples were taken from a quarry (S 42°53'44"; E 171°04'54"). The sediment is a matrix-supported angular gravel. The matrix is composed of clay to sand sized particles with common jigsaw-fractured clasts.

Because there is no exposure in the supraglacial 1991 **Aoraki/Mt. Cook rock avalanche** deposit, the sediment was recovered from a pit, at a depth of about 0.5 m below the surface (S 43º35’40’’; E 171º1’12’’). There was no carapace at this location. The sediment is a matrix-supported greywacke and argillite boulder gravel. Individual clasts are angular to very angular. The matrix is composed of crushed greywacke and is clay to sand size.

Three samples were collected from a quarry in the **Mt. Vora** rock avalanche deposit near Lake Torheimsmyra (N 61°44'23"; E 6°31'44"). This lobe (in total 30-40 m thick) is the result of the single event that occurred sometime between 7100-3600 BP (Aa et al., 2007). The outcrop is ~7 m high and the sample was recovered from about 3 m above the base. The sediment is a matrix-supported angular gravel. The matrix is composed of crushed granitic gneiss and is clay to sand sized with a singular pebbles.

The small **Mt. Beatrice** rock avalanche is interpreted as a large rockfall (Chapter 5) in the current study. The surface of the deposit is covered with large angular boulders which form a carapace and the underlying 3-5 m of the deposits is inaccessible. Fine sediment of silt and clay size was collected from the outcrop surface between boulders (S 43°38'16"; E 171°07'13").

6.2.2. Glacial sediments

Glacial sediment without rock avalanche contributions was sampled from glacier deposits in a variety of different environments. The sampled deposits include pre-Holocene and mostly Holocene moraines and current supraglacial, englacial and subglacial debris. Clean glaciers

with little debris cover and heavily debris covered glaciers with different lithologies from both sides of the Main Divide in the Southern Alps of New Zealand were compared to debris-free outlet glaciers at Jostedalsbreen, Norway. Several samples of continental glacial till associated with the Scandinavian ice sheet were collected from coastal outcrops at the Southern-West Baltic Sea (Kaliningrad region, Western Russia) for comparison with high Alpine glacial deposits and rock avalanche deposits.

6.2.2.1. West Coast glaciers, NZ

Seven samples of glacial sediment from a number of the **Franz Josef Glacier** deposits were also collected. The '1750 moraine' (Wardle, 1973; Shulmeister et al., 2009) was sampled from a 5 m high and over 200 m long outcrop exposed along the Waiho River (S 43°25'13"; E 170°10'33"). The outcrop is largely composed of beds of gravels with thinner interbedded silts. The sample was recovered from the lowest silt bed.

Closer to the modern glacier, sediment was sampled from the 1999 (Davies et al., 2003) moraine, from about 1m above the base of a 2-3 m high outcrop (S 43°26'29.18"; E 170°10'18.76") in the terminal moraine. The sediment is composed of a crudely stratified clast-supported sub-rounded to sub-angular boulder gravel with a silt to fine gravel matrix.

The youngest moraine was also sampled. As observed during the spring of 2009 this is a composite of sediment squeezed beneath and in front of the ice and material avalanched off the surface. The material was recovered from S 43°26'32.16"; E 170°10'21.50". The outcrop is composed of a clast-supported sub-rounded boulder gravel with a silt to fine gravel matrix.

The true left lateral moraine was sampled from the northern part of a 4-5 m high outcrop (S 43°26'36.36"; E 170°10'12.50"). The sample was recovered from 1.5 m above the base of the outcrop composed of a clast-supported sub-angular to angular boulder gravel with a silt to fine gravel matrix.

Modern supraglacial material was collected from two locations on the glacier's lower tongue. Silt was sampled from the surface of the glacier ice in Oct 2008 at S 43°26'32"; E 170°10'23" and in Nov 2009 at S 43°26'35.12"; E 170°10'15.80" In both cases there was a mix of sediment on the glacier surface.

Six samples of glacial sediment from different the **Fox Glacier** deposits were collected. A latero-frontal moraine loop is exposed at Gillespies Beach. Shulmeister et al. (2009) and Evans et al. (2010) provided mapping, lithological and sedimentological descriptions for this

outcrop. The sampled sediment was from a 7 m high and over 200 m long outcrop that is sub-divided into west and east components and is exposed along the coast (S 43°25'20"S; E 169°47'36"). The Gillespie's Beach east outcrop has been described and sub-divided by Shulmeister et al. (2009). The older sediments on the left of the section are brown coloured diamictons containing mixed lithologies (schist, greywacke, granite and volcanics), while the younger sediments to the right of the section are a coarse boulder schist dominated diamicton. Samples of the sediment for the present study were recovered from both units 1.5 m above the base. The older sediments are ice-contact fans and samples were taken from sand and silt lenses in the beds.

Closer to the Fox Glacier, sediment from the moraine remnant at the terminus was sampled (according to the local guides this moraine was formed during 1999 re-advance). The sample was recovered from about 1m above the base of a 2-3 m high outcrop (S 43°26'29"; E 170°10'19") in the terminal moraine. The outcrop is composed of a crudely stratified clast-supported sub-rounded to sub-angular boulder gravel with a silt to fine gravel matrix. In Feb 2010 the glacier retreated some tens of metres from this moraine.

Modern debris was collected from the surface of the dead ice at the true right side of the valley in 2008 and 2009. The origin of this dead ice is attributed to a rockfall that occurred at the beginning of 20th century, and also appears in a photograph taken in 1948. Silt was sampled from the ice surface (S 43°29'49"; E 170°02'35"). The sediment on the ice is a sandy silt with sporadic boulders.

Modern supraglacial material was collected on the glacier lower tongue in Feb 2011. Silt from a variety of sediment types occurring on the glacier surface was sampled at S 43°30'04"; E 170°03'33" from at the bottom of a pond developed on ice.

6.2.2.2. Jostedalsbreen glaciers, Norway

Recent terminal moraines (AD 1997, 2000 and 2001) of Bødalsbreen, Kjenndalsbreen, Brenndalsbreen, Briksdalsbreen, Bergsetbreen were sampled. Bødalsbreen and Kjenndalsbreen sediment is orthogneiss and quartziticmonzonite, while for the other glaciers it is granite, granodiorite and gneiss (augen). The sediment from AD 2000 moraine (up to 2 m high) of Bødalsbreen was recovered about 0.5 m from the top of the moraine at a depth 0.5 m (N 61°47'46"; E 007°06'04"). This was composed of sub-rounded to sub-angular boulders with a silt to fine gravel matrix. Similarly, the sediment from the AD 2000 moraine (1.5 m high) of Kjenndalsbreen was recovered about 0.5 m from the top of the moraine at the depth

0.5 m (N 61°44'38"; E 007°01'54"). The sediment here was composed of sub-angular boulders with a silt to fine gravel matrix. Two samples from the AD 2000 (9 m high) and AD 2001 (5 m high) moraines were collected from Brenndalsbreen. The sediment from the AD 2000 moraine was collected about 2 m from the top of the moraine at the depth 0.5 m (N 61°40'53"; E 006°53'32"). The sediment from the AD 2001 moraine was recovered about 2 m from the top of the moraine at the depth 0.5 m (N 61°40'52"; E 006°53'21"). In both cases, the sediment was composed of sub-rounded to sub-angular boulder with a silt to fine gravel matrix. Two samples from AD 1997 moraine (1.5 m high) of Briksdalsbreen were collected about 1 m from the top of the moraine at the depth 0.5 m (N 61°39'51"; E 006°51'32" and N 61°39'52"; E 006°51'34"). The sediment for both samples was composed of a sub-rounded to sub-angular with a silt to fine gravel matrix. A sample from the 2000 Bergsetbreen moraine was taken at about 1 m from the top of the moraine at the depth 0.5 m (N 61°38'52"; E 007°06'19") and was composed of a sub-angular boulder with a silt to fine gravel matrix.

Modern supraglacial material was collected from the Bødalsbreen and Bergsetbreen lower tongues in June 2010. Silt was sampled from the surface of the Bødalsbreen ice at N 61°47'28"; E 007°06'02", whereas for the Bergsetbreen silt was sampled from the surface of dead ice that is disconnected from the glacier body, (N 61°38'56"; E 007°06'10"). In both cases there was a mix of sediment types on the glacier surface. Additionally, modern basal material (silt) under the Nigardsbreen icefront was collected in Jun 2010 at N 61°40'41"; E 007°12'21" and N 61°40'39"; E 007°12'23".

6.2.2.3. Debris-covered glaciers, NZ

Modern supraglacial material was collected from the lower tongues of the Hooker and Tasman Glaciers. Silt was sampled from the surface of the Hooker ice at S 43°38'40"; E 170°07'22" in Dec 2010. Silt was sampled from the surface of the Tasman ice at S 43°35'33"; E 170°13'15" and S 43°35'28"; E 170°13'13" in Feb 2009. In both cases there was a mix of sediments on the glacier surface. Sample sites for the Mueller, Hooker and Tasman Glaciers lateral and terminal moraines are described in Chapter 7 and Appendix E.

6.2.3. Samples from other environments

Some additional samples from other environment in New Zealand have also been collected and analysed. Two samples were taken from rockfall sediment at the Franz Josef Glacier true

left side wall at S 43°26'32"; E 170°10'23 and from a rock fall on the West Coast Road at S 43°26'32"; E 170°10'23. The finer sediment fraction (silt size) was collected from the bouldery surface layer of these deposits. Samples of suspended sediment from Lake Pukaki were collected from subsurface (< 0.5 m) water at S 44°11'22"; E 170°08'25 and at S 44°10'42"; E 170°11'06. Lake Tekapo sediment was collected from the 8 m high exposure 1.5 m from the base on the southwestern shore of Lake Tekapo at S 43°56'52"; E 170°30'00. The finest (clay size) sediment was recovered from fault gouge at the 6-8 m outcrop roadside of the Smithy's Creek Fault at S 43°26'32"; E 170°10'23, West Coast (see Appendix E).

6.3. LABORATORY TECHNIQUES

6.3.1. Sieving

Silt and clay size fractions from each sample have been used in this study, where the term "clay size particle" is restricted to material < 4μm according to the Wentworth or Udden-Wentworth scales that are commonly used in glaciological research (Evans and Benn, 2004) (Table 6.1). Silts range from 4 to 63μm, with 63 μm being the lower limit of sieve analyses (McManus, 1988) and the silt-sand boundary.

Table 6.1. Particle size conversion and nomenclature after Wentworth (modified from Evans and Benn, 2004).

Milimetres (mm)	Phi unit φ	Psi unit ψ	Particle size category	Particle size sub-category	Micrometres (μm)	Phi unit φ	Psi unit ψ	Particle size category	Particle size sub-category
1024	-10.0	10.0	Gravel	Boulder	1000	0.0	-0.0	Sand	Coarse sand
724	-9.5	9.5			707	0.5	-0.5		
512	-9.0	9.0			500	1.0	-1.0		Medium sand
362	-8.5	8.5			354	1.5	-1.5		
256	-8.0	8.0			250	2.0	-2.0		Fine sand
181	-7.5	7.5		Cobble	177	2.5	-2.5		
128	-7.0	7.0			125	3.0	-3.0		Very fine sand
90.5	-6.5	6.5			88.4	3.5	-3.5		
64.0	-6.0	6.0			62.5	4.0	-4.0		Coarse silt
45.3	-5.5	5.5		Pebble	44.2	4.5	-4.5	Silt	
32.0	-5.0	5.0			31.3	5.0	-5.0		Medium silt
22.6	-4.5	4.5			22.1	5.5	-5.5		
16.0	-4.0	4.0			15.6	6.0	-6.0		Fine silt
11.3	-3.5	3.5			11.0	6.5	-6.5		
8.00	-3.0	3.0			7.81	7.0	-7.0		Very fine silt
5.66	-2.5	2.5			5.52	7.5	-7.5		
4.00	-2.0	2.0			3.91	8.0	-8.0		Coarse clay
2.83	-1.5	1.5		Granule	2.76	8.5	-8.5	Clay	
2.00	-1.0	1.0			1.95	9.0	-9.0		Medium clay
1.41	-0.5	0.5	Sand	Very coarse sand	1.38	9.5	-9.5		
1.00	0.0	0.0			0.977	10.0	-10.0		Fine clay (colloid)
					0.691	10.5	-10.5		
					0.488	11.0	-11.0		

Sieving (15 minutes per sample) was carried out on oven dried samples (< 50º C) using a mechanical shaker and stacked individual sieves with mesh sizes ranging from 1 mm (0φ) and 63 µm (4φ). For better resolution of particle size distribution (PSD) Murray (2002) suggested dissolving the sample in solution of 1 % Calgon dispersant (sodium hexametaphosphate and anhydrous sodium carbonate). However, after testing the samples with distilled water and with a Calgon solution or paste, Dunning (2004) found that the results from each treatment were nearly identical. In the present study no dispersion techniques were used in the sample preparation because of the possibility that this may lead to disruption of the original grain size distribution of the sediment.

6.3.2. PSD by Laser diffraction

6.3.2.1. Method

Sediment finer than 63 µm (4φ) was analysed on the Saturn DigiSizer 5200 (Geology Department, University of Canterbury) and Microtrac X100 (Engineering department, University of Canterbury) Laser Diffraction Particle Size Analyzer. The Laser Diffraction Particle Size Analyzer determines the size of particles based on diffraction caused by those particles as they interfere with a laser beam. The Saturn DigiSizer 5200 used a 658 nm laser source and has a measurement range of particles from 0.1 to 1000 µm. Based on Fraunhofer or Mie diffraction theory, the particle size distribution is calculated from the angle, distribution and intensity of scattered light induced as spherical particles of a known refractive index pass through the laser beam. Although the calculations based on Mie theory of diffraction increased the accuracy for finer silts and clay size particles, it does require knowledge of the mineral composition of a sample, whereas for Fraunhofer theory mineral composition does not need to be known (Murray, 2002; Dunning, 2004). Results are accurate down to 0.4 µm. As a result of damage to the Saturn DigiSizer 5200 Laser Analyzer caused by Christchurch Earthquake of 4 September 2010, the sediments from Norway glaciers and rock avalanche were analysed on a Microtrac X100 Particle Size Analyzer. It is known that this instrument has a lower resolution than the DigiSizer and results may not be directly comparable.

It must be noted that there are significant technical difficulties associated with detecting grains to nanometre sizes and that this is a limitation that must be taken into consideration with respect to interpretation of PSD's. It is likely that such fine particulates are present,

since such grains have been detected in fault gouge and these have similar characteristics, including grain-size distribution, to rock avalanche debris (Kuelen et al., 2007; McSaveney and Davies, 2007).

A series of tests using ultrasonic disaggregation before and during analysis on the Laser Sizer showed insignificant PSD fluctuations for rock avalanche sediment or for sediment of a solely glacial genesis. Therefore, all samples were subjected to ultrasound exposure during analyses on the Laser Analyzer. The graphic plots of volume frequency percent and cumulative finer volume percent versus particle diameter are presented in Appendix F.

6.3.2.2. Results

The distributions of < 63 μm particles for rock avalanche deposits have similar frequencies for the range of measured grain sizes, with no distinctive mode at a particular grain size. The high percentage of clay-size particles is evident where the smaller detected grains were attributed to the minimum size category of 0.2 μm (Fig. 6.1a). In general, rock avalanche particle size distributions are fairly uniform with no obvious dominant mode and a high percentage of finer sized grains (< 5 μm). Sediment from the Aoraki/Mt. Cook rock avalanche deposit was the most uniform with respect to grain size distribution. The least < 5 μm particles were found in the Mt. Vora rock avalanche, however, it should be noted that this result was obtained on the Microtrac X100 Particle Size Analyzer. However, there is no evident mode of the particles < 5 μm in size, in contrast with expectation that clay size particles would dominate in rock avalanche sediment (Fig. 6.1a).

In general, the particle size distributions from the Laser Sizer for rock avalanche sediments show the following:

1. they have no distinctive mode;

1. they have high, but not dominant values of particles < 1μm in size; and

3. a portion of that sediment is composed of sub-micron sized particles (Fig. 6.1a).

For terminal and lateral moraines of clean glaciers, and for supraglacial melt-out deposits, there is noticeable similarity of particle size distributions. In general there is a deficiency of clays < 5 μm in size, and a distinct mode of particles in the 30-60 μm size range (Fig. 6.1b and c). For terminal and lateral moraines there is a distinct increase in the proportion of

particles from 5 to 30 μm, whereas in some supraglacial samples this fraction is very low or even absent. For example, on the Tasman Glacier, supraglacial melt-out upstream from the Aoraki/Mt. Cook rock avalanche deposit contains almost no particles finer than 20-30 μm (Fig. 6.1c). Hooker Glacier supraglacial debris collected about 4 km from the modern terminus had no < 63 μm particles at all (which is why the PSD for this sample is absent on the graph). In the recent moraine of the Jostedalsbreen, clay size particles are mostly absent and the particles are predominantly of 50 μm (coarse silt), as expected for glacial debris (Fig. 6.1b). The sediment from a continental glacier deposit in Western Russia, revealed a similar pattern (Fig. 6.2c).

Therefore, the characteristics of particle size distributions for glacial sediments that are known not to have a rock avalanche contribution are that they:

1) have a distinguishable mode of particles 30-60 μm in size;

2) have insignificant percentage of particles of < 5 μm with absence particles of < 1 μm; and

3) are very similar across all measured deposits (Fig. 6.2b).

Notably, the PSD for sediment from terminal and lateral moraines of debris-covered glaciers showed an intermediate pattern between PSD's for rock avalanche deposits and rock avalanche free glacial sediment. As for rock-avalanche-free glacial sediment, there are sediment modes at 10-20 μm and 30-70 μm but, like rock avalanche deposits, this material has more particles < 5 μm (Fig. 6.2a). The distribution still contrasts with rock avalanche deposits because of the lack of the very small < 1 μm fraction. In general, the mean distributions for sampled lateral and terminal moraines are almost the same (Fig. 6.2a). Because the rock-avalanche-free glacial sediment and the supraglacial debris of known non-rock avalanche origin lacked < 1 μm particles (Fig. 6.1b and c), the sediment in this size fraction in the moraines (Fig. 6.2a) must have originated from another source(s).

These results were compared with PSD for sediments from other environments (Fig. 6.2d). The PSD for suspended sediment in the sub-surface water in the glacially-fed Lake Pukaki, New Zealand, show the presence of particles < 1 μm with modes at 7-9 and 10-20 μm (Fig. 6.2d). The grain size distribution for the glacially-fed Lake Tekapo pre-LGM deposit has just one mode in the 1 - 5 μm range, which represents the size-sorted fraction that settled to the bottom of the lake (Fig. 6.2d). As expected, the lake traps finer available fractions from the catchment which flocculate into clumps while in suspension and are then deposited. The

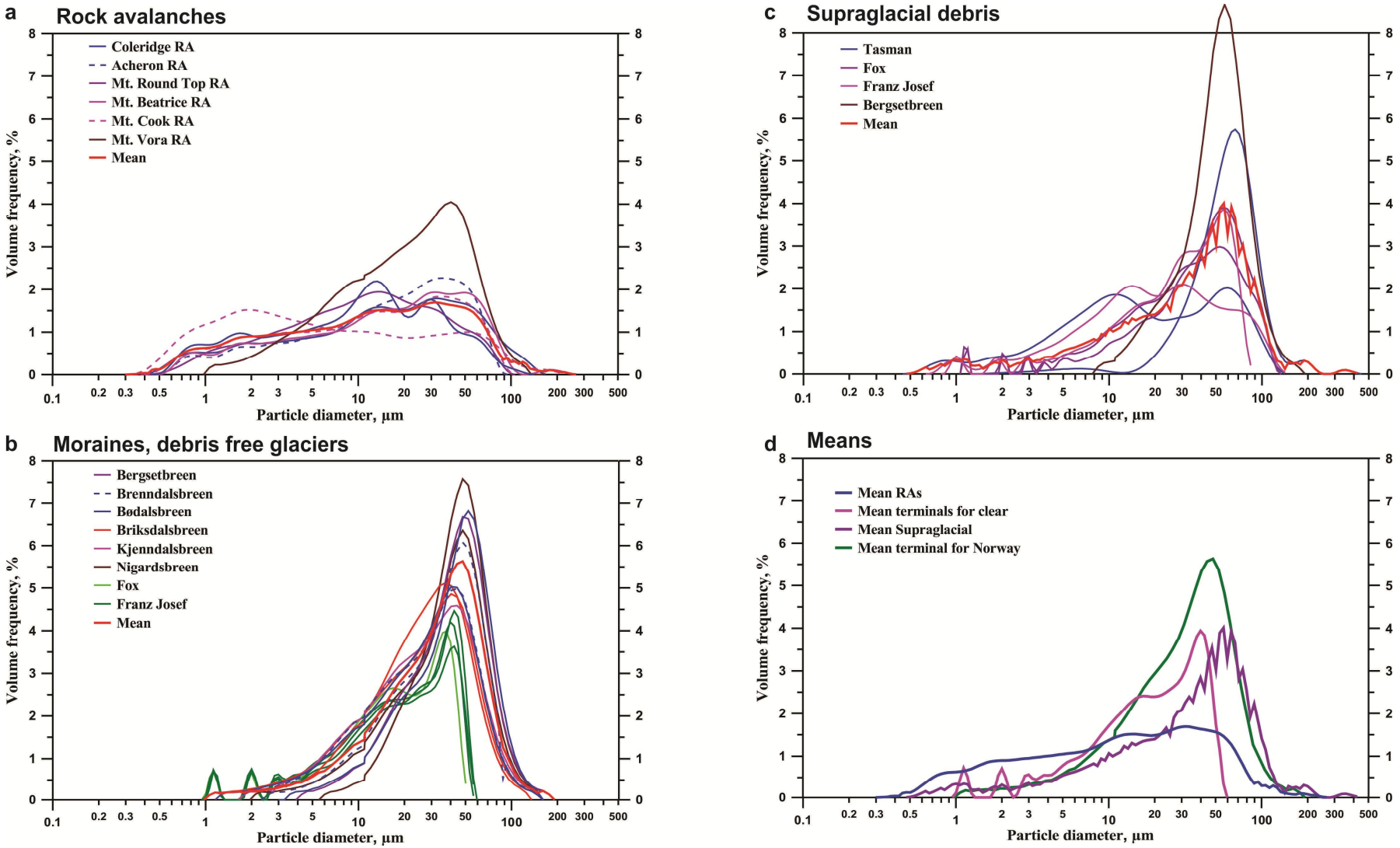

Figure 6.1. Particle size distributions analysed by Laser diffraction for fine sediment (< 63 µm) from rock avalanches, glacial sediment from non-rock avalanche-originated sediment.

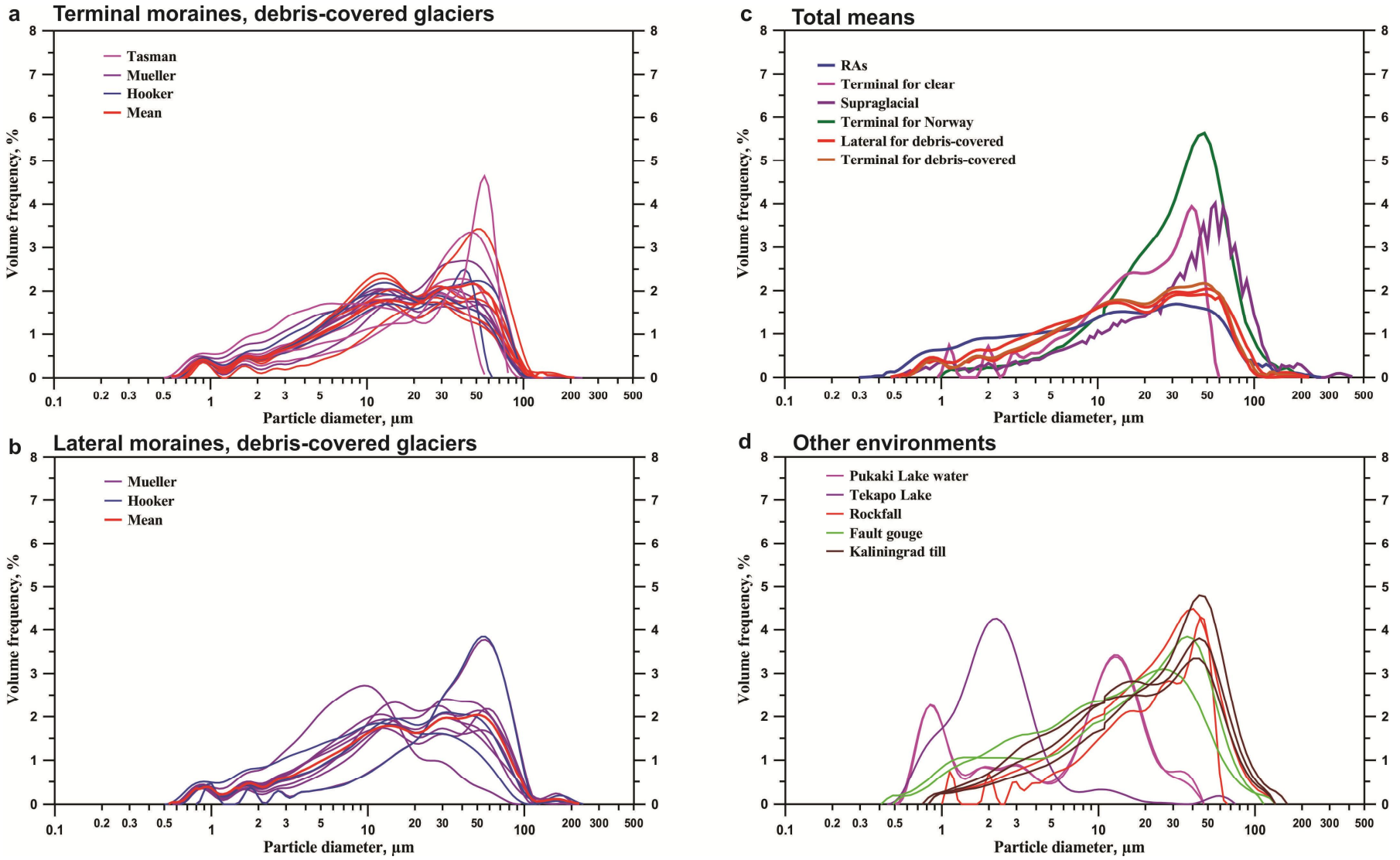

Figure 6.2. Particle size distributions analysed by Laser diffraction for fine sediment (< 63 µm) from glacial sediment for debris-covered glaciers and other environment.

PSD for rockfall sediments lacks particles of a size < 1 μm and is similar to that produced for supraglacial sediment cover. As a result of laser diffraction analysis, the PSD showed different patterns for sediments from contrasting environments, but the expected abundance of fine (clay size) particles in the rock avalanche and fault gouge sediments simply did not eventuate. From that result, the author then hypothesised that the Laser Analyzer was unable to discriminate individual and clumped particles, this being tested by obtaining a PSD for sediment from fault gouge that theoretically should have had only particles of clay size (< 4 μm) (Wilson et al., 2005). The results showed a dominant range between 10-50 μm (Fig. 6.2d). It was concluded that the Laser sizer was unreliable when dealing with rock avalanche deposits. In order to test this, stereoscopic microscope examination of the sediments was the next logical step for this investigation.

6.3.3. Stereomicroscope analysis

Samples of the size fractions 63-1000 μm and < 63 μm were examined and photographed with a "Wild m^3z" stereomicroscope.

Particles of a size 63-1000 μm from different glacial environments (supraglacial or basal) of known non-rock avalanche origin show loose, clean separate fragments of different lithologies with only a few small particles adhering to the surface, and these are easily removed (Fig. 6.3A). Finer fractions (less than 63 μm) also comprise loose and clean particles of mostly quartz for rock avalanche debris-free glaciers in New Zealand and all Norwegian glaciers. Numerous mica particles were present in sediments from the schist-dominated catchments west of the Main Divide in central South Island, New Zealand (the Fox and Franz Josef Glaciers). The particles are loose and easily distinguished from each other. Quartz particles of a size 63-1000 μm were extracted from these samples and mounted for study of surface features using the SEM (see full description of the method and purpose described in Appendix G).

In contrast, rock avalanche sediments of 63-1000 μm size contain heavily-coated grains, where these coatings consist of very fine fragments of undistinguishable lithology. These grains represent different-size fines conglomerated into "snowball"-like clumps (Fig. 6.3B). Some of the clumps are able to be physically broken into smaller ones; however, the size of the finer fragments and their condition (clumped together or separate grains) are impossible to determine under stereomicroscope. After repeated gentle washing with distilled water and

dispersion with sodium hexametaphosphate (Calgon), the clumps still survived, even when the majority of the adhering fines were washed away. Therefore, these clumped grains were also mounted for examination under SEM. However, they were not suitable for examination of surface features as the surface was obscured by remaining fine particulates.

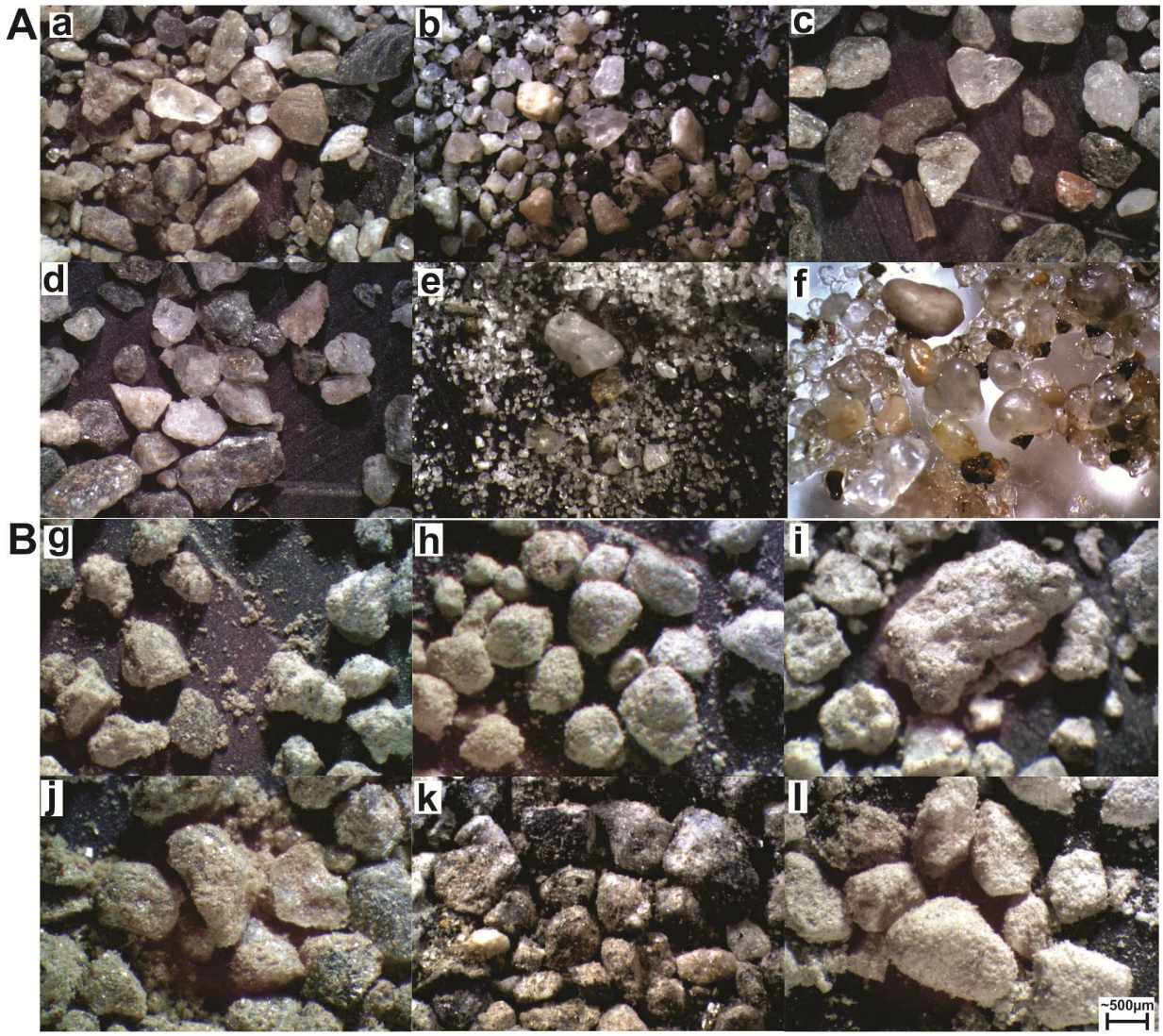

Figure 6.3. Examples of the stereomicroscopy examination of the studies sediment from known rock avalanches and non-rock-avalanche-induced glacier sediments: A. Clean grains of the non-rock avalanche glacial-origin sediment:a – Tasman Glacier supraglacial; b – Briksdalsbreen Glacier moraine 1997, Norway; c – Fox Glacier terminal moraine 1999; d – Franz Josef Glacier terminal moraine 2008/9; e –Nigardsbreen Glacier basal sediment at terminus, 2010; f – continental glaciation till sediment, Western Russia, Baltic state. B. Rock avalanche-origin sediment with heavily coated grains and agglomeration of smaller size particles: g - Coleridge RA, NZ, h – Coleridge RA, NZ; i - Acheron RA, NZ; j –Round Top RA, NZ; k – Mt. Vora RA, Norway; l – Waiho Loop moraine, NZ.

6.3.4. SEM examination

6.3.4.1. Mounted grains

Quartz grains from glacial deposits were examined using a JEOL 7000F Field Emission (FE-SEM) and Leica 440 Scanning Electron Microscopes. The surfaces of grains across the entire range of sizes are clean and have very few smaller particles adhering to that surface (Fig. 6.4 A and Appendix G). Surface features such as sharp or round edges, cleavage faces and plates, conchoidal fractures, grooves, silica precipitation etc are all clearly visible (Appendix G).

This contrasts with grains from rock avalanche deposits. Individual grains from rock avalanche sediment are invariably heavily coated with adhering finer particles which are often less than 1 μm in size or are agglomerated into coarse grains. Host grains may comprise several grains, connected by a matrix of these finer particles (Fig. 6.4 B). Some of the grains are fractured (Fig. 6.4 B). As a result, the identification of surface features for the rock avalanche grains failed because: 1) quartz particles could not be determined with confidence, 2) under SEM the grain surface could not been seen. These results suggested the need to examine the structure of individual grains by examining polished mounts of same under the SEM.

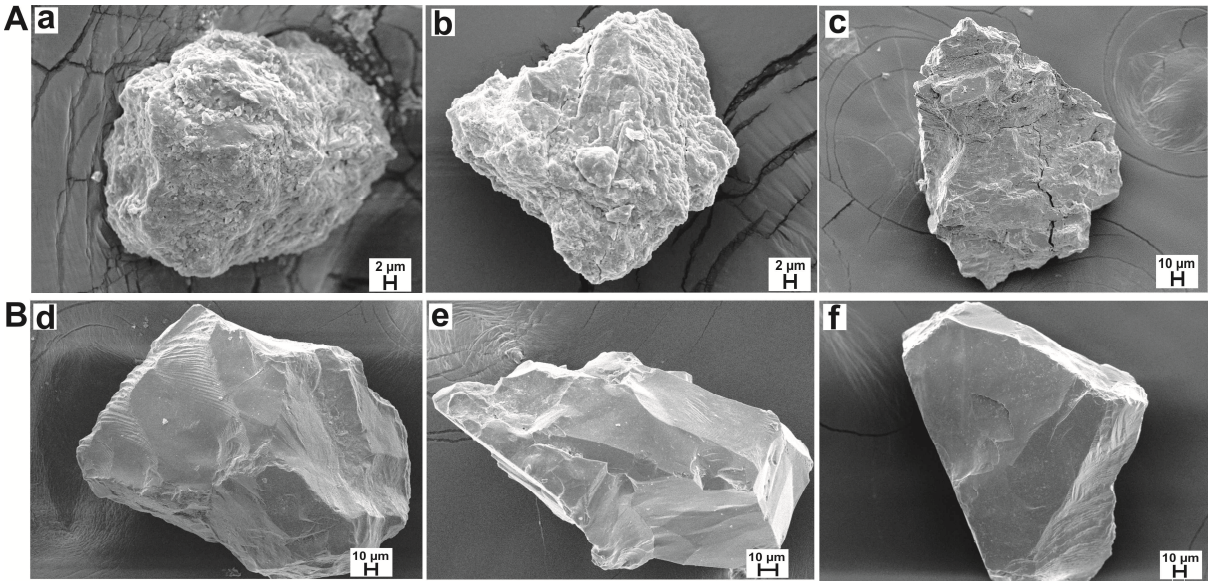

Figure 6.4. Examples of SEM micrographs of grains from: A) the rock avalanche environments, Coleridge rock avalanche, NZ (a, b) and Aoraki/Mt. Cook rock avalanche after washing the sample (c); B) from glacial environments: Franz Josef Glacier LIA (1750) moraine (d, e); Tasman Glacier supraglacial sediment (f).

6.3.4.2. Polished grain mounts

Polished grain mounts of 63-1000 μm sized particles were analysed on SEM. The grains were mounted in a resin block that was then coarse ground to remove approximately 0.5-1 mm of the resin-sediment mix, that surface was then polished (Fig. 6.5). During SEM examination of the polished grains mounts from glacial and rock avalanche sediments both secondary electron and backscattered electron images were taken.

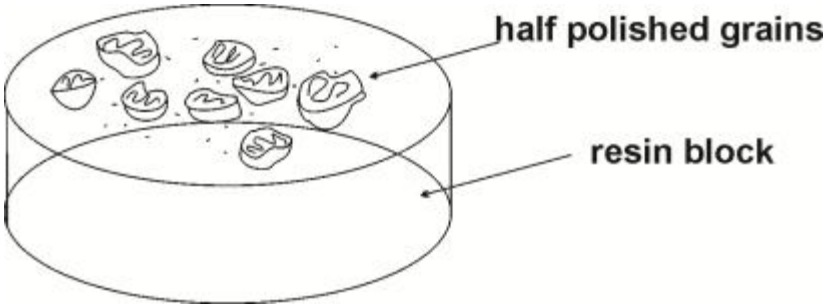

Figure 6.5. Sketch of the mounted grains into the resin blocks and polished through the grains to obtain pictures on SEM.

Examination of polished grain mounts from rock avalanche sediments under the SEM showed that the grains are in fact agglomerations of finer (< 10 μm) particles. [Note that the size of the examined grains is 63-1000 μm.] The coarse fragments are covered with fines, while coarse grains are formed from clumps of smaller (down to submicron scale) grains. The perimeters of larger grains are coated with a matrix of very fine particles, the smallest of which are finer than were able to be resolved by the SEM photomicrograph (Fig. 6.6a). Micrographs of polished grains mounts for all sampled rock avalanche deposits showed these characteristics. Several examples of micrographs of these grains are shown on Fig. 6.6. Sediment from the rock avalanche deposits located in different environments, lithologies and ages (Coleridge, Round Top, Aoraki/Mt. Cook and Mt. Vora rock avalanches deposits) all contain large proportions of the micron and submicron size particles that form the clumps. Thus, the ca. 1000 year-old Round Top rock avalanche sediment has the same characteristics as the 30 years-old Aoraki/Mt. Cook rock avalanche deposit, confirming the high preservation potential with respect to the original fine-particle sedimentological characteristics of the rock avalanche. In all sampled rock avalanche sediments of contrasting lithologies (west and east side of the Main Divide of the Southern Alps, New Zealand, and Norway) are present these clumps.

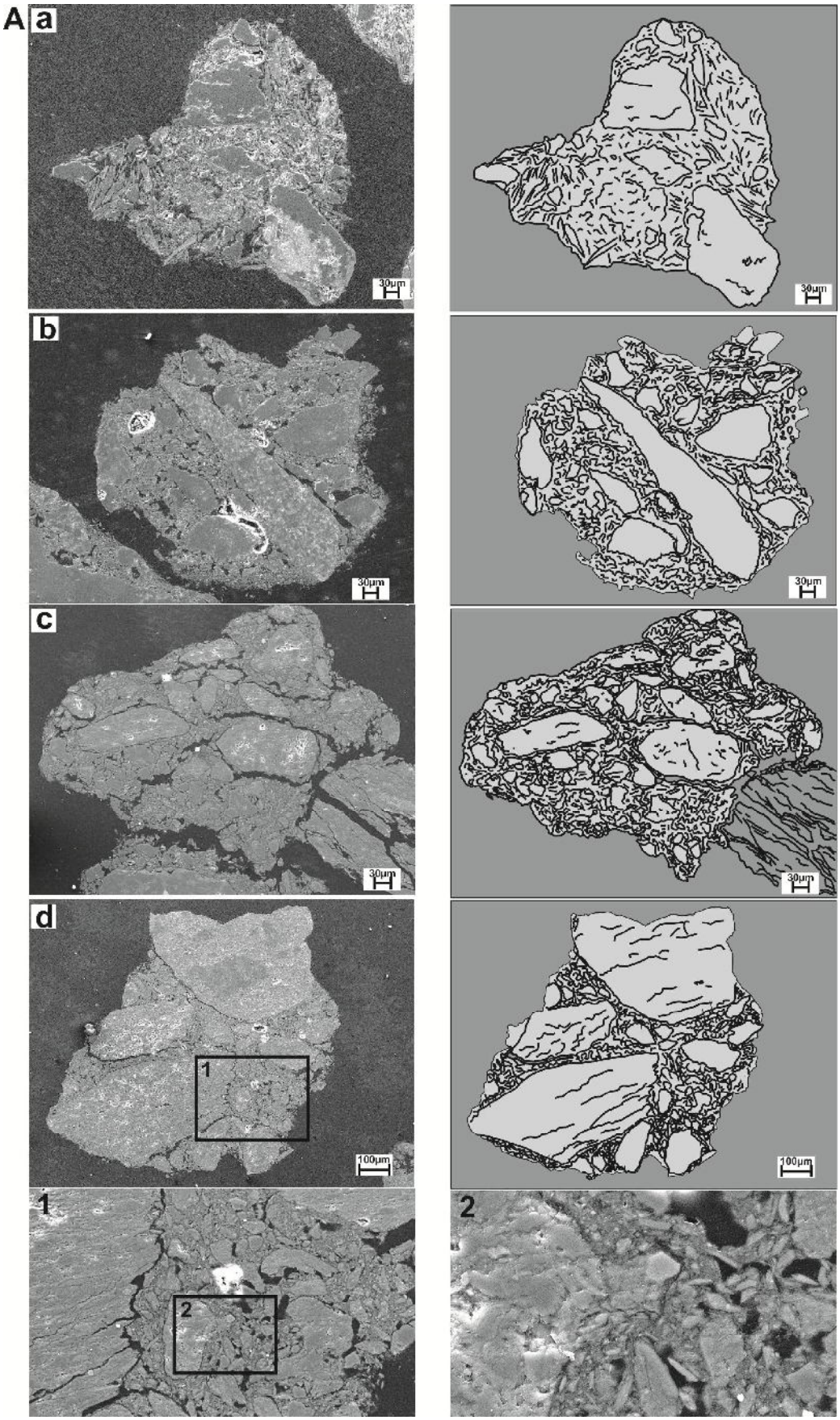

Figure 6.6. SEM micrographs of polished mounted grains of the particles 63-1000 µm for: A. Rock avalanche sediments (a) Mt. Round Top, b) Aoraki/Mt. Cook; c) Coleridge; d) Coleridge with 1 and 2 magnified features.

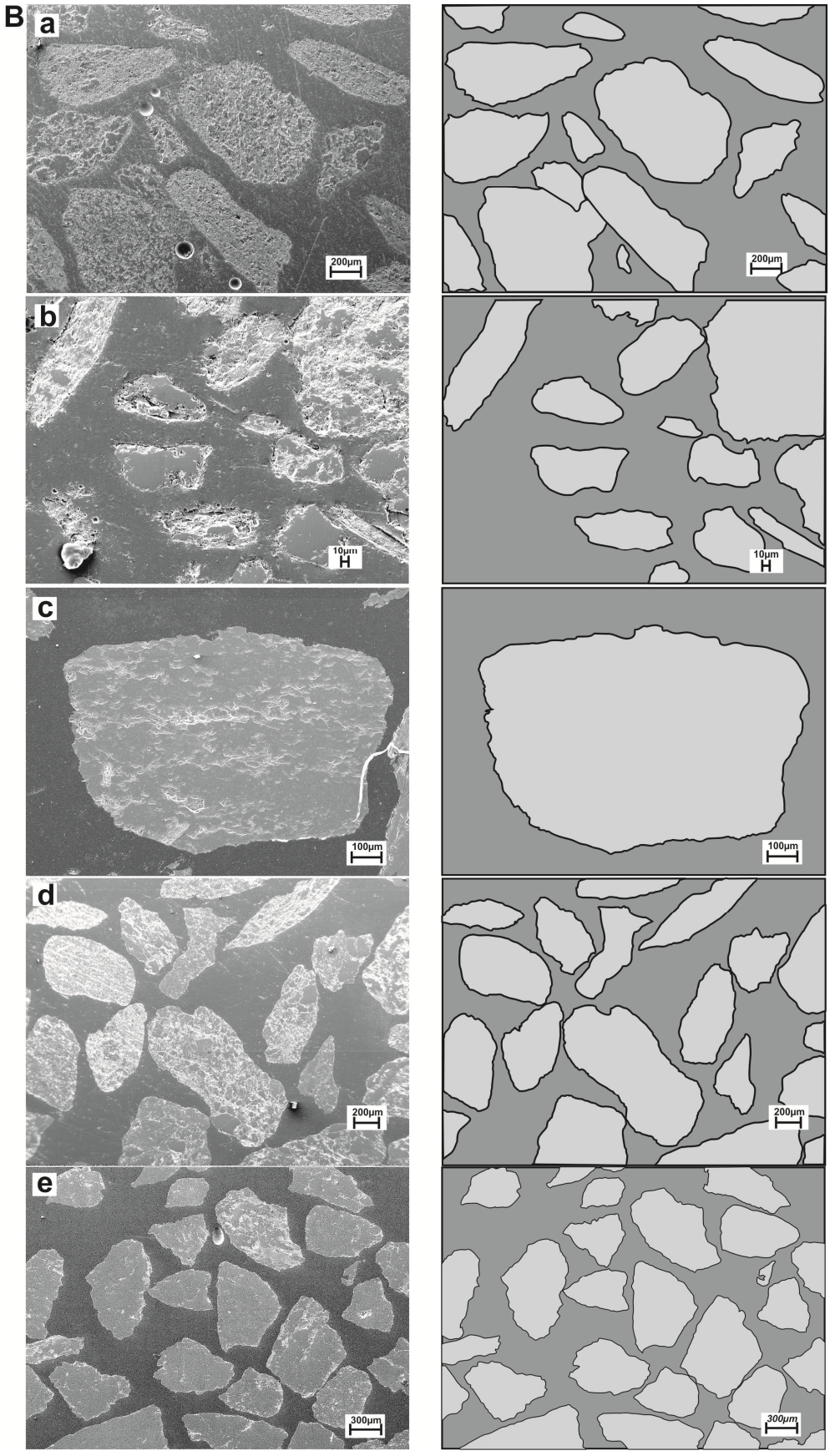

Figure 6.6. (continued) B. Glacial sediment: (a) Franz Josef Glacier terminal moraine; b) Fox Glacier terminal moraine; c) Franz Josef Glacier LIA moraine; d) Mueller Glacier lateral moraine; e) Bødalsbreen Glacier terminal moraine).

The SEM resolution limits (reflecting a sample preparation problem rather than instrument capabilities) do not allow the distinguishing sub-micron particles. The finer grains between larger grains are clearly seen on the SEM as a mixture of sizes, but even under the highest magnification the size of smallest particles is unclear. During X-ray analysis (energy dispersive spectroscopy technique (EDS-SEM) used for the chemical characterization of a specimen) for the determination of particulate composition and to measure the abundance of elements in the sample, the intervening amorphous 'gaps' between particles did not show any obvious source of bonding (organic, carbonates and/or iron oxides), i.e. the material between the larger grains is at this stage indeterminate. The low magnification (the size of the probe used for EDS is 1 μm) makes it impossible to resolve and identify the chemical makeup of the 'bonding' materials that exist between the sub-micron particles.

In contrast, in glacial sediment (from a non-rock avalanche source), grains of different sizes are clean and separate from each other (Fig. 6.6b). No agglomeration of finer particles is found in any glacial sediments of known non-rock avalanche origin. This pattern of separate grains is characteristic for Westland glaciers, New Zealand, the lithology of which is mostly schist, and for Jostedalsbreen, Norway, which are gneiss-derived. The grains from the glacial sediment, therefore, can be easily distinguished from the grains of rock avalanche sediments using SEM also.

Similar sediments to the rock avalanche particle agglomerates were observed in gouge (shear zone material) from the fault gouge, where all grains represented the agglomeration of very fine micron- and nanometre-sized particles. Fig. 6.7 compares polished untreated grains from all glacial environments (where there is no rock avalanche sediment source), with grains from high-stress fragmentation environments (rock avalanche and fault gouge sediment). The former consistently show clear single grains and the latter agglomerates.

6.4. DISCUSSION

From the detailed examination of the fine (< 63 μm) sediments from glacial and rock avalanche environments, the importance of the clay size fraction (< 4 μm) in rock avalanche material is evident. Rock avalanche sediment at a microscopic scale shows unique features of grain clumping that cannot be found in sediment produced from glacial erosion or any other environment except that associated with fault rupture. These features raise significant

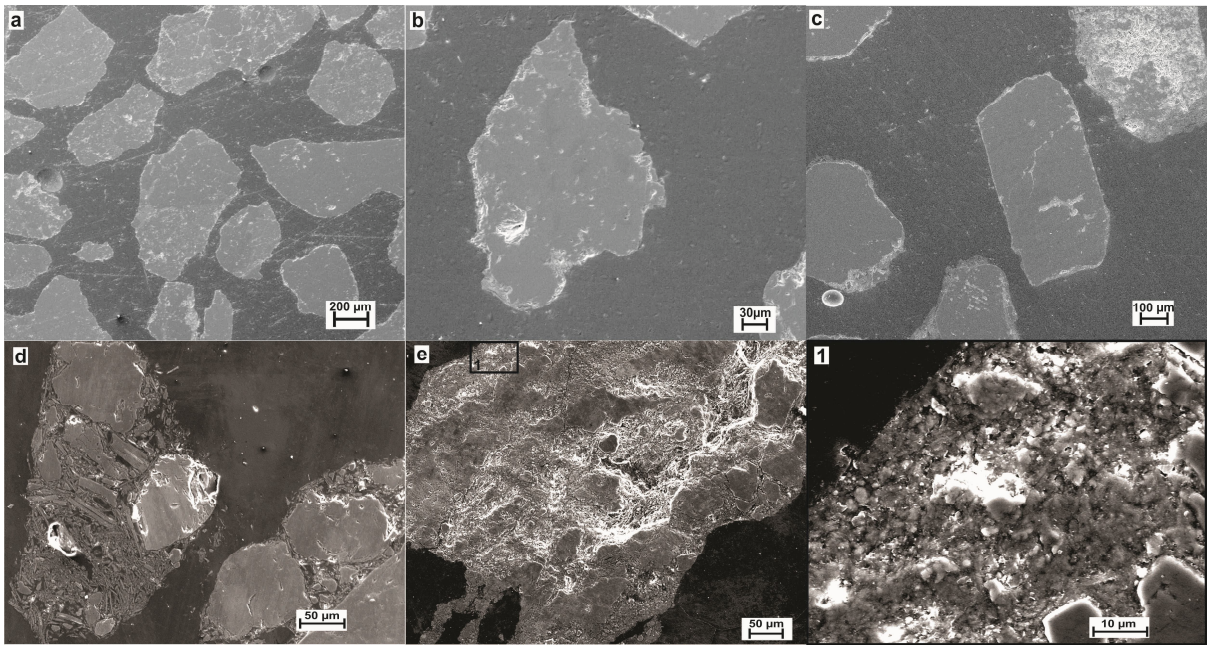

Figure 6.7. Comparison of the polished mounted grains of the particles 63-1000 µm from different environments, SEM micrographs: a. Basal sediment at front position of Nigardsbreen Glacier for 2010, Norway; b. Supraglacial sediment at Bergsetbreen Glacier stagnate ice, Norway; c. Continental glaciation till sediment, Western Russia; d. Mt. Vora RA sediment, Norway; e. Fault gouge sediment, New Zealand, with 1 – magnified feature.

questions about the genesis of those sediments and established methods for their identification.

6.4.1. A diagnostic characteristic of rock avalanche fines: 'agglomerates'

Closer examination of rock avalanche sediment reveals that many 'fine' grains are in fact clumps of many, much smaller particles. These clumps are quite stable and occur in all the studied rock avalanche deposits (Fig. 6.8). These clumps are quite resistant to sieving and disaggregation and are composed of widely-graded (down to sub-micron size) largely sub-angular microclasts of the same lithologies as the parent material. The term 'agglomerates' is proposed for these clumps of particles (which indicates the process of agglomeration rather than any previously established geological terms, Reznichenko et al., 2012). This is the first time such particulates have been recognised as a characteristic of rock-avalanche sediments. Agglomerates occur because, in strongly confined conditions, fragments resulting from comminution cannot disperse when formed (McSaveney and Davies, 2007). The high ratio of surface to inertial forces (characteristic of very fine grains), prevents their later dispersion under shear. Because the finer particles that bond coarser particles were of a sub-micron size

and because no evidence of organic bonding was found during EDS analysis of agglomerates on SEM (X-ray analysis), it is suggested that for rock avalanche deposits, the bonding between fine grains (< 1 μm) is due to the attraction of interparticulate forces exerted by the finer (sub-micron) particles. The fact that agglomerates also occur in fault gouge strongly supports the idea that the sediment is formed by comminution under high stresses (Reches and Dewers, 2005; Wilson et al., 2005; Kuelen et al., 2007; Reches and Lockner, 2010).

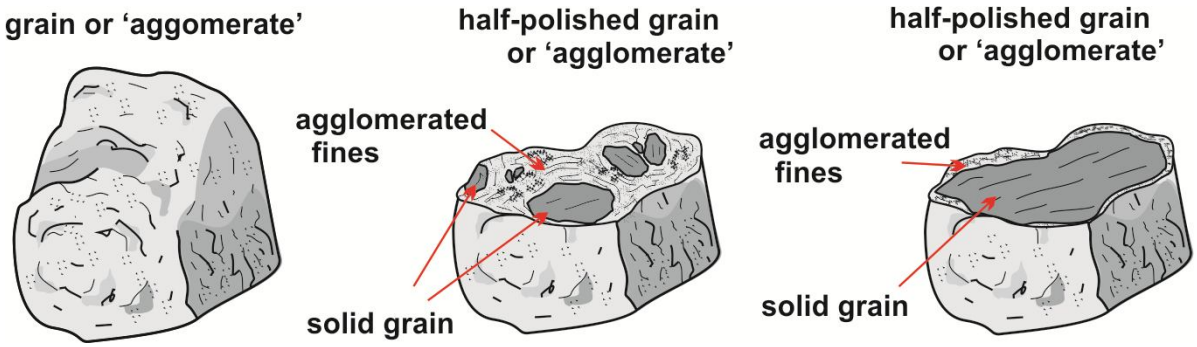

Figure 6.8. Scheme of solid grains or agglomerates and polished agglomerates showing its structure.

Aggregate formation occurs in other environments, but the agglomerates not like the ones observed in rock avalanche sediment or fault gouge. For example, aggregates are typical in soil horizons, where binding agents such as the physical action of the biota, precipitation of salts and clay mineral bonding (Matthews, 1991) are present. Clay minerals (as opposed to clay sized material) are another strong agent for bonding and this is induced by electrochemical forces that commonly operate during moisture loss or gain in soils, resulting in smaller grains becoming attached to larger ones (Towner, 1988). Soil particles are arranged into larger aggregates of different sizes and shapes (usually about 0.5-2 mm in diameter) with the pore spaces between them providing conduits for water and air so crucial for the biota inhabiting that environment. Agglomeration by organic matter does not occur in rock avalanche deposits because organic material is usually completely absent, and there is no evidence for chemical bonding either, acknowledging that this aspect of the research continues. SEM polished mounts of the soil aggregates significantly differ from the polished grains mounts of agglomerates in rock avalanche sediment (Fig. 6.9).

Clumped particles are also found in sediment from alpine lake deposits and these include extensive fine silt/clay-size particles. The micrographs of the clumps from lake sediment

(Fig. 6.10) indicate these are composed of clean grains of similar size and without a mixture of finer (sub-micron size) particles between those grains. Furthermore these grains are very weakly bonded and during washing in water, are easily disintegrated (this was observed under stereomicroscope). This reflects the genesis of the sediment and the deposition process: the lake sediments are slowly deposited by the settling of one size range of particles from suspension in water over a long period of time and the occasional turbidity current, which contrasts with the rapid production of the whole range of clast sizes in a rock avalanche (Davies et al., 1999). Therefore, lake deposits are easily distinguishable from other glacial and rock avalanche deposits because they reflect the sorting resulting in sediment composed of very similar particles with respect to shape and size. In contrast, the agglomerates in the rock avalanche sediment strongly bonded by smaller fines and are much more resistant to disaggregation by physical or chemical means (Fig. 6.10).

The discovery that fine particles in rock avalanche debris comprise agglomerates of even finer grains (sub-micron size) is of significance with respect to the study of fragmentation as a factor in the dynamics and the energy budgets of large-scale, high-stress geodynamic phenomena in general. This is because with grain-size distributions finer than previously thought, more energy is abstracted to form large numbers of finer (nanometre scale) fragments. The 'potential surface energy'of numerous fine particles is assumed to consume the fracture energy in the system (Locat et al., 2006; Ma et al., 2006; Nguyen and Einav, 2009), which, theoretically, makes their formation impossible (McSaveney and Davies, 2009). Clearly as a result of the present study, this is not impossible and the dissipation of energy in this process is of significance to rock avalanche dynamics.

6.4.2. Rock avalanche deposits versus glacial deposits: microsedimentology

Rock avalanche sediment is dominated by fines of particle size < 1 μm size. Glacial deposits from all sampled non-rock-avalanche environments preserve some silt- and clay-size sediments but lack a strong very fine mode. Two questions emerge: 1) what forces could generate clay-size particles in a rock avalanche deposit? and 2) at which stage of emplacement, deposition or preservation are these forces developed? The percentage of silt and clay size particles in glacial sediment decreases during constant transport and modification before deposition. In contrast, in rock avalanche deposits the sediment undergoes modification only during the emplacement itself, which if faithfully preserved will

present grains in their original state. The comminution in large rock avalanches is known to produce large volumes of sub-micron particles (Sammis and Ben-Zion, 2008; Storti and Balsamo, 2010), and communition will continue until motion ceases (Davies et al., 1999). Therefore, particles < 1 μm size are abundant in the deposit. The relative lack of clay size particles in deposits from glacial environments indicates either they are not produced in glacial processes or that they are not preserved in the resultant glacial deposit.

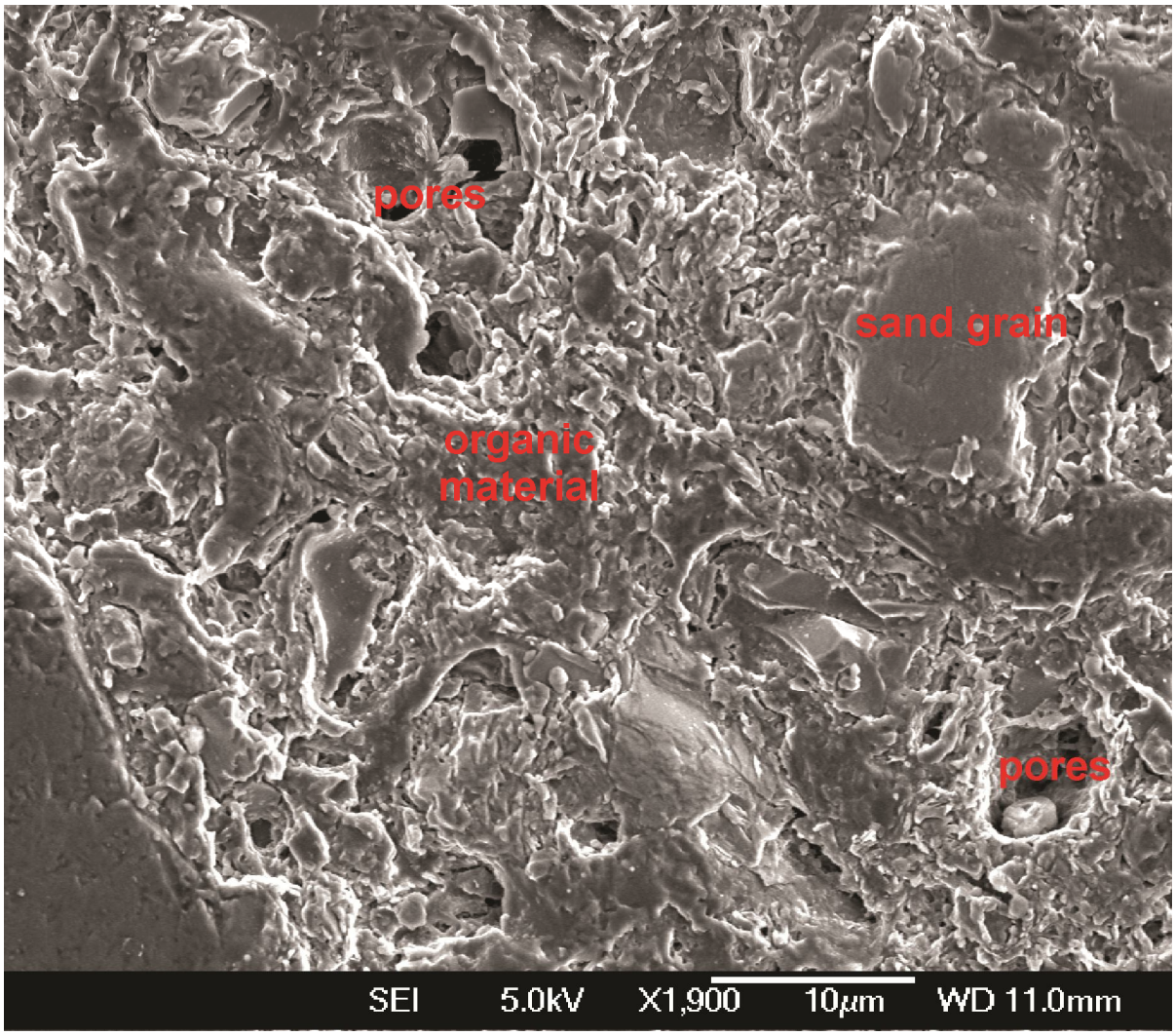

Figure 6.9. The structure of the soil with clay agglomeration that is of different origin that agglomerates found in the rock avalanche deposits (Fig. 6.6). Morphologically similar features produced under contrast conditions and revealed different properties.

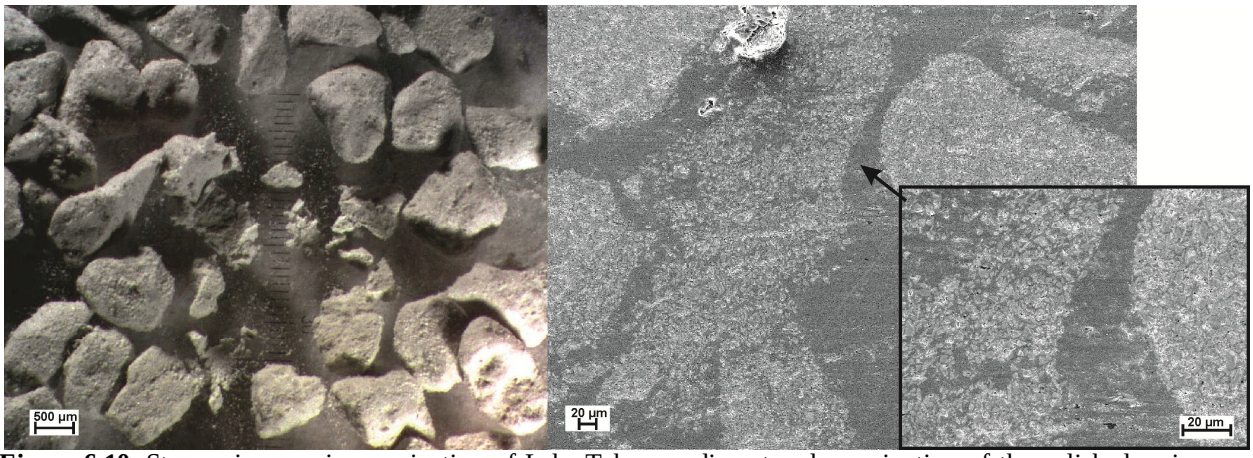

Figure 6.10. Stereomicroscopic examination of Lake Tekapo sediment and examination of the polished grains under SEM showing the grains of similar size between which the risen penetrated.

Glacier abrasion constantly contributes to silt and clay particle production during both substrate erosion and the redistribution of material down glacier (Boulton, 1978), but the associated rates are low. Additionally, the genesis of clay size particles in the glacial environment and in glaciofluvial deposits is complicated due to the difficulty in distinguishing particles originating from direct glacial crushing and abrasion from those resulting from entrainment of pre-existing sediment and/or from colluvial environments. Rockfalls and rock avalanches fall onto a glacier and the associated rock materials are then incorporated into the glaciers sediment transport system. The glacier carries these rock fragments down the valley, and as a result, rock avalanches could be the major source of fines. As previously indicated, the supraglacial rock avalanche deposit travels passively, including enormous quantities of fines produced during emplacement. Supraglacially-emplaced rock avalanches, despite their low frequency of occurrence, may be the major source of fines in glaciated active orogens (Gordon et al., 1978; Hewitt, 2009). This observation requires further, more detailed scientific investigation.

In some studies it has been suggested that the glacial sediment load is comminuted supraglacially. Owen et al. (2003) argue that supraglacial debris transport contributes to glacial sediment production and even exceeds subglacial production, resulting in large volumes of fine sediment as a result of its intense comminution during supraglacial travel. Although these findings suggest that particle comminution and chemical weathering processes are the prevailing mechanisms in the supraglacial transporting system, it is questionable if the grinding forces on the glacier surface are enough to produce abundance of the silt and clay size particles in the relatively thin (1-10 m) passive supraglacial rock

avalanche deposits. Thus, Goodsell et al. (2005) found no evidence of the supraglacial clast comminution during examination of the debris on the Haut Glacier d'Arolla, in Valais, Switzerland. I suggest that the phenomena of increasing fines towards the terminus of debris-covered glaciers (with more quantities of fine than in sub-glacial environment found by Owen et al., 2003), could be explained by the fact that towards the terminus of a debris-covered glacier the debris-cover usually increases in thickness (e.g. Lundstrom et al., 1993; Kirkbride, 1993; Popovnin and Rozova, 2002; Mayer et al., 2006), which more probably has rock avalanche material in it contributing to a high percentage of the fine fraction. Numerous impacts of rock avalanches and big rockfalls in the Himalaya are indicated by Hewitt (1999, 2009) and those observations should be included in the estimation of the sediment production on glaciers, at least in tectonically active regions.

If glaciers produce significant amounts of very fine material (micron and sub-micron size), the fact that there is not significant proportion of these fines in the glacial deposits indicates a modification and redistribution of these fines before deposition. As a result, the sediment does not consist of agglomerates, but of separate, clean grains. In the first instance, glacial ice acts as a conveyor for the redistribution of rock fragments produced either outside the glacier or by the glacial erosion. There is constant modification of these fragments by abrasion and sorting during their travel before their final deposition. Secondly, for warm-based glaciers, water abundance is the key to the preservation of the fines. Subglacial meltwater removes large quantities of sediment from temperate glaciers and this process dominates the sediment budget by exceeding the ice-flow sediment transport rate (Benn and Evans, 2010). Alley et al. (1997) suggested that subglacial streams are exceptionally efficient in transportation of available sediment as a result of abundant surface melt that percolates through moulins to the basal area. The finer particles are more easily suspended and can be transported longer distances by glaciofluvial waters, which are more efficient on steep slopes and in areas of high water discharge.

In both subglacial and rock-avalanche environments fine grains are produced by crushing larger grains, a process that requires stresses that exceed the rock strength. However, these environments have important contrasts that affect the grain-sizes arising from comminution:

1. Fine grains in rock avalanches are produced under high strain rates (Locat et al., 2006), under which conditions rock strength is high (Kobayashi, 1970). This typically causes a grain to break into a large number of small fragments (Zhang et al., 2004), whereas

grains breaking under the much lower strain rates of subglacial environments break into a smaller number of larger fragments.

2. At low subglacial strain rates, which are maintained continuously for long periods, grains break into a smaller number of larger fragments. Stress corrosion (Masuda, 2001) also causes cracks to grow slowly at stresses much lower than the rock strength under these conditions.

3. The environment in a large rock avalanche is mostly dry (as demonstrated by the large volumes of very fine airborne dust produced). In contrast subglacial water enhances stress corrosion and disperses any very fine fragments that are produced by comminution.

Thus, sub-glacially sourced moraine material contains neither the fines-coated grains nor the agglomerates (Reznichenko et al., 2012) found in rock avalanche deposits. Consequently, these characteristics can be used to distinguish the origin of the sediment with respect to either a rock avalanche event or glacial erosion.

6.4.3. Implications for PSD

6.4.3.1. Estimation of PSD

The agglomerates in rock avalanche-derived sediments complicate the PSD in terms of interpretation and genesis. The SEM micrographs of the polished grains mounts clearly show that previously-identified “intact” particles of a particular size are likely to be agglomerates (accumulations of hundreds or thousands of finer fragments), which if not disaggregated prior to analysis will result in a large error in the measured PSD. In many cases, very fine particles adhere to the surfaces of coarser clasts or are bound together into clumps due to inter-particle attractive forces (namely the high surface area to volume ratio), and thus cannot not be recognised as individual grains. Therefore, PSD calculations presented to date for rock avalanche sediments will lead to discrepancies (e.g. Murray, 2002; Wen et al., 2002; Dunning, 2004; Wilson et al., 2005; Crosta et al., 2007) as is the case for the PSDs measured by laser diffraction in this study. This observation is relevant for any sediment produced under high stress conditions, such as rock avalanches and faults gouges, with numerous sub-micron size particles that agglomerate together and lead to a coarser PSD.

In this study I have focussed on agglomerates in rock avalanche deposits, but the same process of sub-micron particles agglomeration was also described for fault gouge sediments. Thus, after prolonged dispersion and disaggregation of fault gouge sediment for 190 hours Wilson et al. (2005) found that the number of finer particles fractions in the PSD increased dramatically with the decrease of the number of coarser particles. Retrospectively I argue that this was caused by the disintegration of agglomerates. This phenomena of agglomeration during the Laser Sizer diffraction is described by Reches et al. (2007) who tested the dispersion of manufactured amorphous silica powder with a mean particle size of 80 nm (equal 0.08 μm). The laser diffraction analysis yielded the PSD with mean of 8-9 μm and no particles smaller than 1 μm (Fig. 6.11), where even after several aggregate dispersion procedures were applied the expected PSD with mean particle size in 80 nm was not reproduced (Reches et al., 2007). It demonstrated that submicron size particles tend strongly to agglomerates during analysis. Thus, the obtained PSD is biased as a result of the presence of large agglomerates in the original sample which require dispersion. Because in reality prolonged dispersion (in > 190 hours) has never has been conducted, the observed PSD for sediment from gouges or rock avalanches reflects the effects of sediment treatment technique rather than the true PSD.

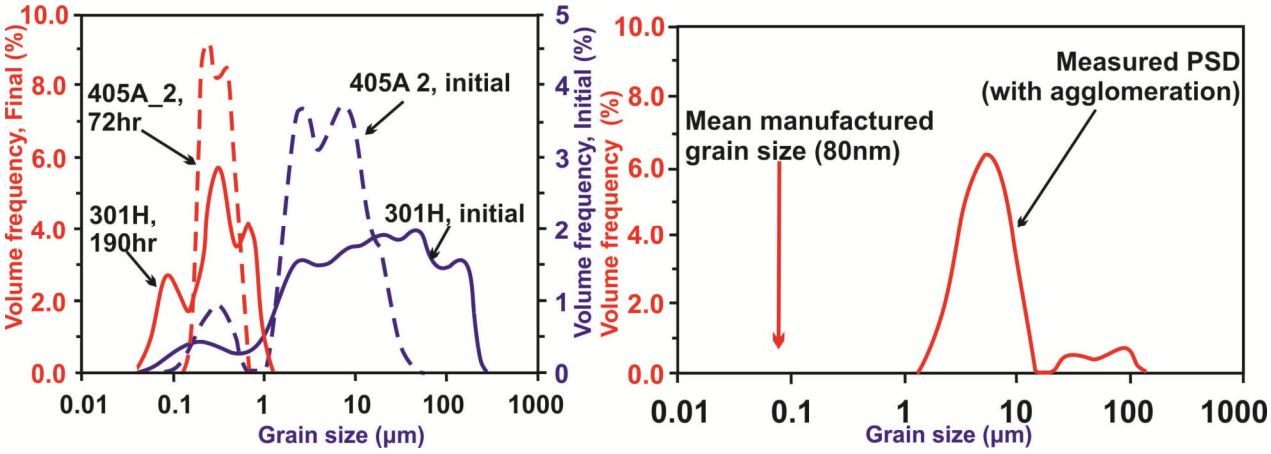

Figure 6.11. Left: PSD for gouge powder dispersed during extended analysis time (Wilson et al., 2005). Right: PSD for amorphous silica powder of uniform size in 80 μm obtained by LDM.

6.4.3.2. Fractal distribution of rock avalanche sediments?

One additional topic also needs comment. Many authors have ascribed fractal distributions to RA sediments (e.g. Dunning, 2004). The fractal distribution of grains in sediment is based on

the grain numbers related to grain diameter. For rock avalanche sediments, the fractal PSD is based on the concept that under high stress concentrations, crushing occurred primarily between equally sized grains (Sammis et al., 1987; Hooke and Iverson, 1995; Ni et al., 2010). Thus, particles of the same size will be fragmented with minimum stress concentration on the grains. As a result, the fractal dimension in such ideal conditions will be 2.58 and the log-normal plot of the number of particles against particle size will fit a straight line. Mathematically, the fractal dimension (*m*) is expressed in formula (6.1), where in such sediment the number of particles (*N*) of diameter (*d*) is the 2^m times the number of size *2d*, where *m* is the fractal dimension and N_o is the number of particles of the reference size, d_o (Hooke and Iverson, 1995).

$$N(d) = N_o \left(\frac{d}{d_o}\right)^{-m} \tag{6.1}$$

Rock avalanche deposit grain size distributions are considered to be 'fractal', indicating crushing between equally sized grains under the largest stress concentrations at all sizes within the avalanche (Sammis et al., 1987; Ni et al., 2010). However, it has been proven by Wilson et al. (2005) and confirmed by the discovery of the agglomerations in this study, that the PSD for sediments produced under high stresses (fault gouges and rock avalanches), to a large extent reflects the sample preparation technique rather than the actual PSD. The actual PSD will have a higher percentage of fines (clays) that led to reinterpretation of the fragmentation during the deposition.

The fractal distribution for subglacial erosion products was also claimed to be diagnostic for solely subglacial erosion (Hooke and Iverson, 1995; Fischer and Hubbard, 1999). The calculated fractal dimension was 3 rather than the theoretical 2.58 (Hooke and Iverson, 1995). Originally this was explained by the additional production of finer size particles from slippage and abrasion that correlates with the transport distance of the sediment. Later, Benn and Gemmell (2002) showed that the fractal dimension of the distribution is the result of mechanical mixing of coarse, medium- and fine-grained sorted sediments and/or by the mixing of Gaussian parent populations. Therefore, a complex set of processes is involved in the production of glacial sediments and these may not be susceptible to simple fractal analysis either.

Therefore, it can be concluded that the fractal dimension of the grain size distribution cannot be used for identification of particular genetic processes.

6.4.4. General discussion of technique

The rock avalanche sediment identification technique proposed and tested in this research is novel and based on the recognition of microscale characteristics of the sediment which can then be related to the process and environment of formation. It has been shown that rock avalanche debris contains large quantities of clay-sized particles. When grains comminute at high strain rate under high confining stress, they form large numbers of fragments; in addition, because the fragments are tightly confined they cannot disperse in response to the high pressures generated by fragmentation. Thus the many small fragments remain in close contact with each other, and intergranular contact forces hold them together as agglomerates, with loose fine grains adhering to the surface. This characteristic structure is expected to change little with variations in lithology and age, because the grain-size distributions and microfabric of different rock-avalanche materials are very similar and are repeated in both fresh and very old (millennial scale) deposits. Therefore, rock avalanche sediment can be identified in any deposit by the occurrence of agglomerates of tightly packed clay-sized particles in the finer fraction of the sediment. If the sediment does not have agglomerates it can be concluded that a) the sediment is neither of direct rock avalanche origin nor contains sediment from a rock avalanche source or b) the deposit was severely reworked in order that the sediment characteristics are changed.

The sample analysis involves minimal treatment with simple drying and sieving followed by examination of the grains (63-1000 μm) under a stereomicroscope and SEM. The examinations of the separate grains and their polished grain mounts on SEM are more useful for detecting agglomerated particles because under stereomicroscope the agglomerates were often heavily coated with very fine particles which mask the internal fabric (i.e. they could be either agglomerates or intact grains).

The constraints associated with the method are:

1. The necessity to have an exposure of the sediment (especially important for moraine sequences where the main body of the deposit is inaccessible). It is important to collect a representative sample of the deposit, and surface sediments should in the main be avoided because of the risk of contamination by soil forming processes and post-depositional admixtures of aeolian and other materials.

2. Laboratory analysis using SEM is expensive and time consuming but necessary to examine the finer fractions of the sediment at a precision where agglomerates can be confirmed.

SEM examination of the polished mounted grains clearly shows the multiple-fragment composition that represents the clay-size and coarser fragments of originally solid grains agglomerated together. On this basis, the absence of any agglomerates is assumed to indicate a lack of rock avalanche sediment, whereas the presence of agglomerates indicates that rock avalanche material is present. This is the first diagnostic test for recognising rock avalanche debris in moraines. It provides a method to identify moraines for which a rock avalanche origin can be eliminated, and thus to reduce the potential confusion associated with palaeoclimatic interpretations resulting from dating of non-climatically-related moraine deposits.

6.5. CONCLUSIONS

1. Analysis of the fine fractions of the sediment (< 63 μm) by Laser diffraction from numerous rock avalanche deposits and glacial sediment of known non-rock avalanche origin (from the Southern Alps of New Zealand, Jostedalsbreen in Norway and Western Russia) showed that there is a distinctive difference between PSD for rock avalanche sediment and glacial sediment. The sediment from rock avalanche deposits has a uniform PSD with high values of particles < 4 μm in size and presence particles of submicron size; however, the expected dominance of particle fraction < 4 μm was not detected. In contrast, the glacial sediment with known non-rock avalanche influence has coarser PSD with a distinct mode of 30-60 μm particles and an absence of submicron size particles. The examination of the individual grains under stereomicroscope and SEM showed that in contrast with clear single grains from glacial sediment the grains from rock avalanche sediment are actually composed of the finer particles agglomerated together. These results indicate that even using the ultrasonic option on the Laser diffraction instrument, is not sufficient to disperse the agglomerations in rock avalanche sediment and produce a true PSD for the rock avalanche sediment.

2. The examination of the mount polished grains under SEM showed that:

- In rock avalanche sediment many grains are not single grains but agglomerations of finer (submicron) particles formed into strong clumps – ‘agglomerates’. These agglomerates are unique to rock avalanches and fault gouge, and produced from characteristic comminution in under high stress and strain-rate conditions. The agglomerates in the sediment have importance in understanding the comminution process and energy

redistribution during the rock avalanche emplacement. Additionally, they are critical to the measurement and interpretations of PSD for the rock avalanche sediments.

- The genesis of the glacial sediment (the result of prolonged comminution under lower strain rates) contrasts with rock avalanche sediment and results in the production of loose grains, mostly of silt size with clear surfaces that do not form agglomerates. The glacial deposits that form after a period of prolonged sediment transportation, often under the influence of water for warm-based glaciers, usually lack particles of submicron size.

3. The presence of agglomerates allows confirmation or rejection of a rock avalanche origin of the any particular deposit. If agglomerates are present in glacial sediment, this will indicate the presence of rock avalanche sediment within the deposit. This can then be used as a diagnostic tool indicating that rock avalanche sediment has contributed to the moraine. Thus, current research shows that along with common techniques such as geomorphology, lithology, clast morphology and fabric description, the microsedimentology (PSD and grain characteristic for finer sediment fractions) can be used as one of the key methods to differentiate rock avalanche-generated moraines from climatically-generated moraines.

How significant is the impact of subaerial or non-glacial processes in total fines production, what portion of fines production is solely the result of glacial processes in high alpine environments, and to what extent have pre-existing fines influenced the sedimentary profile of glacially-derived deposits in the catchment – there are questions that remain to be answered.

7. Application of the technique for rock avalanche induced moraines and paleoclimate implications

7.1. INTRODUCTION

Mountain glaciers are regarded as one of the clearest indicators of climate change on the planet (Meier et al., 2007). Glaciers leave geomorphological evidence of their past extent on the landscape, through features such as terminal and lateral moraines and trimlines. It is widely accepted that terminal moraines are formed from the climatically-driven advances of glaciers (Oerlemans, 2005). Terminal moraines form when a glacier reaches an advanced position. They are abandoned when the glacier retreats, so the moraine records the maximum extent of an advance (Benn and Evans, 2010). Instrumental mass balance measurements have been carried out on glaciers only since the end of the Little Ice Age (Dyurgerov and Meier, 1997) so direct climate/glacier relationships are available only for these younger advances. The formation of all older moraines is assumed to be correlated solely to climatic fluctuations. However, glacierized mountain ranges that are located on active plate margins in highly dynamic geomorphologic environments are characterized by frequent large-scale mass movements such as rock avalanches (Whitehouse and Griffiths, 1983; McSaveney, 2002; Korup et al., 2004) that can cause moraine formation without a change in the climate signal (Reznichenko et al., 2011).

The Southern Alps of New Zealand are one of the few mid-latitude Southern Hemisphere glaciated mountain regions, thus are crucial for comparing glacier variations between the Northern and Southern hemispheres (and any subsequent climatologic interpretation). The presence of modern rock avalanche deposits on glaciers in the Aoraki/Mt. Cook area indicate the probable contribution of earlier rock avalanches to moraine formation in this area. From the work already presented in this thesis (Reznichenko et al., 2011), it is apparent that even small rock avalanches like the 1991 Aoraki/Mt. Cook rock avalanche can alter glacial mass balance. These moraines have been the focus for much research (e.g. Winkler, 2004; Larsen et al., 2005; Schaefer et al., 2009) and have been utilised for global palaeoclimate correlations. Given that their formation may have been influenced by rock avalanches, their origin must be clarified. In this chapter, the new technique for recognising rock avalanche derived glacial sediment, based on the presence of fine-sediment agglomerates (Reznichenko et al., 2012), is applied to glaciers

in three areas; the Holocene moraines of the Mueller, Hooker and Tasman Glaciers in the Aoraki/Mt. Cook area; the Holocene moraines of the Cameron Glacier in the Arrowsmith Range; and the pre-Holocene Waiho Loop moraine of the Franz Josef Glacier. The sediment of the finest available fraction in these moraines was collected and examined for the presence of rock avalanche material.

7.2. APPLYING THE METHOD 1: AORAKI/MT. COOK MORAINES, NZ

7.2.1. Holocene deposits

7.2.1.1. Previous estimations

Large Holocene moraines are preserved in the proglacial valleys of Hooker and Mueller Glaciers. All of these moraines have been assumed to result from climate fluctuations in the Holocene (Schaefer et al., 2009).

Past glacial fluctuations at Aoraki/Mt. Cook are reconstructed from moraine geomorphology and age control (Burrows, 1973; Gellatly, 1984; Winkler, 2005; Schaefer et al., 2009). However, different dating techniques used among these authors have resulted in inconsistencies in the estimated ages for these moraines that complicate climate reconstruction. The estimated ages of the moraine sequences for the Mueller, Hooker and Tasman Glaciers are summarized in Table 7.1. They are related to each other by matching each author's description and/or coordinates. The locations of some moraines were poorly described and may be identified incorrectly.

7.2.1.2. Mueller Glacier

Geomorphological features such as outwash plains, moraine ridges, ice-contact terraces and slopes, lake beaches, alluvial fans, screes and rockfall deposits are found in the Mueller proglacial valley. Well-preserved Holocene moraines are located within 2 km of the present-day terminus. The moraines commonly have steep ice-contact slopes on the proximal side and outwash plains that grade to the distal sides of the moraines. The younger lateral moraines are collapsing into the modern proglacial lake.

These moraines were studied for reconstruction of the Holocene fluctuations of the glacier in the Aoraki/Mt. Cook area by Burrows (1973), Winkler (2004, 2005), Schaefer et al. (2009) and others. In the proglacial area 6 main moraine complexes are distinguished (Fig. 7.1 A): Older moraines of Foliage Hill (a) and White Horse (b), Kea point lateral moraines (c), younger frontal moraines west from the Hooker River (d), younger latero-frontal moraines to the east of the lake along the tourist track (e) and a small complex of lateral moraines between Stocking and Hooker streams (f). The Foliage Hill and White Horse moraines form the largest and oldest moraine complex. During glacier advances around and after the LIA the White Horse moraine caused the glacier ice to flow into the wider open area south from the modern lake. As a result, east from the Alpine Memorial smaller moraine sequences were formed. The White Horse moraines are well-preserved mostly because of the location of the main meltwater outflow running well to the east. However, the enormous volume of the sediment in the moraines suggests that their origins may include one or many rock avalanche events.

Within these complexes the following 9 moraine sequences are distinguishable (Fig. 7.1 B):

(1) Foliage Hill moraine;
(2 and 3) the older moraines of the White Horse;
(4) the longest moraine sequence that is preserved, reaching from the outer edge of the Kea Point area, on the proximal side of the White Horse moraines to the younger moraine complex south of the lake (and a small segment of this moraine can be traced in the eastern latero-frontal moraines complex);
(5) the barely distinguishable moraine south of the look-out point for the Mueller Glacier, which continues after first swing bridge;
(6) the moraine that passes the look-out point for the Mueller Glacier and follows along the track between two swing bridges;
(7) a clearly traced small moraine at the front of the old terminus that follows along the track between two swing bridges;
(8) unclear remnants of a moraine by the lake which could also be traced by Kea point; and
(9) the youngest moraine found at the south of proglacial lake and south from the entrance of the Hooker River into the Mueller Lake.

Table 7.1. A comparison of estimated ages for Holocene moraines of the Mueller, Hooker and Tasman Glaciers.

moraine sequences		Burrows, 1973	Gellatly, 1984 Weathering-rind dating		Black, 2001 Lichenometry	Winkler, 2004/2005 Lichenometry		Schaefer et al., 2009 ^{10}Be chronology	
		date	age	date	date	date	age	age	date
Mueller Glacier	1	-	7200 ± 1870 BP		-		c.5200	6400 BP	
	2	AD <1500	3350 ± 870 BP		-		c.4200	3200 BP	
	3	AD 1600-1700	2500-3000 BP					2100 BP	
	4	AD 1730-50	1490 –2940 BP		AD 1743-45		c. 2000	570 BP	AD 1380
	5	AD 1790	840 ± 218 BP	AD 1110	AD 1761-93	AD 1726			
	6	AD 1850	580 ± 150 BP	AD 1370	AD 1786-1788	AD 1737		400 BP	AD 1550
	7	AD 1890	340 ± 88 BP	AD 1610	AD 1800-1856	AD 1860		200-300 BP	AD 1650-1750
	8	AD 1915	135 ± 35 BP	AD 1815	AD 1887-1874	AD 1895			
	9	AD 1930-47	<100 yr BP	AD 1850	AD 1874-87, 1918	AD 1905		< 200 BP	< AD 1750
Hooker Glacier	1	AD 1200-1300	3350 ± 870 BP		-		c.5200	1400 BP	AD 550
	2	AD 1300-1500	2540 ± 660 BP		-		c.4200	1000 BP	AD 950
	2.1	AD 1500-1600	2160 ± 562 BP			AD 1781	c.4200		
	3	AD 1600-1700	1830 ± 476 BP			AD 1783	AD 1740		
	4	AD 1750	1490–2940 BP		AD 1743-45	AD 1878	x		
	5		840 ± 218 BP	AD 1110	AD 1761-93				
	6		580 ± 150 BP	AD 1370	AD 1786-1788				
	7	AD 1890	340 ± 88 BP	AD 1610	AD 1800-1856	AD 1901	x		
	8	AD 1915	135 ± 35 BP	AD 1815	AD 1887-1874				
	9	AD 1930	<100 yr BP	AD 1850	AD 1874-87, 1918	AD 1916			
Tasman Glacier	0		3790 ± 960 BP					c.6500 BP	
	1	AD 1200-1300	1490 ± 387 BP		-		c. 2000	1650 BP	AD 300
	2				-				
	2.1	AD 1500-1600	1150 ± 300 BP						
	3	AD 1600-1700	840 ± 218 BP					1000 BP	AD 950
	4	AD 1750	580 ± 150 BP			AD 1862			
	5,6	AD 1820-1850	340-580 BP	AD 1370-1610		AD 1845-1860			
	7	AD 1890	135 ± 35 BP	AD 1815		AD 1902			
	8	AD 1950th							

Ages and dates correlated from five studies: lichenometric-dating (Burrows, 1973), modal weathering-rind thickness analysis (Gellatly, 1984), FALL lichenometry measurements (Black, 2001), lichenometric-dating and Schmidt hammer measurements (Winkler, 2004/2005) and ^{10}Be surface exposure dating (Schaefer et al, 2009).

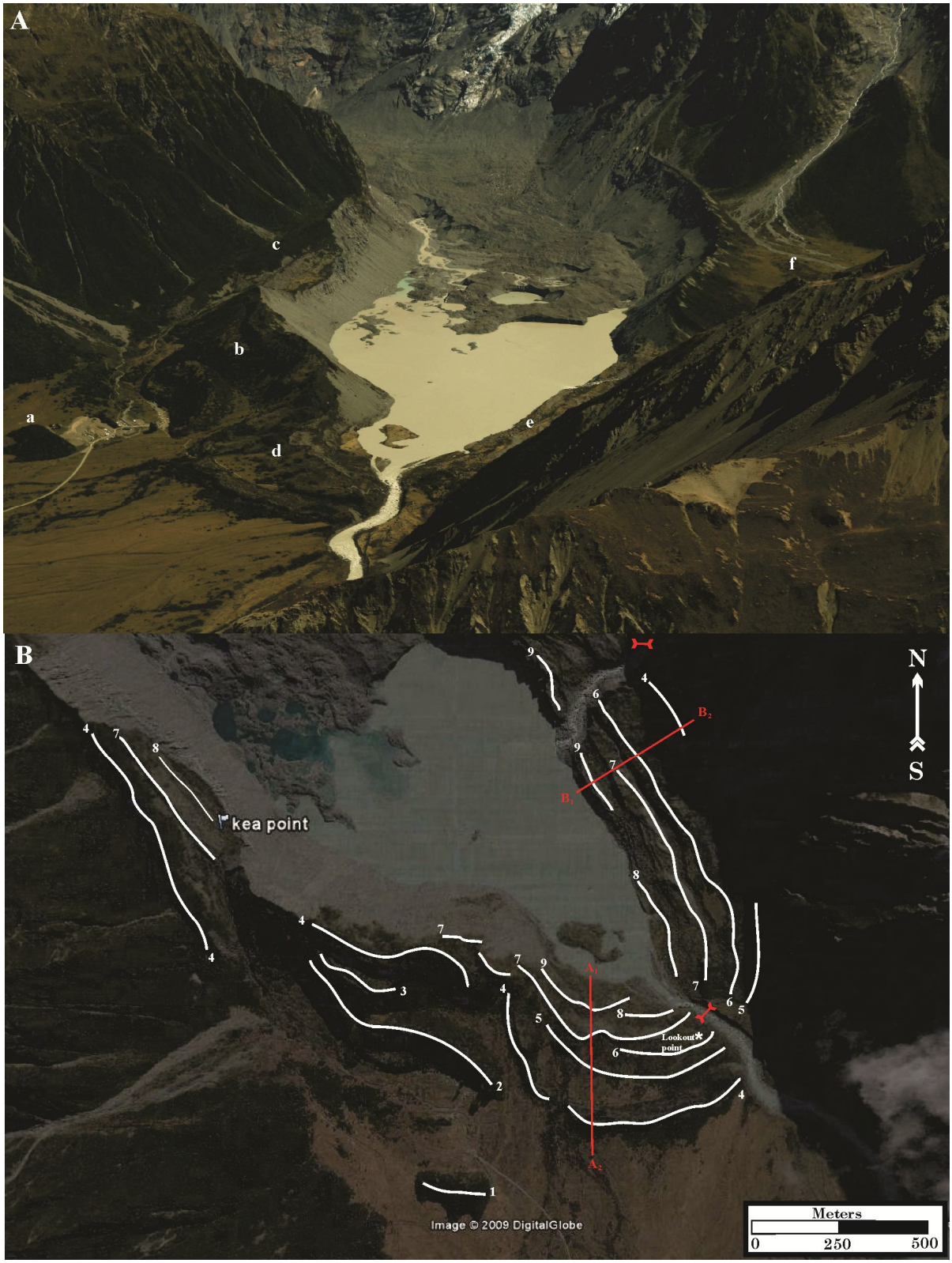

Figure 7.1. A. The terminus of the Mueller Glacier with proglacial lake and moraine complexes. Photo: S. Winkler, Feb 2008. B. The moraine sequences are listed in Table 7.1. Kea and Look-out Points and swing bridges are indicated. Google Earth image, 2006.

7.2.1.3. Hooker Glacier

The Hooker Glacier Holocene moraines border the Hooker proglacial lake, with an outwash plain to the south. The lateral moraines are better preserved than those of the Mueller Glacier and are prominent on both sides of the lake. On the eastern valley wall there are three upper and older pre-LIA moraines with four younger ones below. Despite good preservation, the moraines are dissected by stream courses and buried by alluvium and colluvium, and during the last several years the lowermost moraines have been collapsing into the lake. The lateral moraines on the western valley side have suffered greater erosion by streams and burial from sediment supplied by the Tewaewae, Eugenie and Stewart Glaciers.

The proglacial area of the Hooker Glacier has a series of well-preserved Holocene moraines, which can be divided into 4 complexes (Fig. 7.2A): (a) the frontal moraines south of the lake; (b) the continuation of frontal moraines and older lateral moraines west of the Hooker stream; (c) the well developed lateral moraines on the east side of the lake and (d) older lateral moraines on the south of the eastern wall, which are partially buried under growing screes. Within these complexes the following moraine sequences can be found (Fig. 7.2 B):

(1) the older lateral moraine;
(2 and 2.1) lateral moraines on the south-east slope that continue west from the Hooker stream;
(3 and 4) terminal moraines south from the lake which continue into lateral moraines of around LIA age;
(5 and 6) moraines of uncertain identification from the LIA; and
(7, 8 and 9) younger moraines of the late 19^{th} and early 20^{th} century.

7.2.1.4. Tasman Glacier

In the Tasman Glacier proglacial foreland few Holocene moraines are preserved. The glacier fluctuations during last 1500-2000 years were not large and the terminus stayed close to the AD 1890 moraine sequence (Kirkbride, 2000). Prior to the formation of Tasman Lake, the Tasman Glacier terminus was an outwash head, which redistributed available debris to form the proglacial fan at the expense of moraine construction and preservation. As a result, after the ice level fell to the level of the outwash surfaces in the early 1960s, a moraine formed that consisted of the dumped supraglacial debris that now is resting on the top of the outwash head (labelled here sequence 8). The largest latero-frontal moraines are the so-called Blue

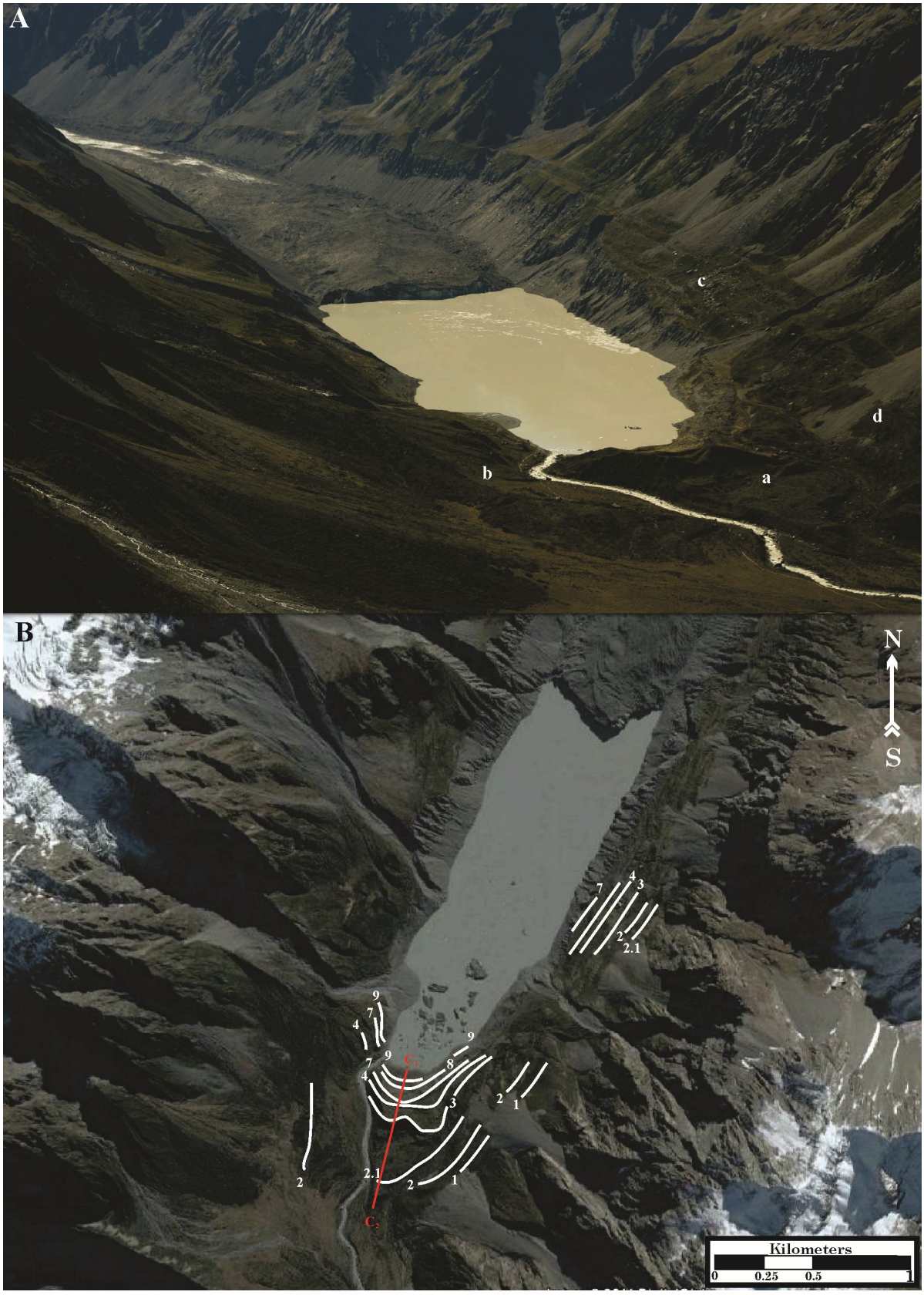

Figure 7.2. A. The terminus of the Hooker Glacier with proglacial lake and moraine complexes. Photo: S. Winkler, Feb 2008. B. The moraine sequences are listed in Table 7.1. Google Earth image, 2006.

Lakes moraines that include moraine complexes formed about 1000 years BP (Schaefer et al., 2009) with the younger moraine ridges of the LIA period on their ice-proximal side. The Blue Lakes themselves are assumed to have formed as a result of dead ice melting after LIA re-advances. The longest continuous moraine marking the glacier terminus is estimated to have been deposited after 1900 AD and can be traced farther north among lateral moraines. Fields of the hummocky moraine with stagnant ice underneath (the thickness of which is unknown) are found at south-western corner of the Tasman Lake and in Murchison Bay.

In the proglacial area of Tasman Glacier the following moraines are distinguished (Fig. 7.3 A): (a) the Blue Lake moraine complex; (b) the main terminus moraine south-east from the Tasman Lake and north from the Blue Lakes; and (c) lateral moraines along the western valley side. Although moraine complexes (b) and (c) can be traced along the east side of the valley, these moraine were not studied due to their difficult access. The main moraine sequences are (Fig. 7.3 B):

(1) a small hill that is a moraine preserved by the road, dated around 6000 years BP (Schaefer et al., 2009);
(2, 3 and 4) pre-LIA moraines preserved in the Blue Lake complex;
(5, 6 and 7) the LIA moraines found in the Blue Lakes morainic complex with small lakes between;
(8) large moraines that trace the last maximum stand of the glacier; and
(9) moraine developed since the melting of stagnant ice at the terminus during the 20th century.

7.2.2. Microsedimentology of sampled moraines

7.2.2.1. Sediment sampling

All identified moraines of the Mueller, Hooker and Tasman Glacier were targeted for sampling of fine sediments (< 1 mm) to determine if agglomerates were present. Sample location information is summarised in Appendix E.

The limited moraine exposures and prohibition of mechanical excavation in the National Park meant sampling was restricted mostly to surficial material on the top or sides of moraines.

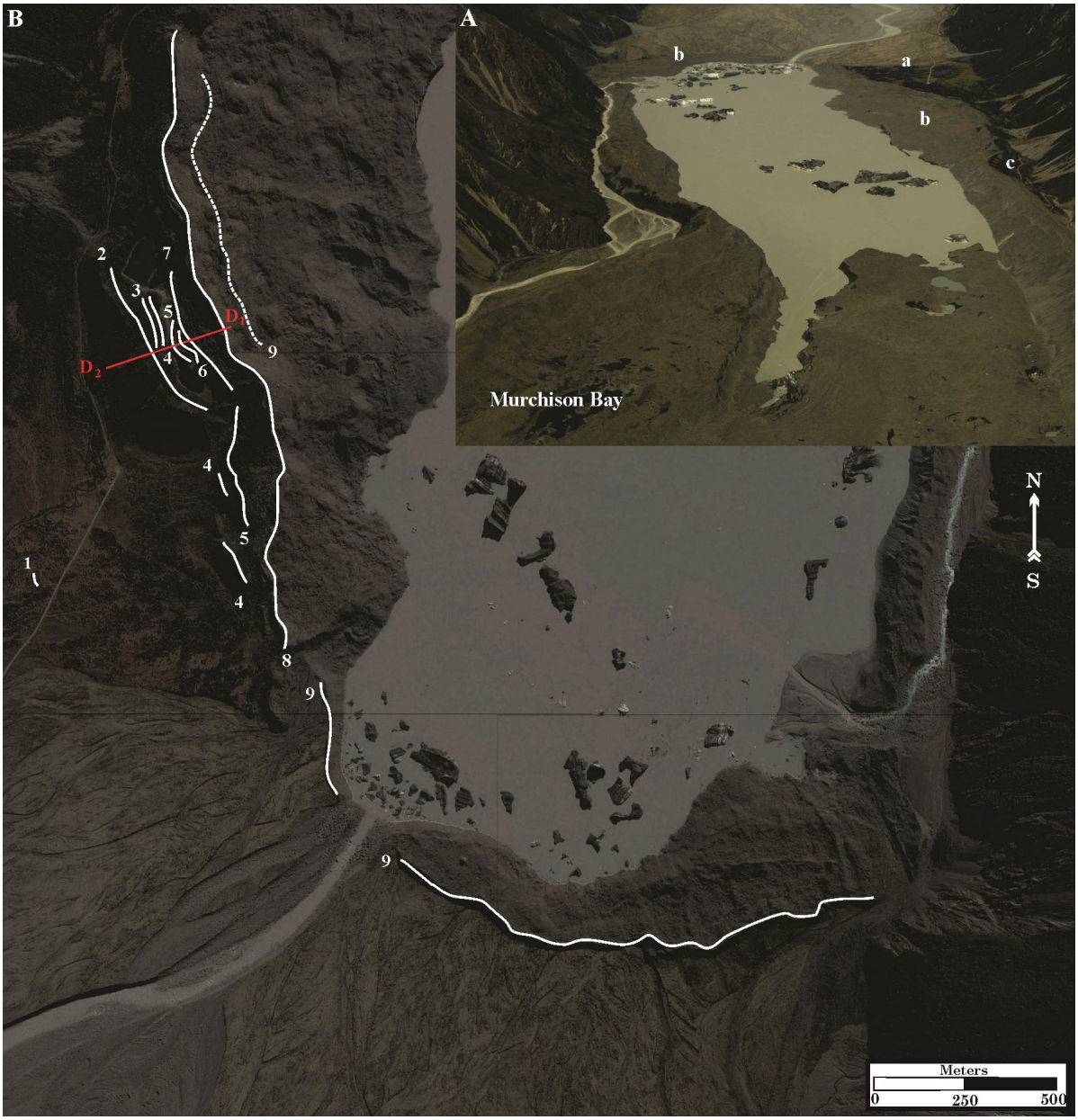

Figure 7.3. A. The terminus of the Tasman Glacier with proglacial lake and moraine complexes. Photo: S. Winkler, Feb 2008. B. The moraine sequences are listed in Table 7.1. Google Earth image, 2006.

The only locations with adequate exposure of internal material within terminal moraines of the Hooker and Mueller Glaciers are two river-cut sections in Mueller Glacier moraines. The majority of the moraines have a carapace of larger angular boulders on the surface that indicate a late stage of supraglacial deposition in their formation. Some LIA and older moraines are covered with a layer of loess (≥ 0.5 m), which restricted sampling of these moraines. Therefore, apart from two Mueller Glacier moraines, all samples were collected from coarse surficial material on the top or sides of the moraines. Cross-sections through the

main moraine ridges are presented in Figures 7.4 and 7.5 (indicated on Figs. 7.1, 7.2 and 7.3) with roundness for pebble-sized clasts highlighted.

7.2.2.2. Results

The Foliage Hill moraine ((a), Fig. 7.1), is covered with a thick layer of loess and vegetation and has no exposures. This moraine is estimated to be of the same age as the small hill by the road at the Tasman Glacier foreland (Schaefer et al., 2009), which is also covered with a thick layer of loess (sequence 1, e Fig. 7.3). The White Horse moraine complex ((b), Fig. 7.1) also has no exposures either. Three moraines of the White Horse moraine complex are the largest ridges of pre-LIA age (Burrows, 1973) or even older (3200 BP, 2100 BP and 570 BP dated by Schaefer et al., 2009). The layer of loess (> 15 cm) on sequences 2 and 3 and vegetation prevent sampling. If rock avalanche material is present in these deposits an outcrop of a minimum of a couple of metres deep would be required for sampling.

The Kea Point terminal moraines ((c), Fig. 7.1), which are mostly of supraglacial origin, are exposed only where the sediment is collapsing into the proglacial lake. The older moraines were sampled for fine sediment, but due to the cover of vegetation and loess, the sample is not representative of the moraine material and has been ignored in the present analysis.

For terminal moraines of complex (d), agglomerates were found in outcrop along the Hooker River for moraine sequence 5 (Figs. 7.1. and 7.6). Access to the sediment of the youngest deposit (sequence 9) was possible due to the undeveloped vegetation, but no agglomerates were found in the surface sediments and it was not possible to sample from deeper in the moraine.

The latero-frontal moraines of complex (e) have 5 moraine sequences that, according to Burrows (1973), have been partially reworked by the Hooker River. Moraine sequences MTOP5, MTOP4 and MTOP3 (Fig. 7.4) have no exposure of internal material and agglomerates were not found in the surficial sediments sampled. The MTOP2 moraine ridge has an exposure at the old swing bridge. Agglomerates were found in the sample taken from here. The MTOP1 moraine was covered with vegetation and loess and the only accessible samples were surficial and not considered representative for this moraine sequence (Fig. 7.4).

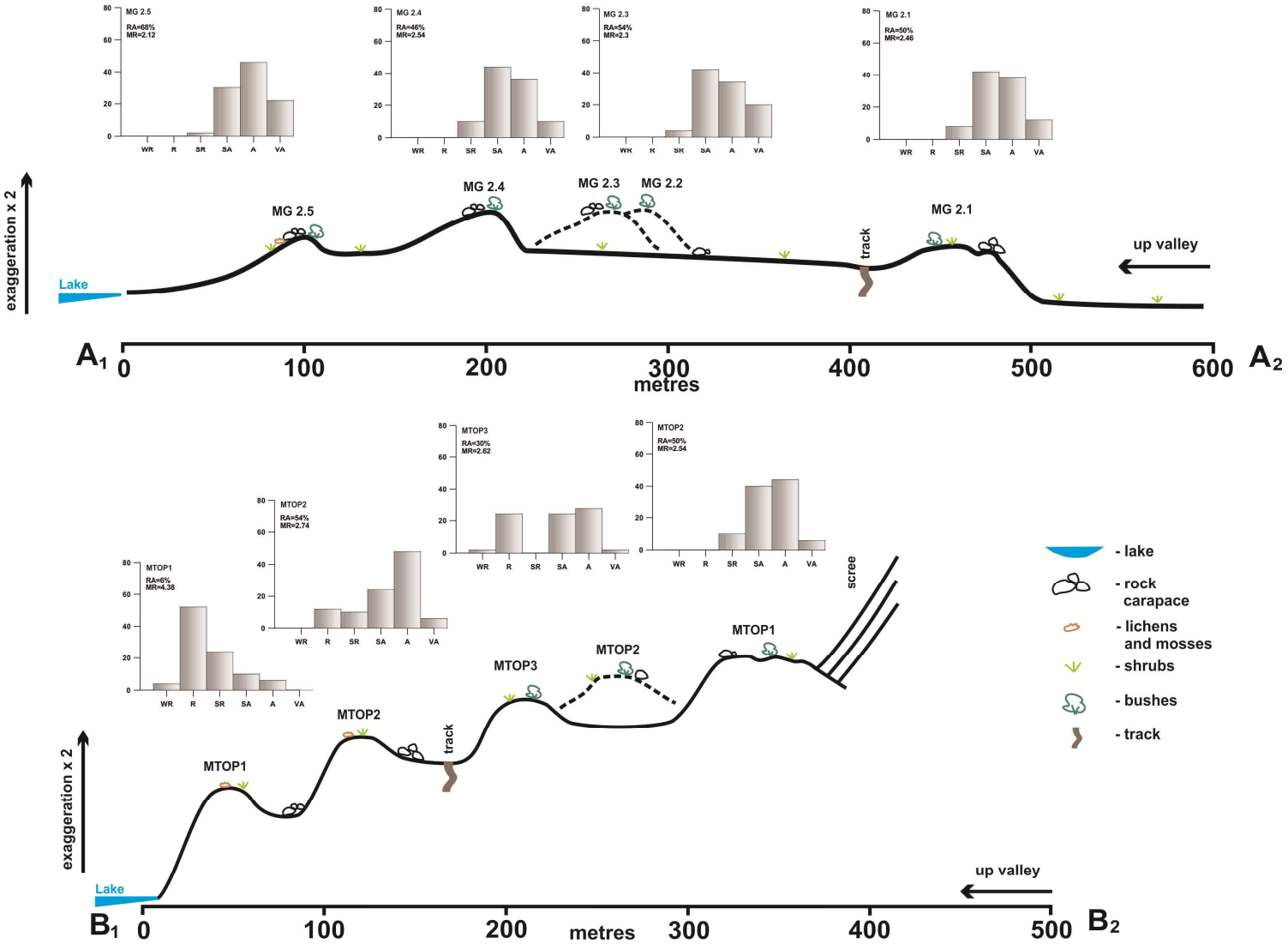

Figure 7.4. The Mueller Glacier moraine cross-sections (see Fig. 7.1): top, cross-section at A_1-A_2 through younger terminal moraines west from the Hooker River; bottom, cross section B_1-B_2 terminal-lateral moraines east from the lake between the two swing bridges.

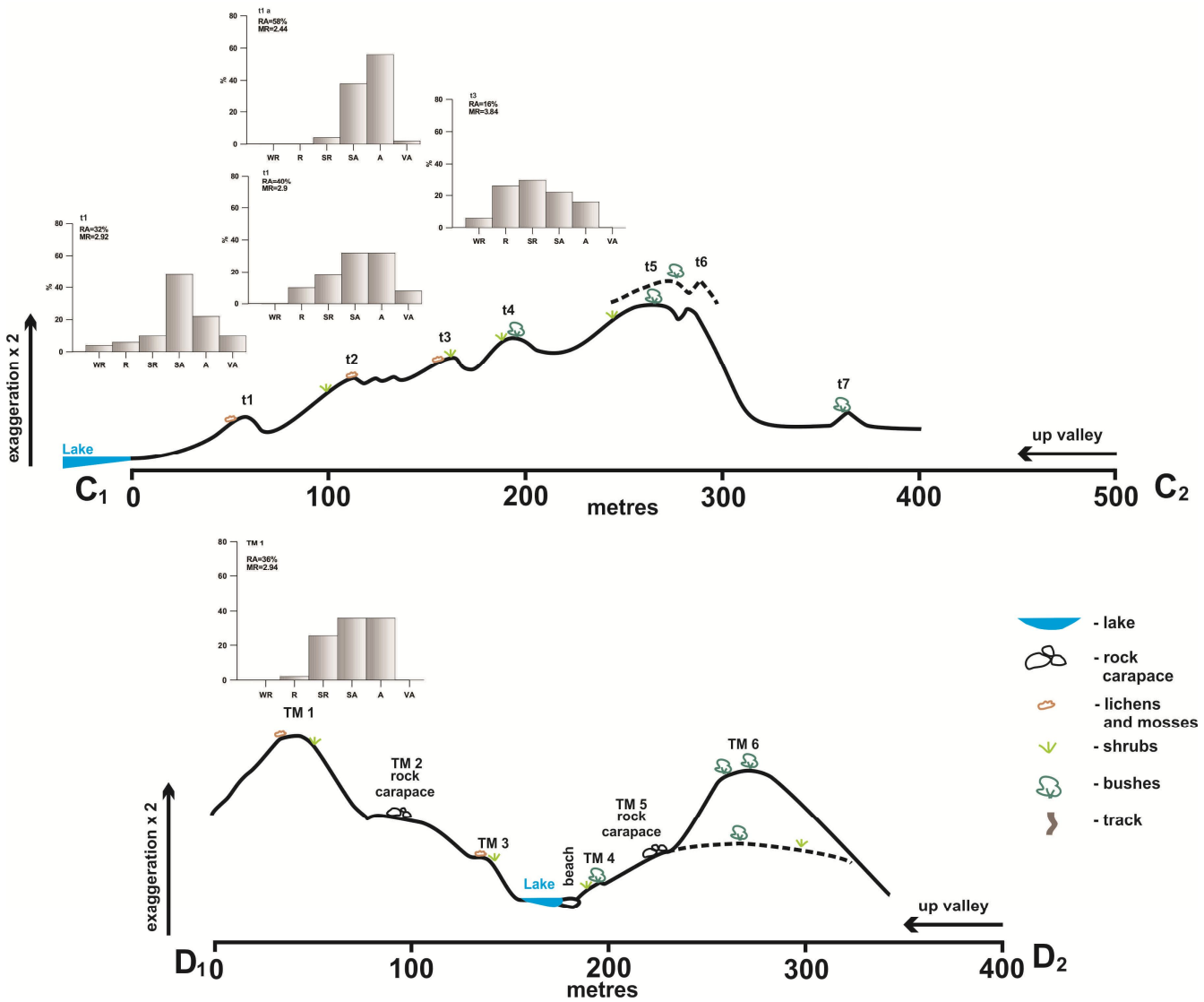

Figure 7.5. Top: the Hooker Glacier moraine cross-section C_1-C_2 (see Fig. 7.2) through the terminal moraines. Bottom: the Tasman Glacier moraine cross-section D_1-D_2 through terminal-lateral moraines of the Blue Lake complex (see Fig. 7.3),

For the Hooker Glacier there are no moraine exposures and only surface reworked material could be sampled. The sediment sampled from morainic complexes (a) and (b) (two lateral moraines) was only taken from the younger moraines, which had no shrub cover. A greater proportion of silt-sized fines was present in the lateral-frontal moraine sequence (9) (Fig. 7.2) than any of the other moraines in this complex. The younger exposure (sequence 7) at the complex of lateral moraines appeared to be composed of much fine sediment (silt), but unstable cliffs made sampling at this site too dangerous. In all samples no rock avalanche agglomerates were detected; however this may be a result of limited exposure sampling rather than absence of rock avalanche sediments.

Agglomerates were not found in any of the Tasman Glacier moraines, but few representative internal materials were sampled. The younger Tasman Glacier terminal moraines were covered with fine materials but lacked adequate exposure of internal material. The older Blue Lakes moraines are covered with a thick rock carapace and dense vegetation making sampling difficult. The younger moraine (sequence 8) had the greatest proportion of fines in the surficial material but no agglomerates were found. At the Lake front where the Tasman River starts, in the sampled outwash sediment no agglomerates were identified. The lateral moraine was sampled at an accessible outcrop where the road had collapsed about 2 km south of the Ball Hut site (see Appendix E). The angular sediment of this outcrop is assumed to be of supraglacial origin and contains some fine silts but no agglomerates.

In total, only two moraines of the Mueller Glacier are exposed along the Hooker River (sequence 4 and 6 are dated to ~600 BP and ~390 BP, respectively, by Schaefer et al. (2009); Table 7.1 and Fig. 7.1). They contain higher percentages of fines. The SEM examination of the separated grains revealed that some of those grains are heavily-coated particles and agglomerates (Fig. 7.6). Although there are fewer agglomerates than in pure rock avalanche deposits, their presence indicates the presence of rock avalanche debris in this deposit.

7.3. APPLYING THE METHOD 2: WAIHO LOOP MORAINE, WESTLAND, NZ

7.3.1. The moraine interpretations

An example of prehistorical rock-avalanche-induced glacier response is the Late Pleistocene/Early Holocene Waiho Loop terminal moraine of the Franz Josef Glacier, the Southern Alps (S 43º21’; N 170º10’). This moraine has received much attention in attempts

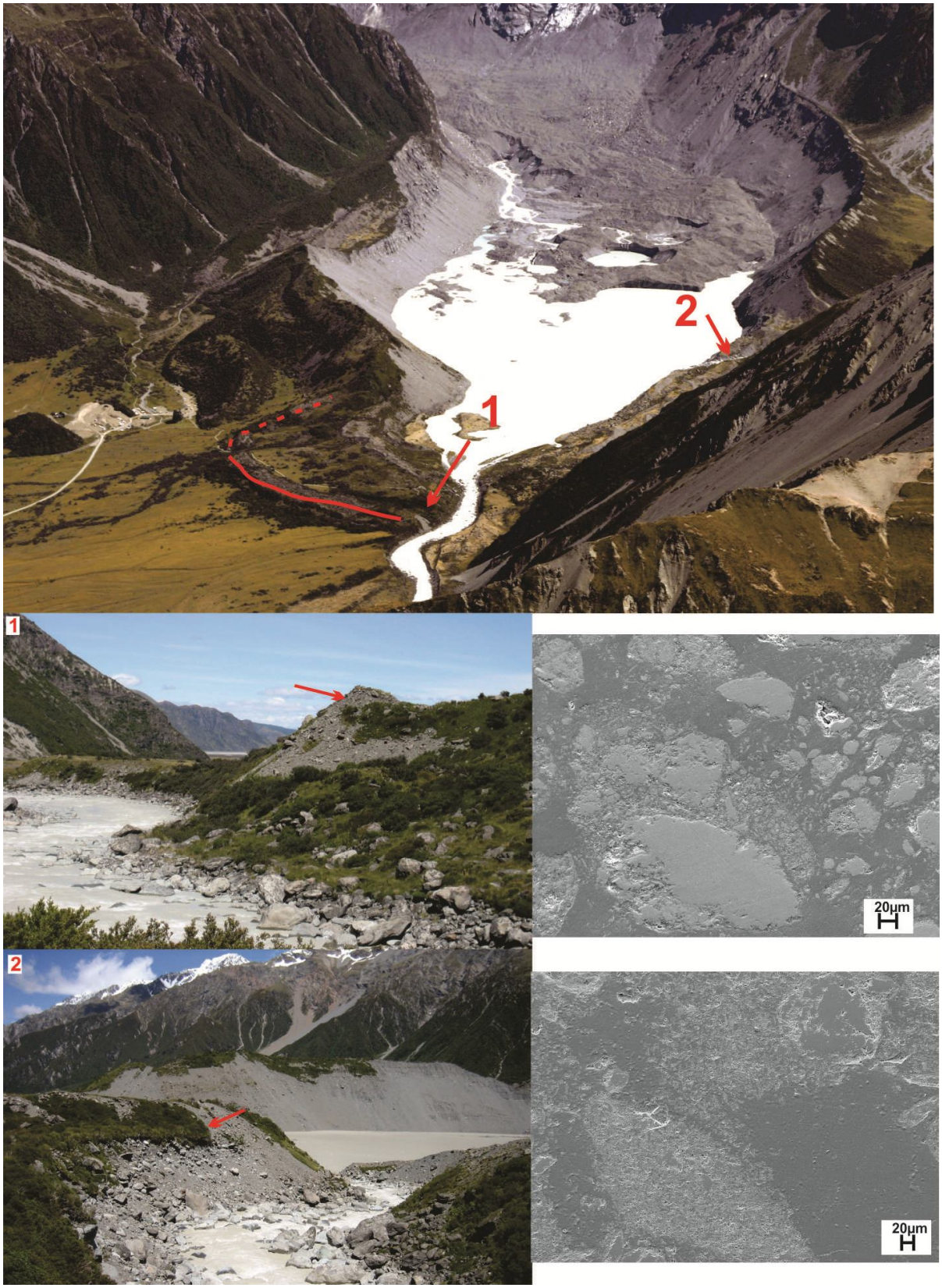

Figure 7.6. Two sampled moraines from the natural exposures that are the most representative in the Aoraki/Mt. Cook area. 1. The outcrop of moraine sequence 4 (see Fig. 7.1) along the Hooker River and the agglomerated fines in this sediment (SEM polished grain mount image). 2. The old swing bridge exposure along the Hooker River (moraine sequence 6, see Fig. 7.1) and the clays found in the sediment (SEM polished grain mount image).

to correlate it to the northern hemisphere Younger Dryas (YD) event (Denton and Hendy, 1994; Mabin, 1995; Barrows et al., 2008) or to the Antarctic Cold Reversal (ACR) about 13,000 BP (Turney et al., 2007; Putnam et al., 2010a). Tovar et al. (2008) in contrast attributed the moraine formation to a catastrophic rock avalanche that, through reduction of surface ablation, either triggered a non-climatic advance (Shulmeister et al., 2009) or without a significant advance held the position of the terminus fixed during the deposition of the bulk of the supraglacial rock avalanche deposit (Evans et al., 2010). Tovar et al. (2008) supported a rock avalanche origin of the moraine through clast lithology and angularity and from the size and morphology of the deposit. Recent modelling and its discussion (Shulmeister et al., 2010a; Vacco et al., 2010; Alexander et al., 2011; Reznichenko et al., 2011) demonstrated how a large rock avalanche could cause the Franz Josef Glacier to advance and create a substantial terminal moraine like the Waiho Loop (discussion in section 5.3.2).

7.3.2. Microsedimentology of moraine

7.3.2.1. Sediment sampling

The deposit at the distal (north) part of the moraine consists mostly of supra-glacially dumped rock avalanche material covering the top of the moraine (WL1) at S 43º21’30’’S; E 170º09’19’’ (Tovar et al., 2008). This material is exposed in a quarry excavation and due to disturbance during quarrying activities, it may not be in-situ (Fig. 7.7). The sediment is very coarse and angular including bouldery diamictons (Tovar et al., 2008). The Tatare River has also incised through and exposed the moraine, revealing more rock avalanche material at the top of the moraine. Fine sediment was collected from true left of the Tatare River outcrop (WL2) at S 43º21’14’’S; E 170º09’59’’, from 2 m below the moraine surface. The sediment is a coarse angular mostly stratified gravel that dips (at 40º) away from the terminus. Two samples were recovered from the outcrop on the true right of the Tatare River (S 43º21’14’’S; E 170º10’05’’) 3 m from the base (WL3) and (S 43º21’12’’S; E 170º10’00’’) further downstream 1 m from the bottom of outcrop (WL4). At these outcrops the sediment is fine gravel that is strongly stratified. Based on the bedding and sorting, it appears to relate to fluvial deposition associated with the Tatare River rather than moraine material (Fig. 7.7).

7.3.2.2. Results

Because of possible reworking and human disturbance, only the samples taken from the Tatare River outcrop at the true left were used in the analysis. The SEM examination showed that abundant agglomerates are present in the Waiho Loop deposit (Fig. 7.8) at least at this location, which confirms that the coarse, angular carapace material identified by Tovar (2008) and Shulmeister et al. (2009) is likely to be rock avalanche debris. The sediment in the quarry site at the West of the moraine has been modified (quarried and replaced) and may not be representative. Similarly, in the true right Tatare River cut the exposed sediment could be the originally reworked moraine sediment deposition beneath the rock avalanche sediment, or it could be the result of recent reworking and re-deposition by the Tatare River.

In absence of the rock avalanche event, the glacier almost certainly would not have produced such a voluminous moraine. As has been noted by others (e.g. Mabin, 1995; Shulmeister et al., 2009), the voluminous Waiho Loop moraine contrasts with the absence of an equivalent moraine in valleys with similar geographic conditions in the immediate vicinity (e.g. the Fox Glacier valley) on the West Coast, South Island.

7.4. APPLYING THE METHOD 3: THE CAMERON GLACIER MORAINES, NZ

7.4.1. Holocene deposits

Sir Julius von Haast in 1864 was the first person to document this glacier and named it the Hawker Glacier in honour of his companion; however, it is now known as the Cameron Glacier. He estimated the terminal face to be 1,500 feet (450 m) wide and at an altitude of 4478 feet (1365 m) above the sea. His notes describe the river flowing out of an ice cave at the terminus of the glacier and high rock walls on each side of the glacier (Haast, 1879 in Burrows, 2005). Burrows (1975) developed the first chronology for the Cameron Glacier moraines, based on lichenometry, growth layers of woody plants, and one radiocarbon date. Later, using new lichen growth curves, Burrows et al. (1990) revised his ages for the younger Marquee and Arrowsmith moraines. Recently, new ages for the Holocene moraines were provided by Denton et al. (2009) based on ^{10}Be exposure-age techniques.

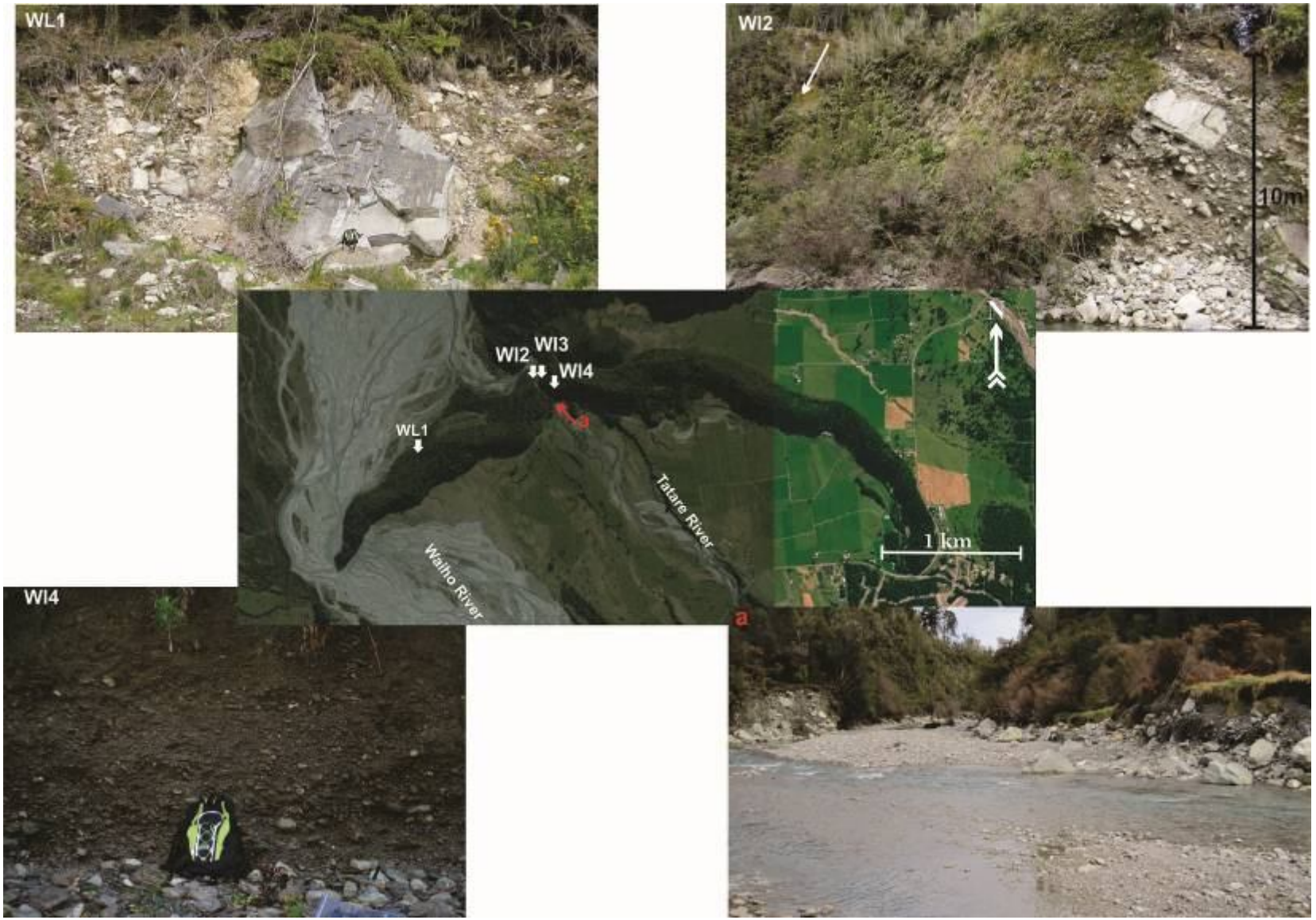

Figure 7.7. Location of the Waiho Loop moraine sampling sites: WL1, WL2, WL3 and WL4 with overview (centre) of the Tatare River cutting through the moraine (a).

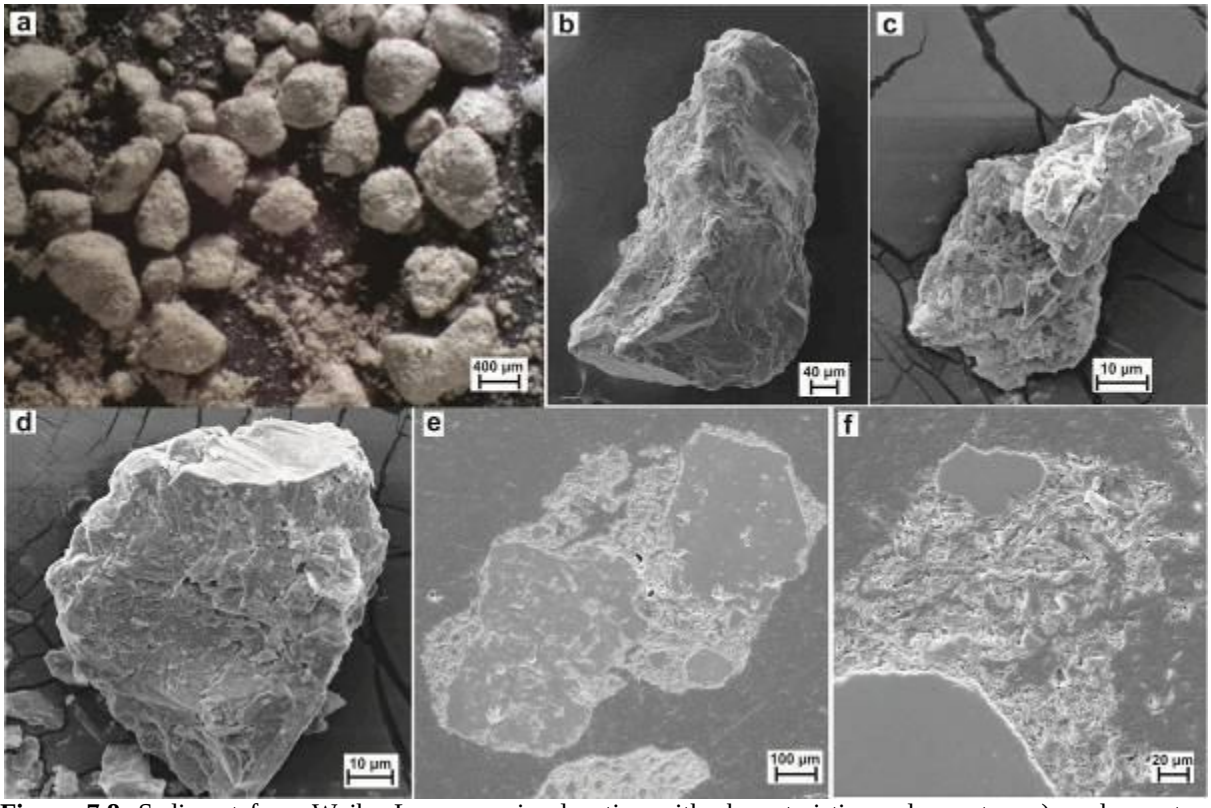

Figure 7.8. Sediment from Waiho Loop moraine location with characteristic agglomerates: a) agglomerates under stereomicroscope (sample WL2); b), c) and d) individual agglomerate grains under SEM; e) and f) polished grain mounts showing internal structure of agglomerates under SEM.

The glacier retreated from its Late Otiran (~17,000-14,000 yrs BP) position at the south end of Lake Heron, where three broad moraine belts surrounded by river and kame terraces mark its location. At that time the Cameron Glacier was a tributary to larger lobe of ice leaving the Rakaia valley; this is evident from the position of kame terraces at low elevations in the Cameron Valley (Pugh, 2008; Evans, 2008). During retreat, the Cameron Glacier produced the 12,000-10,000 BP Wildman moraines (Burrows, 1975). Further moraines were formed in the Holocene (Aranuian), and include the undated Lochaber complex, the Marquee 1 and Marquee 2 moraines (4,500-2,000 yr BP) and the Arrowsmith moraines from 600 yr BP (Burrows et al., 1990) (Figs. 7.9 and 7.10).

The comparison of estimated ages for the 9 moraine sequences is presented in Table 7.2 and shown on Figure 7.9. Additionally, Figure 7.9a shows the old terminus positions for the ice face in AD 1964 and AD 1989 reported by Burrows et al. (1990). The glacier had in (2010) retreated about 1 km since the AD 1964 position.

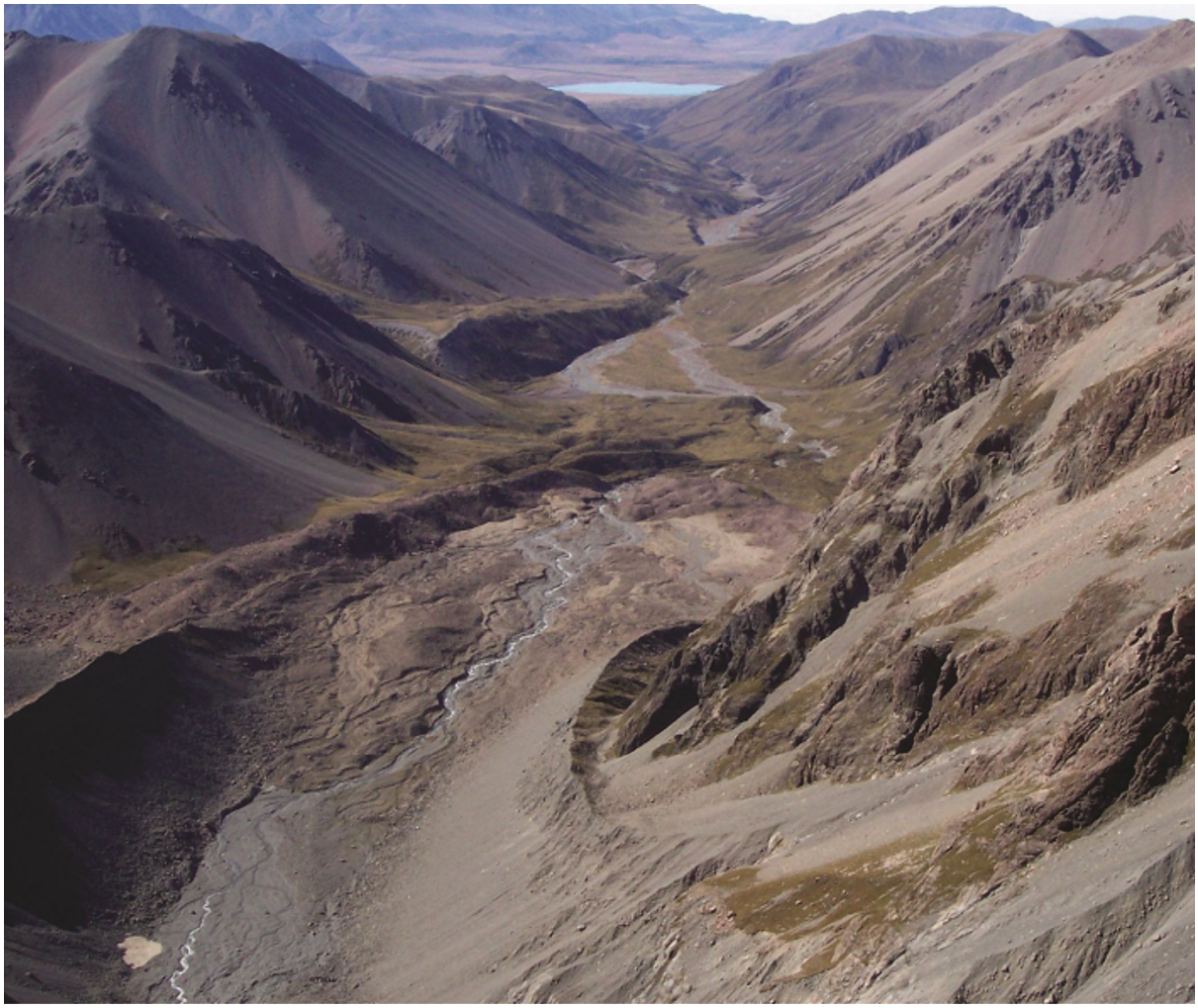

Figure 7.9. Oblique view of the Cameron Valley with Lake Heron at the background. The Cameron River cuts through the studied Holocene moraines (centre). Photo by T. Chinn.

7.4.2. Microsedimentology of sampled moraines

7.4.2.1. Sediment sampling

Half of the targeted Cameron Glacier moraines were able to be sampled for the presence of agglomerates. As with the Aoraki/Mt Cook sites, there were problems with suitable moraine exposure but several good exposures, especially of the younger moraines (Arrowsmith complex), occurred where the Cameron River had incised moraine. The majority of the moraines have an angular boulder carapace, suggesting deposition of supraglacial rockfall or rock-avalanche debris towards the end of their formation. The older moraines (Sequences 1-7) have thick layers of loess and vegetation and only one moraine had suitable exposure for dating; the exposure was created by river incision on the true right of moraine sequence 7.

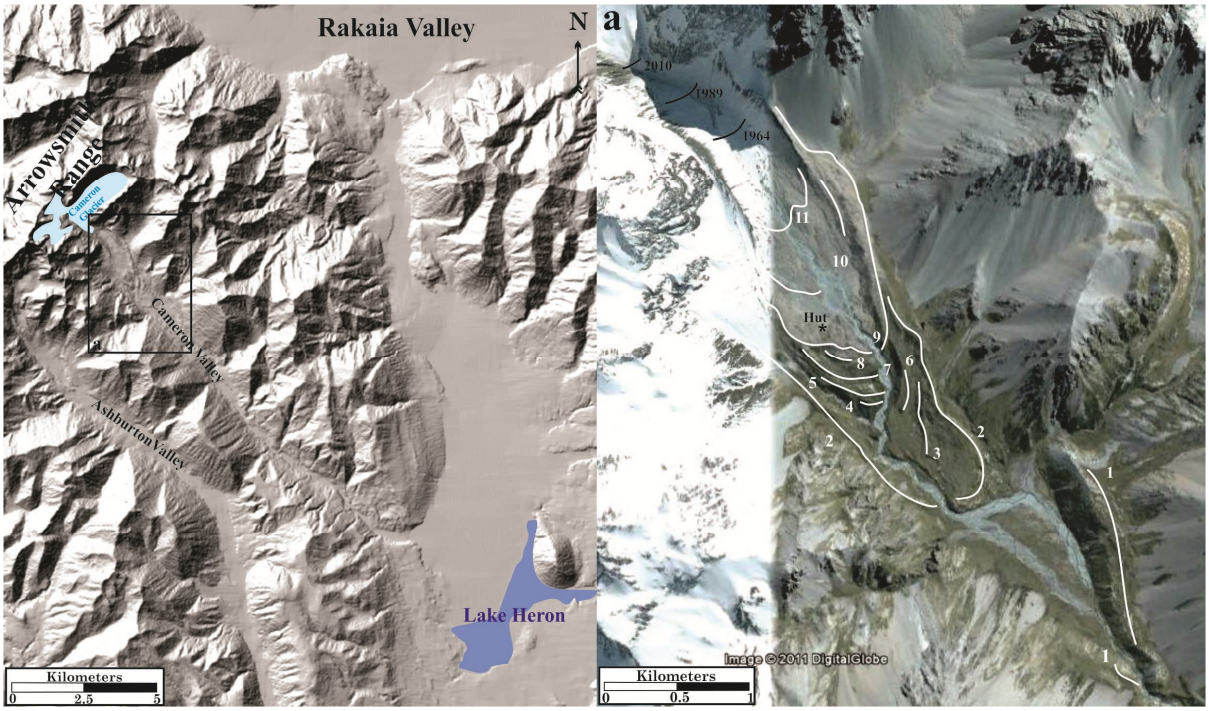

Figure 7.10. The location of the Cameron Valley with a) close view of Holocene moraine sequences for the Cameron Glacier listed in Table 7.2, Google Earth image, 2006.

Table 7.2. A comparison of estimated ages and dates for Holocene moraines of the Cameron Glacier.

moraine complexe	moraine sequences	Burrows, 1975	Burrows et al., 1990	Denton et al., 2009
Wildman	1	12,000-10,000 yrs BP	12,000-10,000 yrs BP	-
Lochaber		-	-	-
Marquee 2	2	4,500-2,000 yrs BP	< 9500 yrs BP	10000-9000 yrs BP
	3			-
Marquee 1	4		2320-5390 yrs BP	8700 yrs BP
	5			8500 yrs BP
	6			8000 yrs BP
	7			7000 yrs BP
Arrowsmith	8	15th century	30 AD	620-827 yrs BP
	9	AD 1740	980 AD	190-280 yrs BP
	10	AD 1890	1580 AD	-
	11	AD 1930	1820 AD	-

Ages and dates correlated from three studies: lichenometric-dating, growth layers of woody plants and one radiocarbon date (Burrows, 1975), revised lichenometric-dating (Burrows et al., 1990) and ^{10}Be surface-exposure dating (Denton et al., 2009). The location of moraine sequences is shown on Fig. 7.7.

Fourteen samples were taken from moraine sequences 7-11 in the Arrowsmith complex; no suitable exposures were found in sequences 1-6. Sample and exposure coordinates, and sediment descriptions are provided in Figure 7.11 and Appendix E. One sample (C14) was collected from the true right lateral moraine (S 43°21'22"; E 171°00'25"). Sediments were analysed with a stereomicroscope and mounted polished grains were examined under a SEM. Unfortunately, the Laser Sizer was knocked out by the Christchurch earthquake so the LDM test was postponed. Additionally, the roundness of the available sediment for sampled moraines was estimated for 50 gravel-sized clasts at each moraine exposure (Appendix E).

7.4.2.2. Results

The sample from moraine sequence 7 (C11) is thought to be unrepresentative because of absence of exposure and presence of vegetation and a loess layer on the surface. The sample from the river outcrop of moraine sequence 7 (C12) did not show the presence of agglomerates. The sample from moraine sequence 8 (C16) is thought to be unrepresentative because of absence of exposure and presence of vegetation on the surface. Two samples of moraine sequence 9 (C1 and C6) from both sides of the stream have fines, but the space between grains on the SEM micrograph indicates that fines do not form agglomerates for C6, but do for C1 (Fig. 7.12). Another two samples from the same sequence (C7 and C8) excavated from the surface downvalley by the river had fines present but not agglomerates. In agglomerates of rock avalanche sediments the space between particles is filled with mixtures of micron and submicron sized grains, and the sample from the large exposure on the true left of the stream of moraine sequence 9 (C10) did have agglomerates (Fig. 7.12).

The younger moraine sequence 10, farther up the incised river section, had four samples taken (C4 and C5), none of which had agglomerates. Moraine sequence 11 is represented by a small hill between lateral moraines, and is covered with a carapace of large boulders. No exposures were available for sampling but sediment between the large boulders on the surface, presumably supraglacial in origin, were sampled (C3) but no clay-sized particles were identified. The river exposure 250 m up-valley of same deposit (C2) shows some presence of clay-size particles adhering on to coarser clasts but no true agglomerates. Sediment from the large lateral moraine (C14) consists of loose grains without agglomerates.

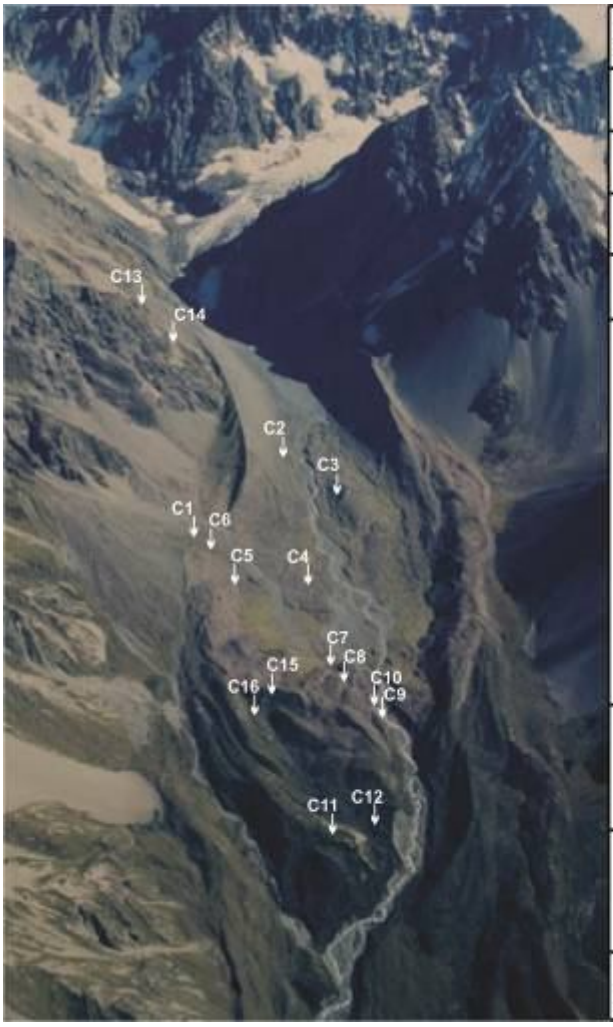

Moraine sequence	Sampled site	Coordinates	Available outcrop	Agglomerates
5	C11	S 43°22'12" E 171°01'18"	no	
6	-		no	
7	C12	S 43°22'11" E 171°01'22"	yes	no
8	C16	S 43°22'06"' E 171°01'06"	no	
9	C1	S 43°21'47" E 171°00'45"	yes	presence
	C6	S 43°21'49" E 171°00'47"	yes	
	C7	S 43°21'58" E 171°01'11"	no	
	C8	S 43°21'59" E 171°01'14"	no	
	C10	S 43°22'04" E 171°01'21"	yes	presence
	C15	S 43°22'04" E 171°01'07"	no	
10	C4	S 43°21'52" E 171°01'04"	yes	no
	C5	S 43°21'52" E 171°00'55"	yes	no
11	C2	S 43°21'30" E 171°00'47"	yes	no
	C3	S 43°21'35" E 171°00'59"	no	
Lateral true right	C14	S 43°21'22" E 171°00'25"	yes	no

Figure 7.11. Location of the sample sites in the Cameron Valley (left) and description of sampled moraines with indicated presence of the rock avalanche sediment.

7.5. DISCUSSION

7.5.1. Using agglomerates for presence of rock avalanche debris in moraines

Burrows (1973) suggested that the size of the moraines in the Aoraki/Mt. Cook area is the result of extensive supraglacial debris cover on glaciers. Porter (2000) discussed the potential rock-avalanche-induced origin of moraines in the Southern Alps, and Larsen et al. (2005) suggested that earthquake shaking generated by faults in the area could have produced large quantities of supraglacial rock avalanche debris. Despite these studies, glacial advances in this area are still attributed to climatic fluctuations and the fact that rock avalanches are common events in the area and could be responsible for the size of moraines and their existence is largely ignored by authors looking at paleoclimate (e.g. Gellatly, 1984; Schaefer et al., 2009). For example, Schaefer et al. (2009: SOM) specifically denied any role that rock

avalanche debris may have played in the glacier fluctuations and moraine formation in this area and their high-resolution ^{10}Be chronology of moraine positions was interpreted by considering climatic fluctuations alone.

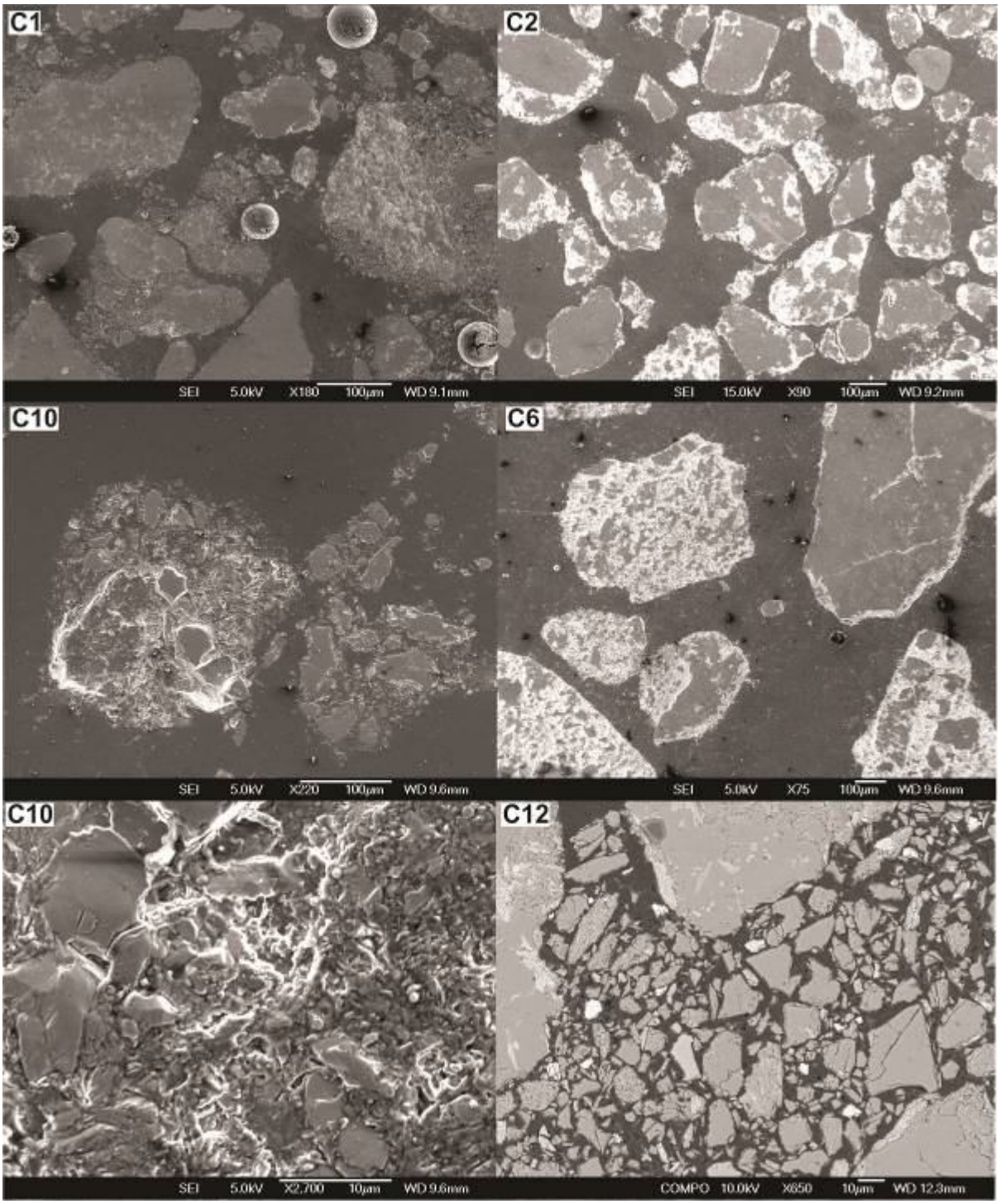

Figure 7.12. Examples of agglomerates found in the Cameron Glacier moraines C1 and C10 compared with clean and separate grains (non-agglomerates) in the sediment from C2, C6 and C12 moraines.

The correlation of similarly-aged moraines between valleys is one of the main arguments for a climatic origin; however, not all moraine complexes are correlated in age (Tabl.7.1). Further, landsliding can occur over extensive areas in response to a single earthquake (Stirling et al., 2005). Therefore, in seismically-active ranges such as the Southern Alps, local climatic correlations may be unreliable. Thus, if we compare the published dates for Alpine Fault earthquakes with four moraine dates by Schaefer et al. (2009) and the AD 1199±56 Hooker moraine of Wardle (1973) they correspond within their margin of error (Fig. 7.14). A large earthquake in South Westland in AD 1826 (179 years BP; Hewitt et al., 2008) coincides with the 160 ± 30 years BP moraine. Because ruptures of the Alpine Fault usually cause M ~ 8 earthquakes (Rhoades and Van Dissen, 2003) and its surface trace lies within 30 km of the glaciers that generated the dated moraines, Alpine Fault earthquakes can certainly cause large rock avalanches in this part of the central Southern Alps. There also are many other known and unrecognised faults in the Southern Alps capable of causing shaking sufficient in magnitude to trigger rock avalanches (Stirling et al., 2005). Moreover, many aseismic supraglacial rock avalanches occur in the glacier catchments (e.g. the 1991 Aoraki/Mt. Cook rock avalanche), that increase the contribution of the rock avalanche sediment to the moraine formation in the area. Therefore, both climate and rock avalanches can affect glacier behaviour and resultant deposition.

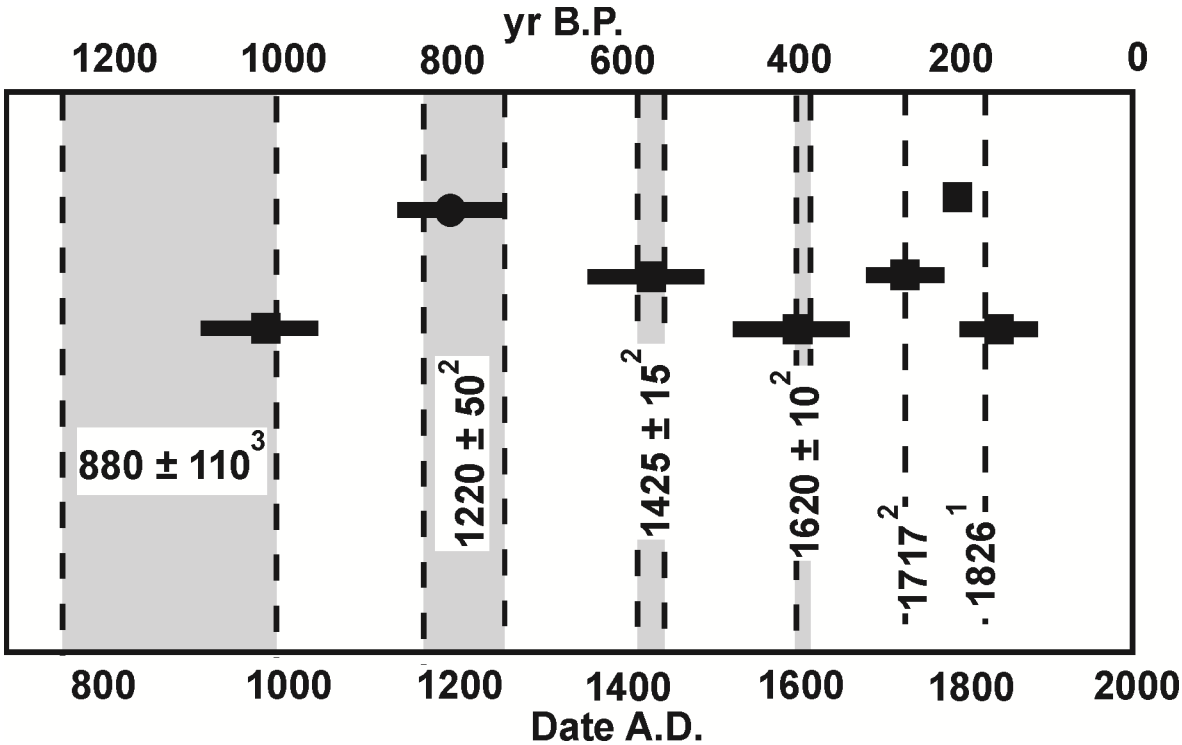

Figure 7.13. Moraine dates in the Aoraki/ Mt. Cook region (horizontal bars; square centres from Schaefer et al, 2009; circular centre from Wardle, 1973) compared with Alpine Fault earthquakes (vertical dashed rectangles): [1]Wells and Goff (2007); [2]Rhoades and Van Dissen (2003); [3]Norris et al. (2001).

Supraglacial rock avalanches are frequent in the Aoraki/Mt. Cook area and more than 20 rock avalanches have been recorded since the 1950s (Allen et al., 2009), including the Murchison Glacier (1979) rock avalanches (Whitehouse, 1983), the Mueller Glacier, Mt. Isabel and Mt. Thomson (1996) rock avalanches and the Mt. Fletcher (1991) rock avalanches onto the Maud Glacier (McSaveney, 2002). The deposits from most of these events are no longer distinct. Modern supraglacially-emplaced rock avalanche deposits are still visible on some glacier surfaces, including the Aoraki/Mt. Cook rock avalanche (1991) on the Tasman Glacier, the Mt. Beatrice rock avalanche (2004) on the Hooker Glacier and numerous rock avalanches from Mt. Vampire on the Mueller Glacier. This study shows that the aseismic Aoraki/Mt. Cook rock avalanche of 1991 had a noticeable effect on glacier local mass balance from reduced surface ablation (Reznichenko et al., 2011, and Chapter 4), despite covering less than 4 % of the glacier area. The ice under the rock avalanche debris now sits proud of the glacier surface by > 25 metres. Furthermore, the rock-avalanche-covered ice is in a stream of very slow moving ice trapped upstream of more active ice from the Hochstetter icefall and has not been able to progress to the terminus region. Although there is no visible response at the terminus yet (which since 1993 has been actively calving into a proglacial lake), the contention of Schaefer et al. (2009, SOM) that the rock avalanche has had no effect on glacier mass balance appears incorrect. The critical point to emphasise is that the Aoraki/Mt. Cook rock avalanche is close to the minimum size for a true rock avalanche but even this small event has affected mass balance on part of the glacier. A larger rock avalanche, of which there is evidence for many in the Aoraki/Mt. Cook area, would have a larger impact on mass balance and if this debris was to be transported to the front of the glacier, it would contribute to terminal moraine formation. The situation for the Cameron Glacier moraines is analogous to the glaciers in the Aoraki/Mt. Cook area. The presence of rock avalanche agglomerates in a sampled moraine (sequence 9) shows the potential contribution of rock avalanche debris to the formation of the moraine. The estimated ages for the moraine are sparse and range from 800-200 yrs BP. Bearing in mind the recent high frequency of aseismic rock avalanches in the Southern Alps (Allen et al., 2011), the climatic significance of these moraines is questionable.

In conclusion, the validity of the palaeoclimate inferences from the dated moraines in areas like Aoraki/Mt. Cook or Cameron Valley is uncertain.

7.5.2. Palaeoclimate implications of identified rock avalanche sediment in moraines

Any rock avalanche large enough to cause a glacier to advance must contribute a significant proportion of the sediment to moraine that formed by that advance. The historical examples of such advances include the Sherman Glacier, whose mass balance was changed by the 1964 rock avalanche that is now contributing to glacier deposition (McSaveney, 1978), the Bualtar Glacier advance and deposition after a 1986 rock avalanche emplacement (Hewitt, 2009), the Brenva Glacier that advanced after a 1920 rock avalanche (Deline, 2009). The 1717 rock avalanche onto the Triolet Glacier caused glacier advance and re-deposition of the rock avalanche sediment (Deline, 2009), and the Waiho Loop moraine formation is attributed to the response of the Franz Josef Glacier to a rock avalanche (Tovar et al., 2008).

The presence of agglomerates in the fine fraction of moraines in tectonically active terrains is evidence that these moraines contain a significant proportion of rock avalanche debris, and are therefore likely to have been influenced by that debris. A moraine that has been affected by a rock avalanche will retain the rock avalanche-origin sediment. The presence of rock avalanche-sediment in a moraine indicates that the rock avalanche volume was significant (in the order of 10^6 m^3 or more) and the rock avalanche therefore may have had more than local effects on the glacier mass balance. It is not necessarily proof that a moraine was the result only of a rock-avalanche-driven advance, because a rock avalanche can fall onto a glacier that is already advancing due to climatic forcing. Also, a rock avalanche deposit may be too small to noticeably affect the mass balance of a very large glacier, but supraglacial rock avalanche sediment can contribute significantly to moraine formation and its further preservation. Therefore, any moraine with rock avalanche material present should be considered very carefully and independent evidence for their paleoclimatic significance is needed. The value of the new technique for identifying rock avalanche sediments (i.e. agglomerates) is clear.

Absence of rock avalanche sediment in a moraine indicates that there has been no rock avalanche contribution, or that the glacier recycled and dispersed or buried a small rock avalanche deposit during its transportation towards the terminus. As a result, it can be assumed that a moraine is not the result of a rock-avalanche-driven advance and so may be safely used to infer past climate.

The technique could be best applied to the Cameron Glacier moraine complex because of the greater number of suitable moraine exposures. From the eight moraines sampled, two

outcrops show the presence of the rock avalanche agglomerates (sequence 9). This demonstrates that the technique can be used to identify moraines that have a component of rock avalanche debris, and also help identify moraines that are suitable for making climate reconstructions. Application of the technique at the Waiho Loop has provided additional support for a rock avalanche-induced origin for the moraine. Abundant agglomerates of silt and clay-sized sediment amongst much coarser particles show that rock avalanche sediment is present. In the ongoing debate with respect to role of climatic forcing in the formation of the Waiho Loop and its regional and global correlation with other events (Applegate et al., 2008; Barrows et al., 2008; Putnam et al., 2010a; section 7.3.1), a rock avalanche event not only provides an appropriate mechanism for a non-climate-forced origin for the moraine, but also explains the documented chronological inconsistencies highlighted by this moraine and its relationship to other events (Denton and Hendy, 1994; Mabin, 1995; Shulmeister et al., 2009).

In a case where rock avalanche sediment is present in the moraines, other indicators, such as the correspondence of moraine ages with known earthquakes which are likely to cause rock avalanches, can be useful. From the test on moraines in the Aoraki/Mt. Cook area it is evident that rock avalanches have contributed to the formation of the Mueller Glacier moraines. Although the area is lacking reliable outcrops, sediment in two exposures of the moraines of the Mueller Glacier has the characteristic rock avalanche signature of agglomerates proposed by the new technique. Both exposures occur in moraines that were dated and used to infer paleoclimate events (Schaefer et al., 2009). These moraines (600 BP and 390 BP dated by Schaefer et al., 2009) correlate well with the AD 1420 and AD 1620 Alpine Fault earthquakes (Wardle, 1973; Fig. 7.13), which is consistent with the presence of rock avalanche debris. This finding alone refutes Schaefer et al.'s (2009) claim that there is no rock avalanche contribution to the moraines in the Aoraki/Mt. Cook area and makes the inferred climate linkage questionable.

The fact that in properly sampled moraines rock avalanche material is present or not indicates the reliability of the proposed technique for areas with possible rock avalanche contribution to the moraines. Thus, the climatic significance of these moraines can be resolved.

7.6. CONCLUSIONS

The research presented in this thesis clearly shows that, in some cases, the assumption of climatic forcing of moraine positions could be wrong. Glaciers advance and retreat in response to changes in mass balance. While climate is the primary cause of mass balance changes, in tectonically active high mountain areas debris cover on a glacier will also change the mass balance characteristics. While this thesis has not examined the actual process of terminal moraine formation in detail (a conceptual model was provided in Chapter 4 and Reznichenko et al., 2011), it has been demonstrated that rock avalanches can provide large volumes of concentrated debris to the terminal zone, which is likely to contribute to moraine formation. The presence of rock avalanche sediments does not preclude a climatic forcing but any moraine rich in rock avalanche debris poses a challenge for paleoclimate interpretation. Rock-avalanche forcing is the only possible non-climatic cause of glacier advance and moraine formation if other factors such as volcanic activity and tidewater calving are absent. If a moraine shows no presence of rock-avalanche sediment, it may be assumed that it is not the result of a rock-avalanche driven advance and thus may be safely used to infer past climate conditions.

New Zealand glaciers are the most intensively studied in the Southern Hemisphere; these studies provide valuable information for global climate modelling and reconstruction of past climate histories (Oerlemans, 2005; Schaefer et al., 2009). Initial analyses (this study) found rock avalanche sediment in some moraine deposits in the Aoraki/Mt. Cook area and in the Cameron valley and reinforced the significance of these processes in similar areas. Therefore, the new technique developed in the current study could be applied to clarify rock avalanche/non-rock avalanche effects in all regions where the glaciers could be affected by rock avalanches and palaeoclimate interpretation of moraines uncertain. Thus, the determination of moraine genesis with some degree of certainty can crucially contribute to the understanding of glacier dynamics in areas such as Alaska and other mountain ranges in the north-western North America, Patagonia, the European Alps, Himalaya.

8. Summary and future work

In this work the main hypothesis is that rock-avalanche-deposited supraglacial debris can disturb the glacier's regime and result in the formation of moraines, or the modification of moraines that might have formed for climatic reasons. This was tested by new approaches developed in this thesis, such as laboratory experiments and field research based on geophysical surveys. In the second part of the thesis, a new technique is developed that distinguishes rock avalanche sediment from glacial sediment at a microscale by using SEM. This is an important new tool to resolve the genesis of some moraines of questionable origin. The newly-discovered agglomerates are fine-sediment signatures characteristic of rapid high-stress comminution. The principal findings of this thesis and some directions for future work are summarized in this chapter.

8.1. SUMMARY OF CONCLUSIONS

8.1.1. Rock avalanche effect on glacier mass balance

The first part of the thesis is focuses on the understanding the effect of rock avalanche deposit material on glacier behaviour and sediment budget, which is covered in Chapters 4 and 5. In Chapter 4 the effect of debris on the melting rate of ice is investigated. The main findings are as follows:

Thick debris-cover from supraglacial rock avalanche *suppresses glacier surface ablation*:

- the diurnal radiation cycle controls the rate of melting beneath debris and the effect of debris cover is increased at high altitude and in lower latitudes;
- the relatively low permeability of rock avalanche sediment in comparison with non-rock avalanche supraglacial debris cover contributes to the suppression of ablation;
- rainfall accelerates ablation under thin non-rock avalanche supraglacial debris cover in a similar degree to that for debris-free ice, whereas rock avalanche sediment suppresses ablation due to rainfall.

These findings have been published as Reznichenko et al. (2010) (see Appendix A).

Having demonstrated that debris cover plays a major role in mass balance, I then investigated the effect of modern rock avalanches on active glaciers. This work was carried out at Aoraki/Mt. Cook National Park and is presented in Chapter 5. The main findings were:

Supraglacial rock avalanche *alters net glacier mass balance*:

- the thickness of the Aoraki/Mt. Cook rock avalanche reached 10 m and the Mt. Beatrice rock avalanche 7 m, causing the underlying ice to thicken by up to 25 and 40 m, respectively;
- in the two case studies, the rock avalanche deposits contribute to a lessening negative mass balance of the Tasman and Hooker Glaciers, but with no noticeable alteration of the glacial regimes;
- in both of the case studies the rock avalanche deposits contribute significantly to supraglacial debris, which is passively transported toward the terminus.

These findings have been published as Reznichenko et al. (2011) (see Appendix B).

These findings supported the hypothesis that glaciers respond to supraglacial rock avalanche through the formation of terminal moraines which do not reflect climate change. From these results and a review of reported supraglacial rock avalanches the minimum rock avalanche sizes required to change glacier mass balance was estimated. A conceptual model of *rock-avalanche-induced advance* of the glacier was proposed.

These findings have been partially published in Reznichenko et al. (2011) and partly in *Zeitschrift für Geomorphologie* (Reznichenko et al., accepted; see Appendix B and C).

8.1.2. Identification of rock avalanche sediment in glacial moraines: a proposed methodology based on microsedimentology and its implications

In the sedimentology section of this thesis a technique for differentiating rock avalanche sediment in moraines was been developed, which is based on genetic differences between rock avalanche and glacial sediment at the microscale. The technique and its development are described in Chapter 6, while in Chapter 7 it has been applied to some moraines in the Southern Alps of New Zealand.

The proposed technique allows *recognition of rock avalanche sediment* by:

- the presence of clay size particles and formation of agglomerates;
- identifying agglomerates through SEM examination of polished grains mounts;
- contrasting the rock-avalanche-derived fines with glacially-derived sediment.

The developed *technique*:

- has crucial importance in measurements and interpretations of PSD for all rock avalanche sediments in that it challenges the ability of standard particle size procedures to identify the true size range of rock avalanche deposits;
- enables differentiation of rock avalanche debris from differently-sourced materials in glacial terminal moraines.

Application of the methodology in the Southern Alps of New Zealand shows:

- that some Holocene moraines contain rock avalanche debris (moraines of the Mueller and Cameron Glaciers at Aoraki/Mt. Cook National Park, the Southern Alps),
- these moraines correlate well with regional seismicity,
- that in rock-avalanche-dominated settings like the Southern Alps, Himalaya, Alaska, Patagonia rock avalanche debris is a significant contributor to glacial moraines,
- that the biggest constraint on the use of the method is the lack of exposure.

Where the rock avalanche sediment exists *in a moraine* this indicates:

- that the moraine has been influenced to some degree by a non-climatic process and is unreliable as a paleoclimatic indicator;
- that potential contamination of palaeoclimatic data by non-climatically-related moraine dates can be reduced, through the use of this technique to screen out moraines with rock avalanche components

These findings are presented in a paper in press in Geology (Reznichenko et al., 2012*;* see Appendix D) and will be published in greater detail a paper that is in preparation for journal submission (provisionally for Quaternary Science Reviews).

8.2. FUTURE WORK

The impact of rock avalanches on glacial mass balance, sediment budget and final moraine deposition patterns requires further investigation in a number of areas. I highlight new directions for future work that stem from the results presented in this thesis.

1. Only in rare studies are the effects of rock avalanches on glaciers reported. This study concentrates on the effects of debris cover on glacier ablation, as a process that modifies glacial mass balance. The laboratory experiments developed in the current research could be adapted to investigate ablation under deposits of rock avalanche and non-rock avalanche origin and under a variety of conditions, such as different diurnal cyclicities and precipitations patterns. The data set from the surveys on two rock avalanches on New Zealand glaciers could be used in further monitoring of deposit evolution and final redeposition as moraine. Repeated geophysical surveys of Mt. Beatrice and Aoraki/Mt. Cook rock avalanche deposits can provide insight into supraglacial deposit evolution and contribution to moraine formation. The effect on glacial ice flow from the deposit and overthickened underlying ice requires a mix of field work and numerical studies to resolve.

2. Agglomerates discovered in rock avalanche sediment have implications for both understanding of rock avalanche size distributions and for identifying it in sediment deposits. Detailed investigation of the proportions of agglomerates and the PSDs of their constituent grains is important for quantifying the possible value of fracture surface energy and to resolve the problem associated with whether rock avalanche deposits have a fractal PSD. This in turn will contribute to understanding of the material fragmentation during a rock avalanche and its further preservation. Additionally, the investigation of how the agglomerates are stable during supraglacial travel of modern rock avalanche deposits on glaciers (e.g., Aoraki/Mt. Cook rock avalanche deposit) will indicate how rock avalanche sediments contribute to the glacial sediment budget and to the final deposition of those sediments in moraines.

3. The diagnostic microsedimentological technique should be applied worldwide to track rock avalanche contribution to moraines. It is particularly important to apply it in areas where global climate teleconnections are derived from moraine chronologies in high mountain regions susceptible to rock avalanches.

4. One sampling problem is the lack of clean outcrop in terminal moraines. Improving the sampling of these moraines can be achieved by coring to obtain sediment from a deeper within the moraine where weathering is less of an issue and a narrow gauge auger would allow the easy recovery of multiple samples so that moraines can be characterised.

5. The processes of moraine formation in response to enhanced debris supply from rock avalanches on glaciers are an unanswered question. Integrated studies of the sedimentology, microsedimentology and geomorphology of established moraines (the Waiho Loop, Westland) and potential rock-avalanche induced moraines (Aoraki/Mt. Cook and the Cameron Glacier moraines, the Southern Alps of New Zealand) can help resolve some of the issues. The monitoring of current supraglacial rock avalanche deposits (on the Sherman Glacier in particular) is likely to yield the easiest insights into the role of RA sediments in moraine formation.

In this thesis it has been shown that rock avalanches onto glaciers constitute a new field of research with wide potential for development. Further study of supraglacial rock avalanches and their effects on glacier mass balance will significantly contribute to understanding and correct reconstruction of the landscape in glaciated valleys.

References

Aa, A.R., Sjåstad, J., Sønstegaard, E. and Blikra L.H., 2007. Chronology of Holocene rock avalanche deposits based on Schmidt-hammer relative dating and dust stratigraphy in nearby bog deposits, Vora, inner Nordfjord, Norway. *The Holocene*, 17: 955-964.

Abbot, P.L., Kerr, D.R., Steven, E.B., Washburn, J.L. and Rightmer, D.A., 2002. Neogene sturzström deposits, Split Mountain area, Anza-Borrego Desert State Park, California. In: Evans, S.G., DeGraff, J.V. (Eds.), Catastrophic Landslides: Effects, Occurrence, and Mechanisms. *Geological Society of America Reviews in Engineering Geology*, 15: 379-400.

Abdrakhmatov, K. and Strom, A., 2002. Rockslides and rock avalanches of the central and northern Tien Shan. In Massive rock slope failure: new models for hazard assessment, abstracts volume, ed. by S.G. Evans & S. Martino. Celano (aq), Abruzzo Italy, 16-21, June, NATO advanced research workshop, p.1-6.

Ackert, R.P. Jr., 1998. A Rock Glacier/Debris-covered Glacier System at Galena Creek, Absaroka Mountains, Wyoming. *Geografiska Annaller*, 80A(3–4): 267-276.

Adhikary, S., Seko, K., Nakawo, M., Ageta, Y. and Miyazaki, N., 1997. Effect of surface dust on snow melt. *Bulletin of Glacier Research*, 15: 85-92.

Adhikary, S., Nakawo. M., Seko, K. and Shakya, S., 2000. Dust influence on the melting process of glacier ice: experimental results from Lirung glacier, Nepal Himalayas. Debris-Covered glaciers. Proceedings of a workshop held at Seattle, Washington, USA, sep 2000. IAHS Publ.no.264, p.43-52.

Agassiz, L., 1840. Etudes sur les Glaciers. (Studies on glaciers). Preceded by the Discourse of Neuchatel, translated and ed. by A. V. Carozzi, 1967. Hefner Publishing Company.

Alean, J., 1984. Ice avalanches and a landslide on Grosser Aletschgletcher. *Zeitschrift fur Gletscgerkunde and Glazialgeologie*, 20: 9-25.

Alexander, D.J., Shulmeister, J. and Davies, T.R.H., 2011. A steady-state mass-balance model for the Franz Josef glacier, New Zealand: testing and application. *Geografiska Annaller*, 93: 41-54.

Allen, S.K., Schneider, D. and Owens, I.F., 2009. First approaches towards modelling glacial hazards in the Mount Cook region of New Zealand's Southern Alps. *Natural Hazards and Earth System Sciences*, 9: 481-499.

Allen, S.K., Cox, S.C. and Owens, I.F., 2011. Rock avalanches and other landslides in the central Southern Alps of New Zealand: a regional study considering possible climate change impacts. *Landslides*, 8 (1): 33-48.

Alley, R.B., Cuffey, K.M., Evenson, E.B., Strasser, J.C., Lawson, D.E. and Larson, G.J., 1997. How glaciers entrain and transport basal sediment: physical constraints. *Quaternary Science Reviews*, 16: l017-1038.

Anderson, R.S., 2000. A model of ablation-dominated medial moraines and the generation of debris-mantled glacier snouts. *Journal of Glaciology*, 46 (154): 459-469.

Anderson, B. and Mackintosh, A., 2006. Temperature is the major driver of lateglacial and Holocene glacier fluctuations in New Zealand. *Geology*, 34 (2): 121-124.

Anderton, P.W., 1975. The Tasman Glacier, 1971-73. Hydrological Research: Annual Report n.33. Ministry of works and development, national water and soil conservation organisation, Wellington.

Andreassen, L. M., Elvehøy, H., Kjøllmoen, B., Engeset, R.V. and Haakensen, N., 2005. Glacier mass-balance and length variation in Norway. *Annals of Glaciology*, 42 (1): 317-325.

Andrews, J.T., 1975. Glacier Systems: An Approach to Glaciers and their Environments. Duxbury Press, North Csituate, Mass, 191 pp.

Angeli, M.G., Gasparetto, P. Menotti, R.M., Pasuto, A., Silvano, S. and Soldati, M., 1996. Rock avalanche. In: Dikau, R., Brunsden, D., Schrott, L., Ibsen, M.-L. (eds.), Landslide Recognition: Identification, Movement and Causes. J. Wiley and Sons, Chichester, p.190-201.

Applegate, P.J., Lowell, T.V. and Alley, R.B., 2008. Comment on "Absence of cooling in New Zealand and the adjacent ocean during the Younger Dryas chronozone". *Science*, 320: 746.

Augustinus, P.C., 1995. Glacial valley cross-profile development: the influence of in situ rock stress and rock mass strength, with examples from the Southern Alps, New Zealand. *Geomorphology*, 14: 87-97.

Ballantyne, C., 2002. Paraglacial geomorphology. *Quaternary Science Reviews*, 21: 1935-2017.

Barla, G. and Barla, M., 2001. Investigation and modelling of the Brenva glacier rock avalanche on the Mount Blanc Range. Proceedings of the ISRM Regional Syposium Eurock 2001, Espoo, Finland, 3-7 June 2001.

Barla, G., Dutto, F. and Mortara, G., 2000. Brenva glacier rock avalanche of 18 January 1997 on the Mount Blanc Range. *Landslide News*, 13: 2-5.

Barrows, T.T., Lehman, S.J., Fifield, L.K. and De Deckker, P., 2008. Absence of cooling in New Zealand and the adjacent ocean during the Younger Dryas chronozone. *Science*, 318: 86-89.

Barry, R.G., 2008. Mountain weather and climate. 3rd ed. Cambridge: Cambridge University Press, 506 pp.

Beck, A.C., 1972. Post-Otiran moraines in Canterbury: further comment. *New Zealand Journal of Geology and Geophysics*, 15: 299.

Benn, D. I. and Evans, D. J. A., 2010. Glaciers and Glaciation. Arnold, London. 734 pp.

Benn, D.I. and Gemmell, A.M.D., 2002. Fractal dimensions of diamictic particle-size distributions: Simulations and evaluation. *Geological Society of America Bulletin*, 114: 528-532.

Benn, D.I., Kirkbride, M.P., Owen, L.A. and Brazier, V., 2003. Glaciated valley landsystems. In: Evans D.J.A. (ed.), Glacial Landsystems. Arnold, London, p.372-406.

Bischoff, J.L. and Cummins, K., 2001. Wisconsin glaciation of the Sierra Nevada (79,000-15,000 yr B.P.), as recorded by rock flour in sedimentary of Owens Lake, California. *Quaternary Research*, (55): 14-24.

Black, J.L., 2001. Can a Little ice Age climate signal be detected in the Southern Alps of New Zealand? M.S. thesis, The University of Maine, USA.

Blikra, L.H. and Anda, E., 1997. Large rock avalanches in Møre og Romsdal, western Norway. *Norges Geologiske Undersøkelse Bulletin*, 433: 44-45.

Blikra, L. H. and Nemec, W., 1998. Postglacial colluvium in western Norway: depositional processes, facies and palaeoclimatic record. *Sedimentology*, 45: 909-959.

Blikra, L.H., Longva, O., Braathen, A., Anda, E., Dehl, J.F. and Stalsberg, K., 2006. Rock slope failures in Norwegian fjord areas: examples, spatial distribution and temporal patterns. In: Evans, S.G., Scarascia Mugnozza, G., Strom, A.L., Hermanns, R.L. (Eds.), Landslides from Massive Rock Slope Failure. Proc. NATO Advanced Workshop, Celano, Italy, June 2002. Springer-Verlag, Dordrecht, p.475-496.

Bottino, G., Chiarle, M., Joly, A. and Mortara, G., 2002. Modelling Rock Avalanches and Their Relation to Permafrost Degradation in Glacial Environments. *Permafrost Periglacial Processes*, 13: 283-288.

Boulton, G.S., 1974. Processes and patterns of glacial erosion. In Glacial Geomorphology: a proceeding volume. (ed. Coats, D.R.), Binghamton: State University of New York, p.41-87.

Boulton, G.S., 1978. Boulder shapes and grain-size distributions of debris as indicators of transport paths through a glacier and till genesis. *Sedimentology*, 25: 773-799.

Boulton, G.S., Smith, G.D., Jones, A.S. and Newsome, J. 1985. Glacial geology and glaciology of the last mid-latitude ice sheets. *Journal of the Geological Society of London*, 142: 447-474.

Boulton, G.S. and Eyles, N., 1979. Sedimentation by valley glaciers; a model and genetic classification. In Schuchter, C. (ed.), Moraines and varves, Balkema, Rotterdam, p.11-23.

Bozhinskiy, A.N., Drass, M.S. and Popovin, V.V., 1986. Role of debris cover in the thermal physics of glaciers. *Journal of Glaciology*, 32(111): 255-266.

Braathen, A., Blikra, L. H., Berg, S. S. and Karlsen, F., 2004. Rock- slope failures in Norway: type, geometry, deformation mechanisms and stability. *Norwegian Journal of Geology*, 84: 67-88.

Broadbent, M., 1974. Seismic and gravity surveys on the Tasman Glacier 1971-72, DSIR Geophysics Division. No. 91, Wellington.

Brugman, M.M. and Meier, M. F., 1981. Response of glaciers to eruptions of Mount St. Helens. *United States Geological Survey professional paper* 1250, p.743-756.

Budd, W.F. and Allison, I.F., 1975. An empirical scheme for estimating the dynamics of unmeasured glaciers. *IAHS-AISH Publ.* 104, (Proceedings of the symposium at Moscow 1975 - *Snow and Ice Symposium*, 1975), p.246-256.

Bull, C., 1969. The 1978–1980 surge of the Sherman Glacier, south-central Alaska. *Canadian Journal of Earth Sciences*, 6(4): 841-843.

Bull, W.B., 1996. Prehistorical earthquakes on the Alpine Fault, New Zealand. *Journal of Geophysical Research*, 101/ B3: 6037-6050.

Bull, C. and Marangunic, C., 1968. Glaciological effects of debris slide on Sherman Glacier. In: the great Alaska earthquake of 1964: Hydrology, Pt. A, Nat. Acad. Sci. Pub. 1603, p.309-317.

Burki, V., Larsen, E., Fredin, O. and Margreth, A., 2009a. The formation of sawtooth moraine ridges in Bødalen, western Norway. *Geomorphology*, 105: 182-192.

Burki, V., Larsen, E., Fredin, O. and Nesje, A., 2009b. Western Norway Glacial remobilization cycles as revealed by lateral moraine sediment, Bødalsbreen glacier foreland. *The Holocene*, 19(3): 415-426.

Burrows, C.J., 1972. Post-Otiran moraines in Canterbury. *New Zealand Journal of Geology and Geophysics*, 15: 296-299.

Burrows, C.J., 1973. Studies on some glacial moraines in New Zealand—2. Ages of moraines of the Mueller, Hooker and Tasman Glaciers. *New Zealand Journal of Geology and Geophysics*, 16: 831-855.

Burrows, C.J., 1975. Late Pleistocene and Holocene Moraines of the Cameron Valley, Arrowsmith Range, Canterbury, New Zealand. *Arctic and Alpine Research*, 7/2: 125-140.

Burrows, C.J., 2005. Julius Haast in the Southern Alps, Canterbury University Press, Christchurch, 215 pp.

Burrows, C.J., Duncan, K.W. and Spence, J. R., 1990. Aranuian vegetation history of the Arrowsmith Range, Canterbury II. Revised chronology for moraines of the Cameron Glacier. *New Zealand Journal of Botany*, 28: 455-466.

Carrara, P.E., 1975. The ice-cored moraines of Akudnirmuit Glacier, Cumberland Peninsula, Baffin Island, N.W.T., Canada. *Arctic and Alpine Research*, 7: 61-67.

Carrivick, J.L., and Rushmer, E.L., 2009. Inter- and Intra-catchment variability in proglacial geomorphology: An example from Franz Josef Glacier and Fox Glacier, South Westland, New Zealand. *Arctic, Antarctic and Alpine Research*, 41/1: 18-36.

Carter, L., Manighetti, B. and Neil, H., 2003. From icebergs to pongas: Antarctica's ocean link with New Zealand. *Water and Atmosphere online*, 11 (3): 30-31.

Chevalier, G., Davies T.R.H. and McSaveney, M.J., 2009. The prehistoric Mt. Wilberg rock avalanche, Westland, New Zealand. *Landslides*, 6: 253–262.

Chinn, T.J., 1975. Late Quaternary snowlines and cirque moraines within the Waimakariri watershed. Master`s thesis, University of Canterbury, Christchurch, New Zealand, 213 pp.

Chinn, T.J., 1979. Moraine forms and their recognition on steep mountain slopes. In: Schluchter, C. ed. Moraines and varves. Rotterdam, A. A. Balkema, p. 51-57.

Chinn, T.J., 1996. New Zealand glacier responses to climate change of the past century. *New Zealand Journal of Geology and Geophysics*, 39: 415-428.

Chinn, T.J., 1999. New Zealand glacier response to climate change of the past 2 decades. *Global and Planetary Change*, 22: 155–168.

Chinn, T. J., 2001. Distribution of the glacial water resources of New Zealand. *New Zealand Journal of Hydrology*, 40: 139-187.

Chinn, T.J.H., Winkler, S., Salinger, M.J. and Haakensen, N., 2005. Recent glacier advances in Norway and New Zealand — a comparison for their glaciological and meteorological causes. *Geografiska Annaler*, 87A, 141–157.

Clark, D.H., Clark, M.M. and Gillespie, A.R., 1994. Debris-Covered Glaciers in the Sierra Nevada, California, and their implication for snowline reconstruction. *Quaternary Research*, 41: 139-153.

Conway, H. and Rasmussen, L.A., 2000. Summer temperature profiles within supraglacial debris on Khumbu Glacier, Nepal. IAHS Publ. 264 (Symposium at Seattle 2000 – Debris-Covered Glaciers), p.89-97.

Cox, S.C., Ferris, B.G. and Allen, S., 2008. Vampire rock avalanches, Aoraki/Mount Cook National Park, New Zealand. GNS Science Report 2008/10, 34 pp.

Cox, S.C. and Allen, S.K., 2009. Vampire rock avalanche of January 2008 and 2003, Southern Alps, New Zealand. *Landslides*, 6: 161-166.

Cox, S.C. and Barrell, D.J.A. (compilers), 2007. Geology of the Aoraki area. Institute of Geological & Nuclear Sciences 1:250 000 geological map 15. 1 sheet + 71 p. Lower Hutt, New Zealand. GNS Science.

Crandell, D.R. and Fahnestock, R.K., 1965. Rockfalls and Avalanches from Little Tahoma Peak on Mount Rainier, Washington. *United States Geological Survey Bulletin* 1221-A, 30 pp.

Crosta, G. B., Frattini, P. and Fusion, N., 2007. Fragmentation in the Val Pola rock avalanche, Italian Alps. *Journal of Geophysical Research*, 112, F01006, doi:10.1029/2005JF000455.

Crozier, M.J., Deimel, M.S. and Simon, J.S., 1995. Investigation of earthquake triggering for deep-seated landslides, Taranaki, New Zealand. *Quaternary International*, 25: 65–73.

Cruden, D.M. and Hu, X.Q., 1993. Exhaustion and steady-state models for predicting landslide hazards in the Canadian Rocky Mountains. *Geomorphology*, 8: 279-285.

Cruden, D.M. and Hungr, O., 1986. The debris of the Frank Slide and theories of rockslide-avalanche mobility. *Canadian Journal of Earth Sciences*, 23(3): 425-432.

Dahl, S. O., Nesje, A., Lie, Ø., Fosheim, K. and Matthews, J. A., 2002. Timing, equilibrium-line altitudes and climatic implications of two early-Holocene glacial re-advances during the Erdalen Event at Jostedalsbreen, western Norway. *The Holocene*, 12: 17–25.

Davies, T. R. and McSaveney, M.J., 1999. Runout of dry granular avalanches. *Canadian Geotechnical Journal*, 36: 313-320.

Davies, T.R. and McSaveney, M.J., 2002. Dynamic simulation of the motion of fragmenting rock avalanches. *Canadian Geotechnical Journal*, 39: 789–798.

Davies, T. R. and McSaveney, M.J., 2009. The role of rock fragmentation in the motion of large landslides. *Engineering Geology*, 109: 67-79.

Davies, T.R. and Smart, C., 2007. Obstruction of subglacial conduits by bedload sediment – implications for alpine glacier motion Journal of Hydrology, 46(2): 51-62.

Davies, T.R. and Smart, C., 2009. Glacial debuttressing. Programme with Abstracts — International Geomorphology Conference, 7, Abstract no. 351.

Davies, T.R., McSaveney, M.J., and Hodgson, K.A., 1999. A fragmentation-spreading model for long-runout rock avalanches. *Canadian Journal of Geotechnics*, 36: 1096-1110.

Davies, T.H.R., Smart, C.C. and Turnbull, J.M., 2003. Water and sediment outbursts from advanced Franz Josef Glacier, New Zealand. *Earth Surface Processes and Landforms,* 28: 1081–1096.

Decaulne, A., Sæmundsson, Þ., Pétursson, H.G, Jónsson, H.P. and Sigurðsson I.A., 2010. A large rock avalanche onto Morsarjökull Glacier, South-East Iceland. Its implications, or Ice-surface evolution and glacier dynamic. In "Iceland in the Central Northern Atlantic: hotspot, sea currents and climate change, Plouzané: France (2010)". Poster, hal-00482107.

Deline, P., 2005. Large rock avalanches on glaciers since 2500 BP on the Italian flank of the Mont Blanc massif. European Geosciences Union, General Assembly 2005 Vienna, Austria, 24–29 April 2005, Abstract # EGU05-A-03434.

Deline, P., 2009. Interactions between rock avalanches and glaciers in the Mont Blanc massif during the late Holocene. *Quaternary Science Reviews*, 28: 1070–1083

Deline, P., 2011. Influences of rock avalanches on glacier behaviour and moraine formation in the Western European Alps. Geophys. Res. Abstr. 13: EGU2011-9961.

Deline, P. and Kirkbride, M.P., 2009. Rock avalanches on a glacier and morainic complex in Haut Val Ferret (Mont Blanc Massif, Italy). *Geomorphology*, 103: 80–92.

Demchenko, V.V. and Sokolov, L.N., 1982. Povyshennaya ablyatsya l`da pod sloem moreny v usloviyakh Vostochnogo Pamira. (Increased ice ablation under a moraine laer in the conditions of the eastern Pamirs). *Materialy Glyasiologicheskikh Issedovaniy (Data of Glaciological Studies). Khronika. Obsuzhdeniya*, 45: 119-121. [in Russian]

Denton, G. H. and Hendy, C. H., 1994. Younger Dryas age advance of Franz Josef Glacier in the Southern Alps of New Zealand. *Science*, 264: 1434-1437.

Denton, G.H., Putnam, A.E., Schaefer, J.M., Barrell, D.J.A., Andersen, B.G., Schwartz, R., Finkel, R.C., Chinn, T.J.H. and Doughty, A.M., 2009. Holocene 10Be surface-exposure chronology of moraines deposited by the Cameron Glacier, Arrowsmith Range, Southern Alps, New Zealand. In. Cortese, G., Vandergoes, M., Bostock, H., 2009. Past Climates Meeting, 2009, Te Papa, Wellington, New Zealand, 15-17 May, 2009. *GNS Science Miscellaneous Series*, 23, p.13.

Dolgushin, L.D., Lebedeva, I.M., Osipova, G.B. and Rototaeva, O.V., 1972. Bliyanie eolovoi sapyilennosti lednikov i poverxnostnow moreni na tayanie lednikov Srednei Asii (The influence of natural dusting and moraines on malting of glaciers in Soviet Central Asia), *Materialy Glyasiologicheskikh Issedovaniy (Data of Glaciological Studies). Khronika. Obsuzhdeniya*, 20: 108-115. [in Russian]

Donner, J.J., 1995. The Quaternary history of Scandinavia. Cambridge, New York: Cambridge University Press, 200 pp.

Dreimanis, A., 1990. Formation, deposition and identification of subglacial and supraglacial tills. In Glacial indicator tracing, Kujansuu R. and Saarnisto M. (ed.), Rotterdam: A.A. Balkema, 252 pp.

Drewry, D., 1986. Glacial geologic processes. London: Edward Arnold, 276 pp.

Driedger, C. L., 1981. Effect of ash thickness on snow ablation. *United States Geological Survey professional paper* 1250, p.757-760.

Driedger, C.L., 1986. A visitor guide to mount Rainer glaciers. Pacific Northwest parks and forests association, Longmire, Washington, USA.

Driscoll, F.G., 1980. Wastage of Klutlan ice-cored moraines, Yukon Territory, Canada. *Quaternary Research*, 14: 19-30.

Dufresne, A. and Davies, T.R., 2009. Longitudinal ridges in mass movement deposits. *Geomorphology*, 105: 171-181.

Dunning, S.A., 2004. Rock avalanches in high mountains. Ph.D. thesis, Luton University, UK.

Dunning, S.A., 2006. The grain-size distribution of rock-avalanche deposits in valley confined settings. *The Italian Journal of Engineering Geology and Environment*, 1: 117-121.

Dykes, R.C., Brook, M.S. and Lube, G., 2011. Buoyancy induced calving at Tasman Glacier, New Zealand. Schedule and Abstracts. Snow and Ice Research Group (SIRG) (NZ) Annual Workshop, Fox Glacier Township, 9th-11th February, p.9.

Dyurgerov, M., 2003. Mountain and subpolar glaciers show an increase in sensitivity to climate warming and intensification of the water cycle. *Journal of Hydrology*, 282(1-4): 164-176.

Dyurgerov, M. B. and Meier, M., 1997. Mass balance of mountain and subpolar glaciers: A new global assessment for 1961–1990. *Arctic and Alpine Research*, 29(4): 379-391.

Eisbacher, G.H., and Clague J.J., 1984. Destructive mass movements in high mountains: hazard and management. *Geological Survey of Canada, Paper* 84-16, 230 pp.

Ensminger, S.L., Alley, R.B., Evenson, E.B., Lawson, D.E. and Larson, G.J., 2001. Basal-crevasse-fill origin of laminated debris bands at Matanuska Glacier, Alaska. *USA Journal of Glaciology*, 47 (158): 412-422.

Evans, D. J. A., 2008. Avalanches and moraines. *Nature Geoscience*, 1: 493–494.

Evans, D.J.A., and Benn, D.I. (eds), 2004. A practical guide to the study of glacial sediments. Arnold, London, 266 pp.

Evans, D.J.A., Shulmeister, J. and Hyatt, O., 2010. Sedimentology of latero-frontal moraines and fans on the west coast of South Island, New Zealand. *Quaternary Science Reviews*, 29: 3790-3811. doi:10.1016/j.quascirev.2010.08.019

Evans, S.G., 1989. Rock avalanche run-up record. *Nature*, 340, 271 pp.

Evans, S.G., 2002. Climate change and geomorphological hazards in the Canadian cordillera; the anatomy of impacts and some tools for adaptation. Scientific Report 1999-2001 – Summary of Activities and Results. Climate Change Action Fund Project A099. p.14.

Evans, S.G., 2006. Single-event landslides resulting from massive rock slope failure: characterizing their frequency and impact on society. In Landslides from massive rock slope failure. Edited by S.G. Evans, G. Scarascia-Mugnozza, A.L. Strom and R. L. Hermanns, Springer, Dordrecht, p.53-73.

Evans, S.G. and Clague, J.J., 1988. Catastrophic rock avalanches in glacial environments. In: Bonnard, C. (Ed.), Proceedings, 5th International Symposium on Landslides, Lausanne, Switzerland, vol. 2, p.1153-1158.

Evans, S.G., and Clague, J.J., 1994. Recent climatic change and catastrophic geomorphic processes in mountain environments. *Geomorphology*, 10 (1-4): 107-128.

Evans, S.G. and Clague, J.J., 1998. Rock avalanche from Mount Munday, Waddington Range, British Columbia, Canada. *Landslide News*, 11: 23-25.

Evans, D.J.A. and Hiemstra, J.F., 2005. Till deposition by glacier submarginal, incremental thickening. *Earth Surface Processes and Landforms*, 30(13): 1633-1662.

Evans, S.G., Clague, J.J., Woodsworth, G.J. and Hungr, O., 1989. The Pandemonium Creek rock avalanche, British Columbia. *Canadian Geotechnical Journal*, 26: 427-446.

Evenson, E.B., Burkhart, P.A., Gosse, G.C., Baker, G.S., Jackofsky, D., Meglioli, A., Dalziel, I., Kraus, S., Alley, R.B. and Berti, C., 2009. Enigmatic boulder trains, supraglacial rock avalanches, and the origin of "Darwin's boulders," Tierra del Fuego. *GSA Today*, 19 (12): 4-10.

Eyles, N., 2006. The role of meltwater in glacial processes. *Sedimentary Geology*, 190: 257-268.

Eyles, N. and Menzies, J., 1983. The subglacial landsystem. In Glacial Geology: An introduction for engineers and earth scientists. (Eyles, N., ed,). Pergamon Press Ltd, Wiltshire, Great Britain, p.19-70.

Fickert, T., Friend, D., Grüninger, F., Molnia, B. and Richter, M., 2007. Did Debris-Covered Glaciers Serve as Pleistocene Refugia for Plants? A New Hypothesis Derived from Observations of Recent Plant Growth on Glacier Surfaces. *Arctic, Antarctic, and Alpine Research*, 39 (2): 245-257.

Field, W.O., 1968. The effect of previous earthquakes on glaciers: in the great Alaska earthquake of 1964: Hydrology, Pt. A, Nat. Acad. Sci. Pub. 1603, p.252-265.

Fischer, U. H. and Hubbard, B., 1999. Subglacial sediment textures: Character and evolution at Haut Glacier d'Arolla, Switzerland. *Annals of Glaciology*, 28: 241-246.

Fitzsimons, S.J., 1997. Late-glacial and early Holocene glacier activity in the Southern Alps, New Zealand. *Quaternary International*, 38/39: 69-76.

Fitzsimons, S.J. and Veit, H., 2001. Geology and geomorphology of the European Alps and the Southern Alp of New Zealand: a comparison. *Mountain Research and Development*, 21/4: 340-349.

Fort, M., Cossart, E., Delin, P., Dzikowski, M., Nicoud, G., Ravanel, L., Schoeneich, P. and Wassmer, P., 2009. Geomorphic impact of large and rapid mass movements: a review. *Geomorphology: relief, processes, environment*, 1: 47-64.

Fujita, K. and Sakai, A., 2000. Air temperature environment on the debris-covered area of Lirung Glacier, Langtang Valley, Nepal Himalayas. *IAHS Publ.* 264 (Symposium at Kathmandu, Nepal 1992 – *Snow and Glacier Hydrology*), p.83-88.

Gardner, J.S. and Hewitt, K., 1990. A surge of Bualtar Glacier, Karakoram range, Pakistan: a possible landslide trigger. *Journal of Glaciology*, 36(123): 159-162.

Geertsema, M., Clague, J.J., Schwab, J.W. and Evans, S.G., 2006. An overview of recent large catastrophic landslides in northern British Columbia, Canada. *Engineering Geology*, 83, 120-143.

Gellatly, A.F., 1984. The use of rock weathering-rind thickness to redate moraines in Mount Cook National Park, New Zealand. *Arctic and Alpine Research*, 16: 225-232.

Gerrard, J., 1994. The landslide hazard in the Himalayas: geological control and human action. *Geomorphology*, 10: 221-230.

Glazyrin, G.E., 1975. The formation of ablation moraines as a function of the climatological environment. Snow and Ice-Symposium-Neiges et Glaces (Proceedings of the Moscow Symposium, August 1971; Actes du Colloque de Moscou, août 1971): IAHS-AISH Publ. No. 104: 106-110.

Glen, J.W., 1952. Experiments on the deformation of ice. *Journal of Glaciology*, 2 (12): 111-114.

Goodsell, B., Anderson, B., Lawson, W.J. and Owens, I.F., 2005. Outburst flooding at the Franz Josef Glacier, South Westland, New Zealand. *New Zealand Journal of Geology and Geophysics,* 48: 95-104.

Gordon, J.E., Birne, R.V. and Timmis, R., 1978. A major rockfall and debris slide on the Lyell Glacier, South Georgia. *Arctic and Alpine research*, 10(1): 49-60.

Gordon, J.E., Haynes, V.M., Hubbard, A. 2008. Recent glacier changes and climate trends on South Georgia. *Global and Planetary Change*, 60 (1-2): 72-84.

Grant-Taylor, T.L. and Rafter, T.A., 1971. New Zealand radiocarbon age measurements – 6. *New Zealand Journal of Geology and Geophysics*, 14: 364-402.

Griffiths, G.A. and McSaveney, M.J., 1983. Distribution of mean annual precipitation across some steepland regions of New Zealand. *New Zealand Journal of Science*, 26: 197-209.

Haeberli, W., Wegmann, M. and Vonder Mühll, D., 1997. Slope stability problems related to glacier shrinkage and permafrost degradation in the Alps. *Eclogae Geologicae Helvetiae*, 90: 407-414.

Hagg, W., Mayer, C., Lambrecht, A. and Helm, A., 2008. Sub-debris melt rates on southern Inylchek Glacier, central Tian Shan. *Geografiska Annaler*, 90A (1): 55-63.

Haidong, H., Yongjing, D. and Shiyin, L., 2006. A simple model to estimate ice ablation under a thick debris layer. *Journal of Glaciology*, 52(179): 528-536.

Haines-Young, R.H. and Petch, J.R., 1983. Multiple working hypotheses: Equifinality and the study of landforms. *Transactions of the Institute of British Geographers*, 8: 458-466.

Haldorsen, S., 1978. Glacial comminution of mineral grains. *Norsk Geologisk Tidsskrift*, 58: 241-243.

Haldorsen, S., 1981. Grain-size distribution of subglacial till and its relation to glacial crushing and abrasion. *Boreas*, 10: 91-105.

Hallet, B., 1979. A theoretical model of glacial abrasion. *Journal of Glaciology*, 23: 39-50.

Hallet, B., 1981. Glacial abrasion and sliding: their dependence on the debris concentration in basal ice. *Annals of Glaciology*, 2: 23-28.

Hallet, B., Hunter, L. and Bogen, J., 1996. Rates of erosion and sediment evacuation by glaciers: A review of field data and their implications. *Global and Planetary Change*, 12: 213-235.

Hambrey, M.J, and Ehrmann, W., 2004. Modification of sediment characteristics during glacial transport in high-alpine catchments: Mount Cook area, New Zealand. *Boreas*, 33: 300-318.

Hambrey, M.J., Quincey, D.J., Glasser, N.F., Reynolds, J.M., Richardson, S.J., and Clemmens, S., 2008. Sedimentological, geomorphological and dynamic context of debris-mantled glaciers, Mount Everest (Sagarmatha) region, Nepal. *Quaternary Science Reviews*, 27: 2361-2389.

Harris, C., 2005. Climate change, mountain permafrost degradation and geotechnical hazard. In: Huber UM, Bugmann HKM, Reasoner MA (eds) Global change and mountain regions. An overview of current knowledge. Springer, Dordrecht, p.215-224.

Hazlett, R.W., Buesch, D., Anderson, J.L., Elan, R. and Scandone, R., 1991. Geology, failure, and implications of seismogenic avalanches of the 1944 eruption at Vesuvius, Italy. *Journal of Volcanology and Geothermal Research*, 47(3-4): 249-264.

Heim, A., 1932. Landslides and human lives. Translated by Skermer, N. (1989), Bi Tech Publishing Ltd, Vancouver.

Hewitt, K., 1988. Catastrophic Landslide Deposits in the Karakoram Himalaya. *Science*, 242 (4875): 64-67.

Hewitt, K., 1998. Catastrophic landslides and the Upper Indus streams, Karakoram Himalaya, northern Pakistan. *Geomorphology*, 26: 47-80.

Hewitt, K., 1999. Quaternary moraines vs. catastrophic rock avalanches in the Karakoram Himalaya, Northern Pakistan. *Quaternary Research*, 51: 220-237.

Hewitt, K., 2001. Catastrophic rockslides and the geomorphology of the Hunza and Gilgit River valleys, Karakoram Himalaya. *Erdkunde*, 55: 72-93.

Hewitt, K., 2002. Styles of rock avalanche depositional complex in very rugged terrain, Karakoram Himalaya, Pakistan. In: Evans, S.G., DeGraff, J.V. (Eds.), Catastrophic Landslides: Effects, Occurrence, and Mechanisms. *Geological Society of America Reviews in Engineering Geology*, 15: 345-378.

Hewitt, K., 2006. Disturbance regime landscapes: mountain drainage systems interrupted by large rockslides. *Progress in Physical Geography*, 30: 365-393.

Hewitt, K., 2009. Rock avalanches that travel onto glaciers and related developments, Karakoram Himalaya, Inner Asia. *Geomorphology*, 103: 66-79.

Hewitt, K., Clague, J.J. and Orwin, J.F., 2008. Legacies of catastrophic rock slope failures in mountain landscapes. *Earth-Science Reviews*, 87: 1-38.

Hochstein, M.P., Claridge, D., Henrys, S.A., Pyne, A., Nobes, D.C. and Leary, S.F., 1995. Downwasting of the Tasman Glacier, South Island, New Zealand: changes in the terminus region between 1971 and 1993. *New Zealand Journal of Geology and Geophysics*, 38: 1-16.

Holm, K., Bovis, M.J. and Jakob, M., 2004. The landslide response of alpine basins to post-Little Ice Age glacial thinning and retreat in southwestern British Columbia. *Geomorphology*, 57: 201-216.

Hooke, R.L. and Iverson, N.R., 1995. Grain-size distribution in deforming subglacial tills: role of grain fracture. *Geology*, 23(1): 57-60.

Hovius, N., Stark, C.P. and Allen, P.A., 1997. Sediment flux from a mountain belt derived by landslide mapping. *Geology*, 25: 231-234.

Hsü, K.J., 1978. Albert Heim: observations on landslides and relevance to modern interpretations. In ed. Voght, Rockslides and avalanches, vol.1, Amsterdam: Elsevier, p.

Hungr, O., Evans, S.G., Bovis, M., and Hutchinson, J.N., 2001. Review of the classification of landslides of the flow type. *Environmental and Engineering Geoscience*, 7: 221-238.

Iturrizaga, L., 2001. Lateroglacial valleys and landforms in the Karakorum Mountains (Pakistan). *GeoJournal*, 54: 397-428.

Ivy-Ochs, S., Poschinger, A.V., Synal, H.A. and Maisch, M., 2009. Surface exposure dating of the Flims landslide, Graubünden, Switzerland. *Geomorphology*, 103(1): 104-112.

Ivy-Ochs, S., Schlüchter, C., Kubik, P. and Denton, G.H., 1999. Moraine exposure dates imply synchronous Younger Dryas glacier advances in the European Alps and in the Southern Alps of New Zealand. *Geografiska Annaler*, 81A: 313-323.

Jansson, P. and Fredin, O., 2002. Ice sheet growth under dirty conditions: implications of debris cover for early glaciation advances. *Quaternary International*, 95/96: 35-42.

Jansson, P., Rosqvist, G. and Schneider, T., 2005. Glacier fluctuations, suspended sediment flux and glacio-lacustrine sediments. *Geografiska Annaler*, 87A (1): 37-50.

Jibson, R.W., 1996. Use of landslides for palaeoseismic analysis. *Engineering Geology*, 43: 291-323.

Jibson, R.W., Harp, E., Schulz, W. and Keefer, D.K., 2004. Landslides Triggered by the 2002 Denali Fault, Alaska, Earthquake and the Inferred Nature of the Strong Shaking. *Earthquake Spectra*, 20 (3): 669-691.

Jibson, R.W., Harp, E.L., Schulz, W. and Keefer, D.K. 2006. Large rock avalanches triggered by the M 7.9 Denali Fault, Alaska, earthquake of 3 November 2002. *Engineering Geology*, 83: 144-160.

Jiskoot, H., 2011. Long-runout rockslide on glacier at Tsar Mountain, Canadian Rocky Mountains: potential triggers, seismic and glaciological implications. *Earth Surface Processes and Landforms*, 36: 203-216.

Johnson, N.M. and Ragle, R.H., 1968. Analysis of flow characteristics of Allen II slide from aerial photographs: in the great Alaska earthquake of 1964: Hydrology, Pt. A, Nat. Acad. Sci. Pub. 1603, p.369-373.

Kalm, V., 2010. Ice-flow pattern and extent of the last Scandinavian Ice Sheet southeast of the Baltic Sea. *Quaternary Science Reviews*, in press. doi:10.1016/j.quascirev.2010.01.019

Kamp, P.J.J., 1992. Tectonic architecture of New Zealand. In: Soons, J.M. and Selby. M.J. (Eds.) Landforms of New Zealand: second edition, Longman Paul, Auckland, p.1-31.

Kaplan, M.R., Schaefer, J.M., Denton, G.H., Barrell, D.J.A., Chinn, T.J.H., Putnam, A.E., Andersen, B.G., Finkel, R.C., Schwartz, R. and Doughty, A.M., 2010. Glacier retreat in New Zealand during the Younger Dryas stadial. *Nature*, 467(7312): 194-197. doi:10.1038/nature09313

Kariya, Y., Sato, G. and Komori, J., 2011. Landslide-induced terminal moraine-like landforms on the east side of Mount Shiroumadake, Northern Japanese Alps. *Geomorphology*, 127: 156-165.

Kaser, G. and Osmaston, H., 2002. Tropical Glaciers. Cambridge University Press, 228 pp.

Kääb, A. and Weber, M., 2004. Development of transverse ridges on rock glaciers: field measurements and laboratory experiments. *Permafrost and Periglacial Processes*, 15: 379-391.

Kayastha, R. B., Takeuchi, Y., Nakawo, M. and Ageta, Y., 2000. Practical prediction of the ice melting beneath various thickness of debris cover on Khumbu Glacier, Nepal using a positive degree-day factor. *IAHS Publ.* 264 (Symposium at Kathmandu, Nepal 1992 – *Snow and Glacier Hydrology*): p.71-81.

Keefer, D.K., 1984. Landslides caused by earthquakes. *Geological Society of America Bulletin*, 95: 406-421.

Keefer, D.K., 1994. The importance of earthquake-induced landslides to long-term slope erosion and slope-failure hazards in seismically active regions. *Geomorphology*, 10: 265-284.

Keefer, D.K., 1999. Earthquake-induced landslides and their effects on alluvial fans. *Journal of Sedimentary Research*, 69: 84-104.

Keefer, D.K., 2002. Investigating Landslides Caused by Earthquakes – A Historical Review. *Surveys in Geophysics*, 23(6): 473-510.

Kellerer-Pirklbauer, A., Lieb, G.K., Avian, M. and Gspurning, J., 2008. The response of partially debris-covered valley glaciers to climate change: the example of the Pasterze Glacier (Austria) in the period 1964 to 2006. *Geografiska Annaler*, 90 A(4): 269-285.

Khodakov, V. G., 1972. Raschet ablyatsii l`da pod sloem moreni. (A calculation of ice ablation under the moraine layer). *Materialy Glyasiologicheskikh Issedovaniy (Data of Glaciological Studies). Khronika Obsuzhdeniya*, 20: 105-108. [in Russian]

Kick, W., 1989. The decline of the last Little Ice Age in High Asia compared with that in the Alps. In: Oerlemans J, editor. Glacier Fluctuations and Climate Change. Dordrecht, The Netherlands, Kluwer: p.129-142.

Kirkbride, M.P., 1989. The influence of sediment budget on the geomorphic activity of the Tasman Glacier, Mount Cook National Park, New Zealand. Unpublished Ph.D. dissertation, University of Canterbury, Christchurch, New Zealand.

Kirkbride, M.P., 1993. The temporal significance of transistions from melting to calving at glaciers in the central Southern Alps of New Zealand. *The Holocence*, 3: 232-240.

Kirkbride, M.P., 1995. Processes of transportation. In: Menzies, J. (Ed.), Glacial Environments, vol. 1. Modern Glacial Environments— Processes, Dynamics and Sediments. Butterworth-Heinemann, Oxford: p.261-292.

Kirkbride, M. P., 2000. Ice marginal geomorphology and Holocene expansion of debris-covered Tasman Glacier, New Zealand. In Debris-covered glaciers Debris-covered glaciers (M. Nakawo, C. Raymond and A. Fountain, Eds.), IAHS Publication, 264: p.211–217.

Kirkbride, M.P. and Brazier, V., 1998. A critical evaluation of the use of glacier chronologies in climatic reconstruction, with reference to New Zealand. In- Mountain Glaciation (ed. L.A. Owen). Quaternary Proceedings N6, John Wiley and Sons Lyd., Chichester, p.55-64.

Kirkbride, M.P. and Dugmore, A.J., 2003. Glaciological response to distal tephra fallout fromthe 1947 eruption of Hekla, south Iceland. *Journal of Glaciology*, 49(166): 420-428.

Kirkbride, M.P. and Spedding, N., 1996. The influence of englacial drainage on sediment-transport pathways and till texture of temperate valley glaciers. *Annals of Glaciology*, 22: 160-166.

Kirkbride, M.P. and Sugden, D. 1992. New Zealand loses its top. *Geographical Magazine*, 64(7): 30-34.

Kirkbride, M.P. and Warren, C.R., 1999. Tasman glacier, New Zealand: 20th-century thinning and predicted calving retreat. *Global Planetary Change*, 22: 11-28.

Kobayashi, R., 1970. On mechanical behaviors of rocks under various loading rates. *Rock Mechanics in Japan*, 1: 56-58.

Kobayashi, Y., 1994. Effects of basal guided waves on landslides. *Pure and Applied Geophysics*, 142(2): 329-346.

Komorowski, J.C., Glicken, H.X. and Sheridan, M.F., 1991. Secondary electron imagery of microcracks and hackly fracture surfaces in sandstone-sized clasts from the 1980 Mount St. Helens debris avalanche deposits: implications for particle-particle interactions. *Geology*, 19(3): 261-264.

Konovalov, V., 2000. Computations of melting under moraine as a part of regional modeling of glacier runoff. *IAHS Publ.* 264 (Workshop at Seattle 2000 – *Debris-Covered Glaciers*): 109-118.

Korup, O. and Clague, J.J., 2009. Natural hazards, extreme events, and mountain topography. *Quaternary Science Reviews*, 28: 977–990.

Korup, O., McSaveney, M.J. and Davies, T.R.H., 2004. Sediment generation and delivery from large historic landslides in the Southern Alps, New Zealand. *Geomorphology*, 61(1-2): 189-207.

Korup, O., Clague, J.J., Hermanns, R.L., Hewitt, K., Strom, A.L. and Weidinger, J.T., 2007. Giant landslides, topography, and erosion. *Earth and Planetary Science Letters*, 261: 578-589.

Korup, O., Densmore, A.L., Schlunegger, F. 2010. The role of landslides in mountain range evolution. *Geomorphology*, 120: 77-90.

Krenek, L.O., 1958. The formation of dirt cones on Mount Ruapehu, New Zealand. *Journal of Glaciology*, 3 (24): 312-14.

Krinsley, D. H., and Doornkamp, J. C., 1973. Atlas of quartz sand surface textures. Cambridge, Cambridge University Press, 91 pp.

Kuelen, N., Heilbronner, R., Stünitz, A., Bouiller, A. M. and Ito, H., 2007. Grain size distributions of fault rocks: a comparison between experimentally and naturally-formed granitoids. *Journal of Structural Geology*, 29: 1282-1300.

Kulkarni, A.V., 1992. Mass balance of Himalayan glaciers using AAR and ELA methods. *Journal of Glaciology*, 38(128); 101-104.

Larsen, S., Davies, T.R.H. and McSaveney, M.J., 2005. A possible coseismic landslide origin of late Holocene moraines of the Southern Alps, New Zealand. *New Zealand Journal of Geology and Geophysics*, 48: 311–314.

Laznicka, P., 1988. Breccias and coarse fragmentites: petrology, environments, associations, ores. *Elsevier Developments* in *Economic Geology*, 25: 832 pp.

Lee, J., 2004. Engineering Geological investigation of the Lake Coleridge rock avalanche deposits, Inland Canterbury. Master`s thesis, University of Canterbury, New Zealand.

Lee, J., Davies, T.R. and Bell, D.H., 2009. Successive Holocene rock avalanches at Lake Coleridge, Canterbury, New Zealand. *Landslides*, 6: 287-297.

Lipovsky, P.S., Evans, S.G., Clague, J.J., Hopkinson, C., Couture, R., Bobrowsky, P., Ekström, G., Demuth, M.N., Delaney, K.B., Roberts, N.J., Clarke, G. and Schaeffer, A., 2008. The July 2007 rock and ice avalanches at Mount Steele, St. Elias Mountains, Yukon, Canada. *Landslides*, 5(4): 445-455. DOI 10.1007/s10346-008-0133-4

Locat, P., Couture, R., Leroueil, S., Locat, J. and Jaboyedoff, M., 2006. Fragmentation energy in rock avalanches. *Canadian Geotechnical Journal*, 43: 830-851.

Lundstrom, S.C., McCaferty, A.E. and Coe, J.A., 1993. Photogrammetric analysis of 1984-89 surface altitude change of the partially debris-covered Eliot glacier, Mount Hood, Oregon, USA. *Annals of Glaciology*, 17: 167-170.

Ma, K.F., Tanaka, H., Song, S.-R., Wang, C.Y., Hung, J.H., Tsai, Y.B., Mori, J., Song, Y.F., Yeh, E.C., Soh, W., Sone, H., Kuo, L.W. and Wu, H.Y., 2006. Slip zone and energetics of a large earthquake from the Taiwan Chelungpu-fault Drilling Project. *Nature*, 444: 473-476.

Mabin, M.C.G., 1995. Age of the Waiho Loop glacial event: Comment. *Science*, 271: 868.

Mahaney, W. C., 2002. Atlas of sand grain surface textures and applications. Oxford; New York: Oxford University Press, 237 pp.

Mahaney, W. C., and Kalm, V. 2000. Comparative scanning electron microscopy study of oriented till blocks, glacial grains and Devonian sands in Estonia and Latvia. *Boreas*, 29: 35-51.

Mahaney, W.C., Vortisch, W. and Julig, P., 1988. Relative differences between glacially crushed quartz transported by mountain and continental ice – some examples from North America and East Africa. *American Journal of Science*, 288: 810–826.

Malamud, B.D., Turcotte, D.L., Guzzetti, F. and Reichenbach, P., 2004a. Landslide inventories and their statistical properties. *Earth Surface Processes and Landforms*, 29: 687–711.

Malamud, B.D., Turcotte, D.L., Guzzetti, F. and Reichenbach, P., 2004b. Landslides, earthquakes, and erosion. *Earth and Planetary Science Letters*, 229: 45-59.

Mangerud, J., Larsen, E., Longva, O. and Sønstegaard, E., 1979. Glacial history of western Norway 15,000–10,000 B.P. *Boreas*, 8: 179-87.

Marangunic, C. and Bull, C., 1968. The landslide on Sherman glacier: in the great Alaska earthquake of 1964: Hydrology, Pt. A, Nat. Acad. Sci. Pub. 1603: p.383-394.

Marks, L., 2010. Timing of the Late Vistulian (Weichselian) glacial phases in Poland. *Quaternary Science Reviews*, in press. doi.org/10.1016/j.quascirev.2010.08.008

Marshall, S.J., 2009. Modeling glacier response to climate change. In Glacier Science and environmental change, ed. by Knight, P.G.: p.163-173.

Masuda, K., 2001. Effect of water on strength in a brittle regime. *Journal of Structural Geology*, 23: 1653-1657.

Matthews, M.D., 1991. The effect of pretreatment on size analysis. Ch.3 in principles, methods and application of particle size analysis. Ed. By Syvitski, J.P.M. Cambridge University Press, Cambridge, New York, 368 pp.

Mattson, L.E., 2000. The influence of the debris-cover on the midsummer dischatge o Dome Glacier, Canadian Rocky mountains. IAHS Publication N264: p.25-33.

Mattson, L.E. and Gardner J.S., 1989. Energy exchange and ablation rates on the debris-cover Rakhio Glacier, Pakistan. *Zeitschrift fur Gletscherkunde und Glazizlgeologie*, 25 (1): 17-32.

Mattson, L.E., Gardner, J.S. and Young, G.J., 1993. Ablation on debris covered glaciers: an example from the Rakhiot Glacier, Punjab, Himalaya. IAHS Publ. 218 (Symposium at Kathmandu, Nepal 1992 – *Snow and Glacier Hydrology*), p.289-296.

Mayer, C., Lambrecht, A., Belò, Smiraglia, C. and Diolaiuti, G., 2006. Glaciological characteristics of the ablation zone of Baltoro glacier, Karakoram, Pakistan. *Annals of Glaciology*, 43: 123-131.

McColl, S.T. and Davies, T.R.H., 2011. Evidence for a rock-avalanche origin for The Hillocks moraine, Otago, New Zealand. *Geomorphology*, 127(3-4): 216-224.

McColl, S.T., Davies, T.R.H. and McSaveney, M.J., 2010. Glacier retreat and rock-slope stability: Debunking debuttressing. In: Williams A.L., Pinches, G.M., Chin, C.Y., McMorran, T.J., Massey, C.I. (Eds) Geologically Active: Proceedings of the 11th IAEG Congress. Auckland, New Zealand.

McKenzie, G.D., 1969. Observations on a collapsing kame terrace in Glacier Bay National Monumant, South-East Alaska. *Journal of Glaciology*, 8: 413-425.

McManus, J., 1988. Grain size determination and interpretation. In: Tucker, M. (ed.) techniques in sedimentology, Blackwell Scientific, Oxford, p.63-85.

McSaveney, M.J., 1975. The Sherman glacier rock avalanche of 1964: its emplacement and subsequent effects on the glacier beneath it. PhD thesis, Ohio State University, Columbus, Ohio.

McSaveney, M.J., 1978. Sherman Glacier rock avalanche. In: Voight, B (Ed.) Rockslides and Avalanches, Vol. 1, Elsevier Publishing Company, NY, p.71-96.

McSaveney, M.J., 2002. Recent rockfalls and rock avalanches in Mount Cook National Park, New Zealand. In: Evans, S.G., DeGraff, J.V. (Eds.), Catastrophic Landslides: Effects, Occurrence, and Mechanisms. *Geological Society of America Reviews in Engineering Geology*, 15: 35-70.

McSaveney, M.J. and Davies, T.R., 2007. Rockslides and their motion. In Sassa K, Fukuoka H, Wang F, Wang G (Eds) Progress in Landslide Science Springer-Verlag, p.113-134.

McSaveney, M.J. and Davies, T.R.H., 2009. Surface energy is not one of the energy losses in rock comminution. *Engineering Geology*, 109: 109-113. doi: 10.1016/j.enggeo.2008.11.001

McSaveney, M.J. and Whitehouse, I.E., 1989. An Early Holocene glacial advance in the Macaulay River valley, central Southern Alps, New Zealand. *New Zealand journal of geology and geophysics*, 32(2): 217-223.

Meier, M.F. and Post, A.S., 1962. Recent variations in mass net budgets of glaciers in western North America: Variations of the Regime of Existing Glaciers, IAHS Publication, 58, p. 63-77.

Meier, W. N., Stroeve, J. and Fetterer, F., 2007. Whither Arctic sea ice?: A clear signal of decline regionally, seasonally, and extending beyond the satellite record. *Annals of Glaciology*, 46(1): 428-434.

Melosh, H.J., 1987. The mechanics of large rock avalanches. *Geological Society of America Reviews in Engineering Geology*, 7: 41-49.

Mihalcea, C., Mayer, C., Diolaiuti, G., Lambrecht, A., Smiraglia, C. and Tartari, G. 2006. Ice ablation and meteorological conditions on the debris-covered area of Baltoro glacier, Karakoram, Pakistan. *Annals of Glacio*logy, 43: 292-300.

Molnia, B.F., 2008. Glaciers of North America - Glaciers of Alaska. *In* Williams, R.S., Jr., and Ferrigno, J.G., eds., Satellite image atlas of glaciers of the world: U.S. Geological Survey Professional Paper 1386-K, 525 pp.

Montgomery, D.R. and Brandon, M.T., 2002. Topographic controls on erosion rates in tectonically active mountain ranges. *Earth and Planetary Science Letters*, 201: 481-489.

Morris, E.M., 1976. An experimental study of the motion of ice past obstacles by process of regelation. *Journal of Glaciology*, 17(75): 79-98.

Morris, E.M., 1979. The flow of ice, treated as Newtonian viscous liquid, around a cylindrical obstacle near the bed of glacier. *Journal of Glaciology*, 23(89), 117-30.

Muller, E.H. and Coulter, H.W., 1957. The Knife Creek glaciers of Katmai National Monument, Alaska. *Journal of Glaciology*, 3(22): 116-122.

Murray, M.R., 2002. Is particle size determination possible for carbonate-rich lake sediments? *Journal of Palaeontology*, 27: 173-183.

Murray, T., Strozzi, T., Luckman, A., Jiskoot, H. and Christakos, P., 2003. Is there a single surge mechanism? Contrasts in dynamic between glacier surges in Svalbar and other regions. *Journal of Geophysical Research*, 108(B5): 2237. doi:10.1029/2008GL031207

Nakawo, M., and Rana, B., 1999. Estimate of ablation rate of glacier ice under a supraglacial debris layer. *Geografiska Annaler*, 81A(4): 695-701.

Nakawo, M. and Young, G.J., 1981. Field experiments to determine the effect of a debris layer on ablation of glacier ice. *Annals of Glacioogy*, 2: 85-91.

Nakawo, M. and Young, G.J., 1982. Estimate of glacier ablation under a debris layer from surface temperature and meteorological variables. *Journal of Glacio*logy, 28(98): 29-34.

Nakawo, M., Yabuki, H. and Sakai, A., 1999. Characteristics of Khumbu Glacier, Nepal Himalaya: recent changes in the debris-covered area. *Annals of Glaciology*, 28: 118-122.

NGU Report, 2009. Rock avalanches - distribution and frequencies in the inner part of Storfjorden, Møre og Romsdal County, Norway. Report no. 2009.002, p.23.

Nesje, A., 1994. A gloomy 250-year memory; the glacier destruction of the Tungøyane farm in Oldedalen, western Norway, 12 December 1743. *Norsk Geografisk Tidsskrift*, 48: 133-35.

Nesje, A., 2005. Briksdalsbreen in western Norway. AD 1900–2004 frontal fluctuations as a combined effect of variations in winter precipitation and summer temperature. *The Holocene*, 15: 1245–1252.

Nesje, A., Bakke, J., Dahl, S.O., Lie, Ø. and Matthews, J.A., 2008. Norwegian mountain glaciers in the past, present and future. *Global and Planetary Change*, 60: 10-27.

Nguyen, D.G. and Einav, I., 2009. The energetics of cataclasis based on breakage mechanics. *Pure* and *applied geophysics. Special issue: Mechanics, structure and evolution of fault zones*, 166: 1-32.

Ni, H., Zheng, W., Liu, X. and Gao, Y., 2010. Fractal-statistical analysis of grain-size distributions of debris-flow deposits and its geological implications. *Landslides*, 8(2): 253-259. DOI 10.1007/s10346-010-0240-x

Nicholson, L. and D.I. Benn, 2006. Calculating ice melt beneath a debris layer using meteorological data. *Journal of Glaciol*ogy, 52(178): 463-470.

Nicoletti, P.G., and Sorriso-Valvo, M., 1991. Geomorphic controls of the shape and mobility of rock avalanches. *Geological Society of America Bulletin*, 103: 1365-1373.

NIWA CliFlo, 2007. The National Climate Database: http://cliflo.niwa.co.nz/

Nobes, D.C., 2011. Ground penetrating radar measurements over glaciers. In Singh, V. P., Singh, P., and Haritashya, U. K. (eds.), Encyclopedia of Snow, Ice and Glaciers, Springer Verlag, Heidelberg, p.490-504.

Noetzli, J, Hoelzle, M. and Haeberli, M., 2003. Mountain permafrost and recent Alpine rock-fall events: a GIS-based approach to determine critical factors, in: Proceeding of the 8th International Conference on Permafrost, Zurich, Switzerland, 2003, eds. M. Philipps et al., p.827-832.

Norris, R. J., Cooper, A. F., Wright, T. and Berryman, K. R., 2001. Dating past Alpine Fault Rupture in South Westland: EQC Research Report 99/341.

Nye, J., 1959. The deformation of a glacier below an ice-fall. *Journal of Glaciology*, 3: 387-408.

Oerlemans, J., 1997. Climate sensitivity of Franz Josef Glacier, New Zealand, as revealed by numerical modeling. *Arctic and Alpine Research*, 29: 233-239.

Oerlemans, J., 2000. *Glaciers and climate change*. Lisse (Netherlands): A.A. Balkema, 160 pp.

Oerlemans, J., 2005. Extracting a climate signal from 169 glacier records. *Science*, 308: 675-677.

Oerlemans, J. and Fortuin, J. P. F., 1992. Sensitivity of glaciers and small ice caps to greenhouse warming. *Science*, 258: 115-117.

Ogilvie, I.H., 1904. The effect of superglacial debris on the advance and retreat of some Canadian Glaciers. *Journal of Geology*, 12: 722-743.

Olesen, O., Blikra, L.H., Braathen, A., Dehls, J.F., Olsen, L., Rise, L., Roberts, D., Riis, F., Faleide, J.I. and Anda, E., 2004. Neotectonic deformation in Norway and its implications: a review. *Norwegian Journal of Geology*, 84: 3-34.

Orombelli, G. and Porter, S.C., 1988. Boulder deposit of upper Val Ferret (Courmayeur, Aosta valley): Deposit of historic giant rockfall and debris avalanche or a late-glacial moraine? *Eclogae Geologicae Helvetiae*, 81(2): 365-371.

Owen, L.A., Derbyshire, E. and Scott, C.H., 2003. Contemporary sediment production and transfer in high-altitude glaciers. *Sedimentary Geology*, 155: 13-36.

Owen, G., Hiemstra, J.F., Matthews, J.A. and McEwen, L.J., 2010. Landslide-glacier interaction in a neoparaglacial setting at Tverrbytnede, Jotunheimen, Southern Norway. *Geografiska Annaler*, 92A(4): 421-436.

Østrem, G., 1959. Ice melting under a thin layer of moraine and the existence of ice cores in moraine ridges. *Geografiska Annaler*, 41A: 228-230.

Østrem, G., 1965. Problem of dating Ice-Cored Moraines. *Geografiska Annaler*, 47A(1):1-38.

Østrem, G. and Brugman, M., 1991. Glacier mass-balance measurements. NHR1 Science Report No. 4, Environment Canada, 224 pp.

Paterson, W.S.B., 2004. The Physics of Glacier. 3rd ed. Pergammon, New York, 496 pp.

Pelto, M.S., 2000. Mass balance of adjacent debris-covered and clean glacier ice in the North Cascades, Washington. Debris-Covered glaciers. Proceedings of a workshop held at Seatle, Washington, USA, sep 2000. IAHS Publ.no.264, p.35-42.

Petrakov, D.A., Chernomorets, S.S., Evans, S.G. and Tutubalina, O.V., 2008. Catastrophic glacial multi-phase mass movements: a special type of glacial hazard. *Advanced* Geosciences, 14: 211-218.

Plafker, G., 1968. Source area of the Shattered Peak and Pyramid Peak landslides at Sherman Glacier: in the great Alaska earthquake of 1964: Hydrology, Pt. A, Nat. Acad. Sci. Pub. 1603: 374-383.

Plafker, G., Ericksen, G.E. and Concha, J.F., 1971. Geological aspects of the May 31, 1970, Peru earthquake. *Bulletin of the Seismological Society of America*, 61: 543-578.

Popovin, V.V. and Rozova, A.V., 2002. Influence of sub-debris thawing on ablation and runoff of the Djankuat glacier in the Caucasus. *Nordic Hydrology*, 33(1), 79-94.

Porter, S.C., 2000. Onset of neoglaciation in the Southern Hemisphere. Journal of Quaternary Science 15, 395-408. Reid JR (1969) Effects of a debris slide on “Sioux Glacier”, south-central Alaska. *Journal of Glaciology*, 8 (54): 353-367.

Porter, S. C. and Orombelli, G., 1980. Catastrophic rockfall of September 12, 1717 on the Italian flank of the Mont Blanc massif. *Zeitschrift für Geomorphologie*, 24: 200-218.

Porter, S.C. and Orombelli, G., 1981. Alpine rockfall hazards. *American Scientist*, 69: 67-75.

Post, A.S., 1967. Effects of the March 1964 Alaska earthquake on glaciers. United States Geological Survey Professional Paper 544-D, 42 pp.

Post, A.S., 1968. Effects on Glaciers: in the great Alaska earthquake of 1964: Hydrology, Pt. A, Nat. Acad. Sci. Pub. 1603: 266-308.

Post, A., 1969. Distribution of surging glaciers in North America. *Journal of Glaciology*, 8(53): 229-240.

Prager, C., Ivy-Ochs, S., Ostermann, M., Synal, H.A. and Patzelt, G., 2009. Geology and radiometric 14C-, 36Cl- and Th-/U-dating of the Fernpass rockslide (Tyrol, Austria). *Geomorphology*, 103(1): 93-103.

Pugh, J.M., 2008. The late Quaternary environmental history of the Lake Heron Basin, Mid Canterbury, New Zealand. Master`s thesis, University of Canterbury, New Zealand.

Purdie, J. and Fitszharris B., 1999. Processes and rates o ice loss at the terminus of Tasman Glacier, New Zealand. *Global and Planetary Change*, 22: 79-81.

Purdie, H.L., Brook, M.S. and Fuller, I.C., 2008. Seasonal Variation in Ablation and Surface Velocity on a Temperate Maritime Glacier: Fox Glacier, New Zealand. *Arctic, Antarctic, and Alpine Research*, 40(1): 140-147.

Putnam, A.E., Denton, G.H., Schaefer, J.M., Barrell, D.J.A., Andersen, B.G., Finkel, R.C., Schwartz, R., Doughty, A.M., Kaplan, M.R. and Schlüchter, C., 2010a. Glacier advance in southern middle-latitudes during the Antarctic Cold Reversal. *Nature Geoscience*, 3: 700-704.

Putnam, A.E., Schaefer, J.M., Barrell, D.J.A., Vandergoes, M.J., Denton, G.H., Kaplan, M.R., Finkel, R.C., Schwartz, R., Goehring, B.M. and Kelley, S.E. 2010b. In situ cosmogenic ^{10}Be production-rate calibration from the Southern Alps, New Zealand. *Quaternary geochronology, 5(4):* 392-409. doi:10.1016/j.quageo.2009.12.001

Quincey, D.J. and Glasser, N.F., 2009. Morphological and ice-dynamical changes on the Tasman Glacier, New Zealand, 1990–2007. *Global and Planetary Change*, 68, 185-197.

Ramberg, I.B., Bryhni, I., Nøttvedt, A. and Rangnes, K. (Ed.), 2008. The making of a land - Geology of Norway. *Trondheim: Norsk Geologisk Forening*, 624 pp.

Rana, B., Nakawo, M., Fukushima, Y. and Ageta, Y., 1997. Application of a conceptual precipitation–runoff model (HYCY-MODEL) in a debris-covered glacierized basin in the Langtang Valley, Nepal Himalaya. *Annals of Glaciology*, 25: 226-231.

Reches, Z. and Dewers, T., 2005. Gouge formation by dynamic pulverization during earthquake rupture. *Earth and Planetary Science Letters*, 235: 361-374.

Reches, Z. and Lockner, D.A., 2010. Fault weakening and earthquake instability by powder lubrication. *Nature*, 467: 452-455. doi:10.1038/nature09348

Reches, Z., Mishima, T. D., Strout, G., Lockner, D. A., Hamilton, M., and Heesakkers, V., 2007. Gouge powder from earthquakes rupture-zones and laboratory rupture experiments: sub-microscopic observations and particle size distribution. EOS Transactions AGU, 88, Abstract T11A-0338.

Reid, J.R., 1969. Effects of a debris slide on "Sioux Glacier", south-central Alaska. *Journal of Glaciology*, 8(54): 353-367.

Reynolds, R.C., 1971. Clay mineral formation in Alpine environment. *Clays and Clay Minerals*, 19: 361-374.

Reznichenko, N.V., Davies, T.R.H., Shulmeister, J. and McSaveney, M.J., 2010. Effects of debris on ice-surface melting rates: an experimental study. *Journal of Glaciology*, 56(197): 384-394.

Reznichenko, N.V., Davies, T.R.H. and Alexander, D.J., 2011. Effects of rock avalanches on glacier behaviour and moraine formation. *Geomorphology*, 132(3-4): 327-338.

Reznichenko, N.V., Davies, T.R.H., Shulmeister, J. and Winkler, S. Accepted. Influence of rock avalanches upon the formation of moraines and their subsequent palaeoclimatic interpretation: a critical appraisal. *Zeitschrift für Geomorphologie*.

Reznichenko, N.V., Davies, T.R.H., Shulmeister, J. and Larsen S.H., 2012. A new technique for identifying rock-avalanche-sourced sediment in moraines and some paleoclimatic implications. *Geology*, in press. doi: 10.1130/G32684.1

Rhoades, D.A. and Van Dissen, R.J., 2003. Estimates of the time-varying hazard of rupture of the Alpine fault, New Zealand, allowing for uncertainties. *New Zealand Journal of Geology and Geophysics*, 46: 479-488.

Richardson, J. and Brook, M., 2010. Ablation of debris-covered ice: Some effects of the 25 September 2007 Mt. Ruapehu eruption. *Journal of the Royal Society of New Zealand*, 40(2): 45-55.

Rogers, J.J.W., Krueger, W.C. and Krog, M., 1963. Sizes of naturally abraded materials. *Journal of Sedimentary Petrology*, 33(3): 628-632.

Rogerson, R.J., Olson, M.E. and Branson, D., 1986. Medial moraines and surface melt on glaciers of the Torngat Mountains, Nothern Labrador, Canada. *Journal of Glaciology*, 32(112): 350-354.

Rosenbaum, J.G. and Reynolds, R.L., 2004. Record of Late Pleistocene glaciation and deglaciation in the southern Cascade Range: II. Flux of glacial flour in a sediment core from Upper Klamath Lake, Oregon. *Journal of Paleolimnology*, 31: 235-252.

Röhl, K., 2008. Characteristics and evolution of supraglacial ponds on debris-covered Tasman Glacier, New Zealand. *Journal of Glaciology*, 54(188): 867-880.

Röthlisberger, H., 1969. Evidence for an ancient glacier surge in the Swiss Alps. *Canadian Journal of Earth Science*, 6: 863-865.

Sammis, C. G. and Ben-Zion, Y., 2008. The Mechanics of Grain-Size Reduction in Fault Zones. *Journal of Geophysical Research*. 113: B02306. doi:10.1029/2006JB004892

Sammis, C., King, G. and Biegel, R., 1987. The kinematics of gouge deformation. *Pure and Applied Geophysics*, 125: 777-812.

Sara, W.A., 1968. Franz Josef and Fox Glaciers, 1951-1967. *New Zealand Journal of Geology and Geophysics*, 11(3): 768-780.

Schaefer, J.M., Denton, G.H., Kaplan, M., Putnam, A., Finkel, R.C., Barrell, D.J.A., Andersen, B.G., Schwartz, R., Mackintosh, A., Chinn, T. and Schluechter, C., 2009. High-frequency Holocene glacier fluctuations in New Zealand differ from the northern signature. *Science*, 324(5927): 622-625. doi:10.1126/science.1169312

Scheidegger, A.E., 1973. On the prediction of reach and velocity of catastrophic landslides. *Rock Mechanics*, 5: 231-236.

Scherler, D., Bookhagen, B. and Strecker, M.R., 2011. Spatially variable response of Himalayan glaciers to climate change affected by debris cove. *Nature Geoscience*, 4: 156-159.

Schulz, W.H., Harp, E.L. and Jibson, R.W., 2008. Characteristics of large rock avalanches triggered by the November 3, 2002 Denali Fault earthquake, Alaska, USA: in: Proceedings of the 10th International Symposium on Landslides, Xian, China, June 30-July 4, 2008, Taylor and Francis Group, London.

Schytt, A., 1967. A study of “ablation gradient”. *Geografiska Annaler*, 49A: 327-332.

Sharp, R.P., 1949. Studies of superglacial debris on valley glacier. *American Journal of Science*, 22(86): 43-52.

Sharp, M. and Gomez, B. 1986. Processes of debris comminution in the glacial environment and implications for quartz sand grain micromorphology. *Sedimentary Geology*, 46, 33-47.

Sharp, M., Tranter, M., Brown, G.H. and Skidmore, M., 1995. Rates of chemical denudation and CO_2 drawdown in a glacier-covered alpine catchment. *Geology*, 23: 61-64.

Shreve, R.L., 1966. Sherman Landslide: Alaska. *Science*, 154: 1639-1643.

Shreve, R.L., 1968. Leakage and fluidization in air-layer lubricated avalanches. *Geological Society of America Bulletin*, 79(5): 653-657.

Shugar, D. H., 2011. Rock avalanches on glaciers. PhD Dissertation, Simon Fraser University, Burnaby, British Columbia, Canada

Shugar, D. H. and Clague, J.J., 2011. The sedimentology and geomorphology of rock avalanche deposits on glaciers. *Sedimentology*, 58: 1762-1783.

Shugar, D. H., Rabus, B., Clague, J.J. and Capps, D.M., 2011. The response of Black Rapids Glacier, Alaska, to the Denali earthquake rock avalanches, *Journal of Geophysical Research*, in press. doi:10.1029/2011JF002011

Shulmeister, J., Davies, T.R.H., Evans, D.J.A., Hyatt, O.M. and Tovar, D.S., 2009. Catastrophic landslides, glacier behaviour and moraine formation - a view from an active plate margin. *Quaternary Science Reviews*, 28: 1085-1096.

Shulmeister, J., Davies, T.R., Reznichenko, N. and Alexander, D.J., 2010a. Comment on "Glacial Advance and stagnation caused by rock avalanches" by Vacco, D., Alley, R.B. and Pollard, D. *Earth and Planetary Science Letters*, 297: 700-701.

Shulmeister, J., Fink, D. and Augustinus, P.C. 2005. A cosmogenic nuclide chronology of the last glacial transition in North-West Nelson, New Zealand - new insights in Southern Hemisphere climate forcing during the last deglaciation. *Earth and Planetary Science Letters*, 233:455-466.

Shulmeister, J., Goodwin, I., Renwick, J., Harle, K., Armand, L., McGlone, M.S., Cook, E., Dodson, J., Hesse, P.P., Mayewski, P. and Curran, M., 2004. The Southern Hemisphere Westerlies in the Australasian sector during the last glaciation cycle: a synthesis. *Quaternary International*, 118/119: 23-53.

Shulmeister, J., Thackray, G.D., Rieser, U, Hyatt, O.M, Rother, H., C.C. Smart, and Evans, D.J.A., 2010b. The stratigraphy, timing and climatic implications of pre-LGM glaciolacustrine deposits in the middle Rakaia Valley, South Island, New Zealand. *Quaternary Science Reviews*, 29: 2362-2381.

Sigurðsson O. and Williams R., 1991. Rockslides on the terminus of "Jökulsárgilsjökull", Southern Iceland. *Geografiska Annaler*, 73A: 129-140.

Singh, P., Kumar, N., Ramasastri, K.S. and Singh, Y., 2000. Influence of a fine debris layer on the melting of snow and ice on a Himalayan glacier. *IAHS Publ.* 264 (Workshop at Seattle 2000 – *Debris-Covered Glaciers*), p.63-69.

Slaymaker, O. and Kelly, R.E.J., 2009. The cryosphere and global environmental change. Malden, MA: Blackwell Pub., p.225-253.

Small, R.J., 1987. Moraine sediment budgets, A.M. Gurnell, M.J. Clark, Editors, *Glacio-Fluvial Sediment Transfer*, Wiley, New York, p.165–197.

Smalley, I.J., 1966. The properties of glacial loess and the formation of loess deposits. *Journal of Sedimentary Research,* 36(3): 669-676.

Smalley, I.J. and Krinsley, D.H., 1978. Loess deposits associated with deserts. *Catena*, 5: 53-66.

Smalley, I.J. and Vita-Finzi, C., 1968. The formation of fine particles in sandy deserts and the nature of 'desert' loess. *Journal of Sedimentary Petrology*, 38: 766-774.

Smith, G.M., Davies, T.R., McSaveney, M.J. and Bell, D.H., 2006. The Acheron rock avalanche, Canterbury, New Zealand—morphology and dynamics. *Landslides,* 3: 62-72.

Soldati, M., Corsini, A. and Pasuto, A., 2004. Landslides and climate change in the Italian Dolomites since the Late glacial. *Catena*, 55(2): 141-161.

Speight, R., 1940. Ice wasting and glacier retreat in New Zealand. *Journal of Geomorphology*, 3: 131-143.

Stevens, G. R., 1990. Rugged Landscape: The Geology of Central New Zealand, Including Wellington, Wairarapa, Manawatu and the Marlborough Sounds, Wellington, A.H. and A.W. Reed. DSIR Publishing.

Stirling, M.W., McVerry, G.H. and Berryman, K.R., 2005. A new seismic hazard model for New Zealand. *Bulletin of the Seismological Society of America,* 92(5): 1878-1903.

Storti, F. and Balsamo, F. 2010. Impact of ephemeral cataclastic fabrics on laser diffraction particle size distribution analysis in loose carbonate fault breccia. *Journal of Structural Geology*, 32(4): 507-522.

Strom, A.L., 1999. The Morphology and Internal Structure of Large Rockslides as Indicators of Their Formational Mechanisms. *Doklady Earth Sciences*, 369(8): 1079-1081.

Strom, A.L., 2004. Rock avalanches of the Ardon River valley at the southern foot of the Rocky Range, Northern Caucasus, North Osetia. *Landslides,* 1(3): 237-241.

Strom, A. and Korup, O., 2006. Extremely large rockslides and rock avalanches in the Tien Shan Mountains, Kyrgyzstan. *Landslides*, 3(2): 125-136.

Sturm, M., Benson, C. and MacKeith, P., 1986. Effects of the 1966-68 eruptions of Mount Redoubt on the flow of Drift Glacier, Alaska, U.S.A. *Journal of Glaciology,* 32(112): 355-362.

Suggate, R.P. (ed.), 1978. The geology of New Zealand. 1.E.C.Keating, Wellington.

Suggate, R.P., 1990. Late Pliocene and quaternary glaciations of New Zealand. *Quaternary Science Reviews,* 9: 175-197.

Swift, D.A., Nienow, P.W., Spedding, N. and Hoey, T.B., 2002. Geomorphic implications of subglacial drainage configuration: rates of basal sediment evacuation controlled by seasonal drainage system evolution. *Sedimentary Geology*, 149: 5-19.

Swithinbank, C.W.M., 1950. The origin of dirt cones on glaciers. *Journal of Glaciology*, 1: 461-465.

Takeuchi, N., Kayastha, R.B. and Nakawo, M., 2000. Charateristics of ablation and heat balance in debris-free and debris-covere areas on Khumbu Glacier, Nepal Himalaya, in the pre-monsoon season. IAHS publication no 264 (Workshop at Seattle 2000 – *Debris-Covered Glaciers*), p.53-63.

Tangborn, W. and Rana, B., 2000. Mass balance and runoff of the partially debris-covered Langtang glacier, Nepal. IAHS publication no 264 (Workshop at Seattle 2000 – *Debris-Covered Glaciers*), p.99-108.

Tarr, R.S. and Martin, L., 1912. The earthquakes at Yakutat Bay, Alaska in September, 1899. US geological survey, professional paper 69, 135 pp.

Tarr, R.S. and Martin, L., 1914. Alaskan Glacier Studies. National Geographical Society, Washington, 498 pp.

Tovar, D.S., Shulmeister, J. and Davies, T.R.H., 2008. Evidence for a landslide origin of New Zealand's Waiho Loop Moraine. *Nature Geosciences*, 1(8): 524-526.

Towner, G.D., 1988. The influence of sand- and silt-size particles on the cracking during drying of small clay-dominated aggregates. *Journal of Soil Science*, 39: 347-356.

Turnbull, J.M., Davies, T.R.H., 2002. Subglacial sediment accumulation and basal smoothing - a possible mechanism for initiating glacier surging. *New Zealand Journal of Hydrology*, 41 (2): 105-123.

Turnbull, J.M. and Davies, T.R.H., 2006. A mass movement origin for cirques. *Earth Surface Processes and Landforms*, 31(9): 1129-1148.

Turney, C.S.M., McGlone, M.S. and Wilmshurst, J.M., 2003. Asynchronous climate change between New Zealand and the North Atlantic during the last deglaciation. *Geology*, 31(3): 223-226.

Tuthill, S.J., 1966. Earthquake origin of superglacial drift on the glaciers of the Martin River area, south-central Alaska. *Journal of Glaciology*, 6: 83-88.

Tuthill, S.J., Field, W.O. and Clayton, L., 1968. Postearthquake studies at Sherman and Sheridan glaciers: in the great Alaska earthquake of 1964: Hydrology, Pt. A, Nat. Acad. Sci. Pub. 1603, p.318-328.

Vacco, D. A., Alley, R. B. and Pollard, D., 2010. Glacial advance and stagnation caused by rock avalanches. *Earth and Planetary Science Letters*, 294: 123-130.

Veblen, T. T., Ashton, D. H., Rubulis, S., Lorenz, D. and Cortes, M., 1989. Nothofagus stand development on in-transit moraines, Casa Pangue Glacier, Chile. *Arctic and Alpine Research*, 21(2): 144-155.

Vilímek, V., Klimeš, J. and Zapata, M., 2008. Delimitation of prehistoric rock fall from Huascaran Mt., Peru. In: Proceedings of The First World Landslide Forum, Tokyo, 18. 2008, United Nations University, Tokyo, Japan, p.631-634.

Voight, B. (Ed.), 1978. Rockslides and Avalanches, 1 Natural Phenomena. Elsevier, NY. 843 pp.

Voight, B. and Pariseau, W.G., 1978. Rockslides and avalanches: An Introduction. In Rockslide and avalanches. Vol. 1: Natural Phenomena. Elsevier, NY, 843 pp.

Voight, B., and Sousa, J., 1994. Lessons from Ontake-San: a comparative analysis of debris avalanche dynamics. *Engineering Geology*, 38(3-4): 261-297.

Voight, B., Janda, R.J., Glicken, H. and Douglass, P.M., 1983. Nature and mechanics of the Mount St. Helens rockslide-debris avalanche of 18 May 1980. *Geotechnique*, 33(3): 243-273.

Wardle, P., 1973. Variations of the glaciers of Westland National Park and Hooker Range, New Zealand. *New Zealand Journal of Botany*, 11: 349-388.

Warren, G., 1967. Sheet 17, Hokitika (1st Ed.) Geological Map of New Zealand. 1; 250,000. New Zealand Geological Survey, Wellington.

Warren, C.R. and Kirkbride, M.P., 2003. Calving speed and climatic sensitivity of New Zealand lake-calving glaciers. *Annals of Glaciology*, 36: 173-178.

Watson, M.I., 1995. Geophysical and glaciological studies of the Tasman and Mueller Glaciers. MSc thesis. University of Auckland, Auckland, New Zealand.

Wells, A., and Goff, J., 2007. Coastal dunes in Westland, New Zealand, provide a record of palaeoseismic activity on the Alpine fault. *Geology*, 35(8): 731-734.

Wen, B., Aydin, A. and Duzgoren-Aydin, N.S., 2002. A comparative study of particle size analyses by sieve-hydrometer and laser diffraction methods. *Geotechnical Testing Journal*, 25(4): 1-9.

Whalley, W. B., 1978. An SEM examination of quartz grains from sub-glacial and associated environments and some methods for their characterization. *Scanning Electron Microscopy*, 1: 353-60.

Whalley, W. B., 1996. Scaning Electron Microscopy. In Menzies, J., (Ed.) Past Glacial Environments: Sediments, Forms and Techniques. Oxford, Butterworth-Heinemann, pp. 357-75.

Whitehouse, I.E., 1983. Distribution of large rock avalanche deposits in the central Southern Alps, New Zealand. *New Zealand Journal of Geology and Geophysics*, 25: 271-279.

Whitehouse, I. and Griffiths, G., 1983. Frequency and hazard of large rock avalanches in the central Southern Alps, New Zealand. *Geology*, 11: 331-334.

Wieczorek, G. F., 1996. Chapter 4: Landslide triggering mechanisms. In: Landslides: Investigation and Mitigation. A. K. Turner and R. L. Schuster (Eds). U.S. Transportation Research Board, p.76-90.

Wilson, D., Dewers, T., Reches, Z. and Brune, J., 2005. Particle size and energetics of gouge from earthquake rupture zones. *Nature*, 434: 749-752.

Wilson, P., 2009. Storurdi: a Late Holocene rock-slope failure (sturzstrom) in the Jotunheimen, southern Norway. *Geografiska Annaler*, 91A(1): 47-58.

Winkler, S., 2004. Lichenometric dating of the 'Little Ice Age' maximum in Mt Cook National Park, Southern Alps, New Zealand. *The Holocene*, 14(6): 911-920.

Winkler, S., 2005. The 'Schmidt hammer' as a relative-age dating technique: potential and limitations of its application on Holocene moraines in Mt Cook National Park, Southern Alps, New Zealand. *New Zealand Journal of Geology and Geophysics*, 48: 105-116.

Winkler, S. and Matthews, J.A., 2010. Observations on terminal moraine-ridge formation during recent advances of southern Norwegian glaciers. *Geomorphology*, 116: 87-106.

Winkler, S. and Nesje, A., 1999. Moraine formation at an advancing temperate glacier: Brigsdalsbreen, western Norway. *Geografiska Annaler*, 81A: 17-30.

Wright, C.A., 1998. The AD 930 long-runout Round Top debris avalanche, Westland, New Zealand. *New Zealand Journal of Geology and Geophysics*, 41(4): 493-497.

Wright, J.S., 1995. Glacial comminution of quartz sand grains and the production of loessic silt: a simulation study. *Quaternary Science Reviews*, 14: 669-680.

Yamaguchi, S., Matsumoto, T., Sawagakit, T., Muravyev, Y.D., Ovsyannikov, A.A. and Naruse, R., 2000. Glaciological research of Bilchenok glacier in Kamchatka, 1998. *Bull Glaciological Research*, 17: 43-50.

Yamaguchi, S., Sawagakit, T, Matsumoto T., Muravyev Y.D. Naruse R. 2007. Influence of Debris Cover on Ogive-like Surface Morphology of Bilchenok Glacier in Kamchatka. *Arctic, Antarctic and Alpine Research*, 39(2): 332-339.

Yarnold, J.C. and Lombard, J.P., 1989. A facies model for large rock avalanche deposits formed in dry climates. In: Colburn, I.P., Abbott, P.L., Minch, J. (Eds.), Conglomerates in Basin Analysis: A Symposium Dedicated to A.O. Woodford. Soc. Econ. Paleontol. Mineral., Pacific Sect. 62: 9-31.

Yde, J.C. and Paasche, Ø., 2010. Reconstructing climate change: not all glaciers suitable. *EOS transactions, American Geophysical Union*, 91(21, 25): 189-196.

Zhang, Y.Q., Lu, Y. and Hao, H., 2004. Analysis of fragment size and ejection velocity at high strain rate. *International Journal of Mechanical Sciences*, 46: 27-34.

Zhang, Y., Liu, S. and Ding, Y., 2007. Glacier meltwater and runoff modelling, Keqicar Baqi glacier, southwestern Tien Shan, China. *Journal of Glaciology*, 53(180): 91-98.